

GRISPE

Guidelines and Recommendations for Integrating Specific Profiled steel sheets in the Eurocodes (**GRISPE**)

Test report

Interlocking planks

Annex

28.02.2016

Deliverable D 4.3

Guidelines and Recommendations for Integrating Specific Profiled Steel sheets in the Euro-codes (GRISPE)

Project co-funded under the Research Fund for Coal and Steel
Grant agreement No RFCS-CT-2013-00018
Proposal No RFS-PR-12027

Author(s)	
<i>C. Fauth, KIT</i>	
Drafting history	
<i>Final Version</i>	<i>28th February 2016</i>
Dissemination Level	
<i>PU</i>	<i>Public</i>
<i>PP</i>	<i>Restricted to the Commission Services, the Coal and Steel Technical Groups and the European Committee for Standardisation (CEN)</i>
<i>RE</i>	<i>Restricted to a group specified by the Beneficiaries</i>
<i>CO</i>	<i>Confidential, only for Beneficiaries (including the Commission services)</i>
Verification and Approval	
<i>Coordinator:</i>	
<i>WP4 Leader:</i>	
<i>Other Beneficiaries</i>	
Deliverable	
<i>D 4.3 Test report</i>	<i>Due date: 28th February 2016</i> <i>Completion date: 28th February 2016</i>

Content

1	Annex A: Object of testing	4
2	Annex B: Single span positive bending tests (pressure tests).....	5
3	Annex C: Single span negative bending test (suction tests)	18
4	Annex D: Double span positive bending tests (pressure tests)	38
5	Annex E: Double span negative bending tests (suction tests)	62
6	Annex F: End support tests (pressure)	112
7	Annex G: Measurement of the profile geometry	128
8	Annex H: Tensile tests	130

1 Annex A: Object of testing

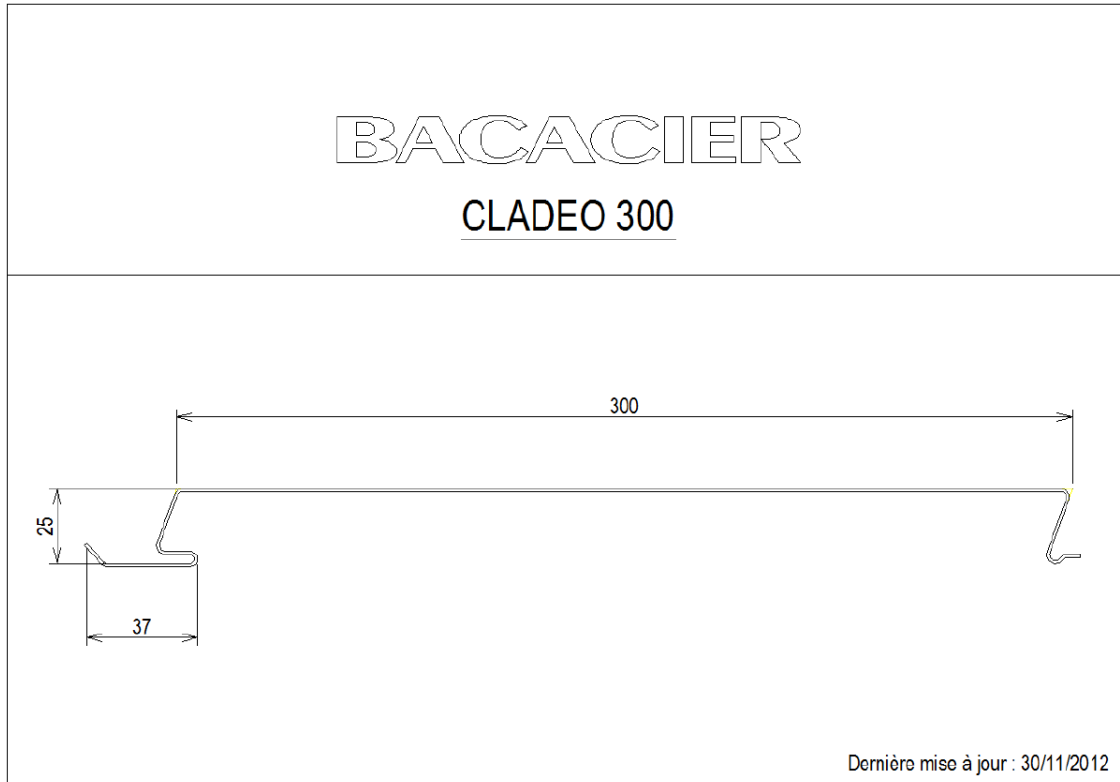


Figure A.1: Cross-section of Cladeo 300 (Bacacier)

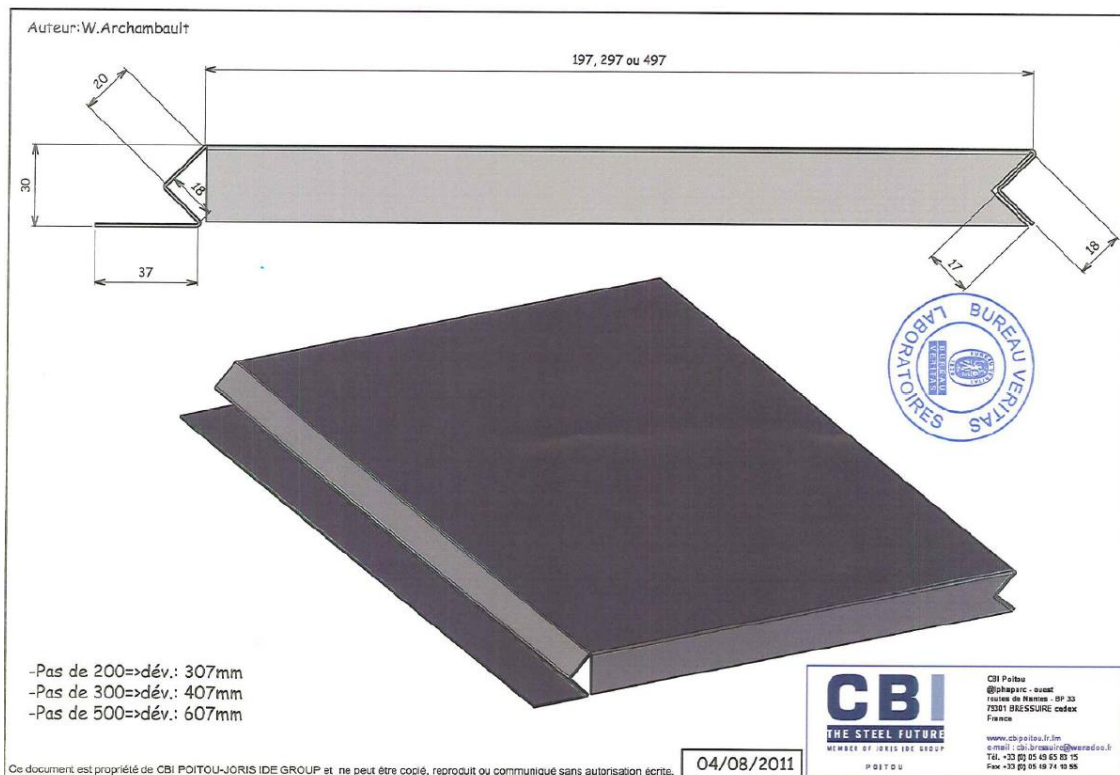


Figure A.2: Cross-section of Zephir 300 (Joris Ide)

2 Annex B: Single span positive bending tests (pressure tests)

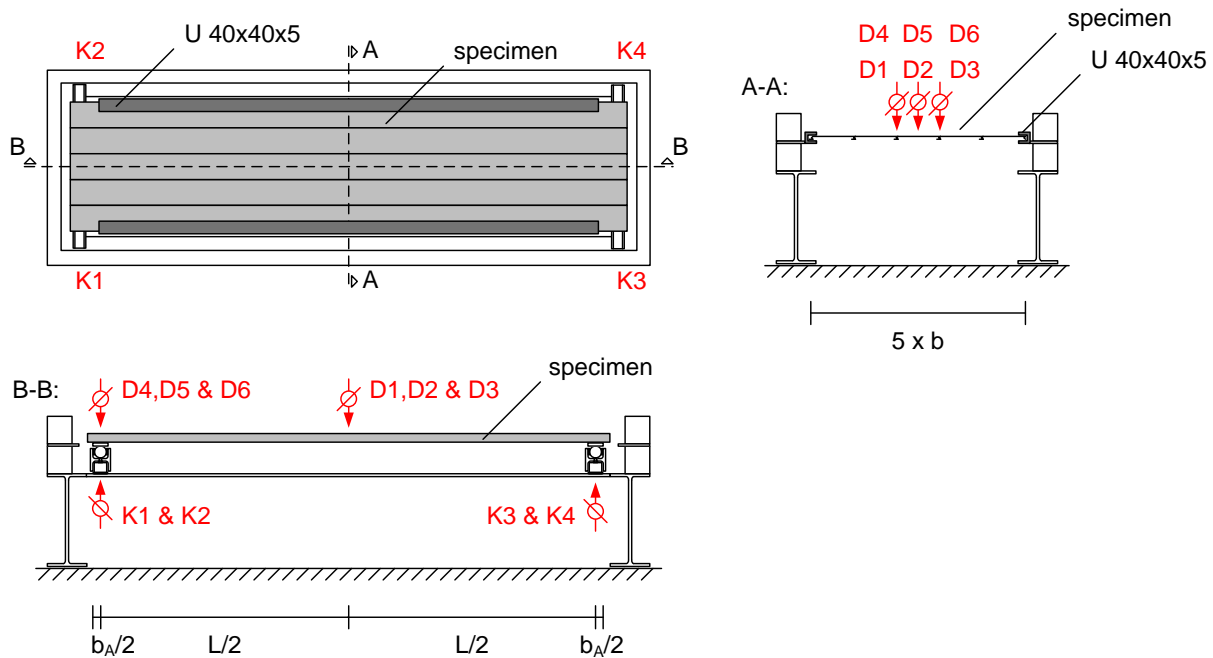


Fig. B.1: Schematic test setup



Fig. B.2: Test setup

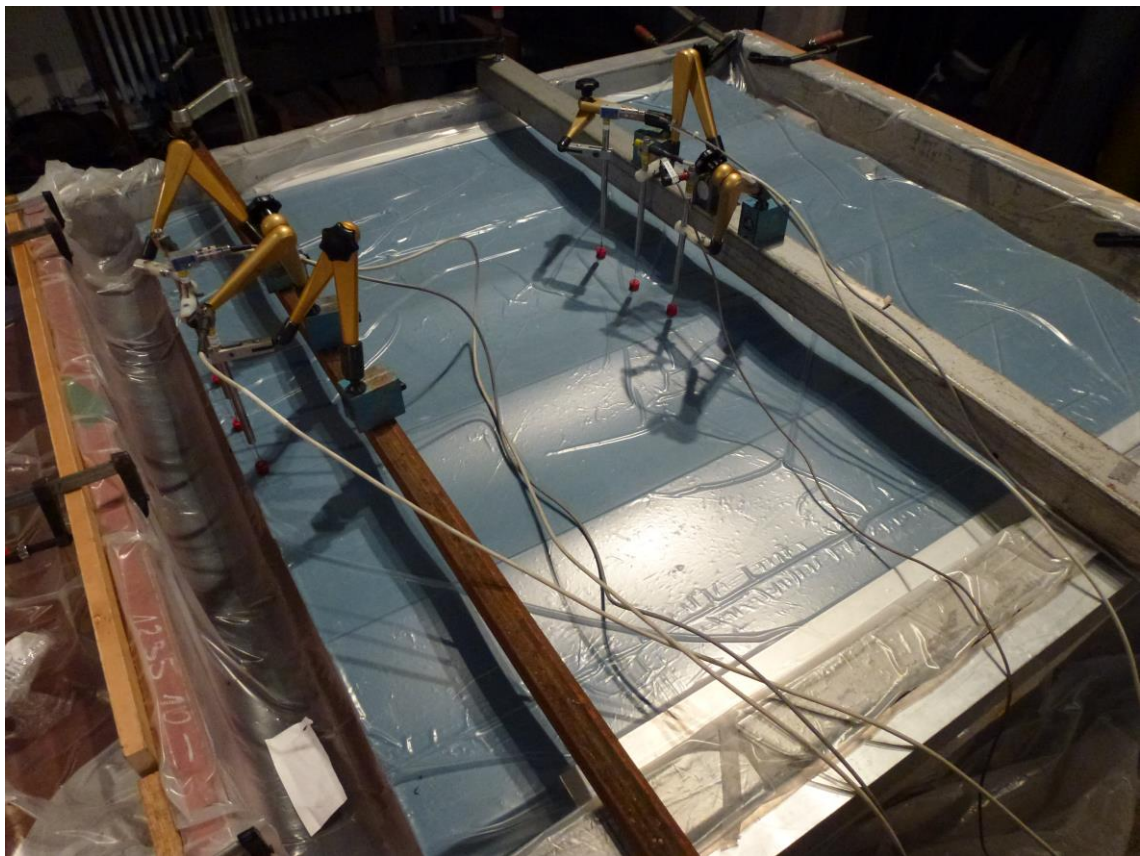


Fig. B.3: Deformation before failure load was reached (Cladeo)

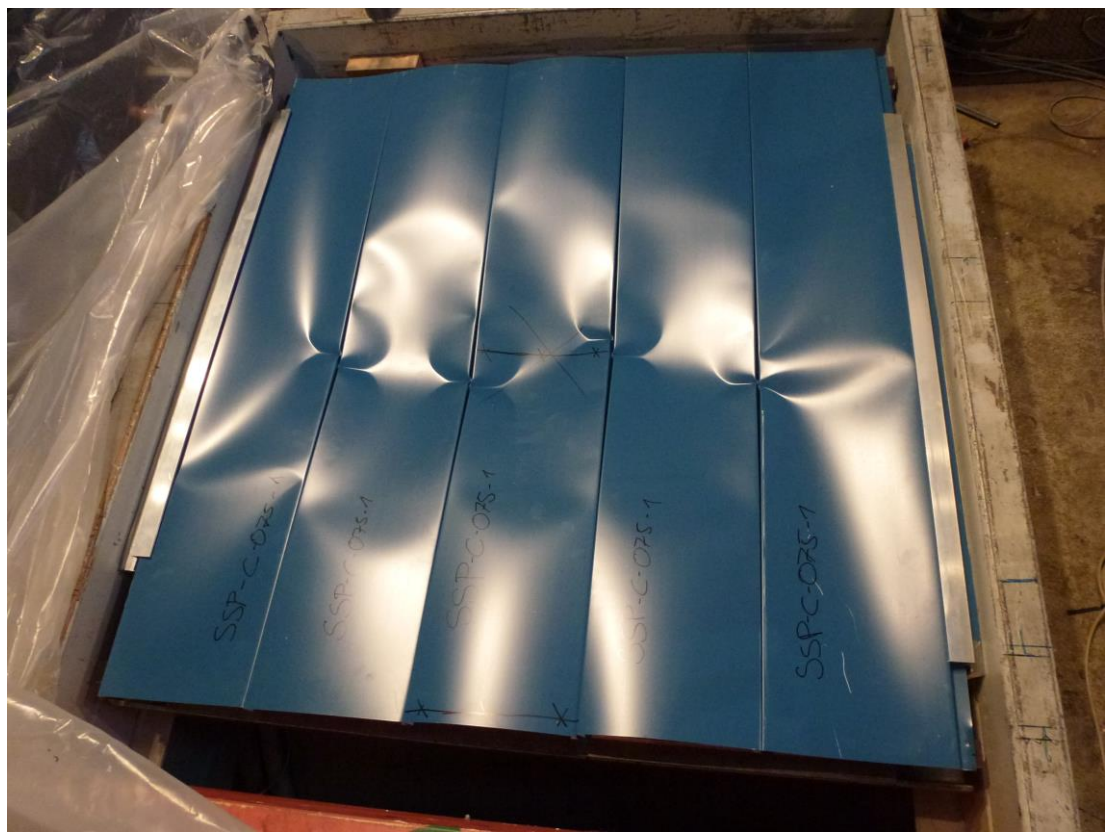


Fig. B.4: Failure mode (local buckling of the compressed flange, Cladeo $t_N = 0.75$ mm)

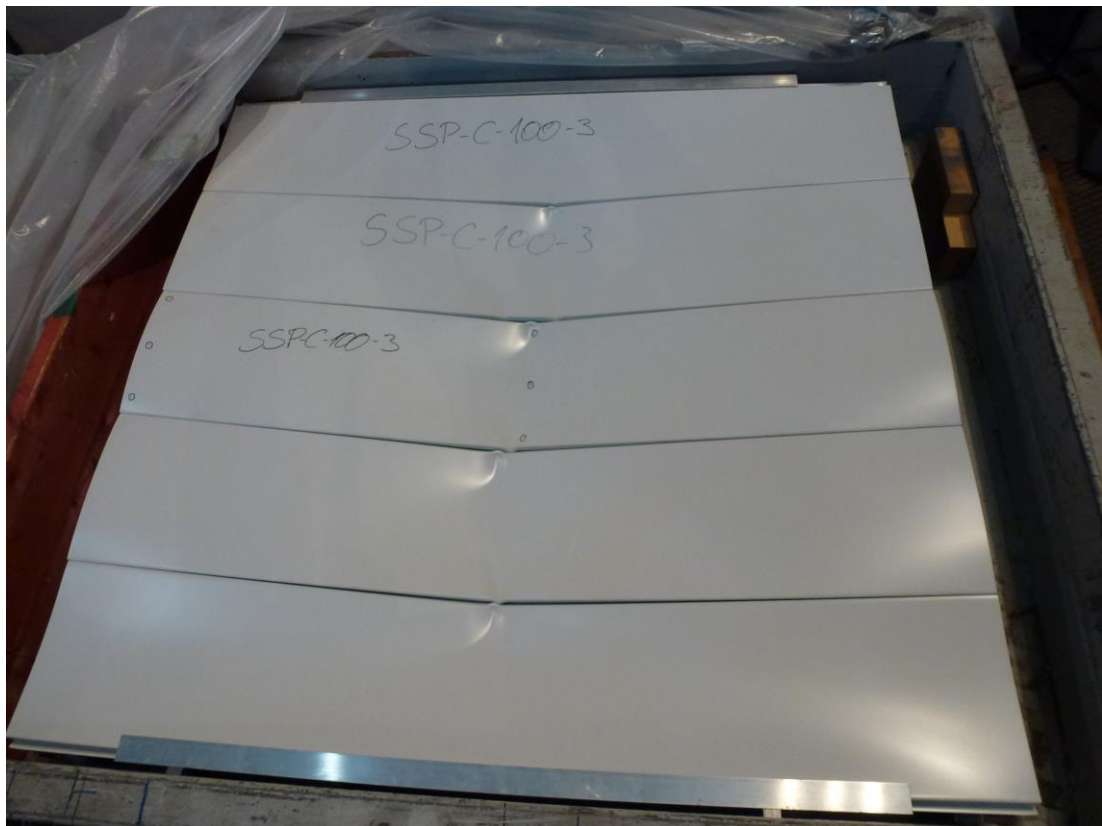


Fig. B.5: Failure mode (local buckling of the compressed flange, Cladeo $t_N = 1.00$ mm)

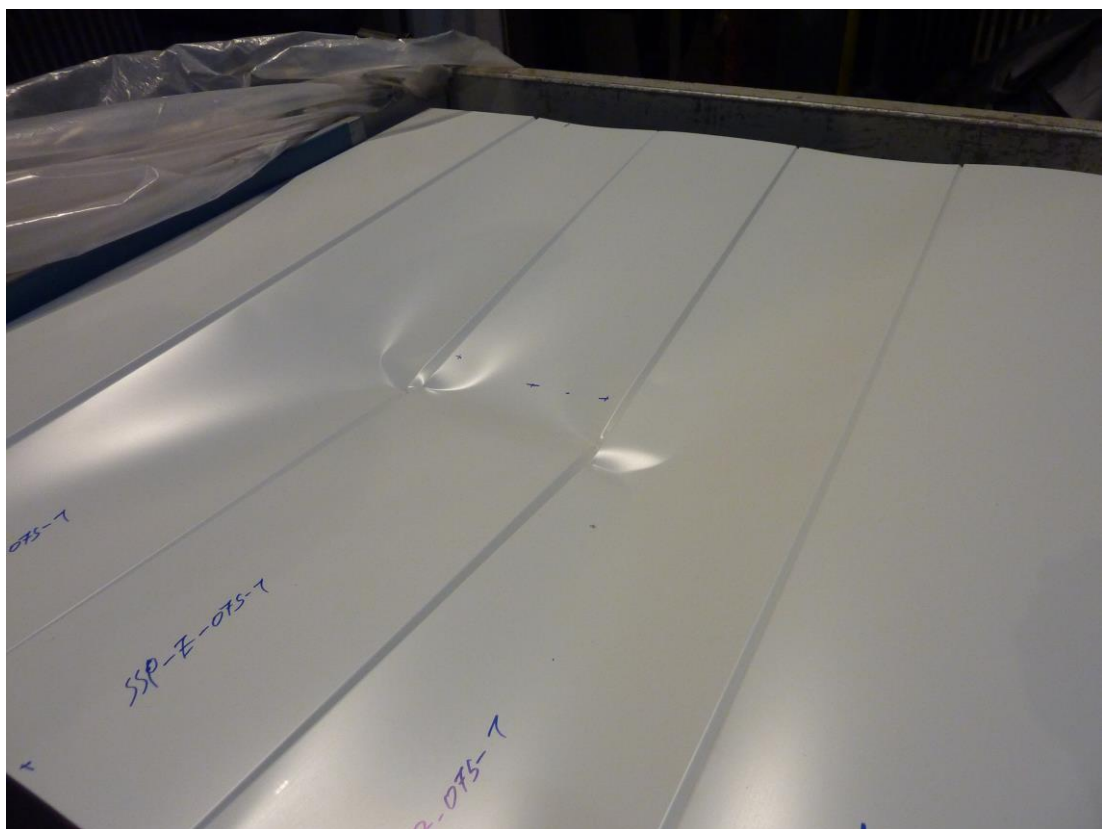


Fig. B.6: Failure mode (local buckling of the compressed flange, Zephir $t_N = 0.75$ mm)

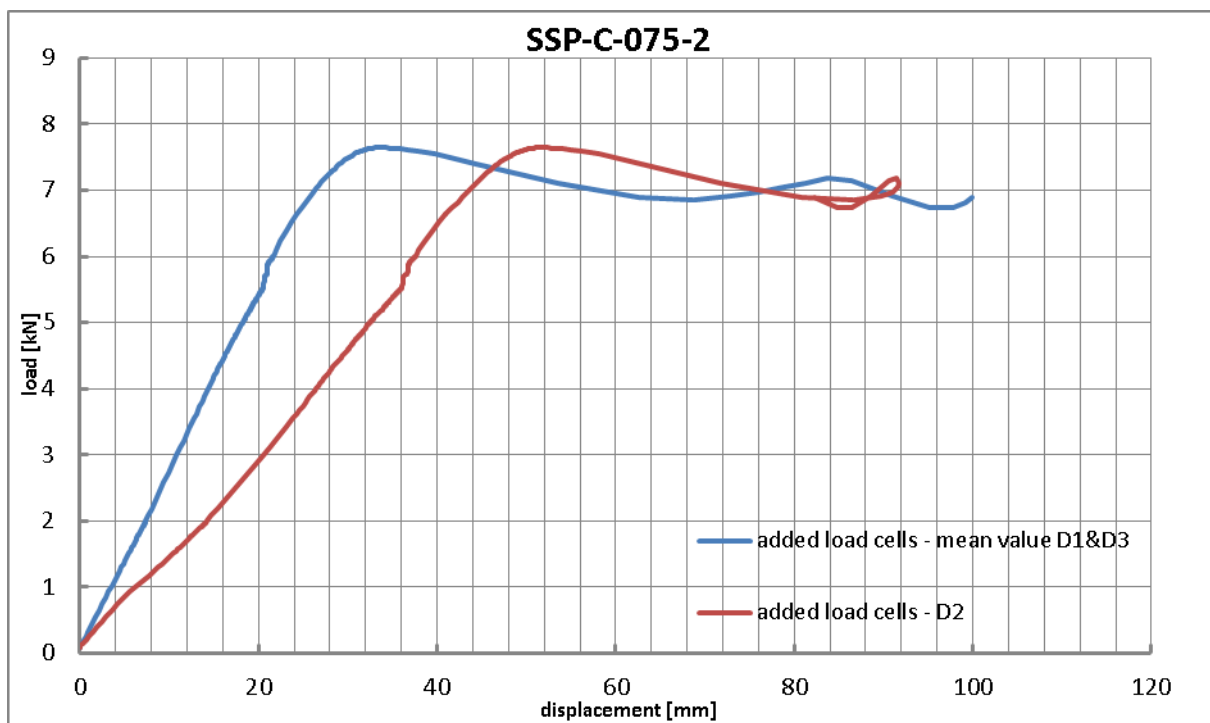
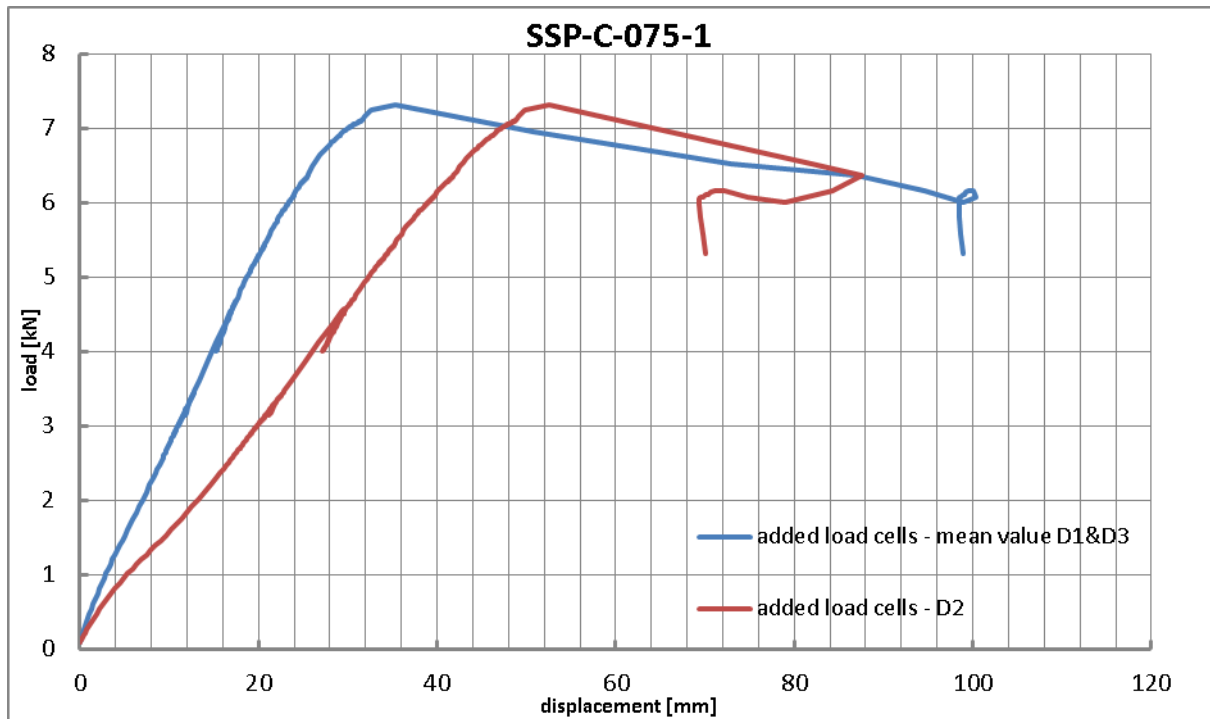


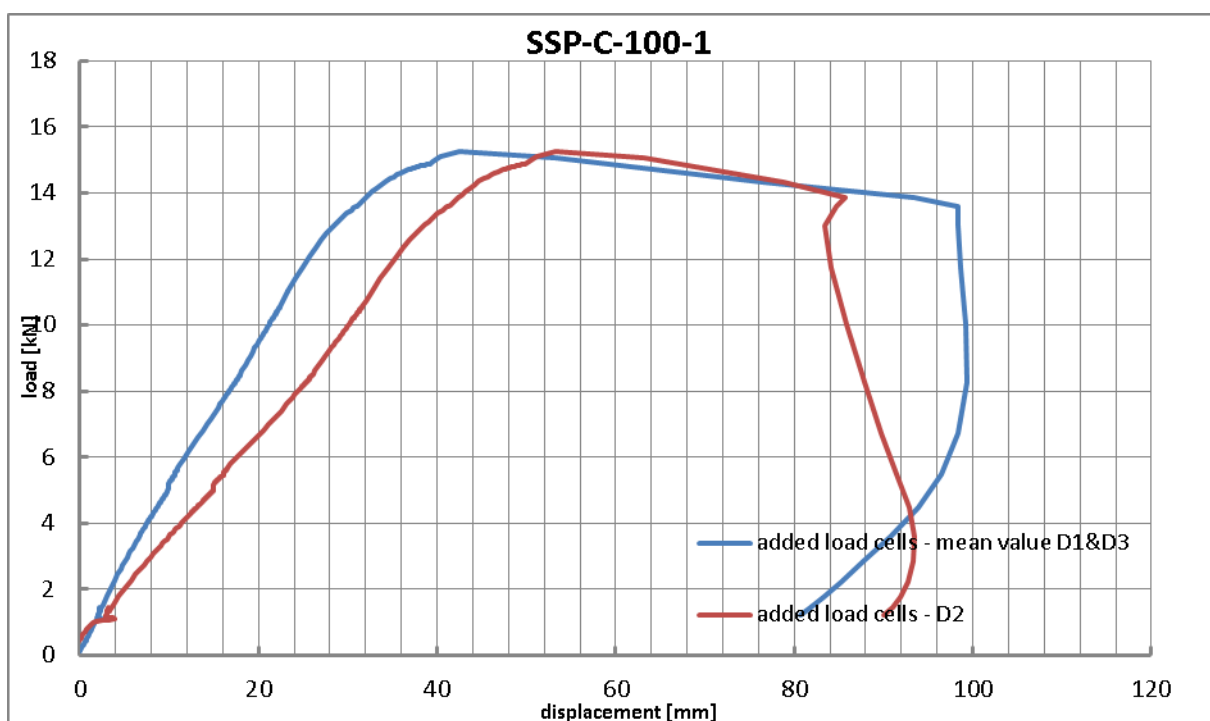
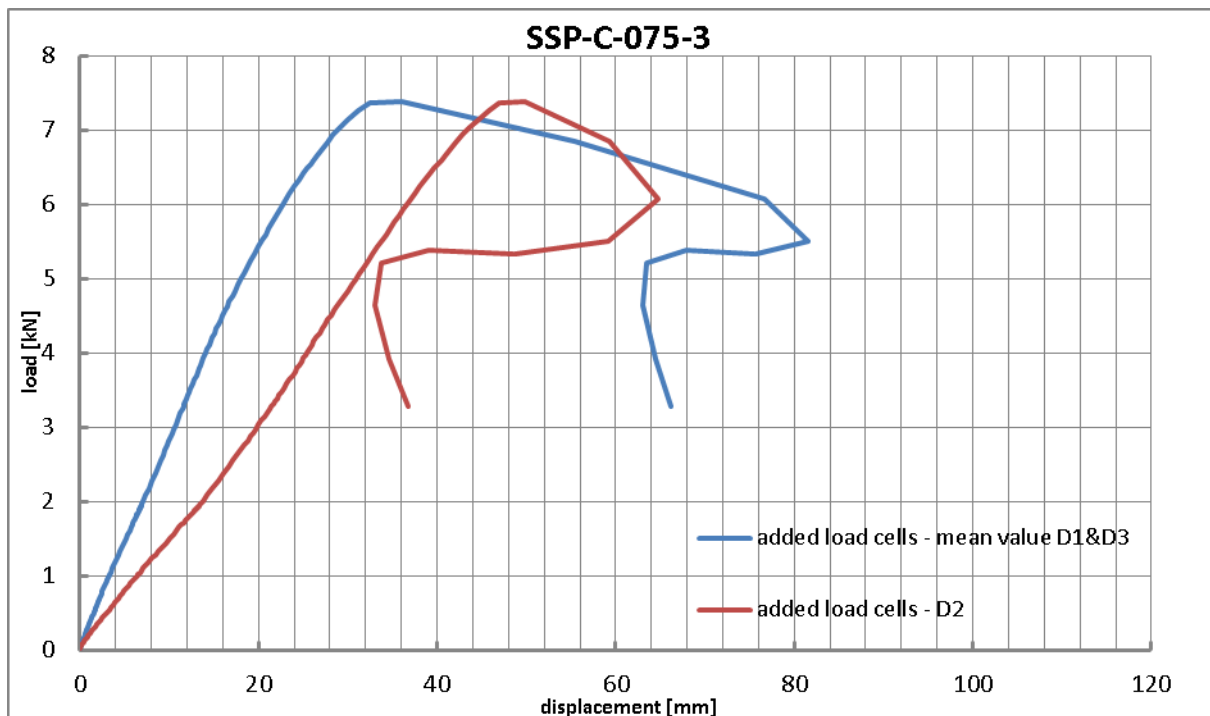
Fig. B.7: Failure mode (local buckling of the compressed flange, Zephyr $t_N = 1.00$ mm)

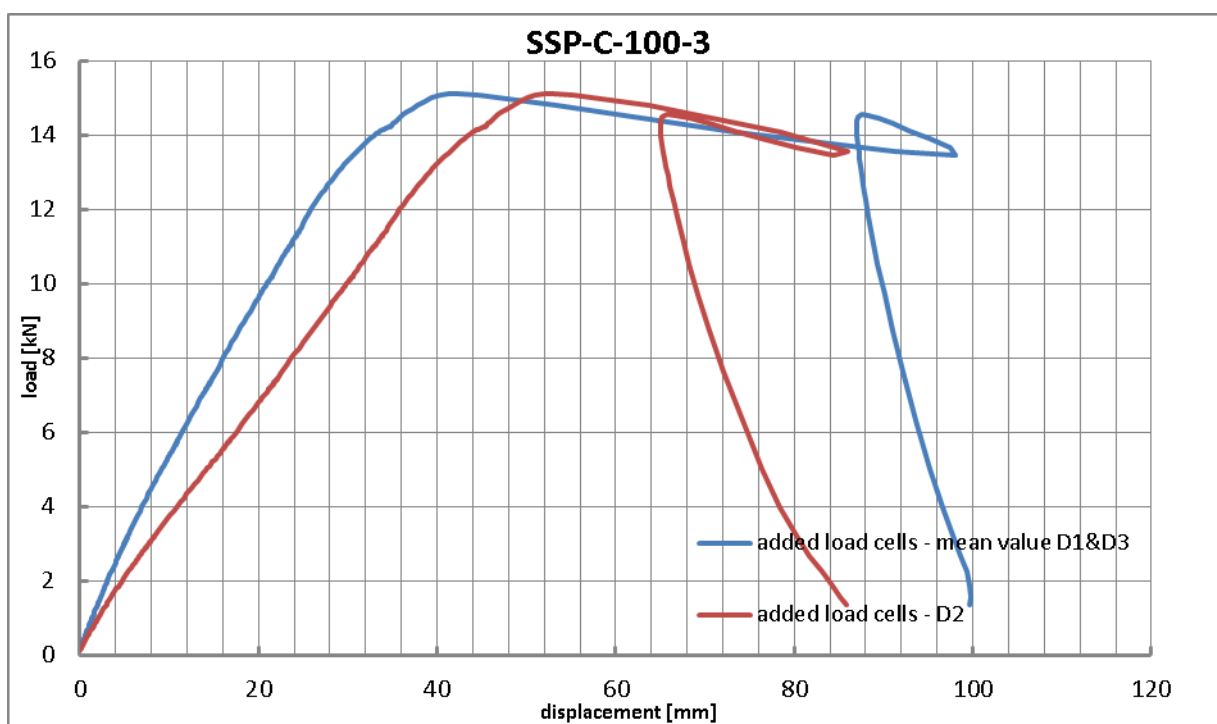
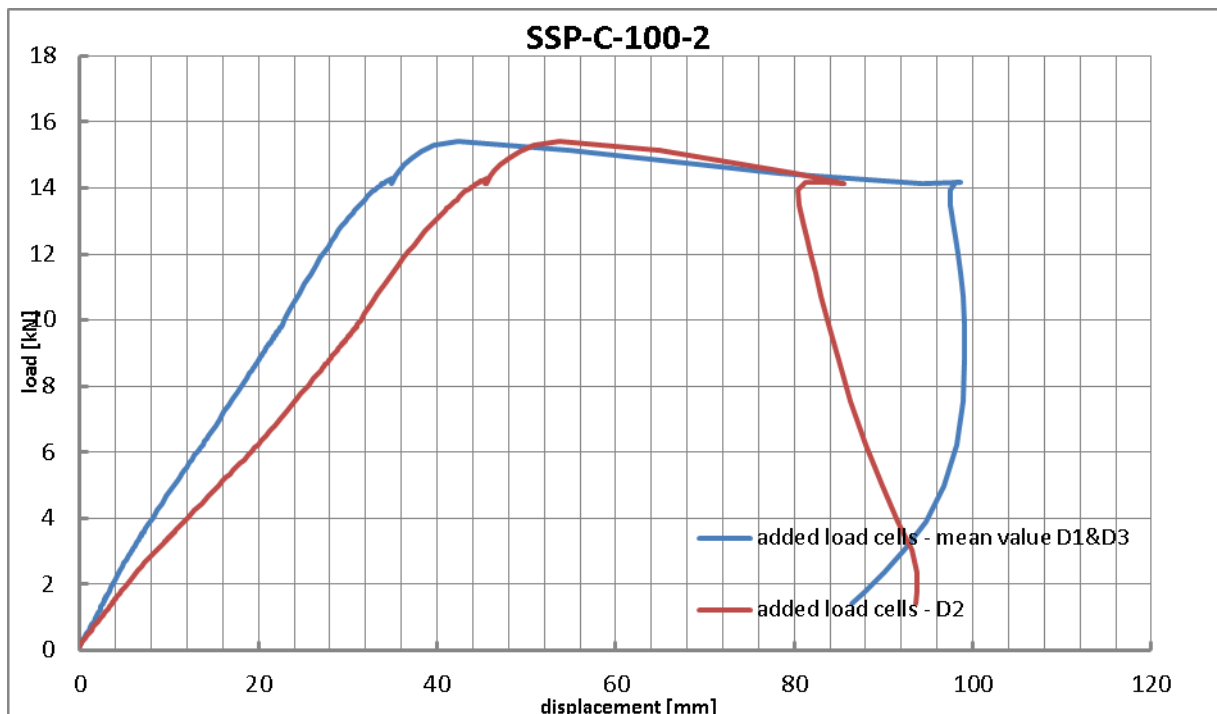


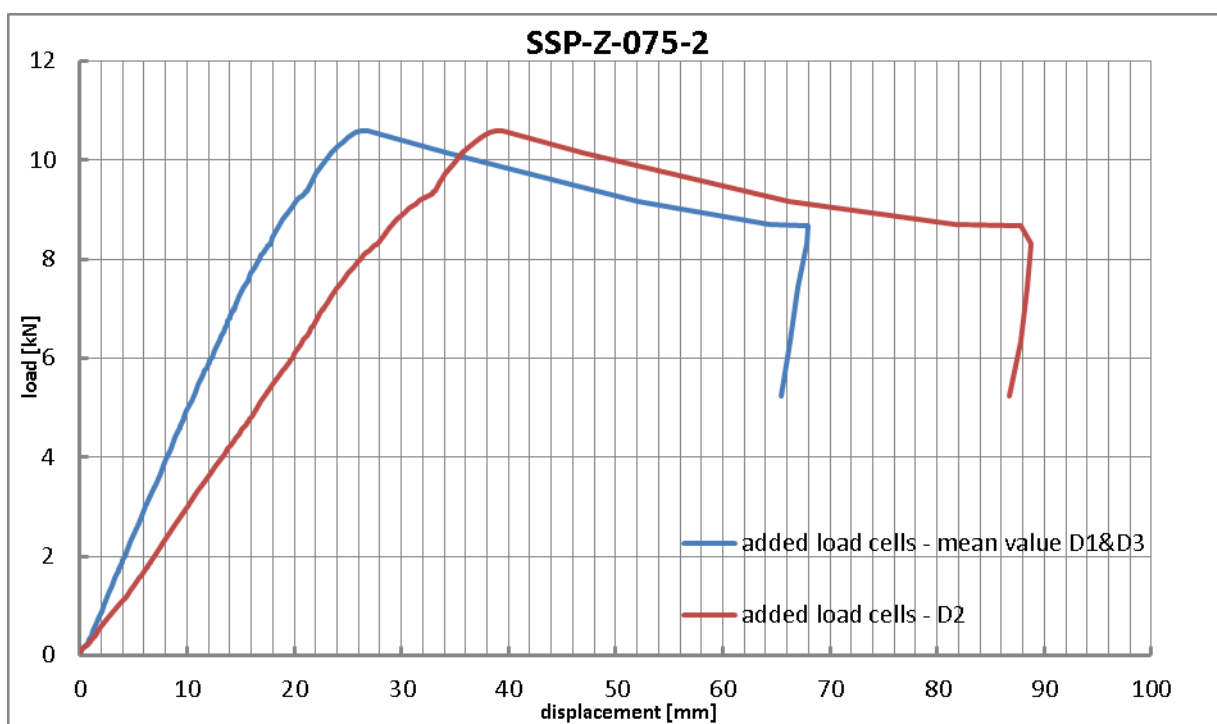
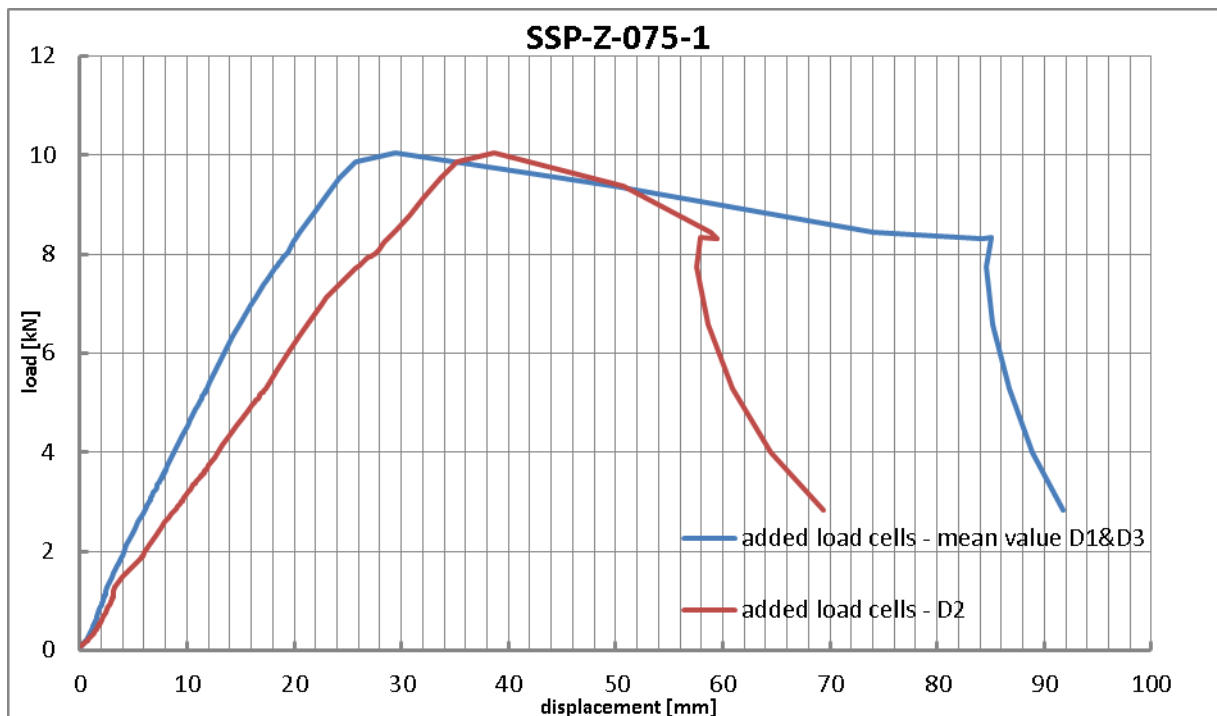
Fig. B.8: Failure mode (local buckling of the compressed flange, Zephyr $t_N = 1.00$ mm)

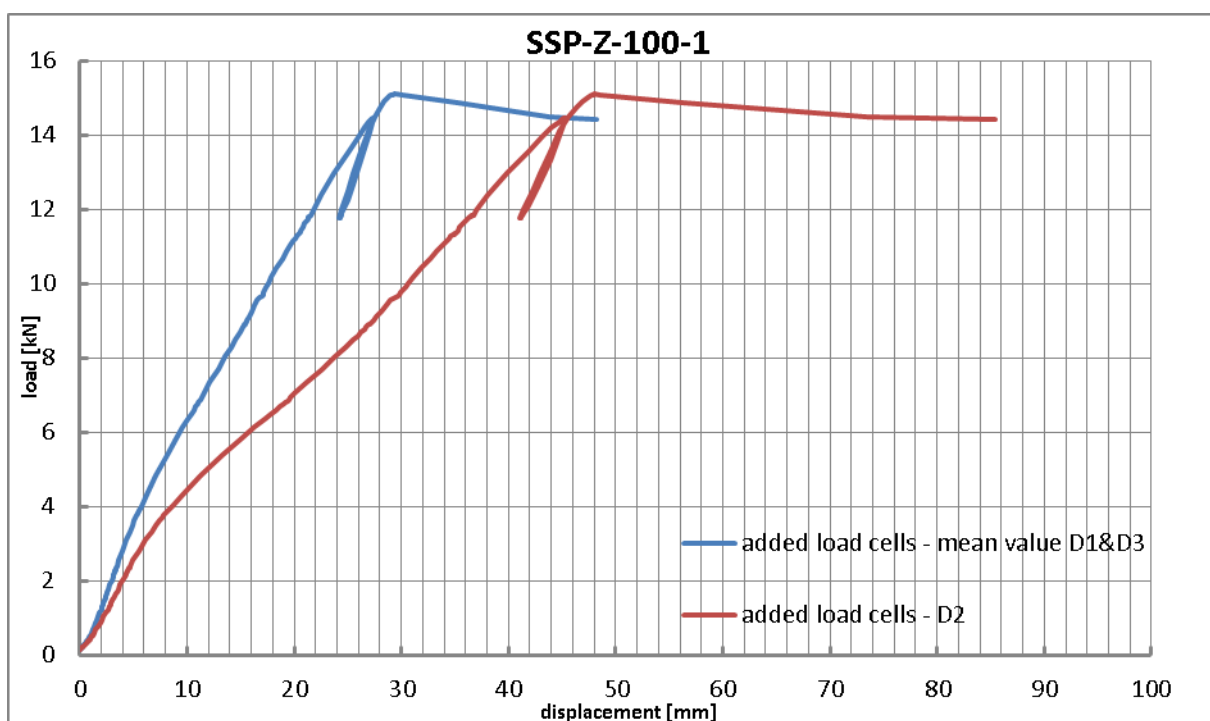
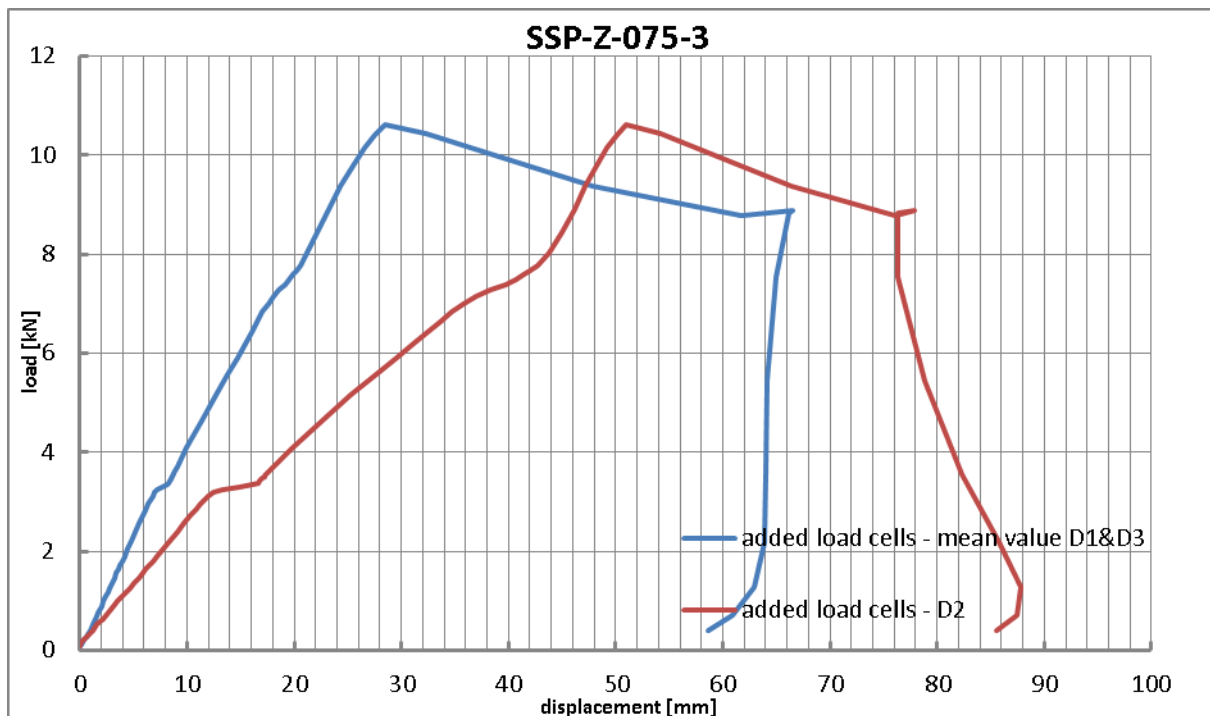
Load-deflection-curves:

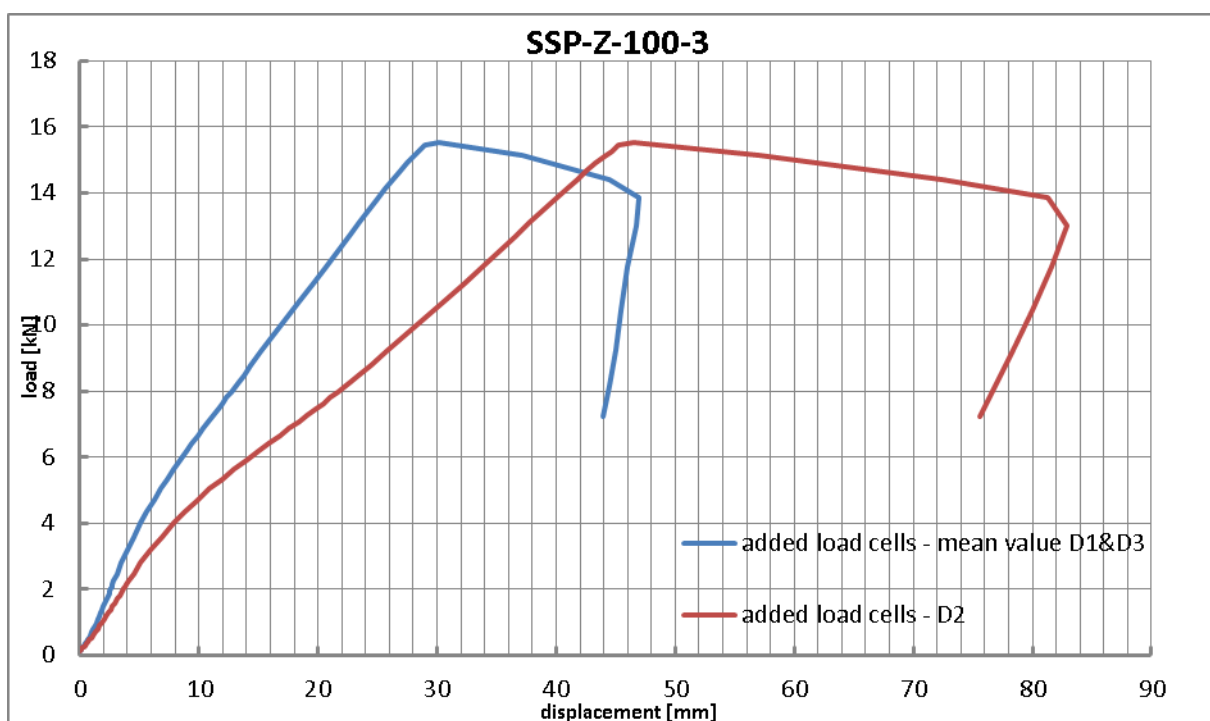
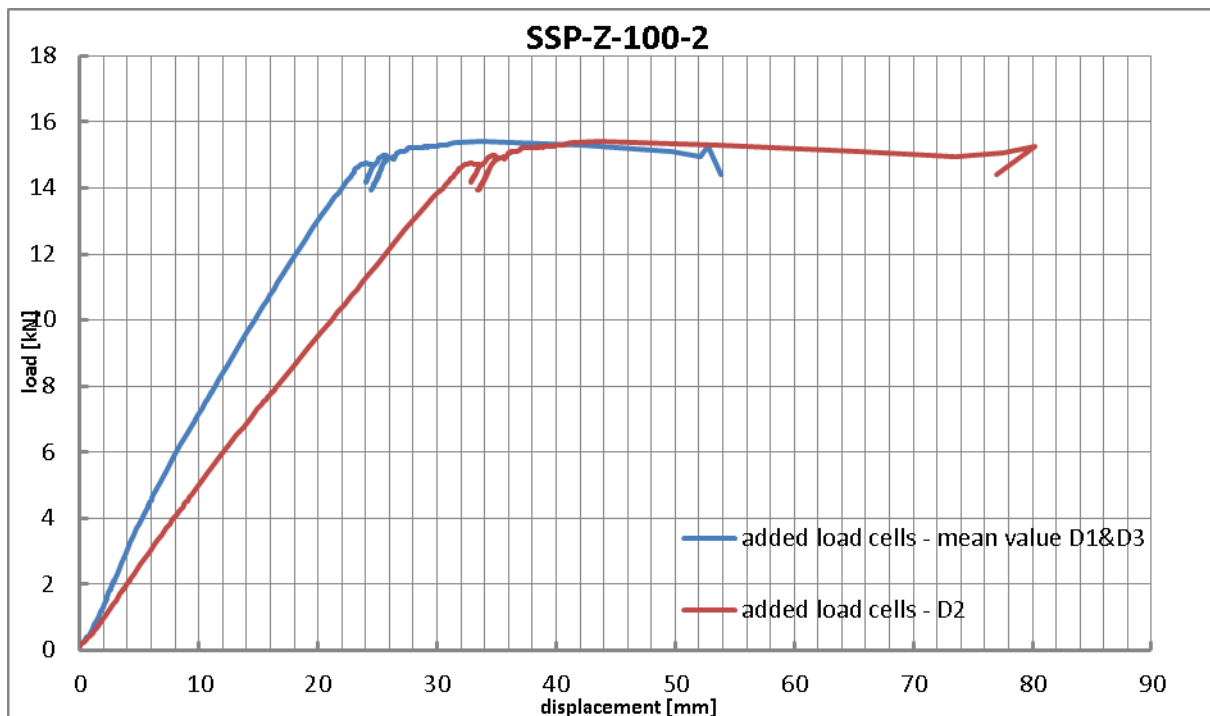


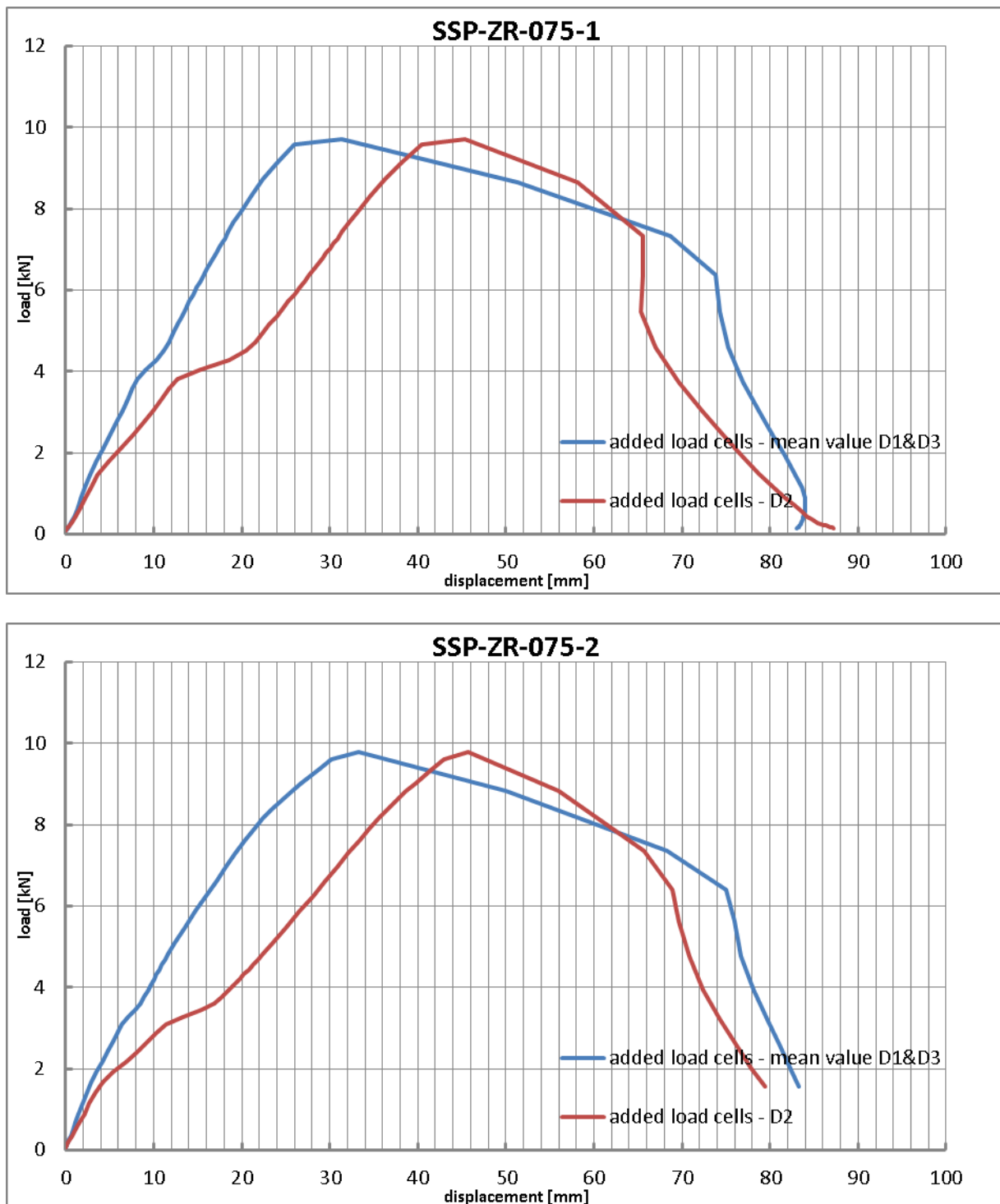


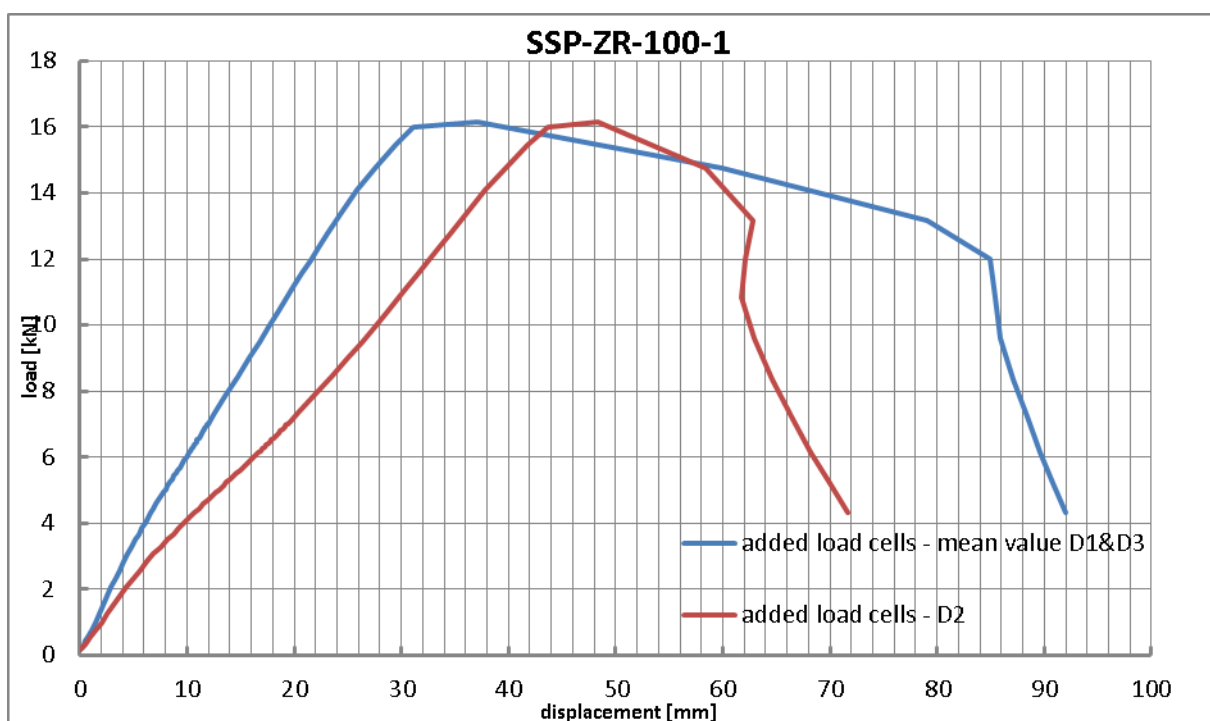
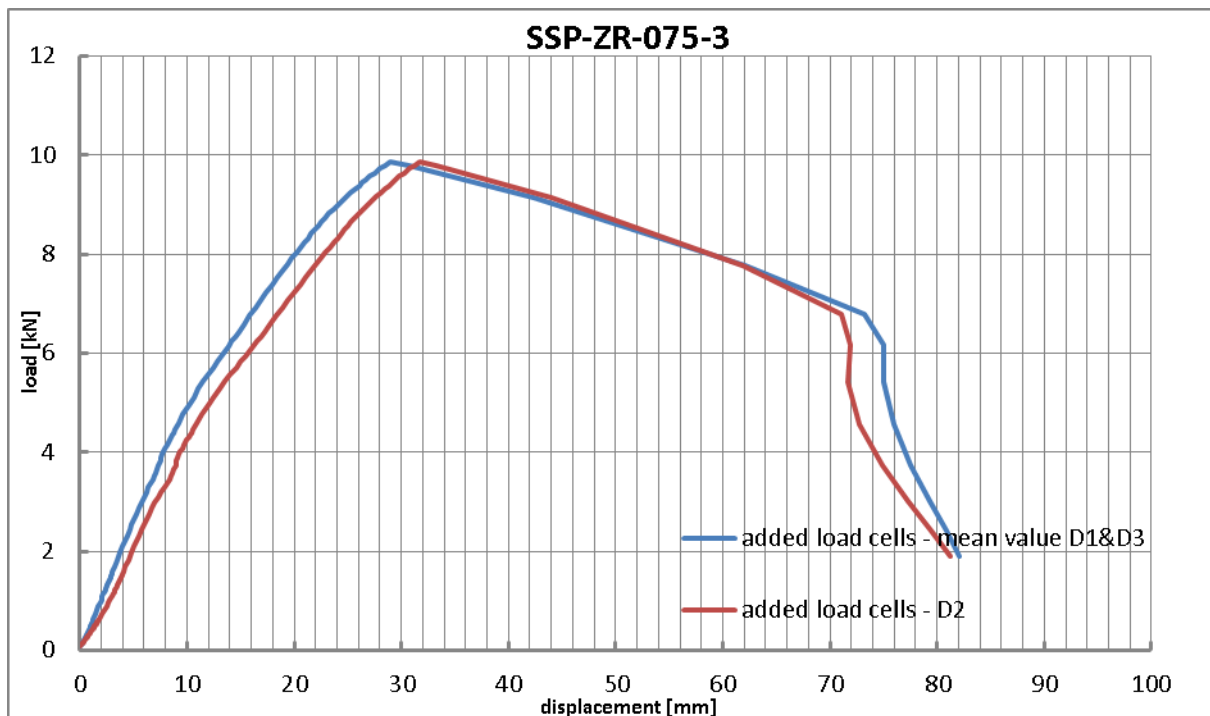


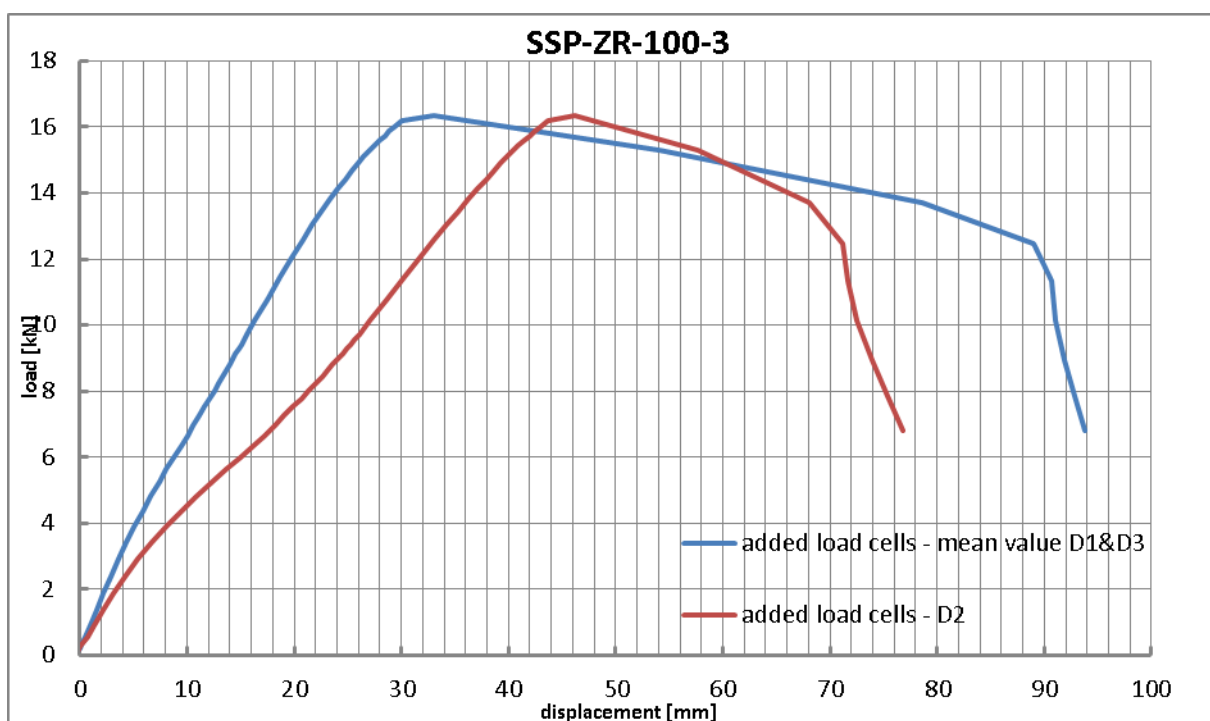
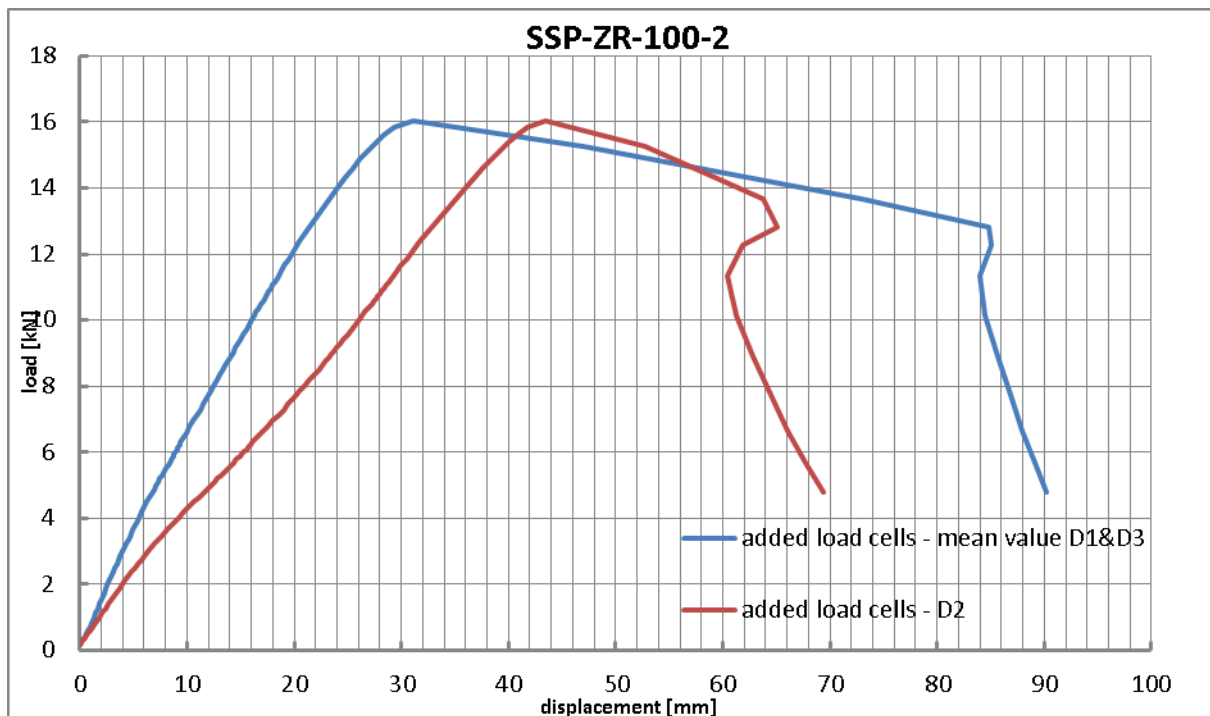












3 Annex C: Single span negative bending test (suction tests)

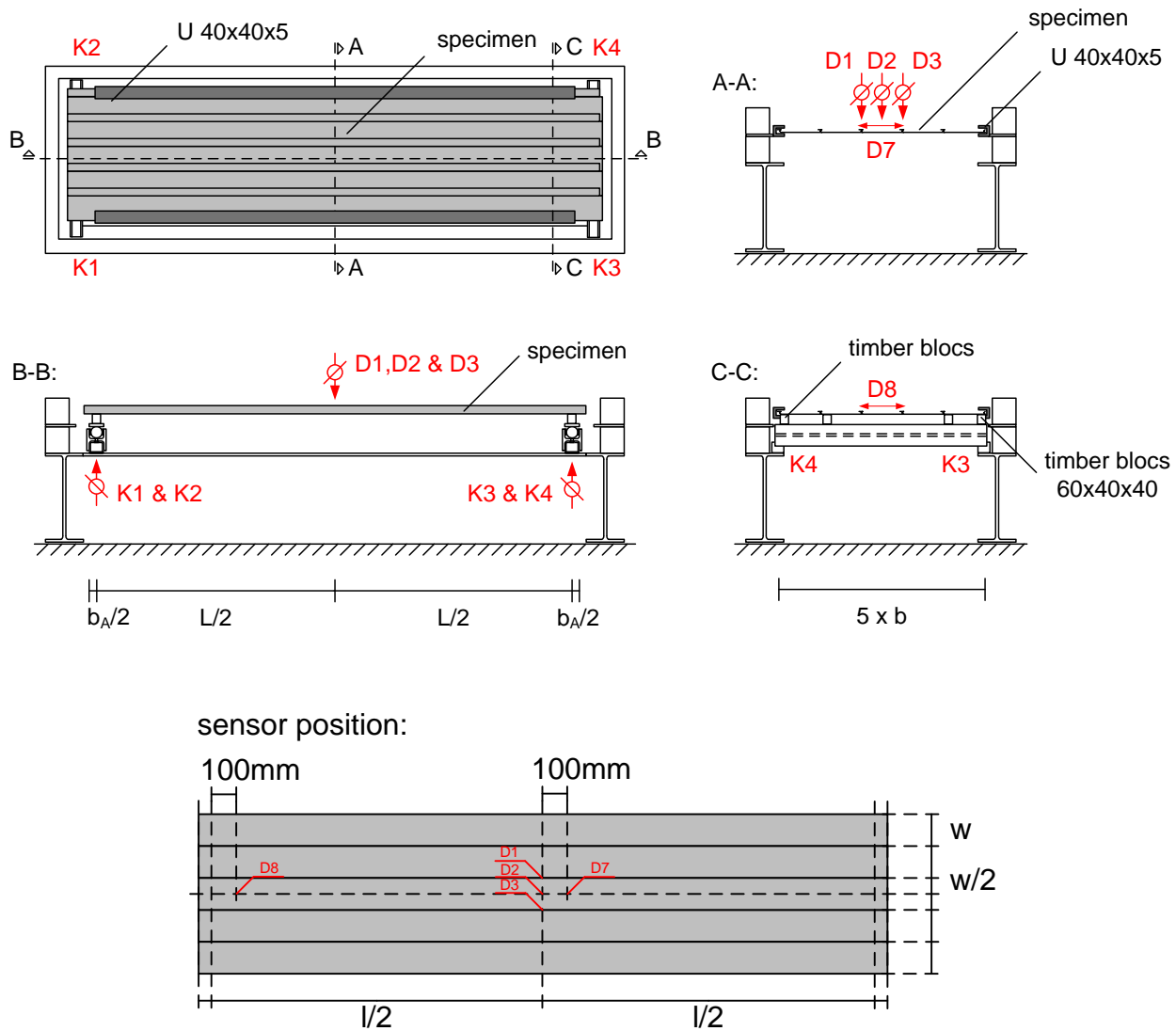


Fig. C.1: Schematic test setup



Fig. C.2: Test setup



Fig. C.3: Failure mode (local buckling of the compressed flanges) of SSN-Z-075-3

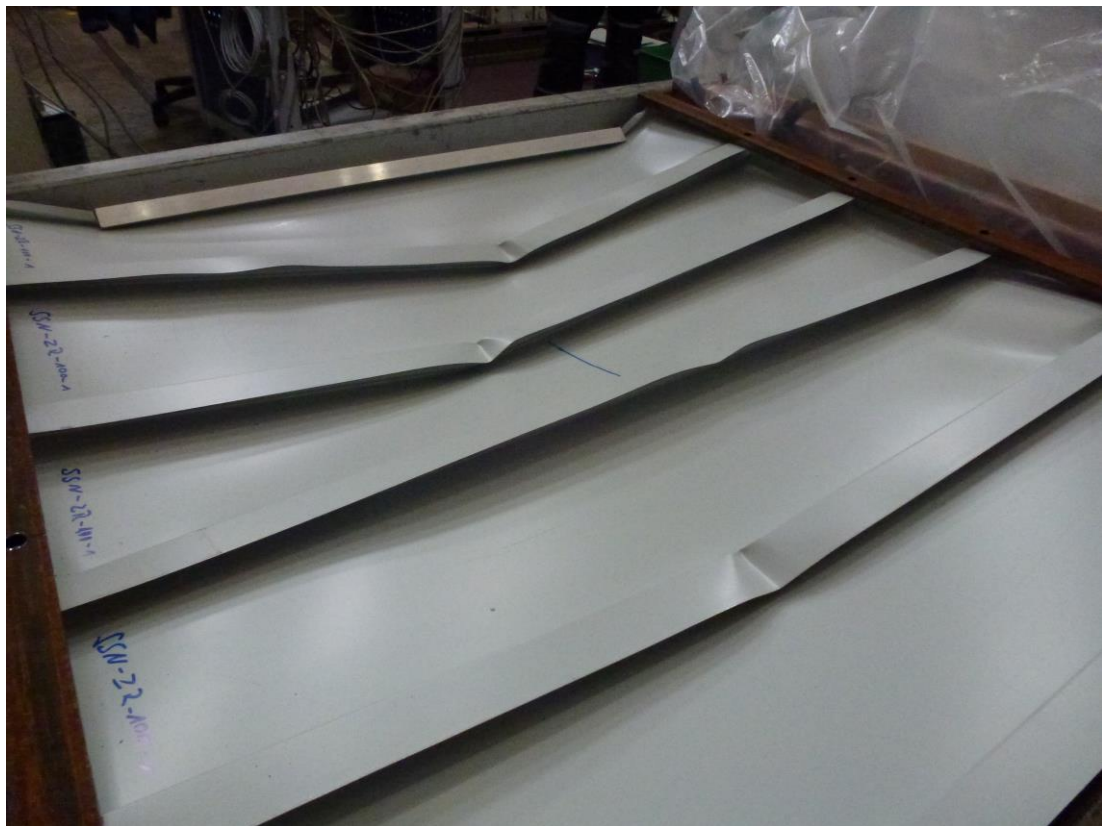


Fig. C.4: Failure mode (local buckling of the compressed flanges) of SSN-ZR-100-1

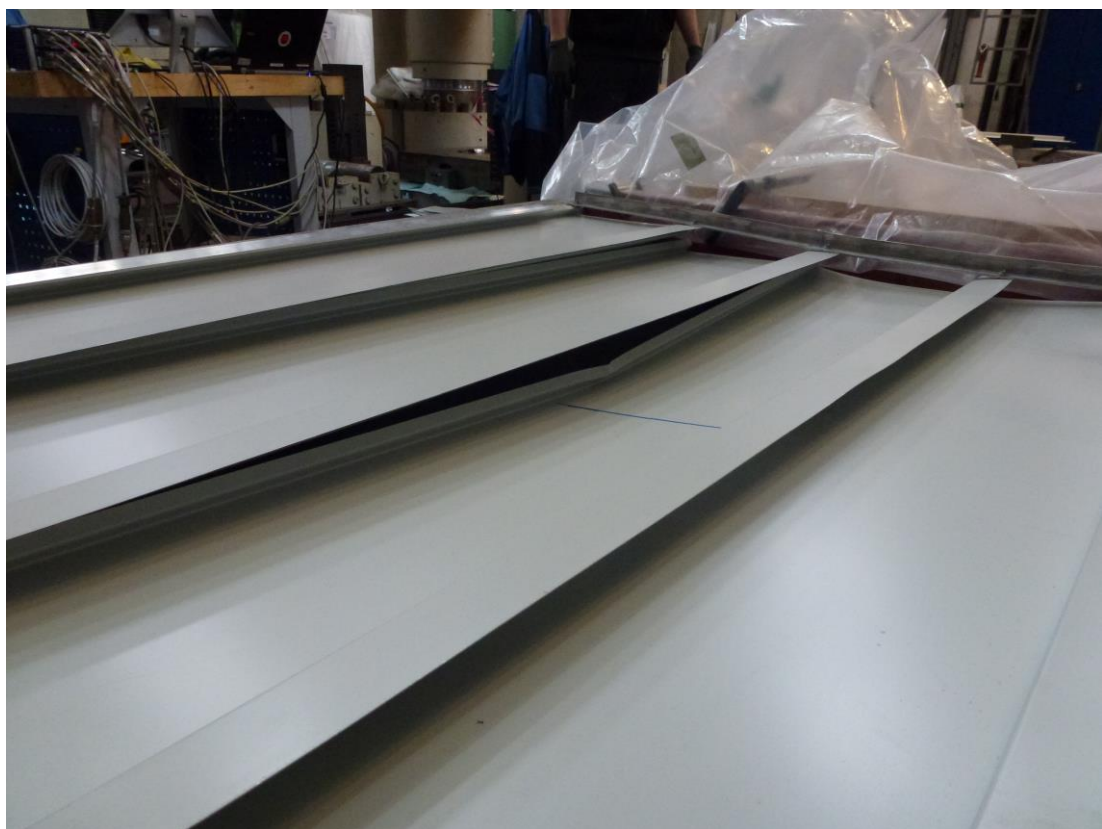
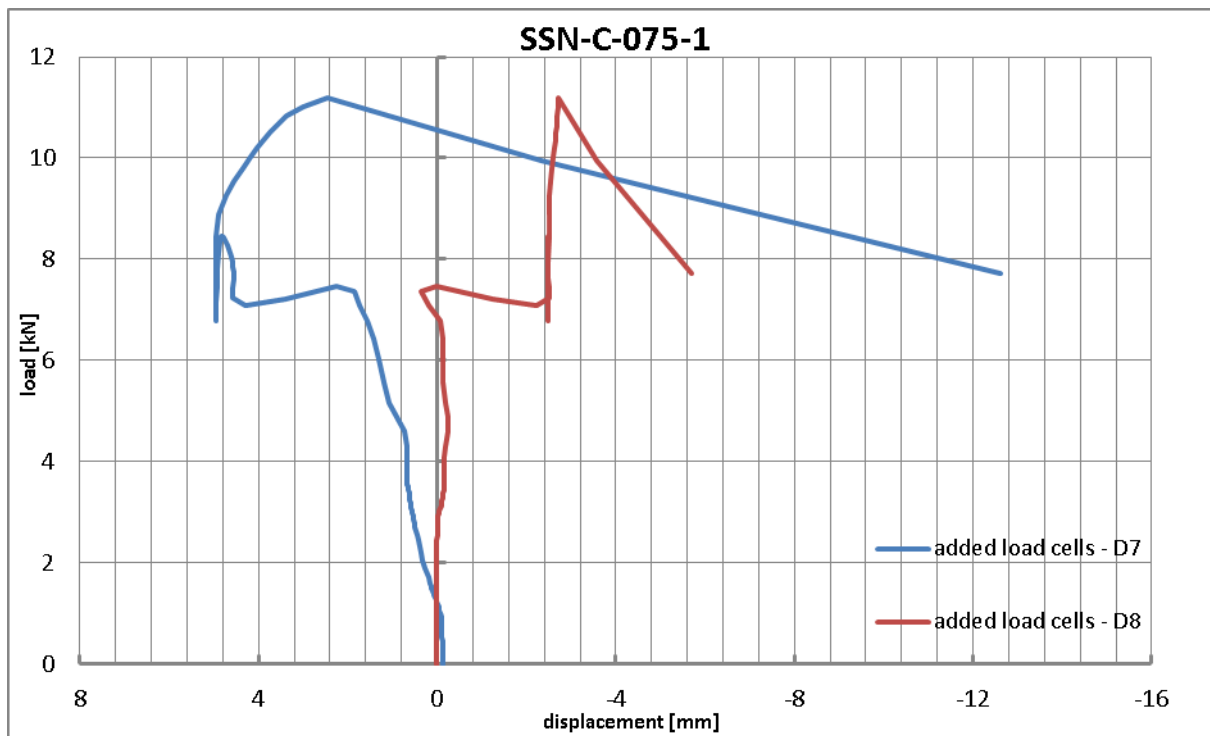
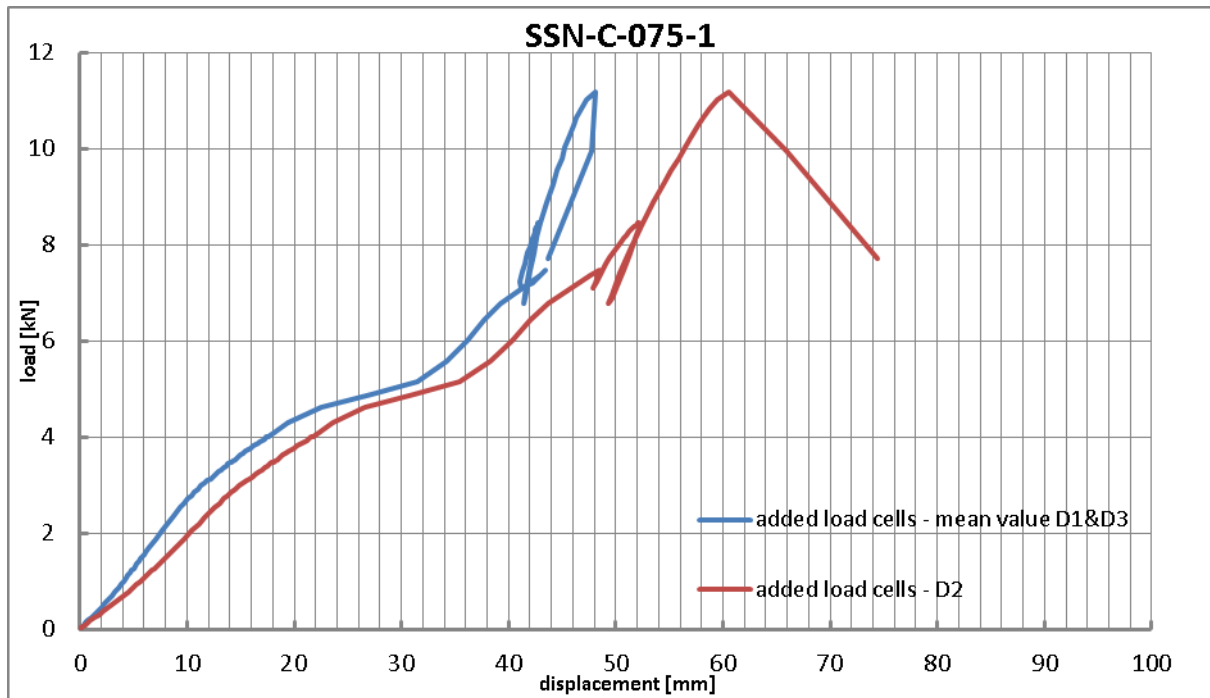


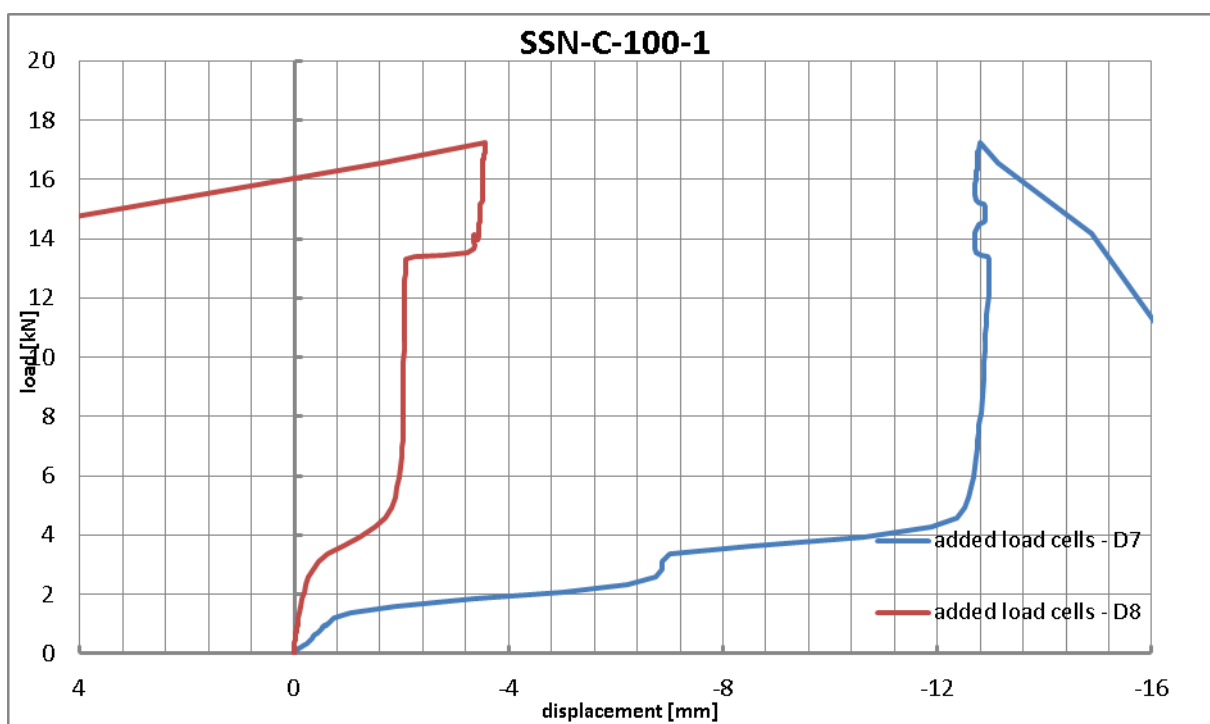
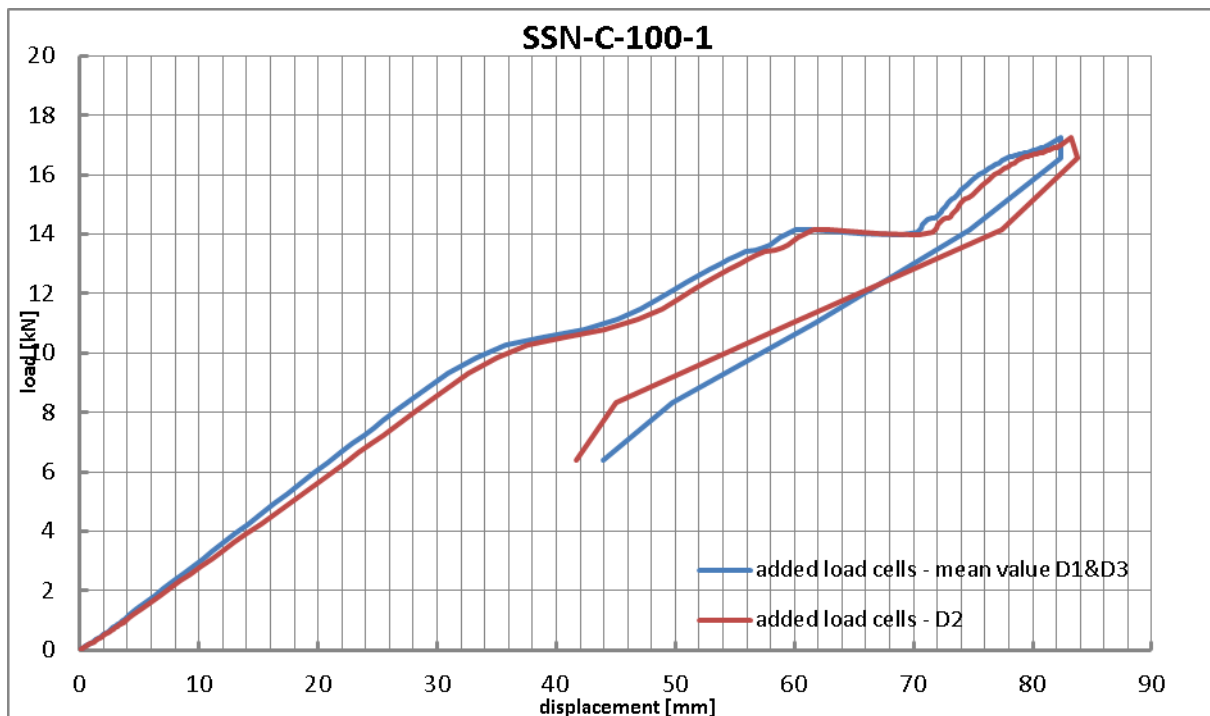
Fig. C.5: Failure mode (dislocation) of SSN-Z-100-2

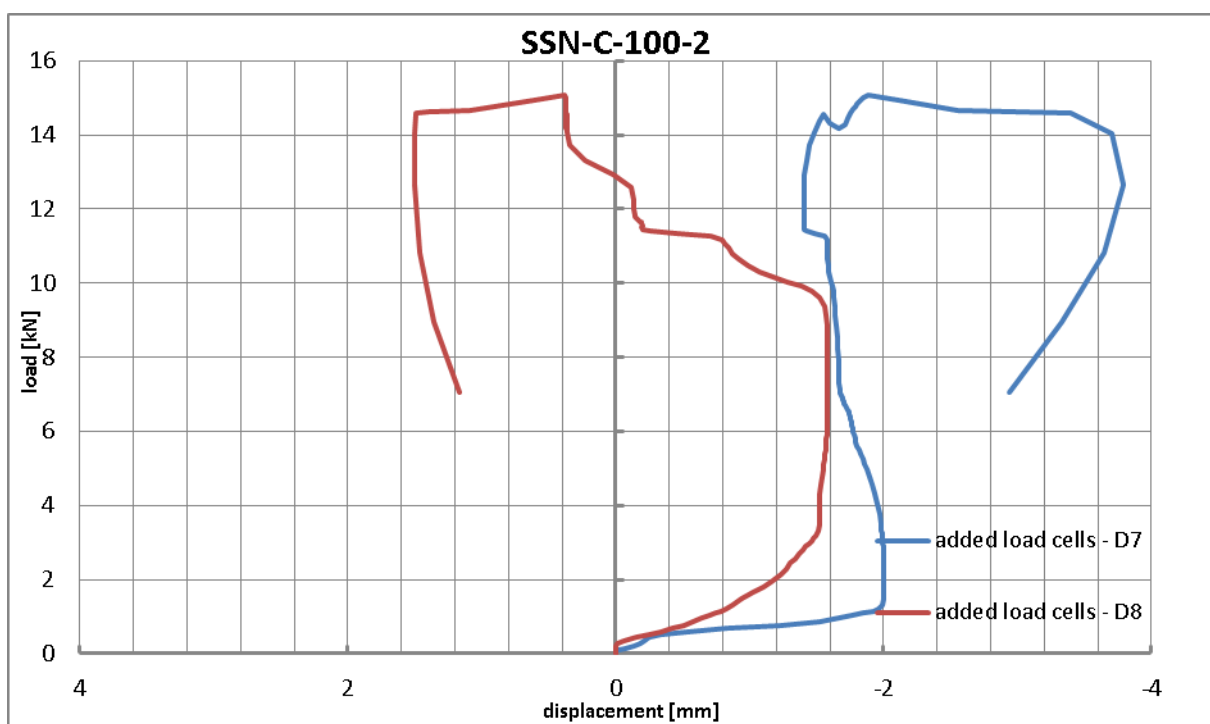
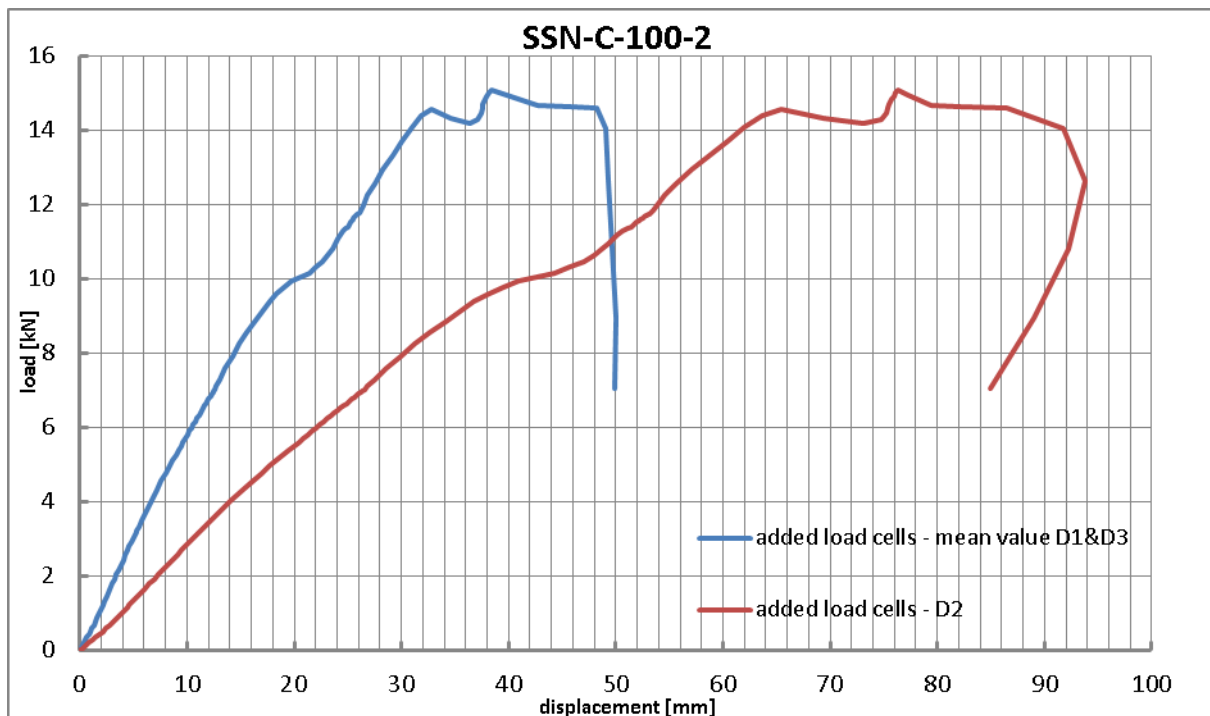


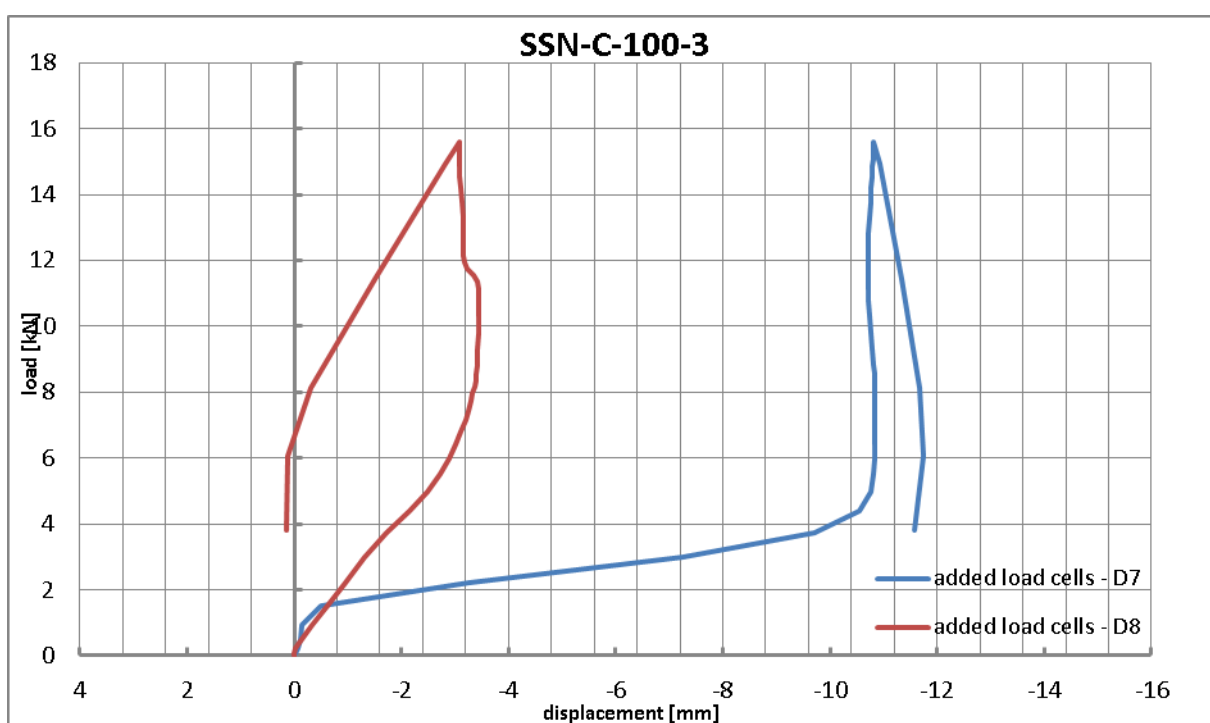
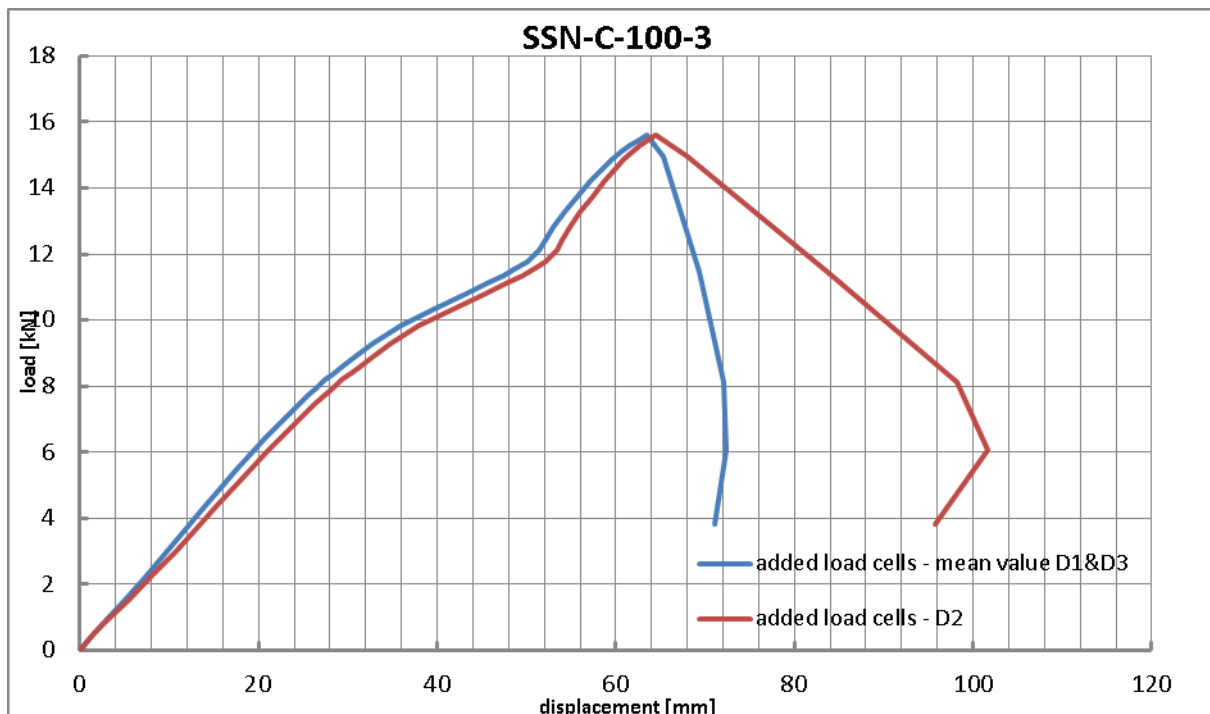
Fig. C.6: Failure mode (local buckling of the compressed flanges) of SSN-C-100-3

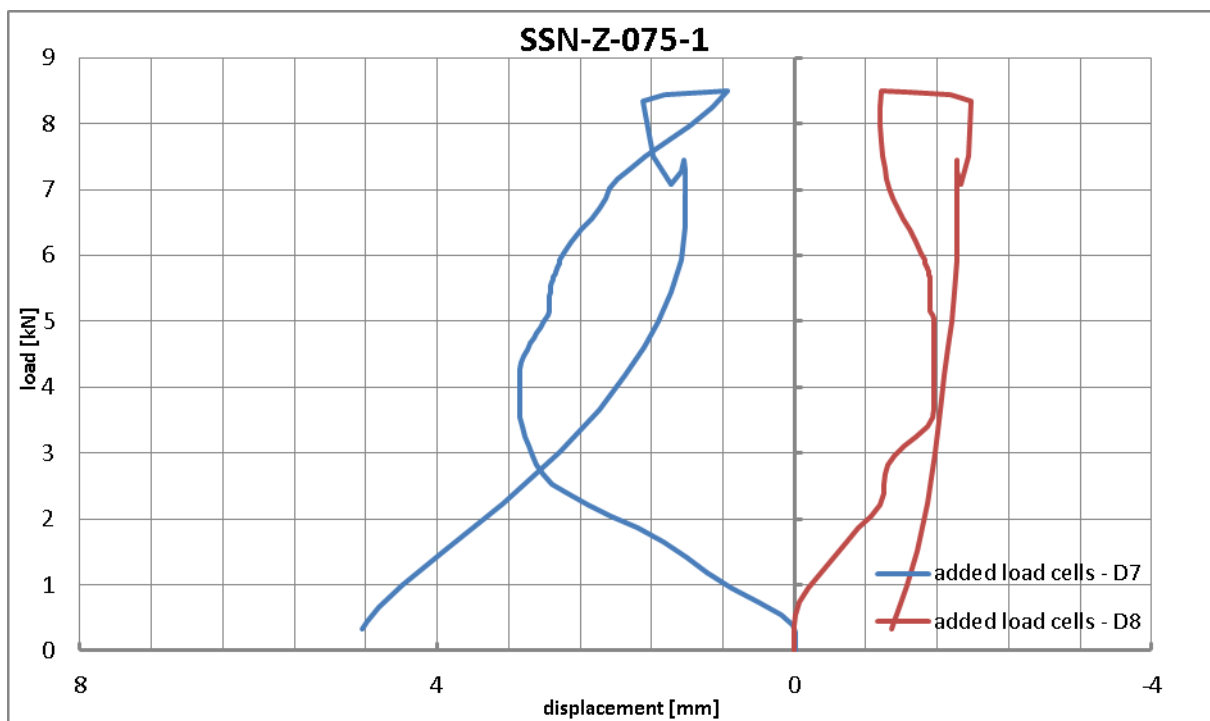
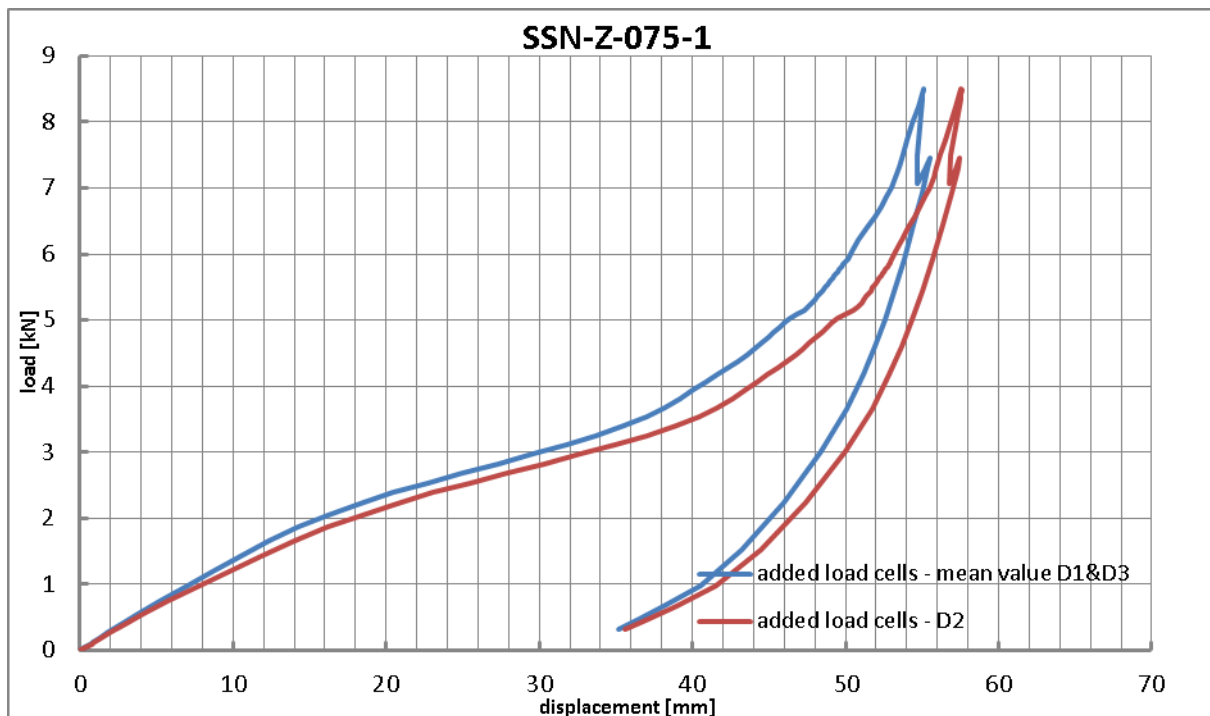
Load-deflection-curves:

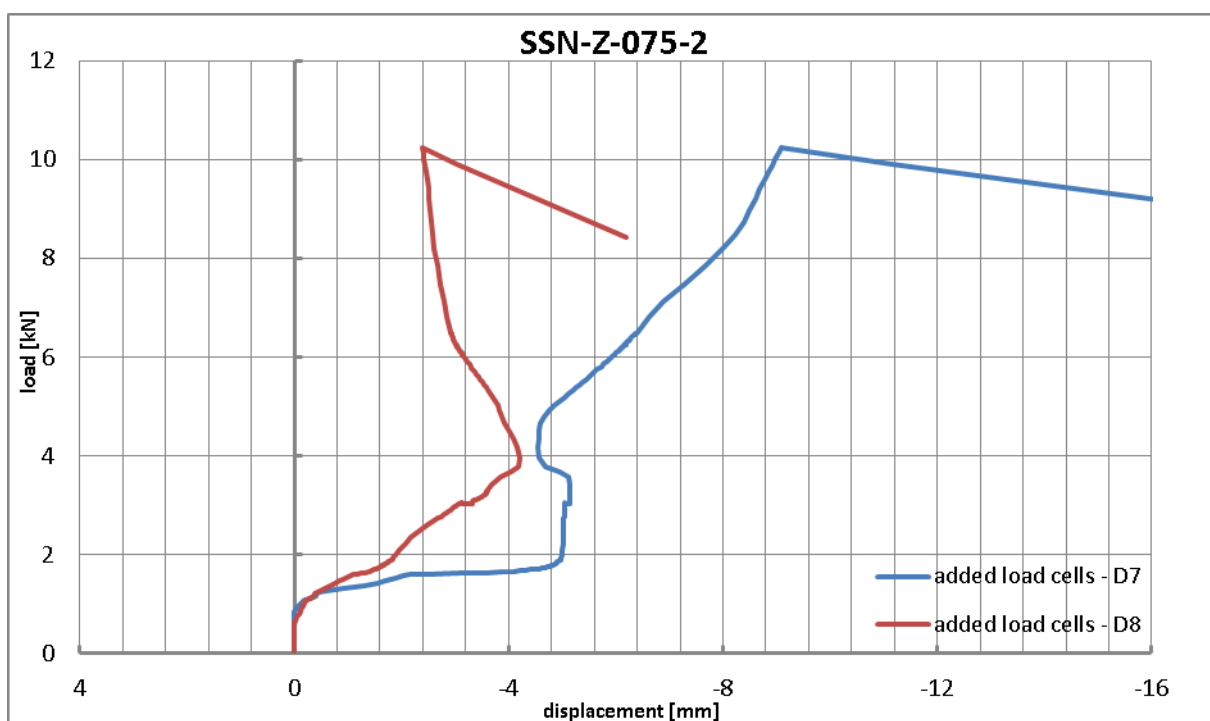
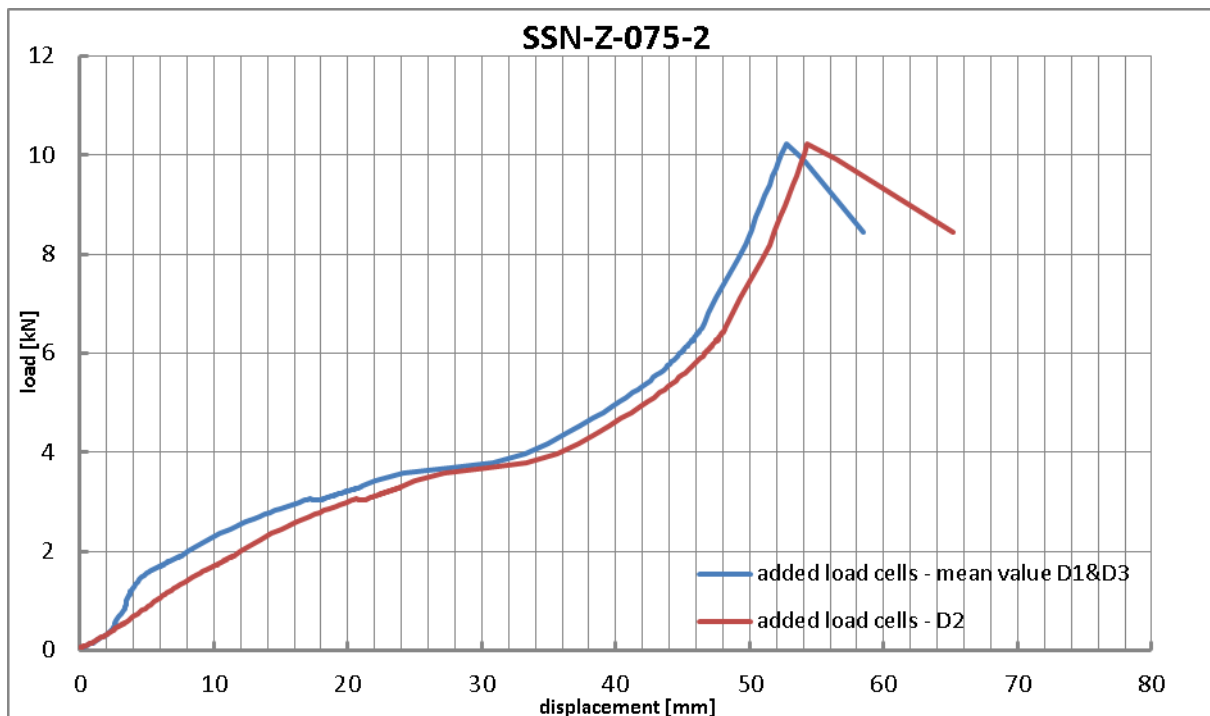


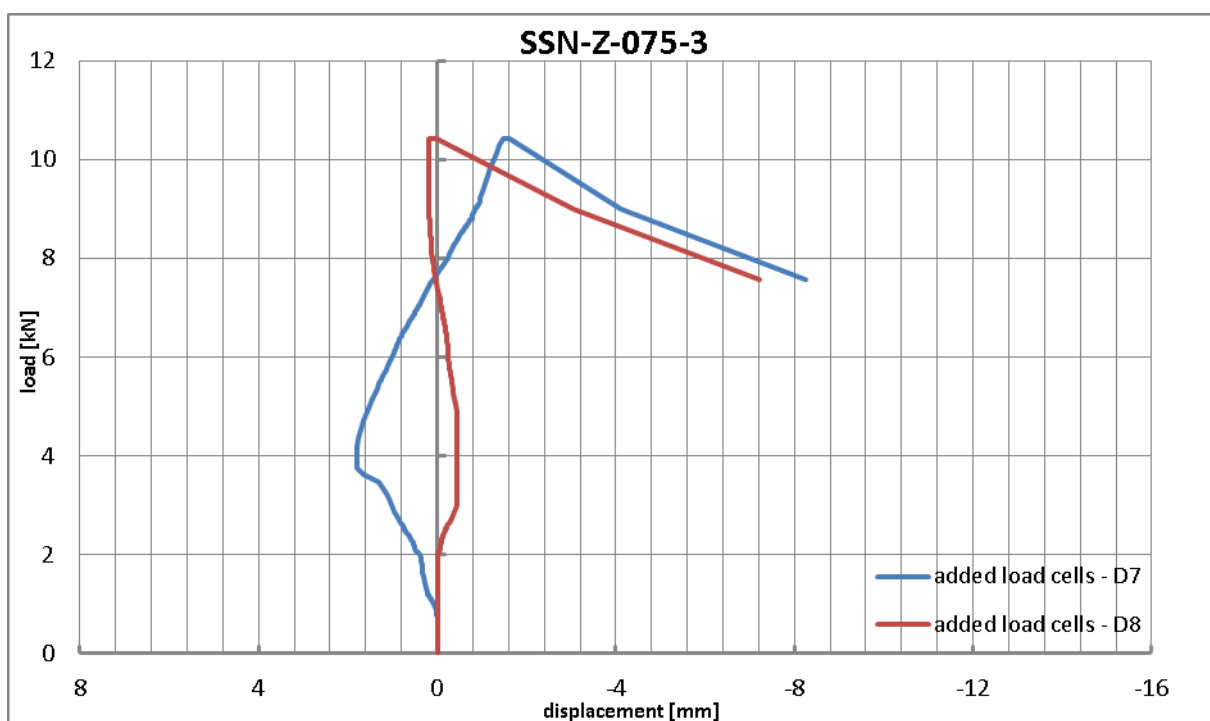
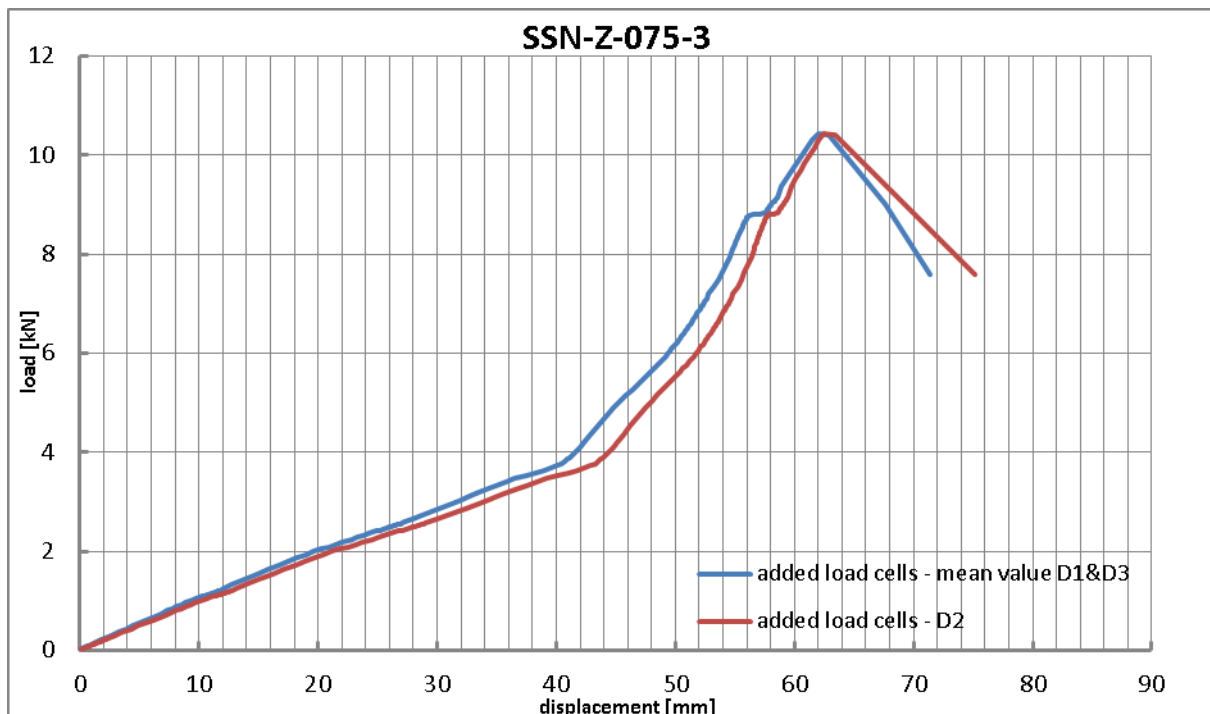


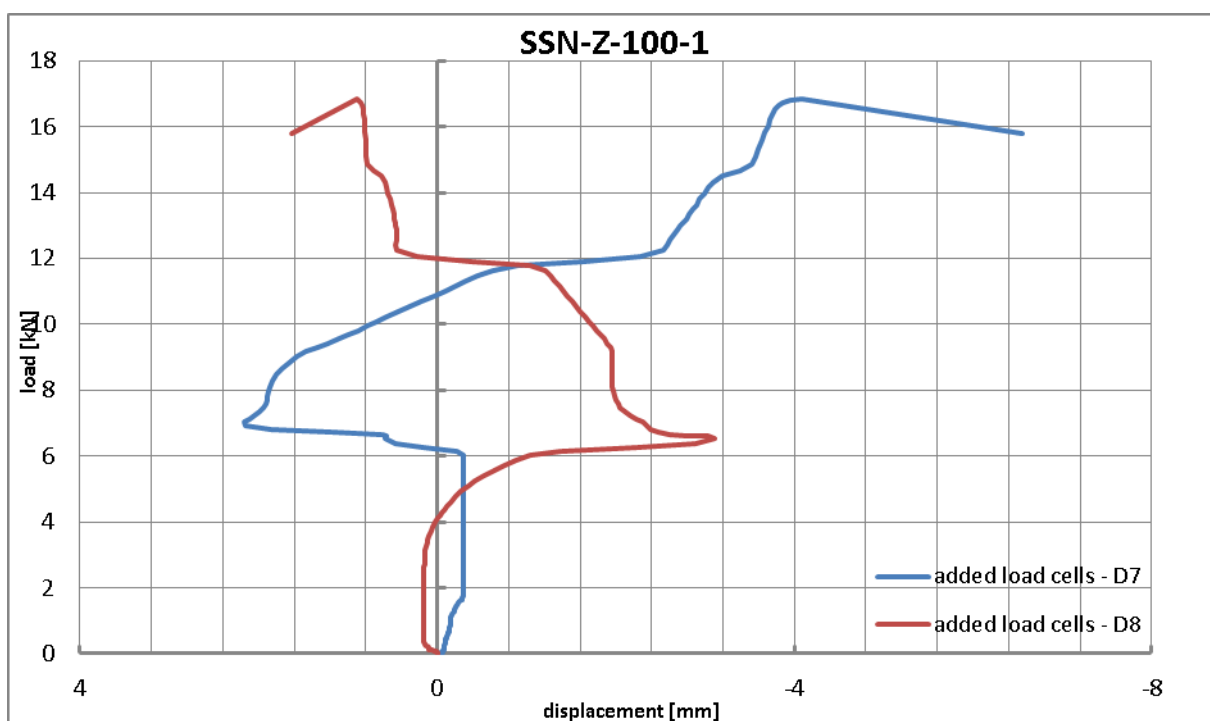
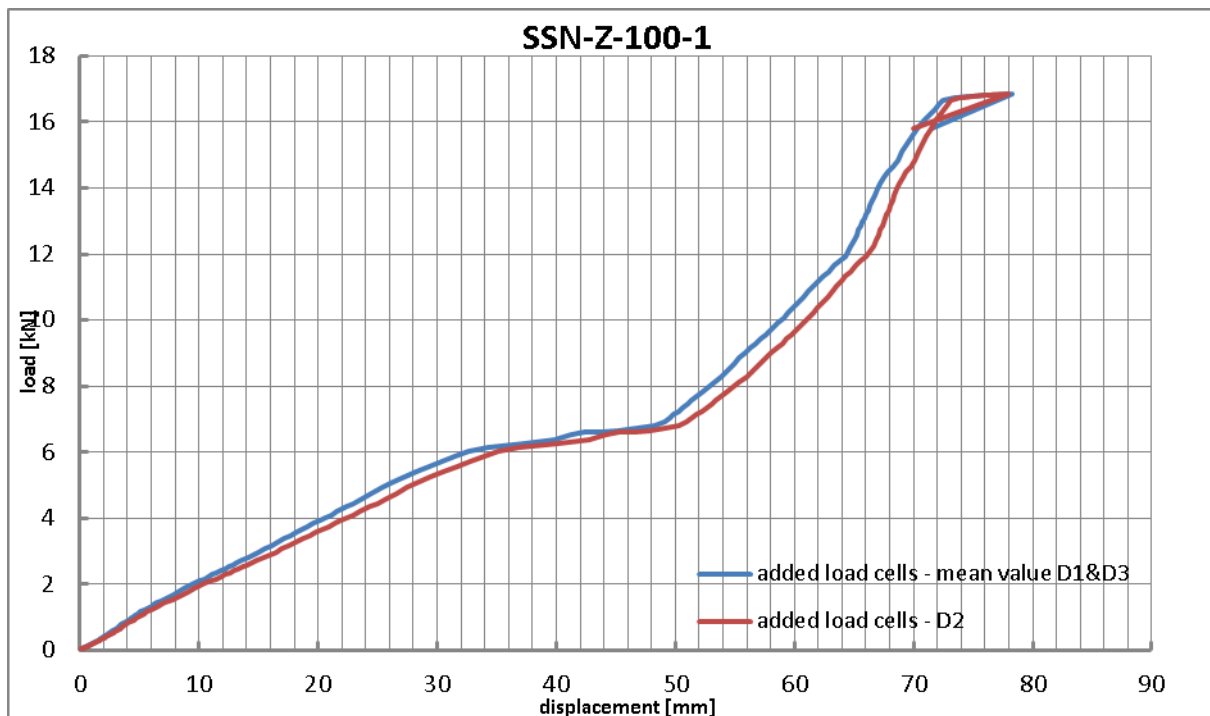


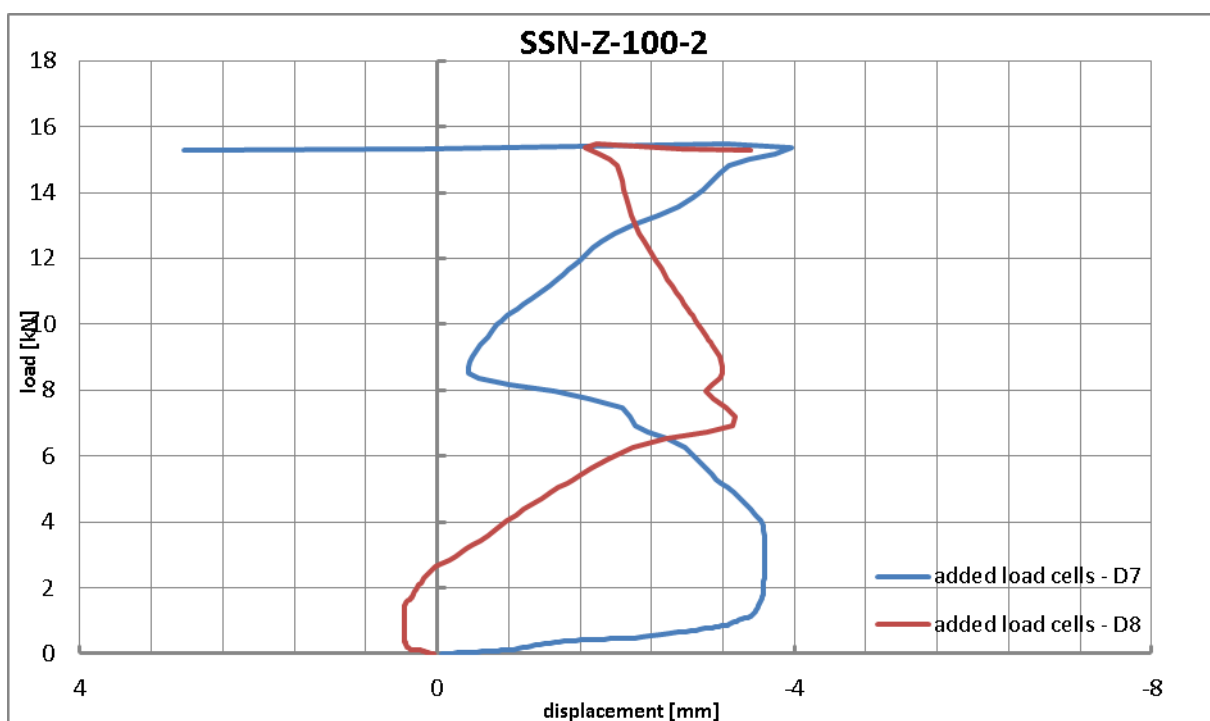
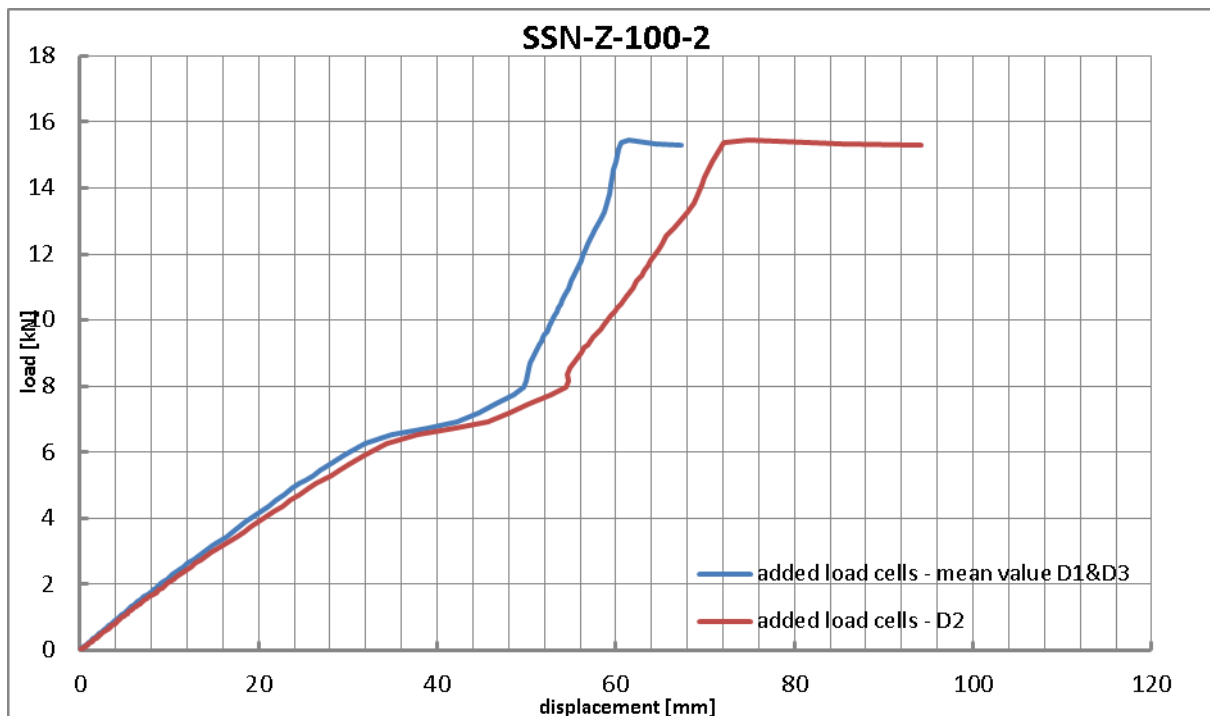


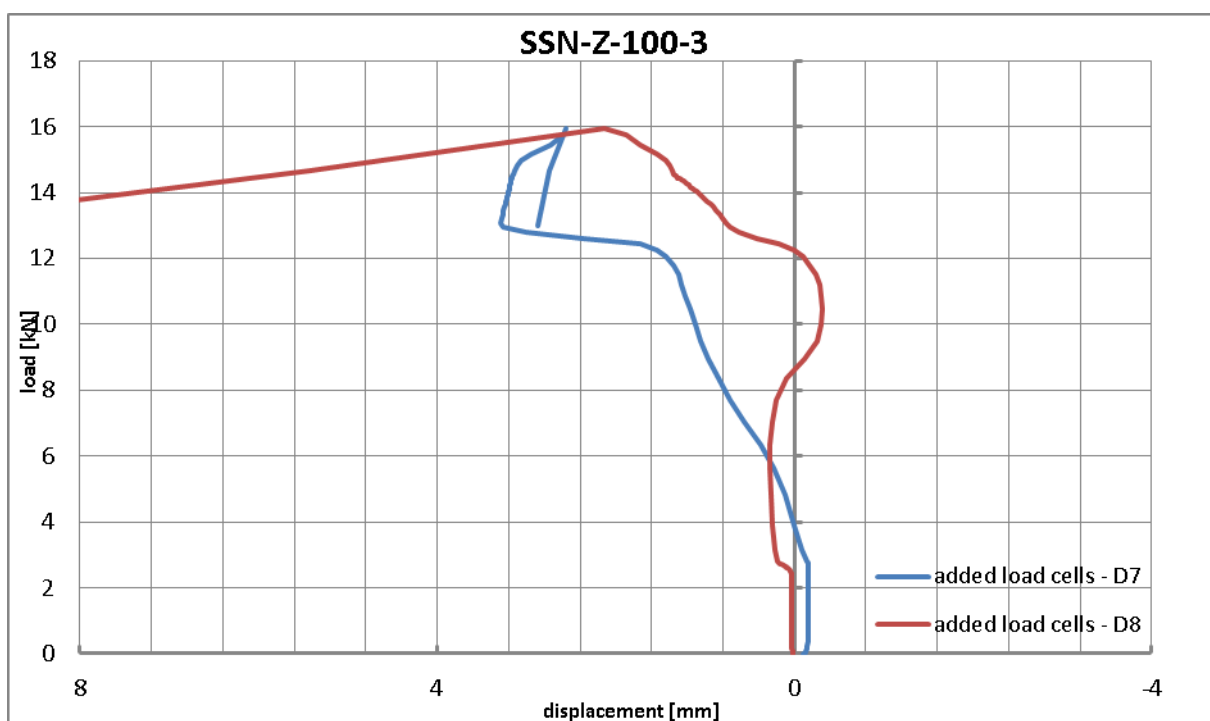
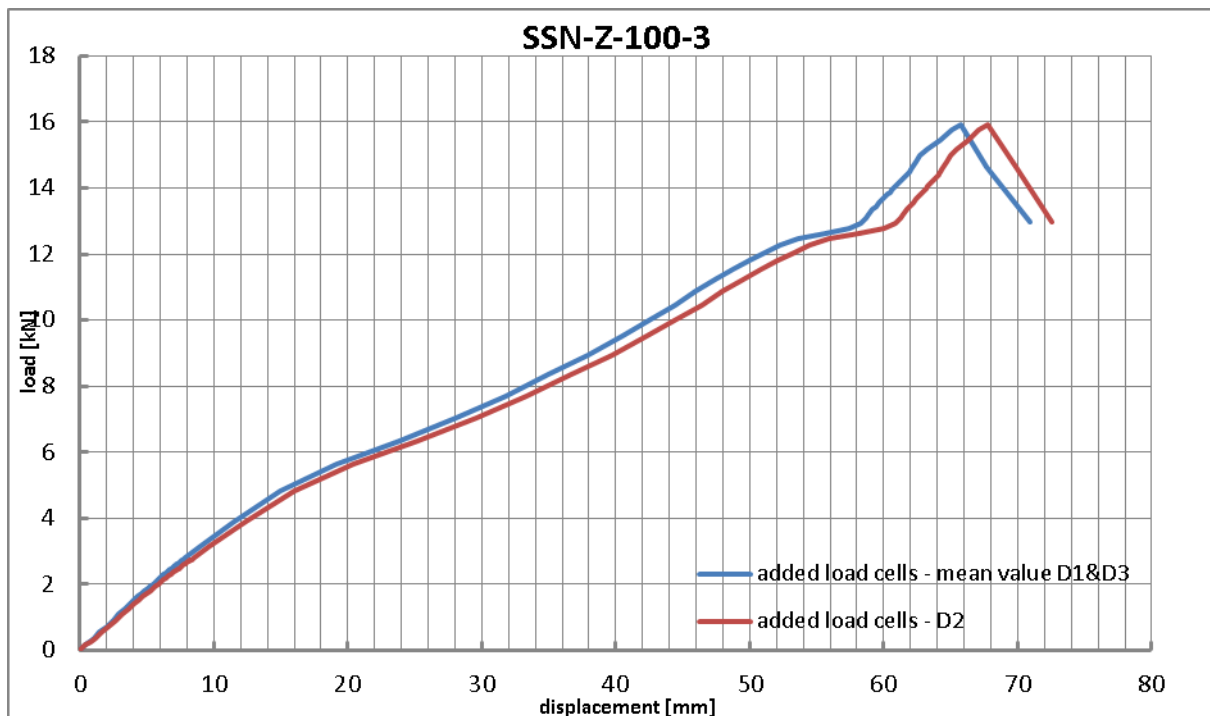


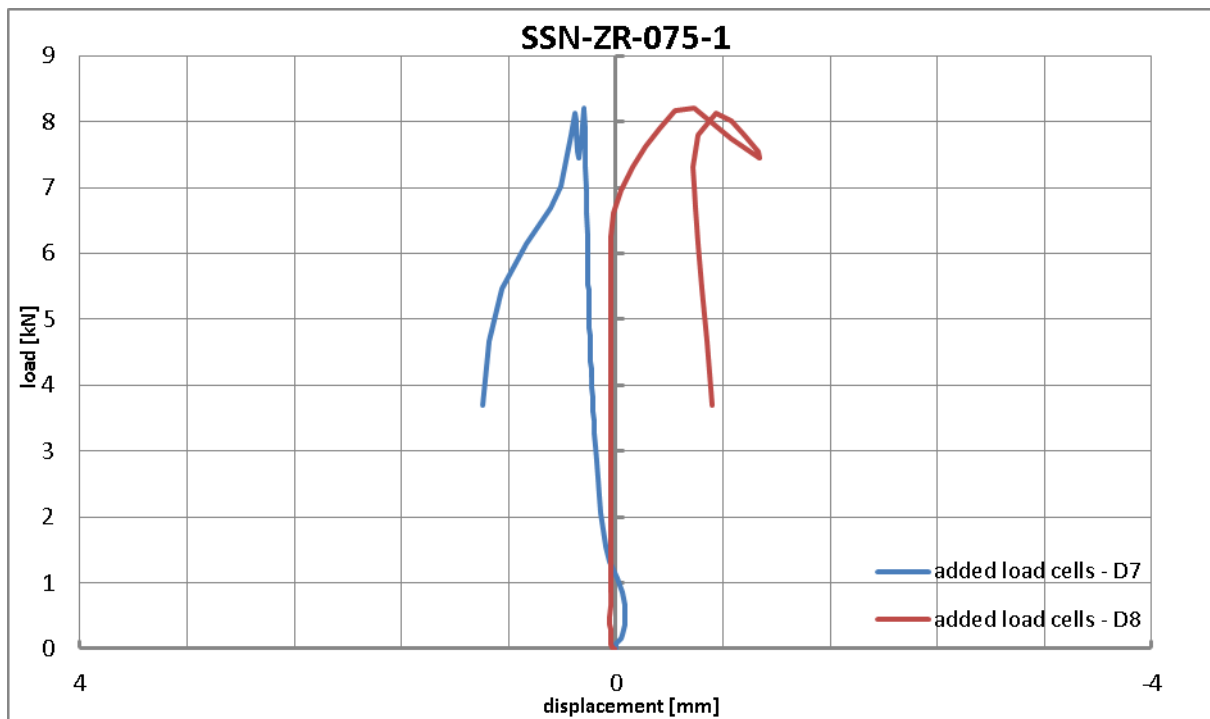
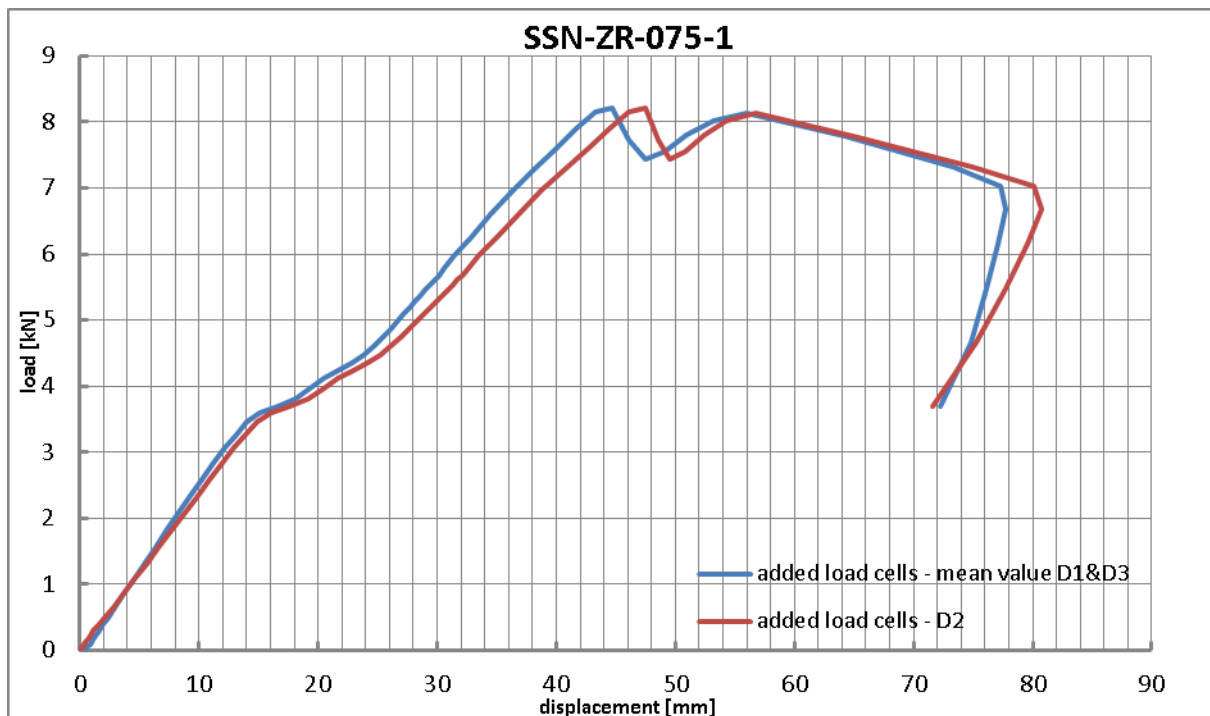


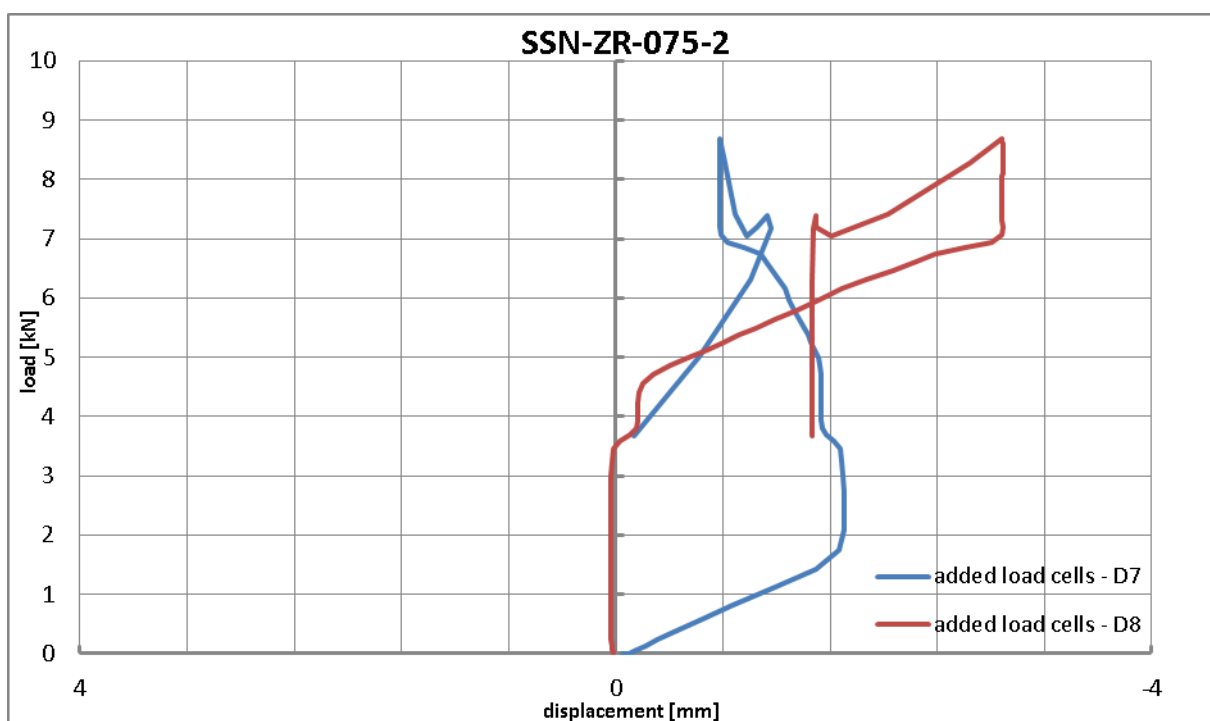
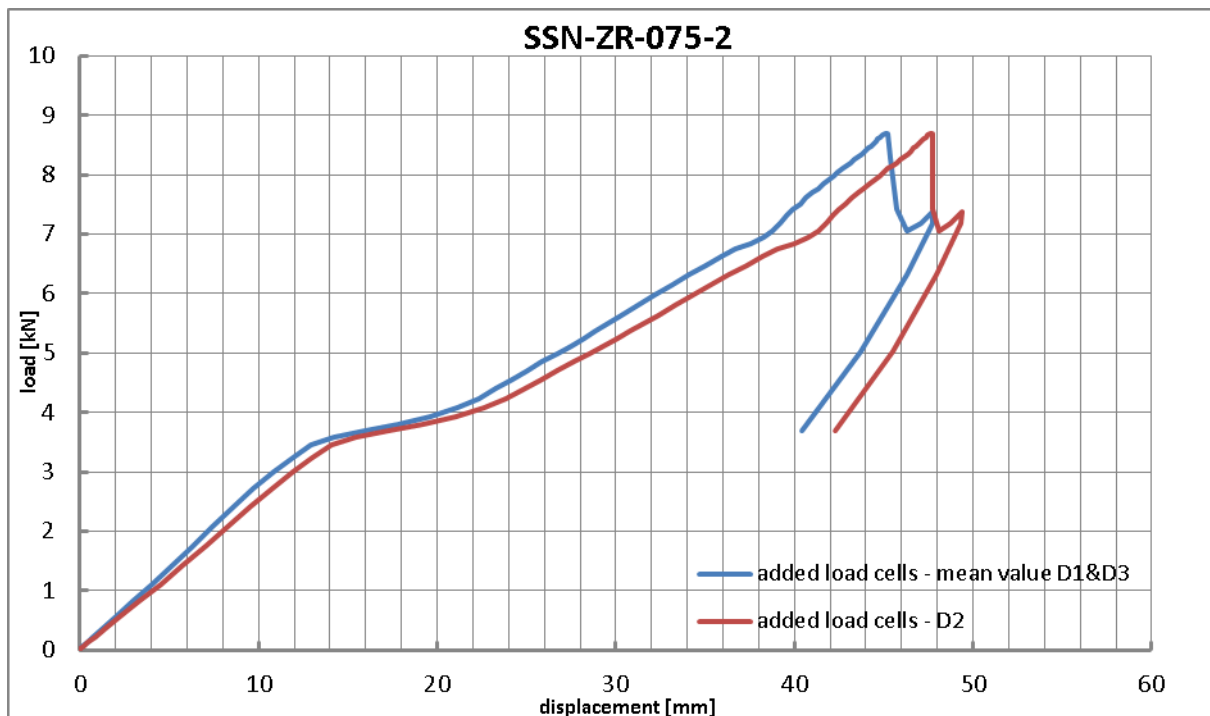


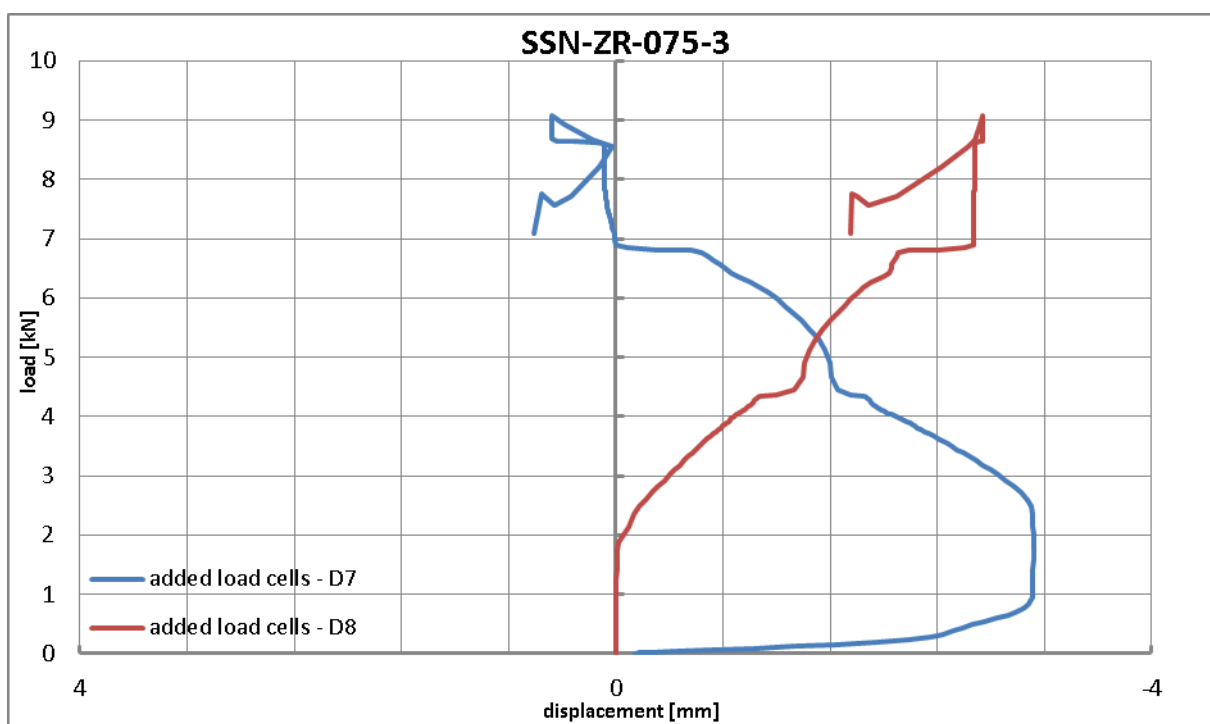
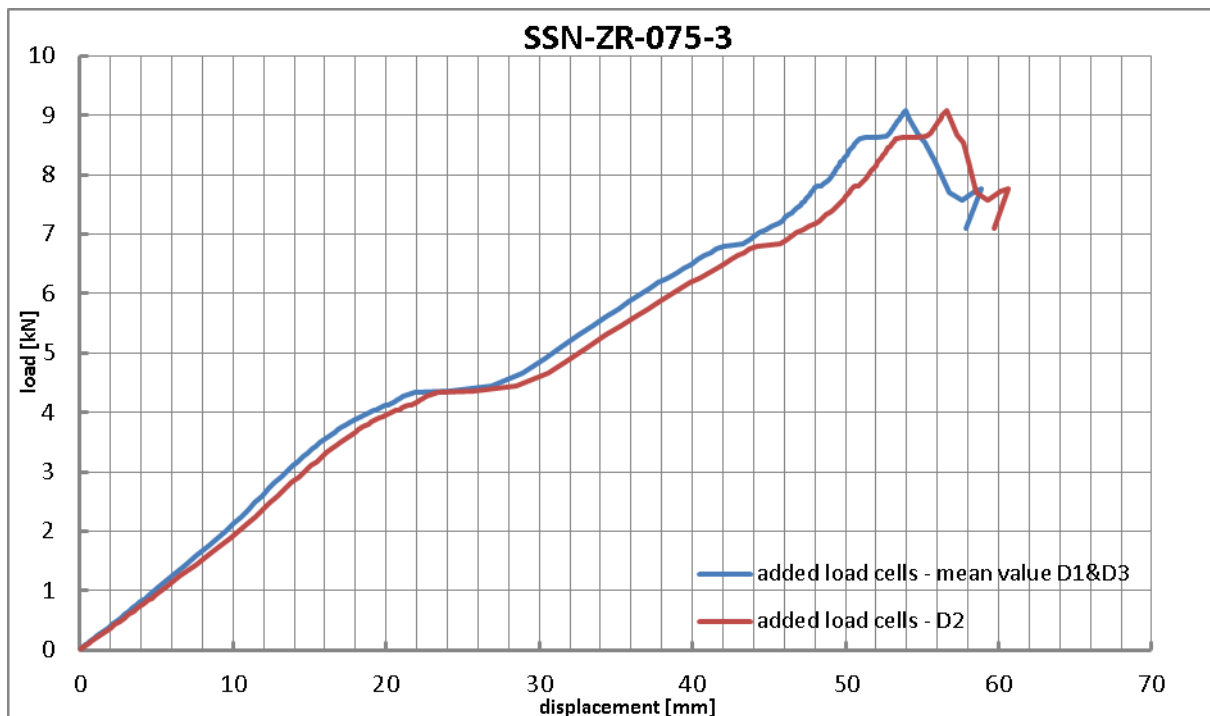


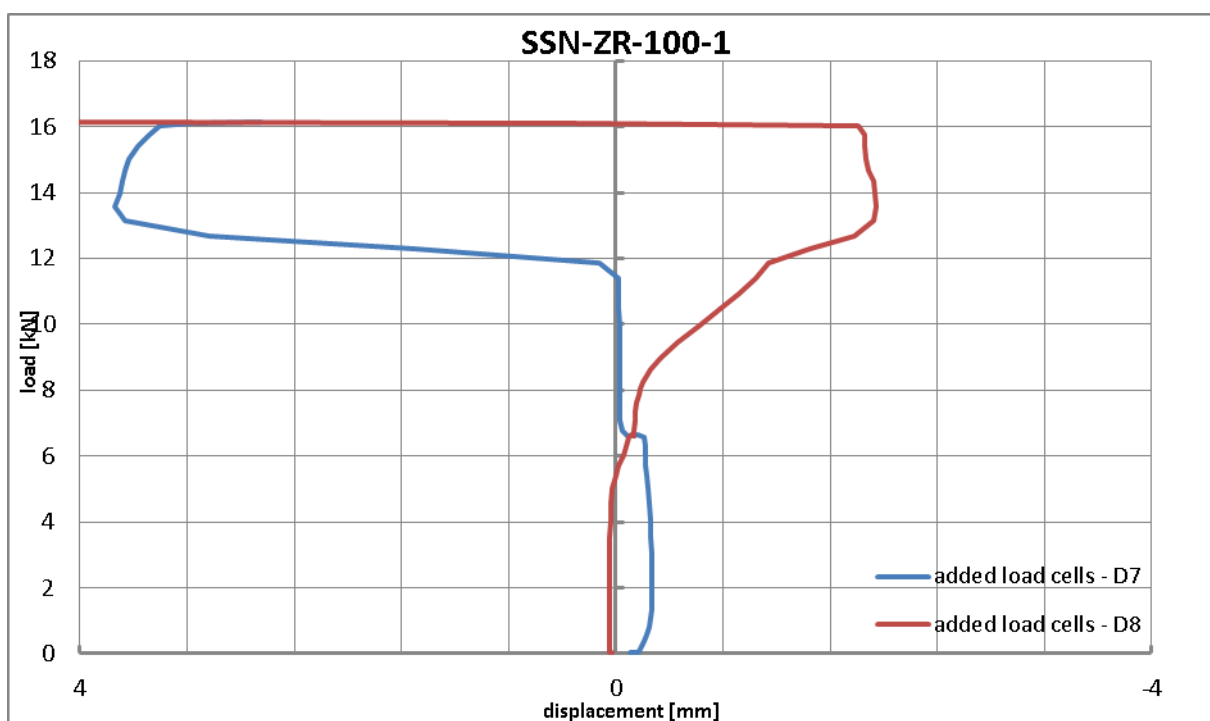
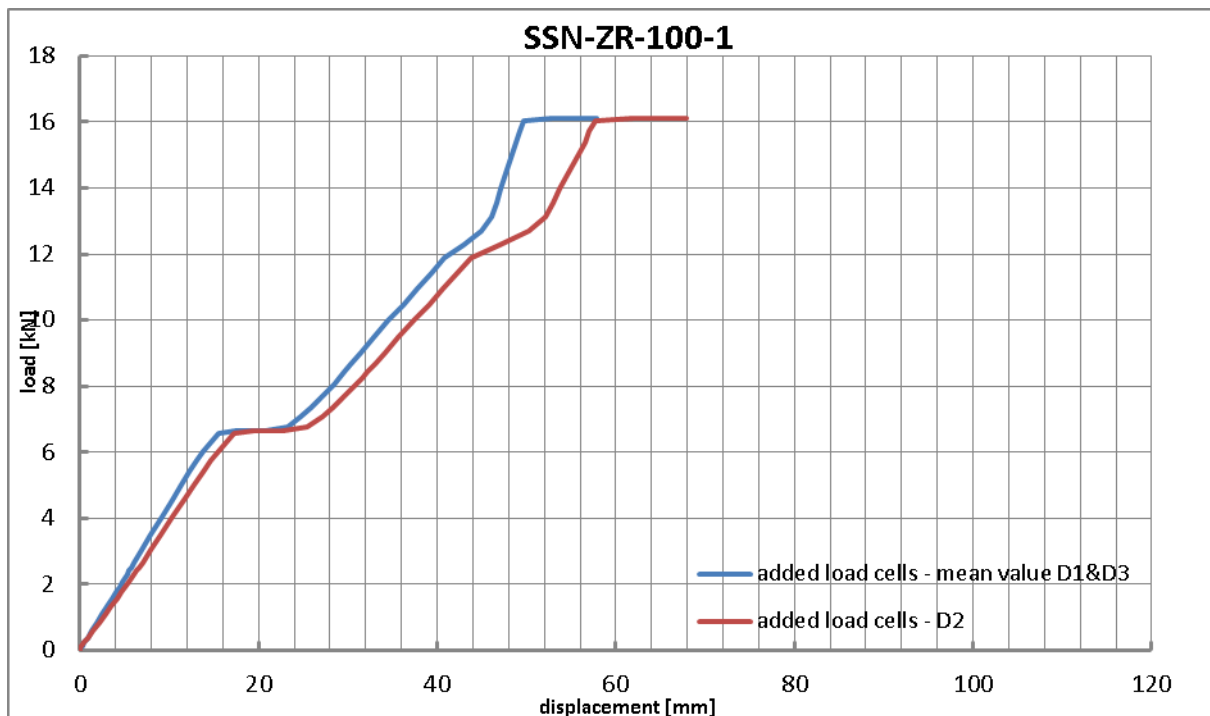


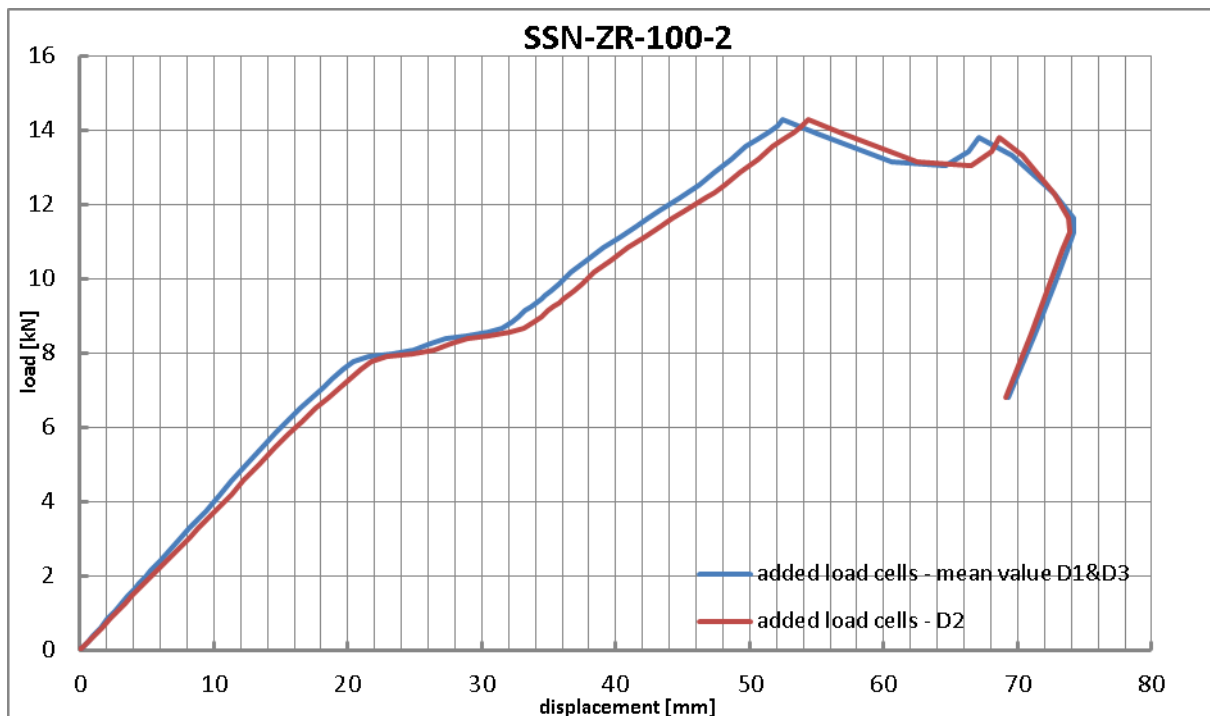


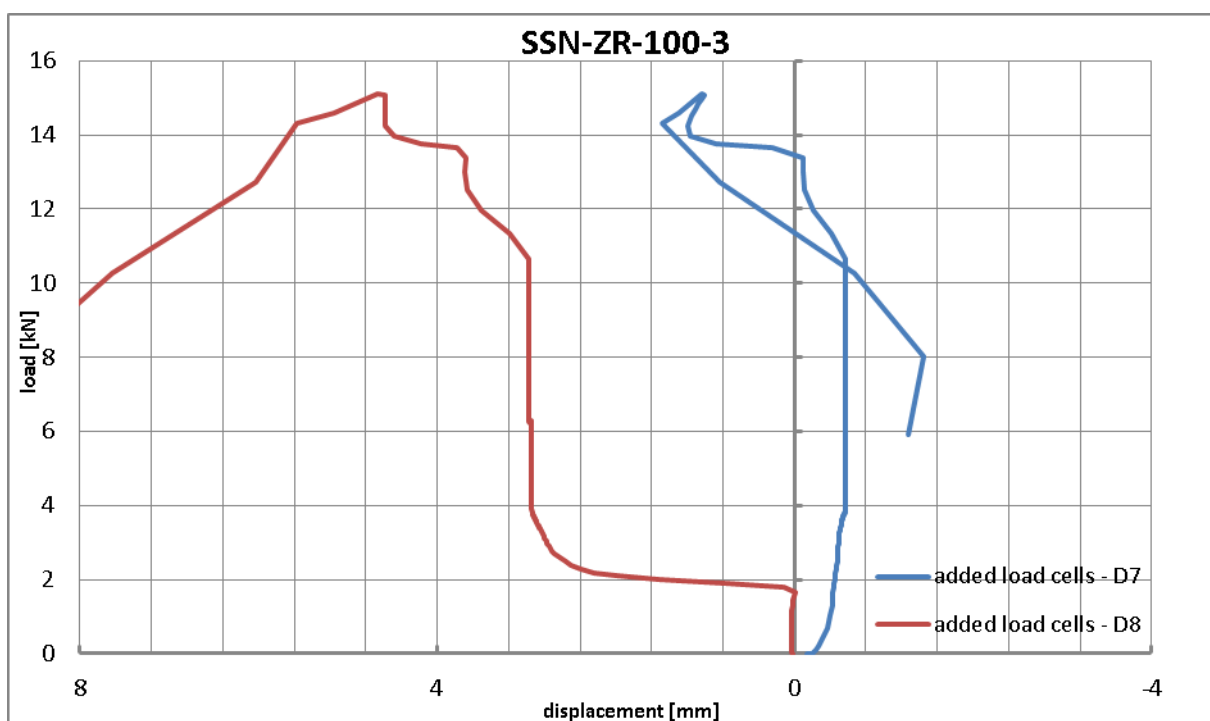
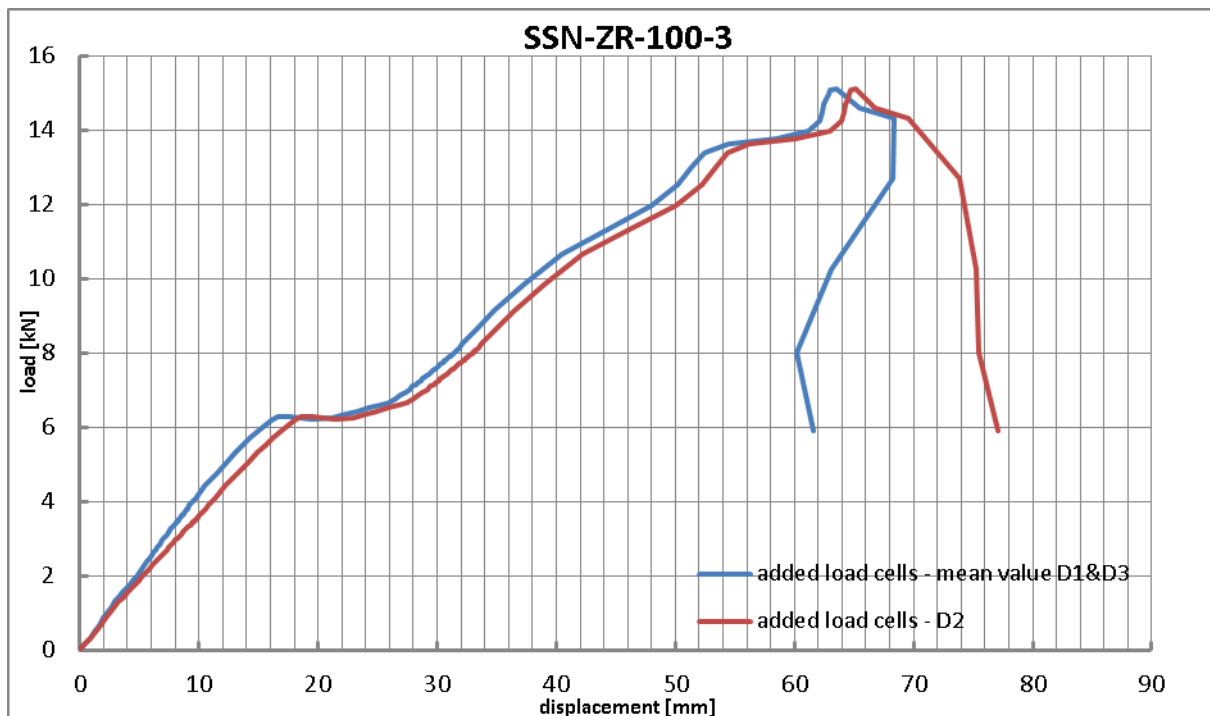












4 Annex D: Double span positive bending tests (pressure tests)

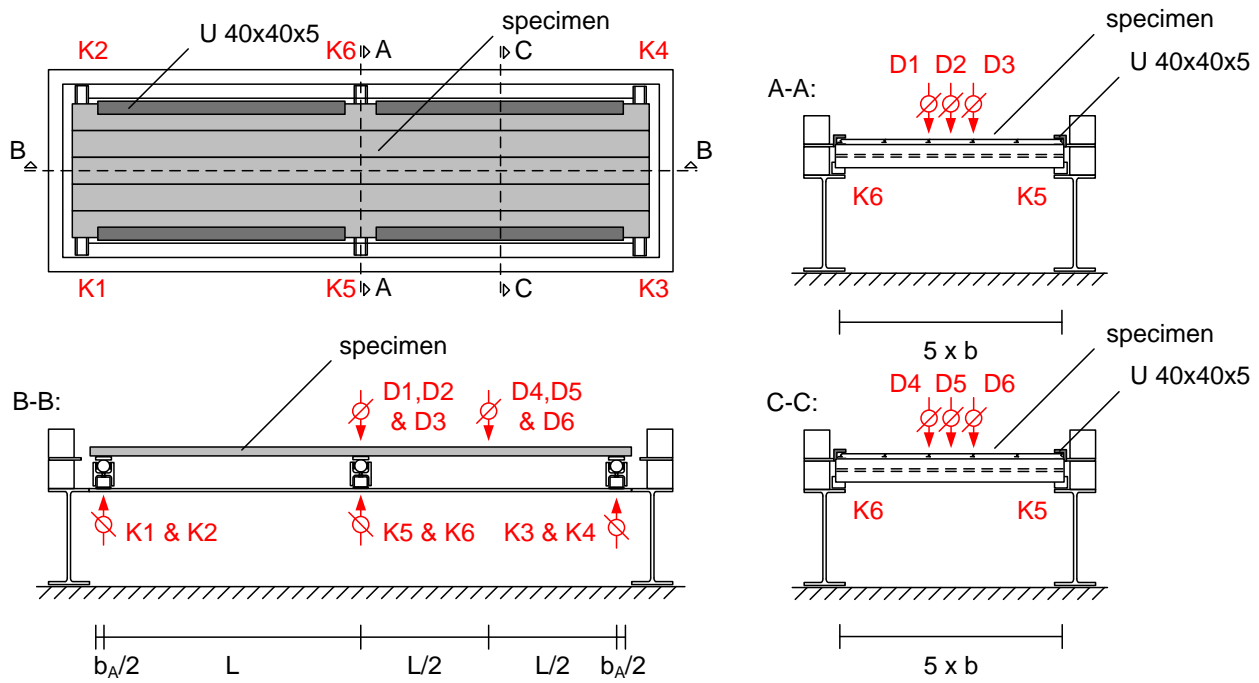


Fig. D.1: Schematic test setup

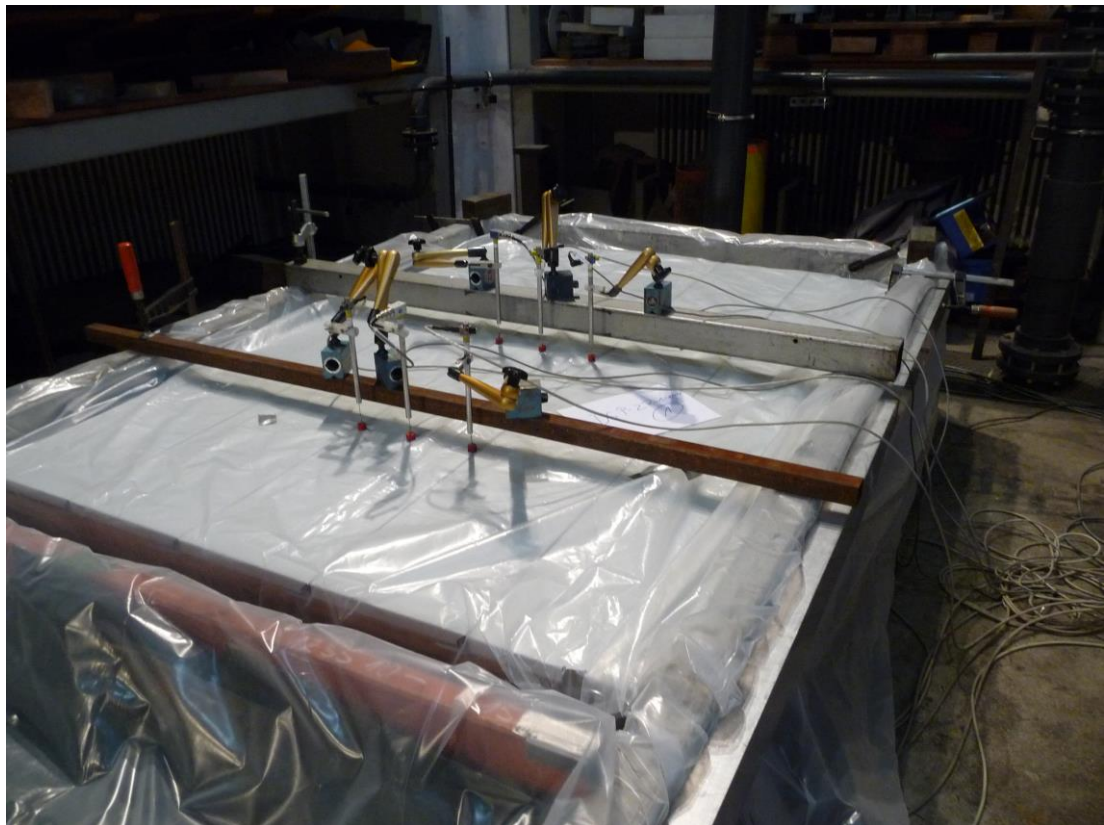


Fig. D.2: Test setup

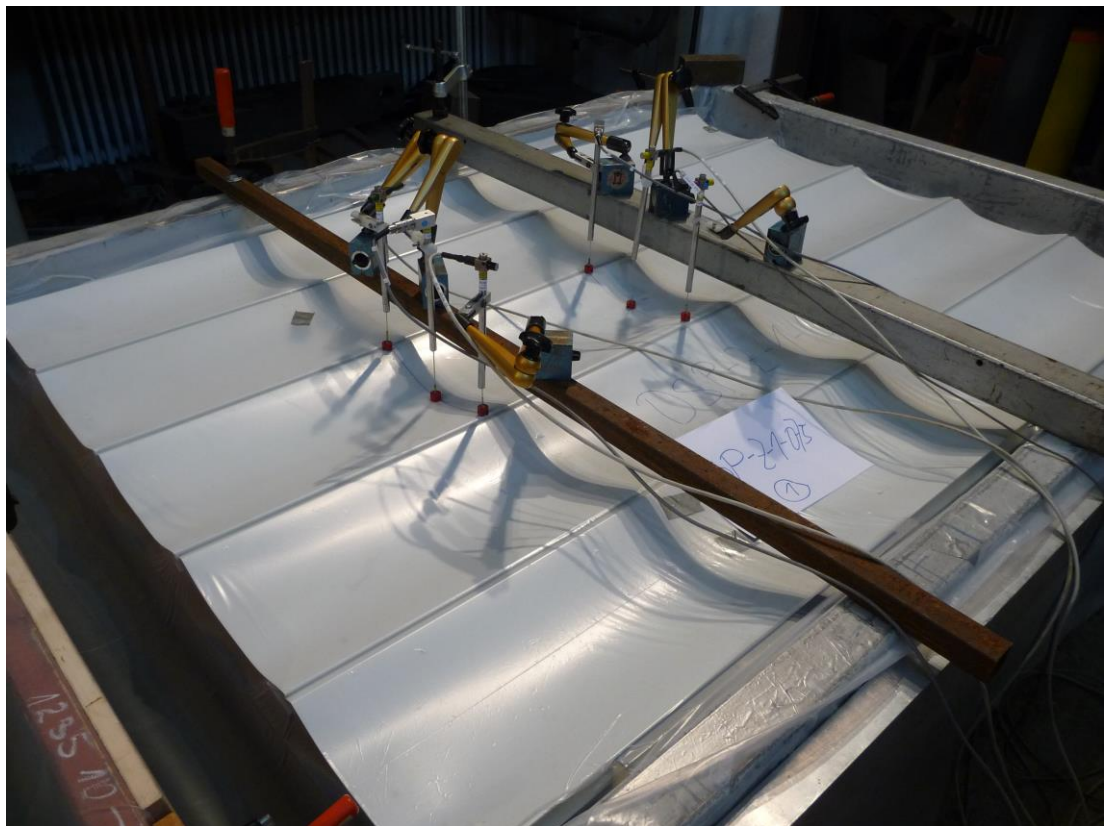


Fig. D.3: Deformation when maximum load of the vacuum chamber was reached (DSP-Z-1-075-1)



Fig. D.4: Deformation when maximum load of the vacuum chamber was reached (DSP-C-1-075-1)

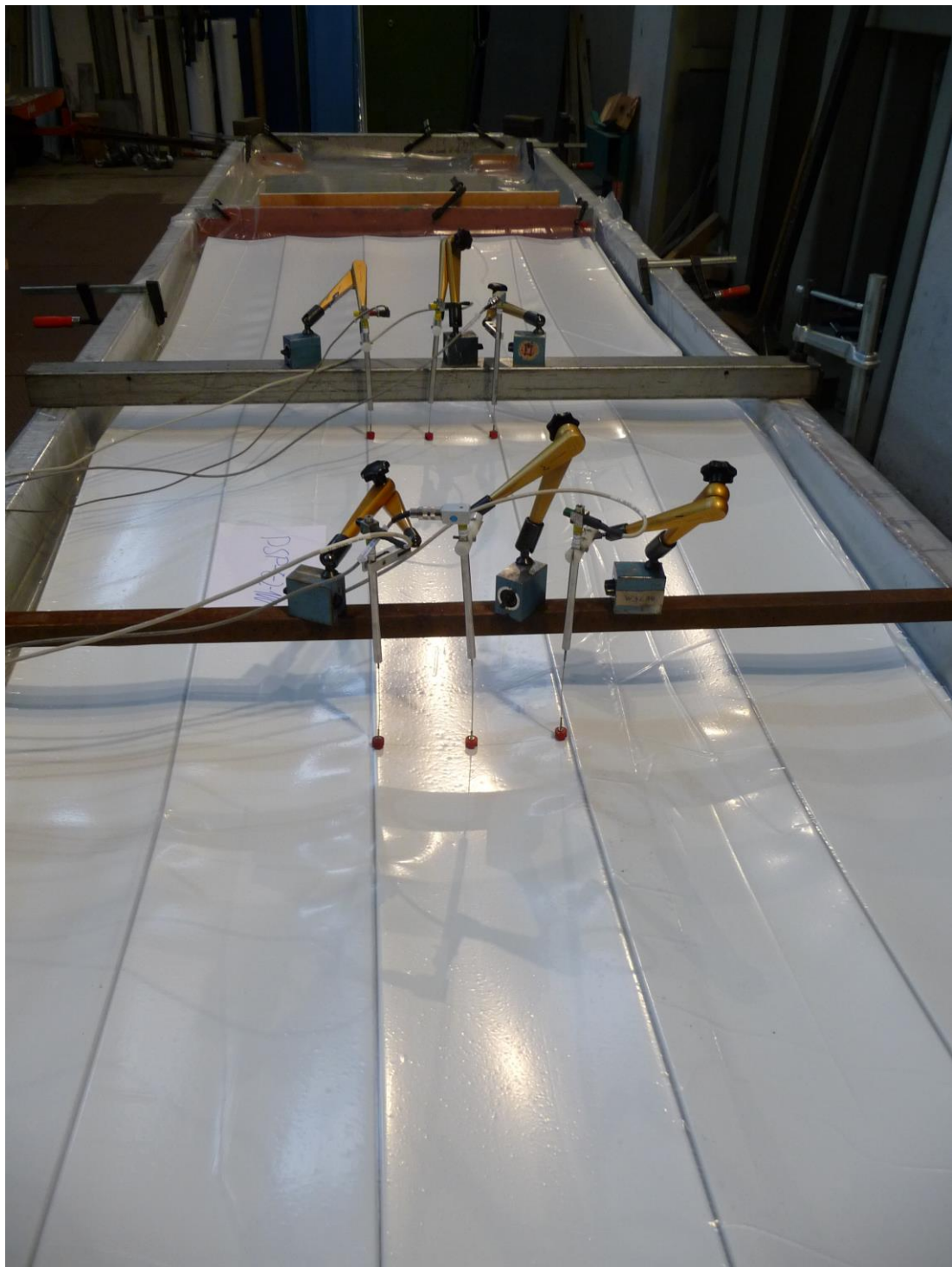


Fig. D.5: Deformation before failure load was reached (DSP-C-2-100-1)



Fig. D.6: Failure by local buckling of the compressed flanges (DSP-C-2-100-1)

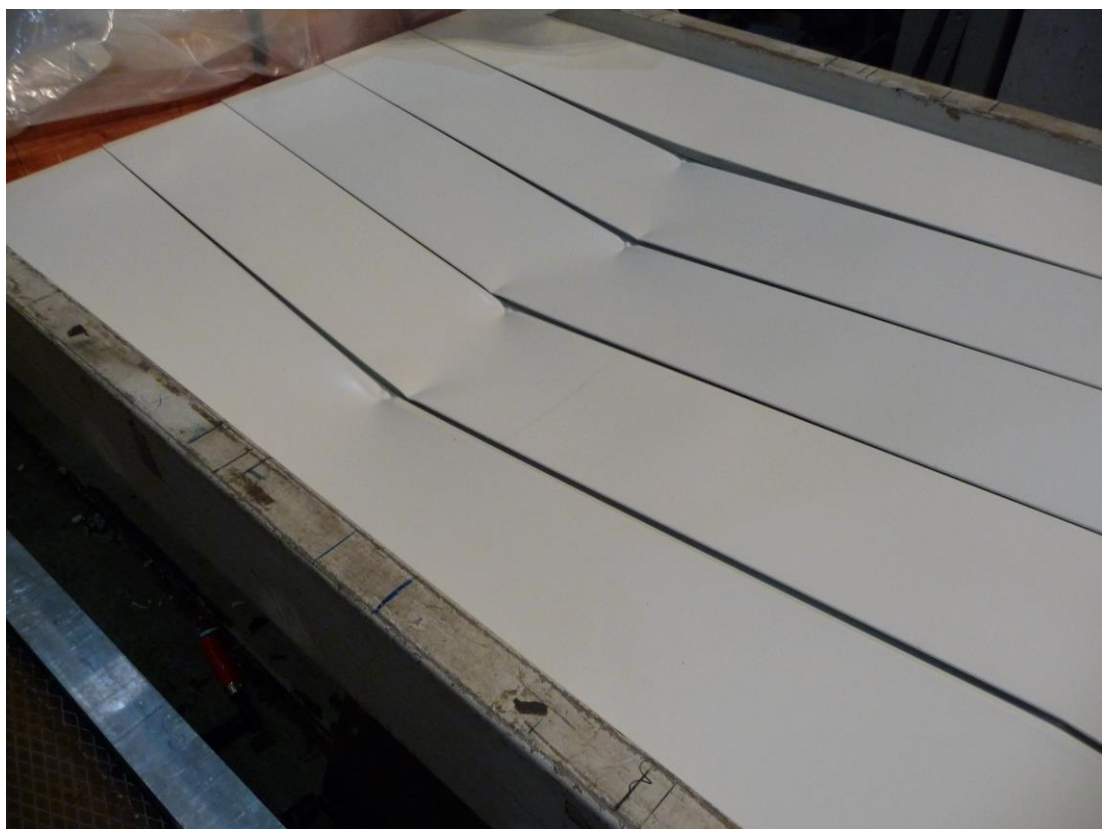


Fig. D.7: Failure by local buckling of the compressed flanges (DSP-ZR-2-100-3)

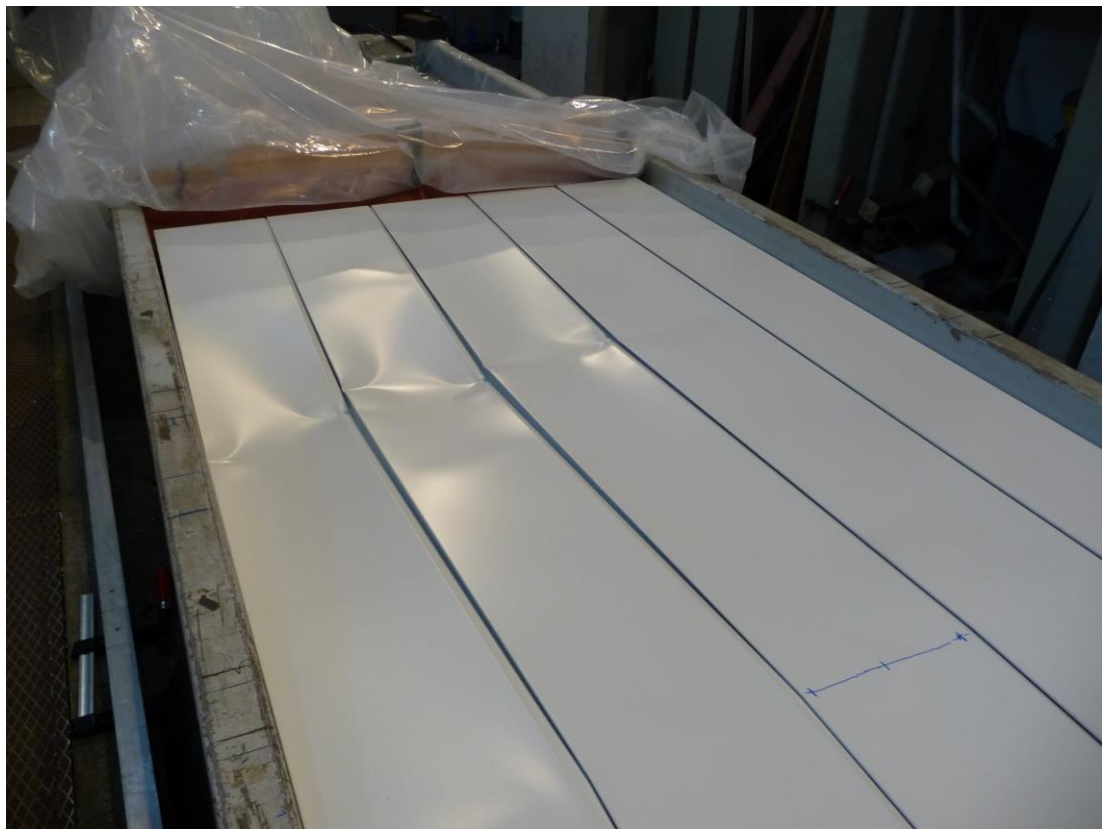


Fig. D.8: Failure by local buckling of the compressed flanges (DSP-ZR-2-075-1)

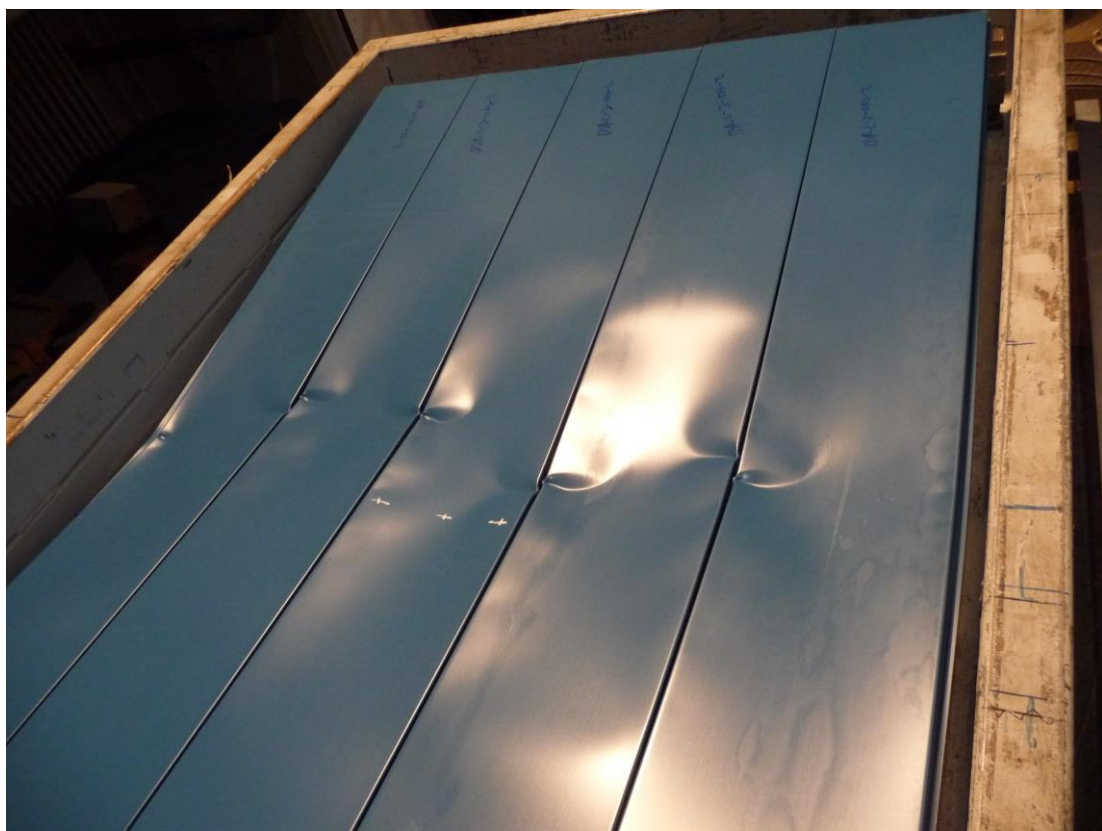
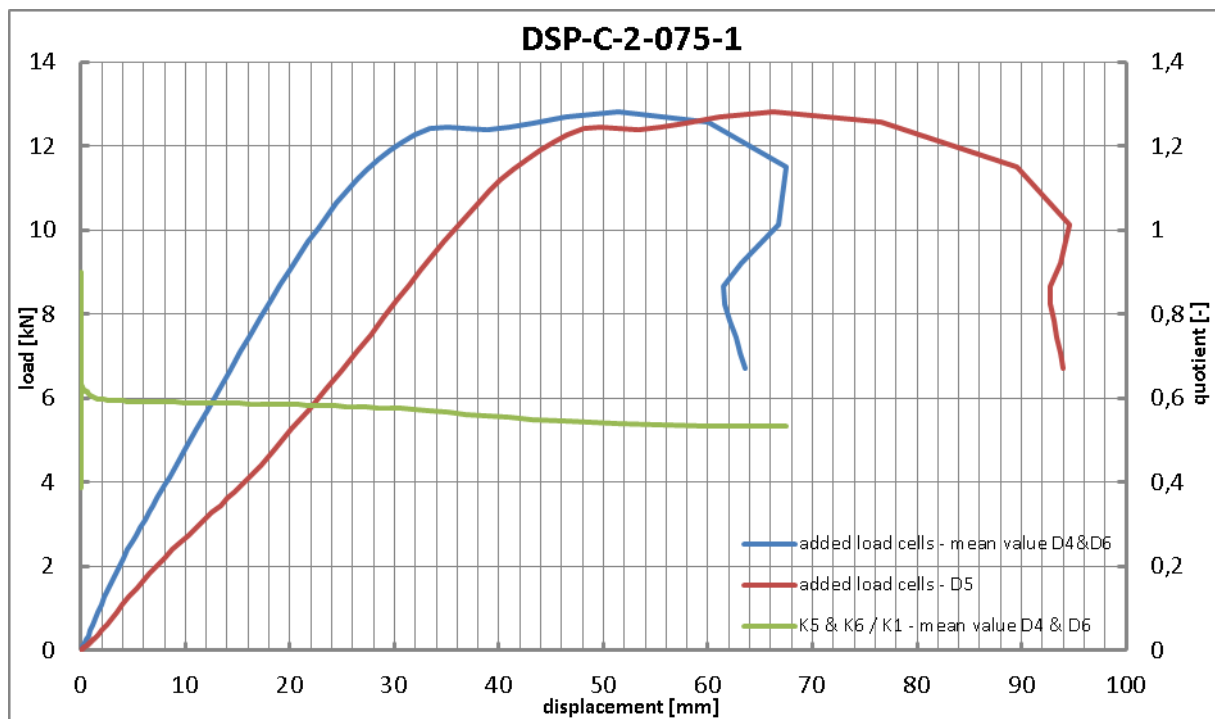


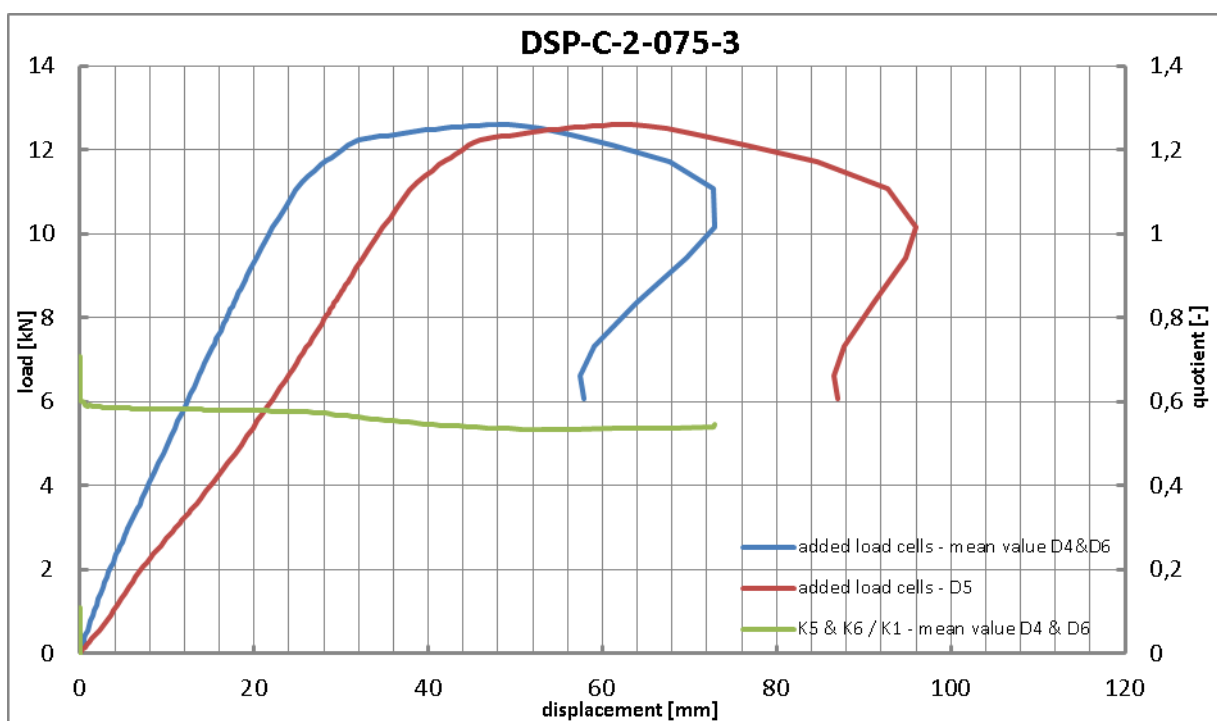
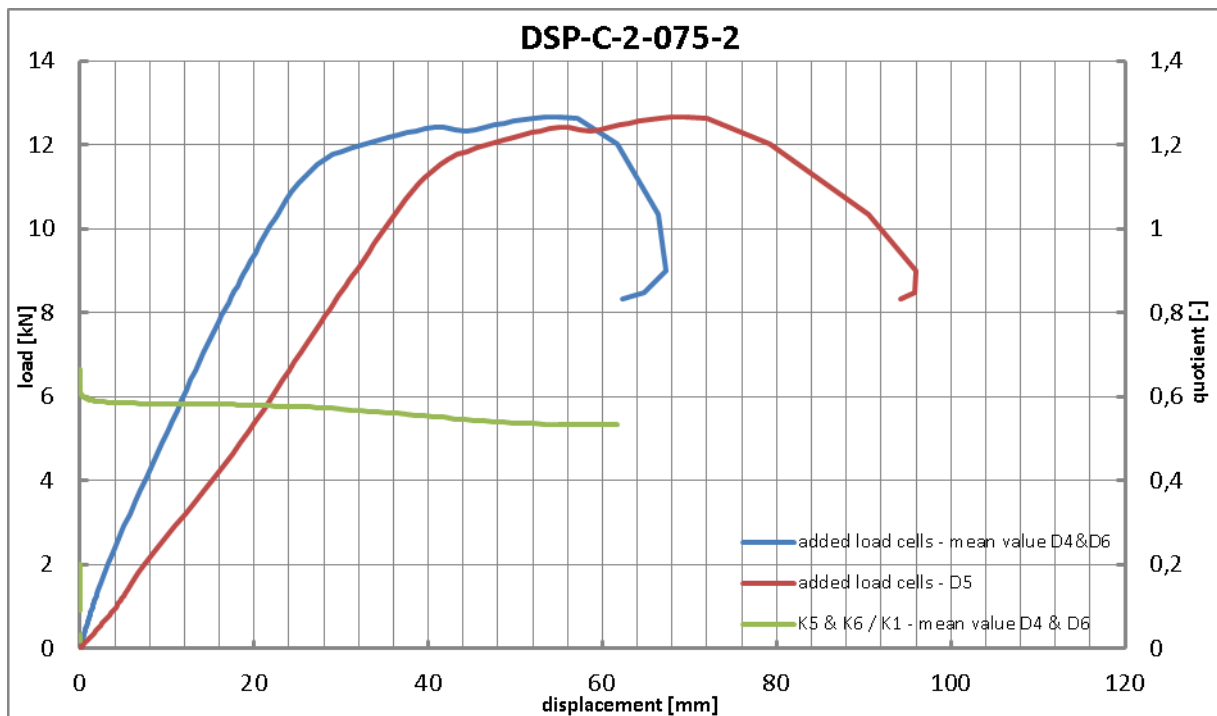
Fig. D.9: Failure by local buckling of the compressed flanges (DSP-C-3-075-2)

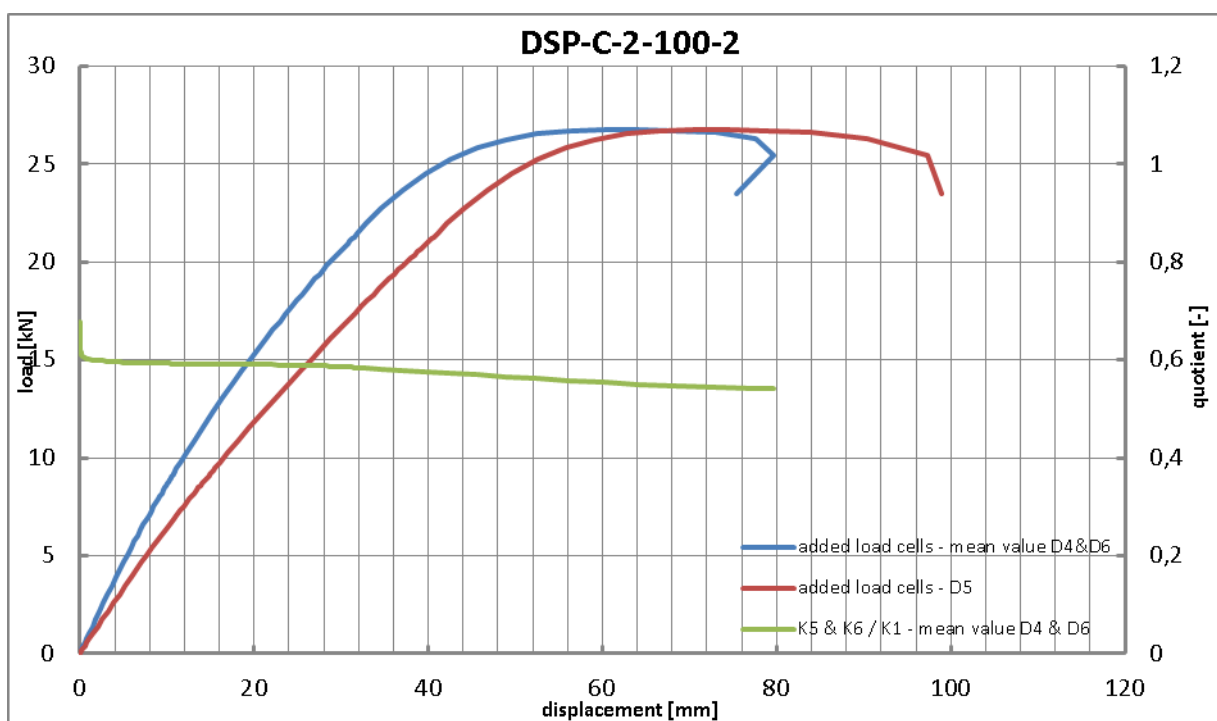
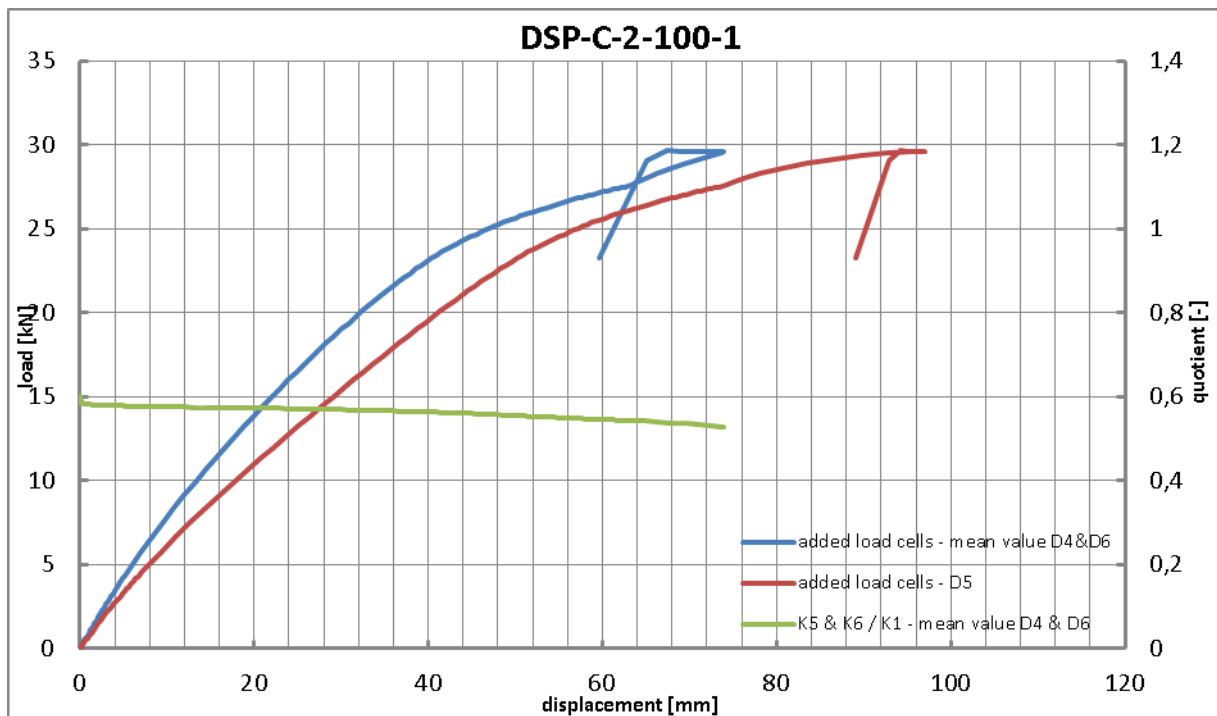


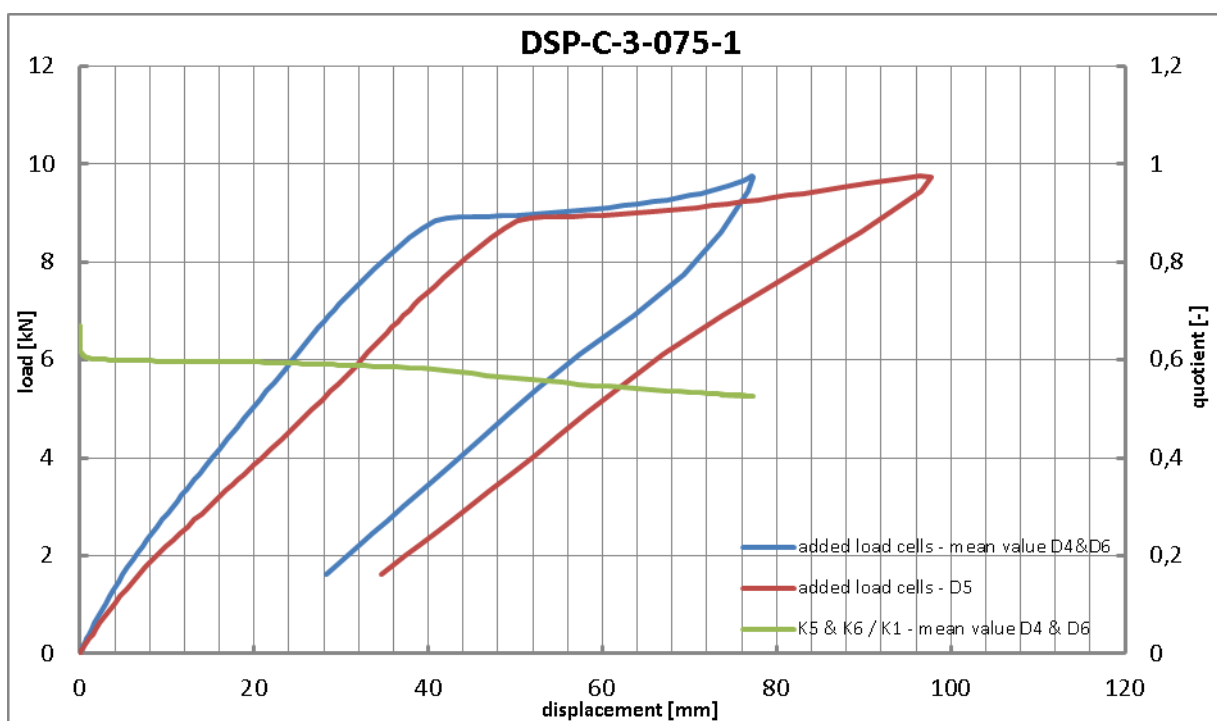
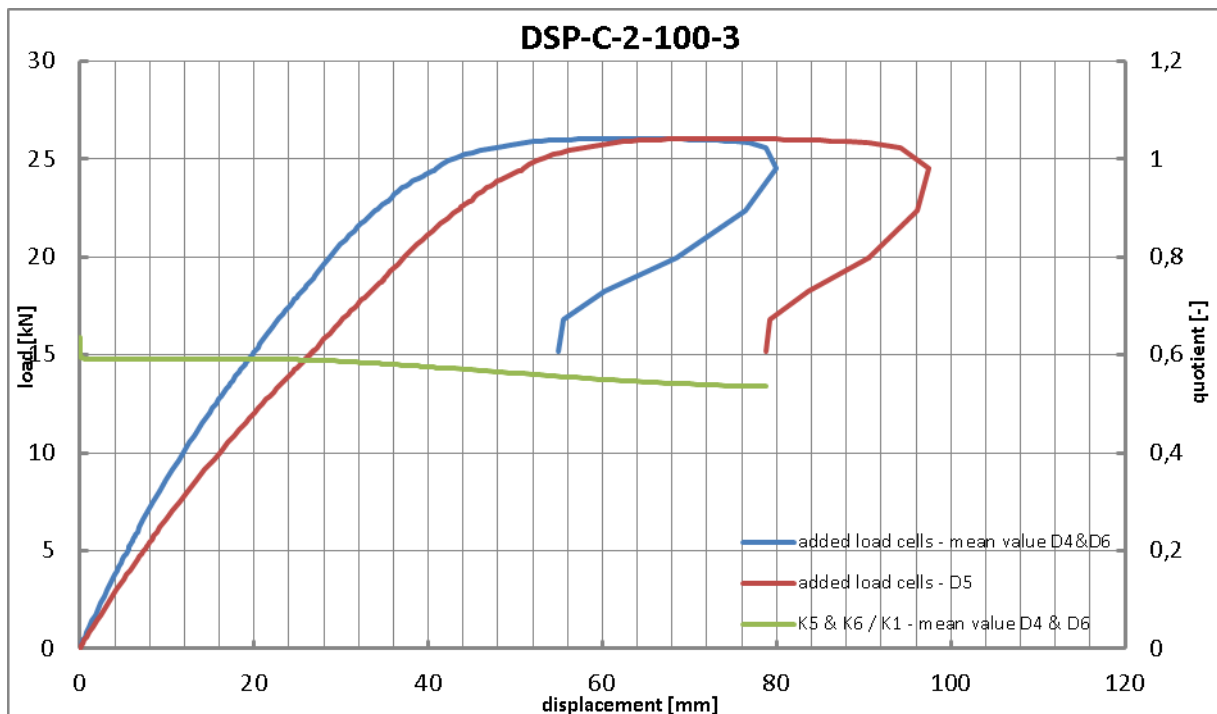
Fig. D.10: Failure by local buckling of the compressed flanges (DSP-ZR-3-100-3)

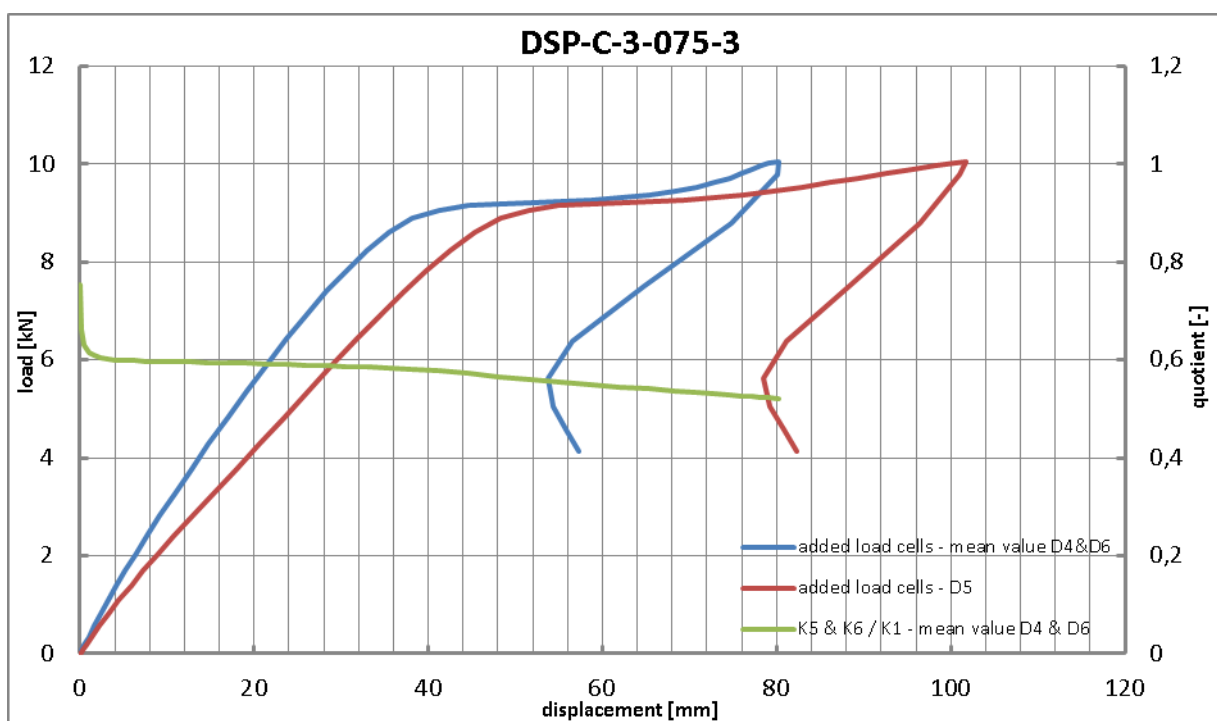
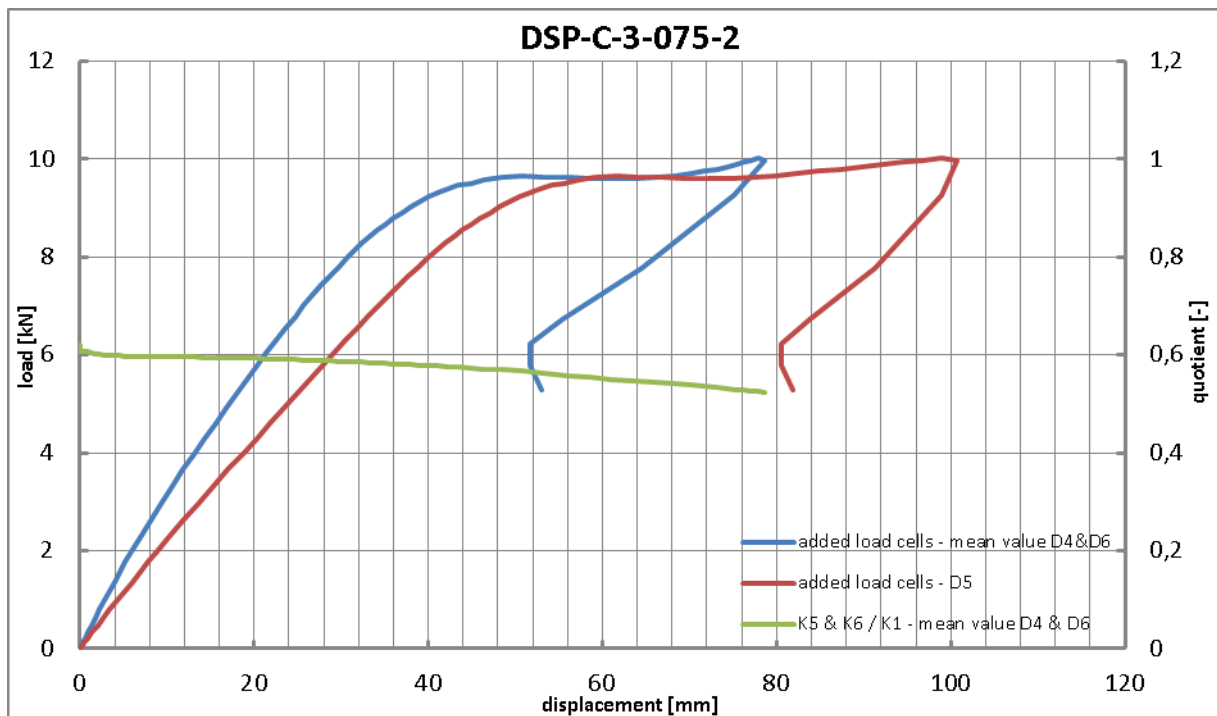
Load-deflection-curves:

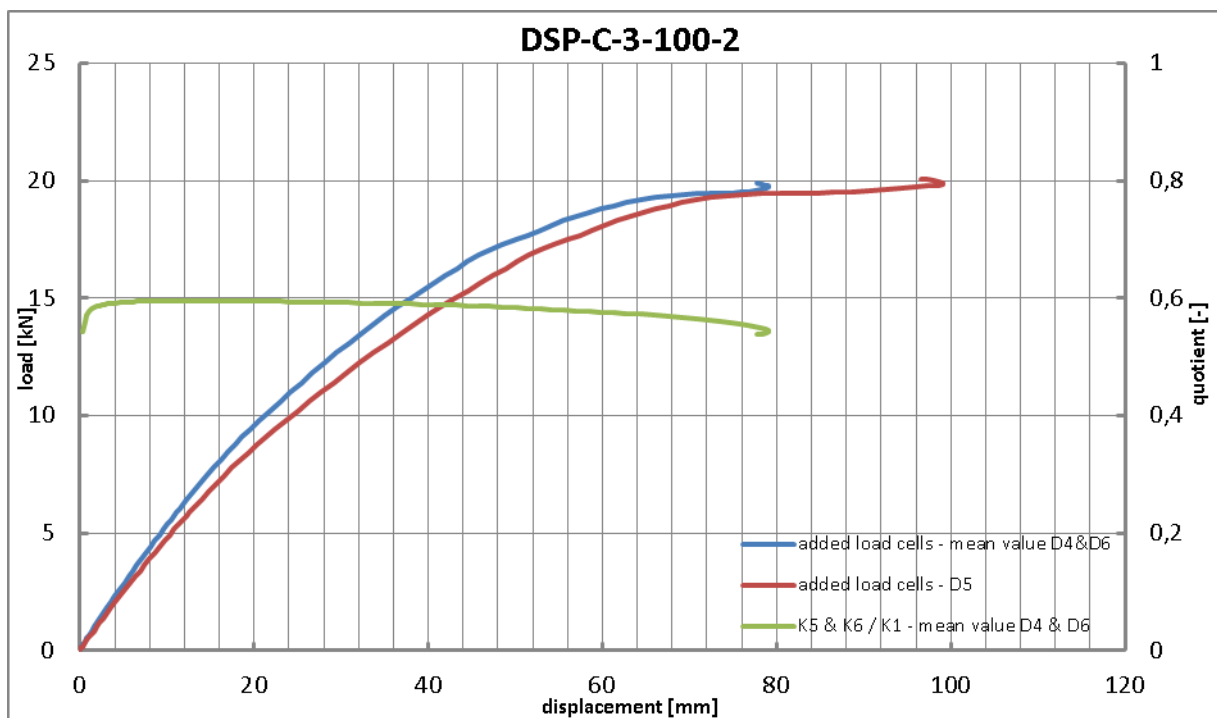
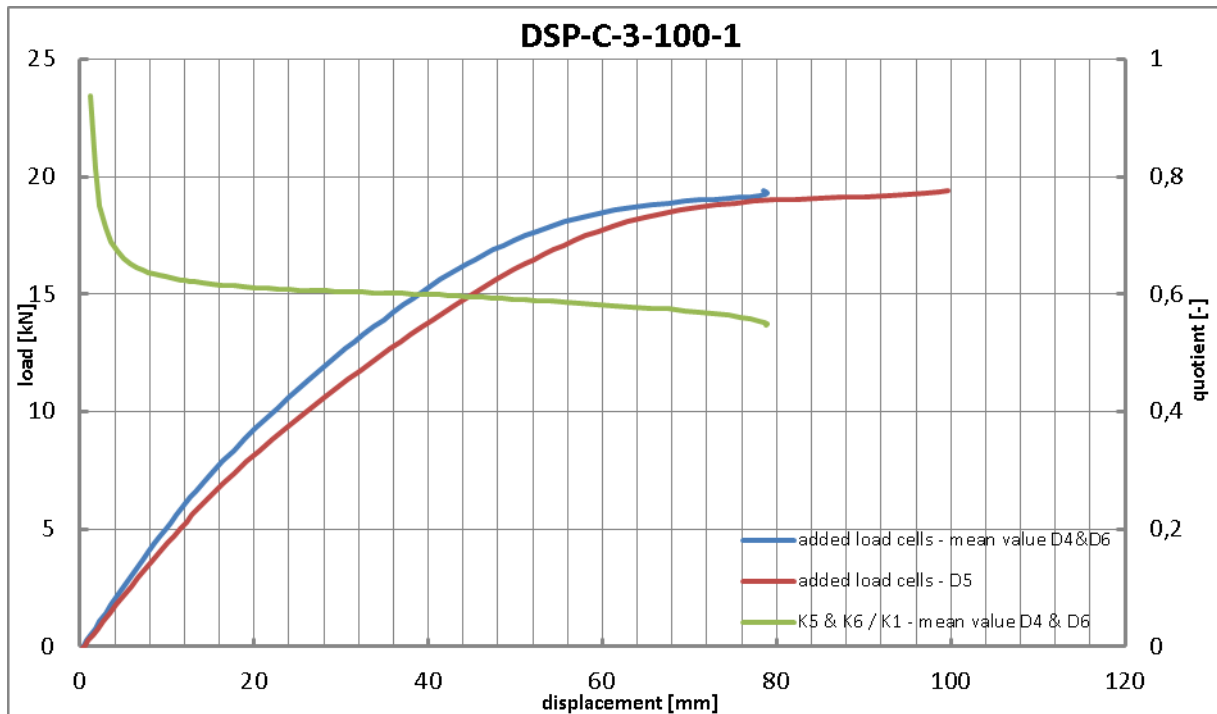


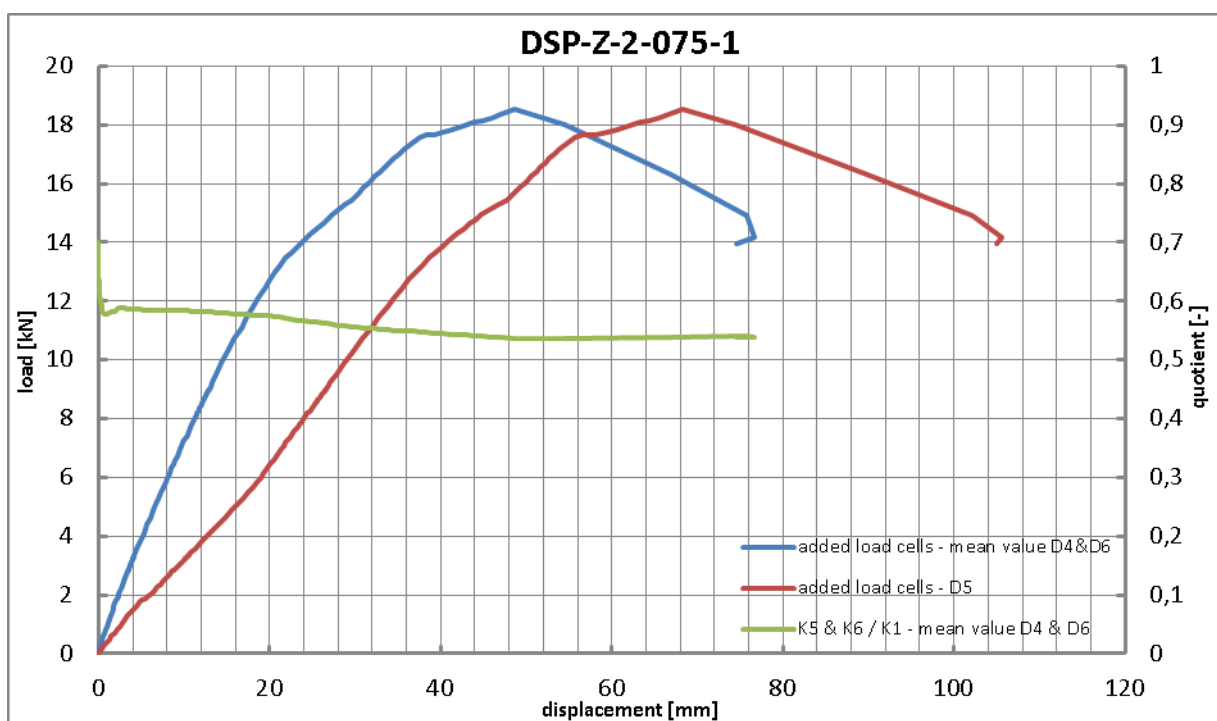
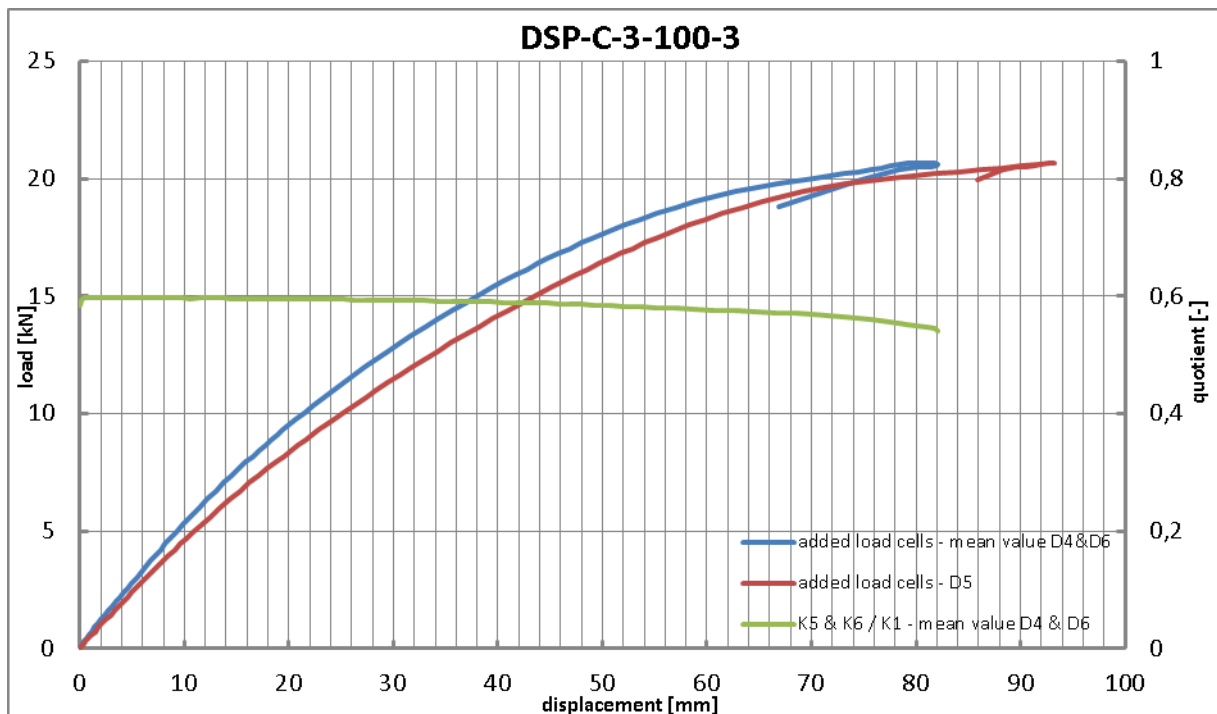


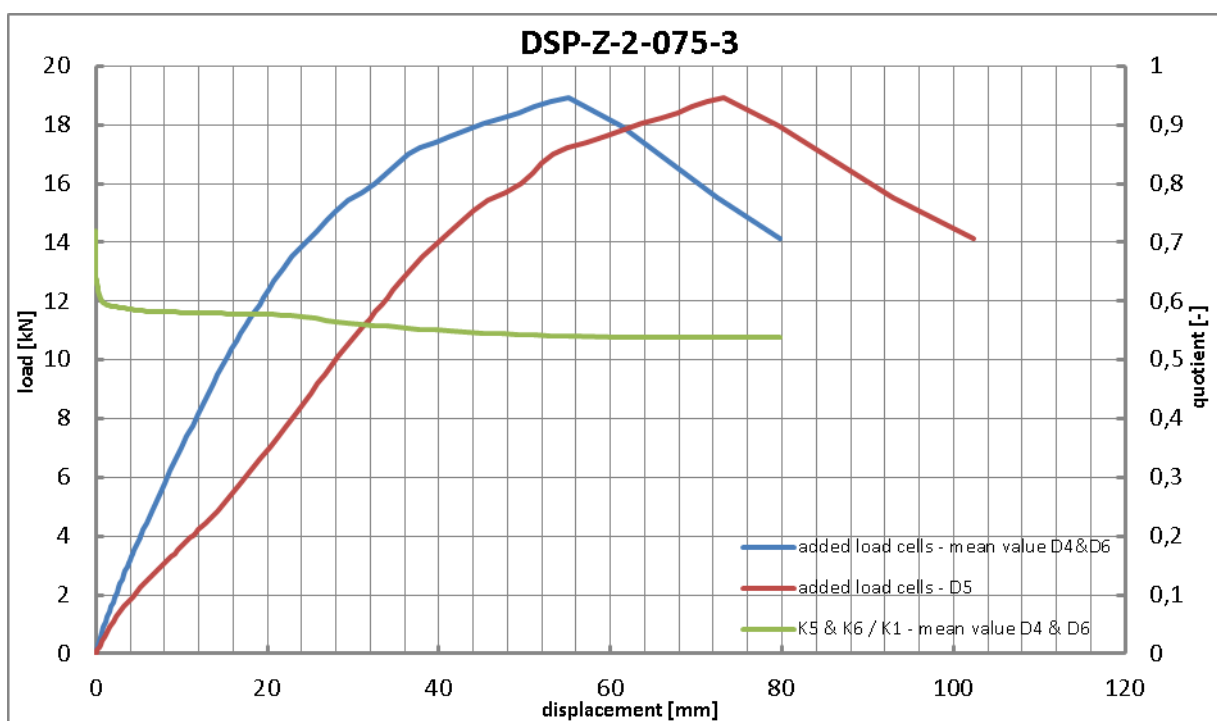
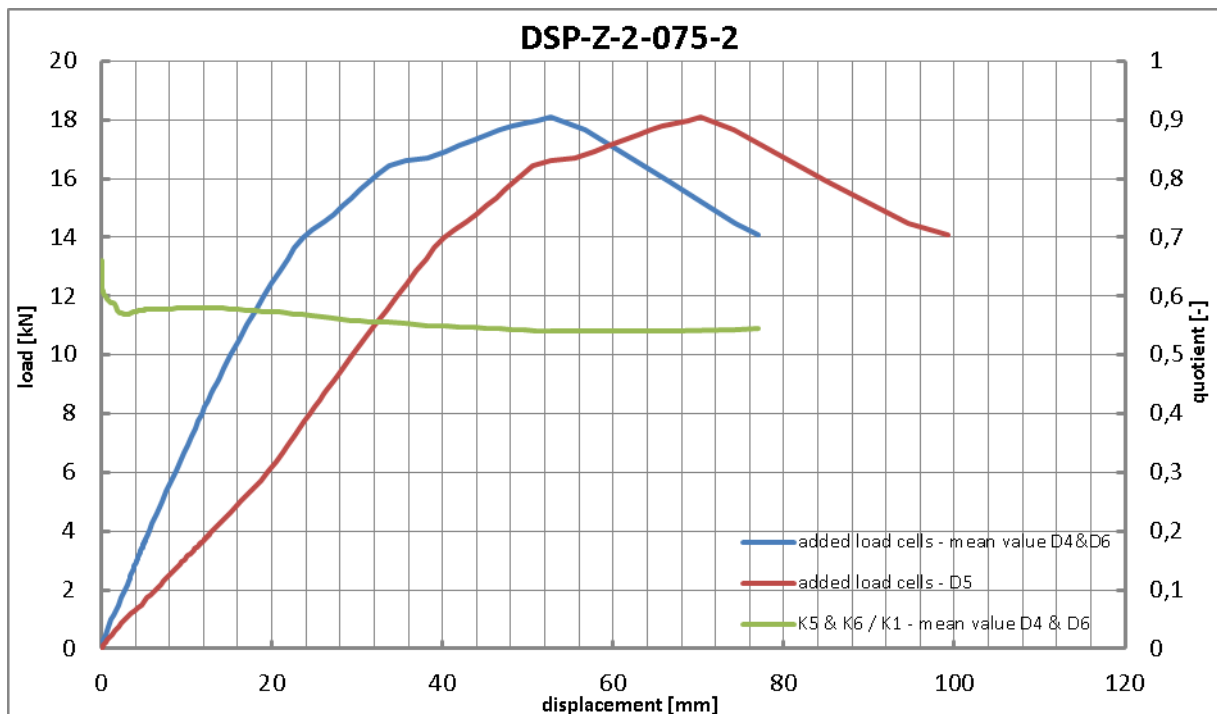


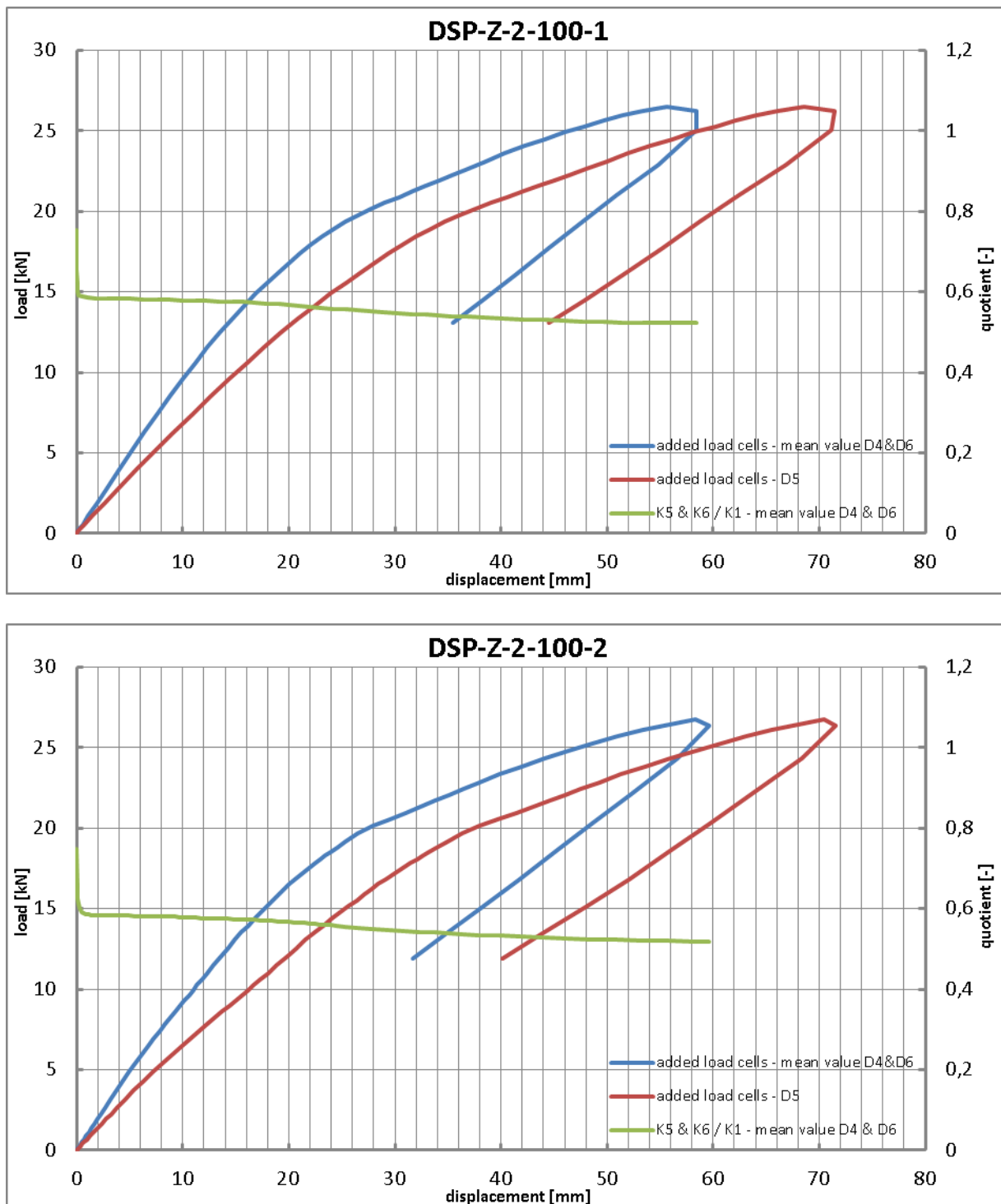


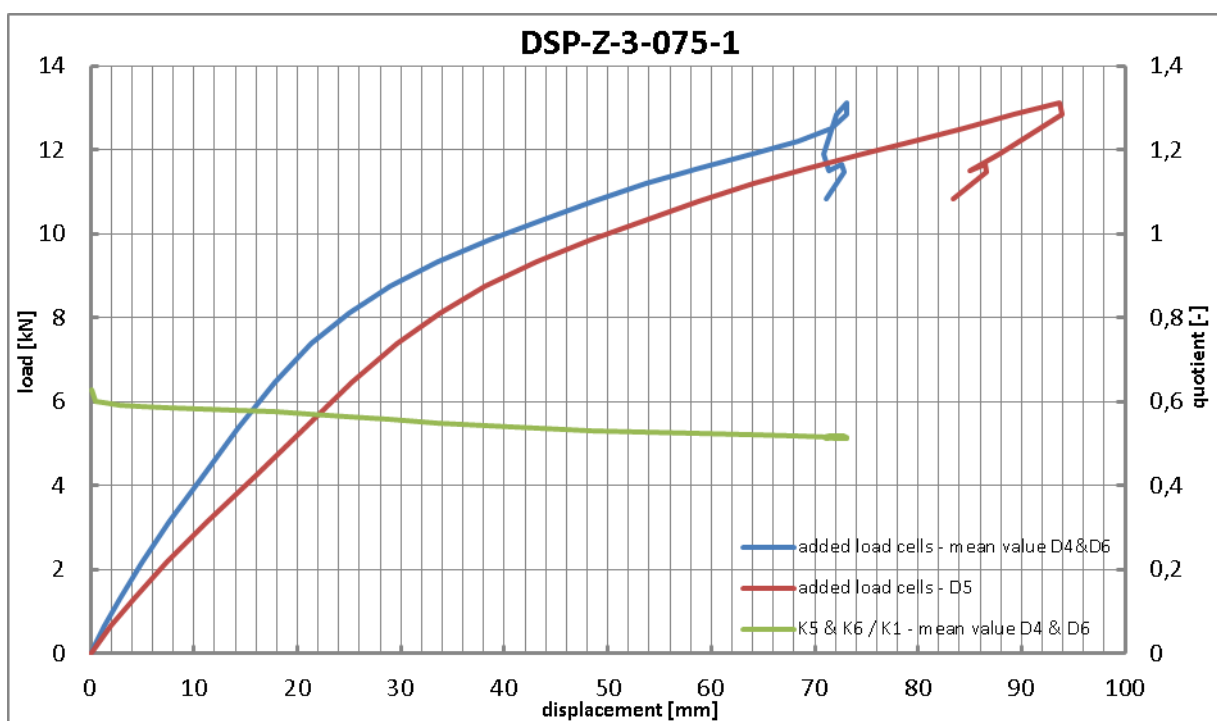
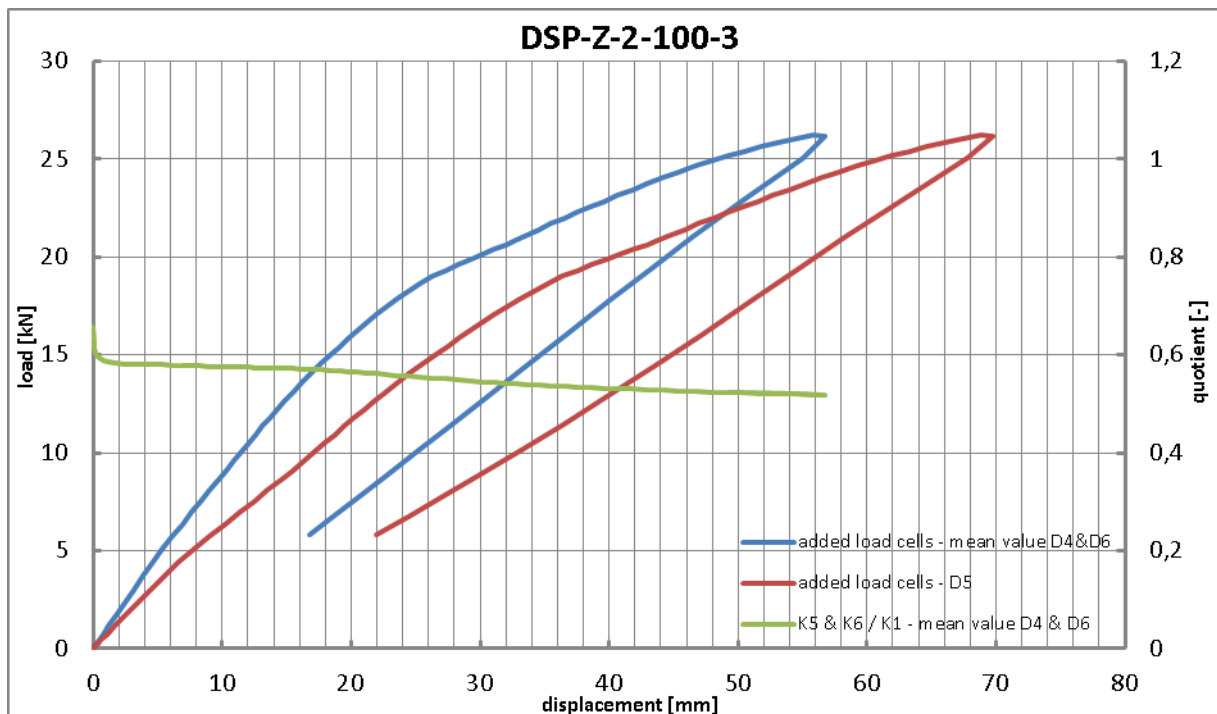


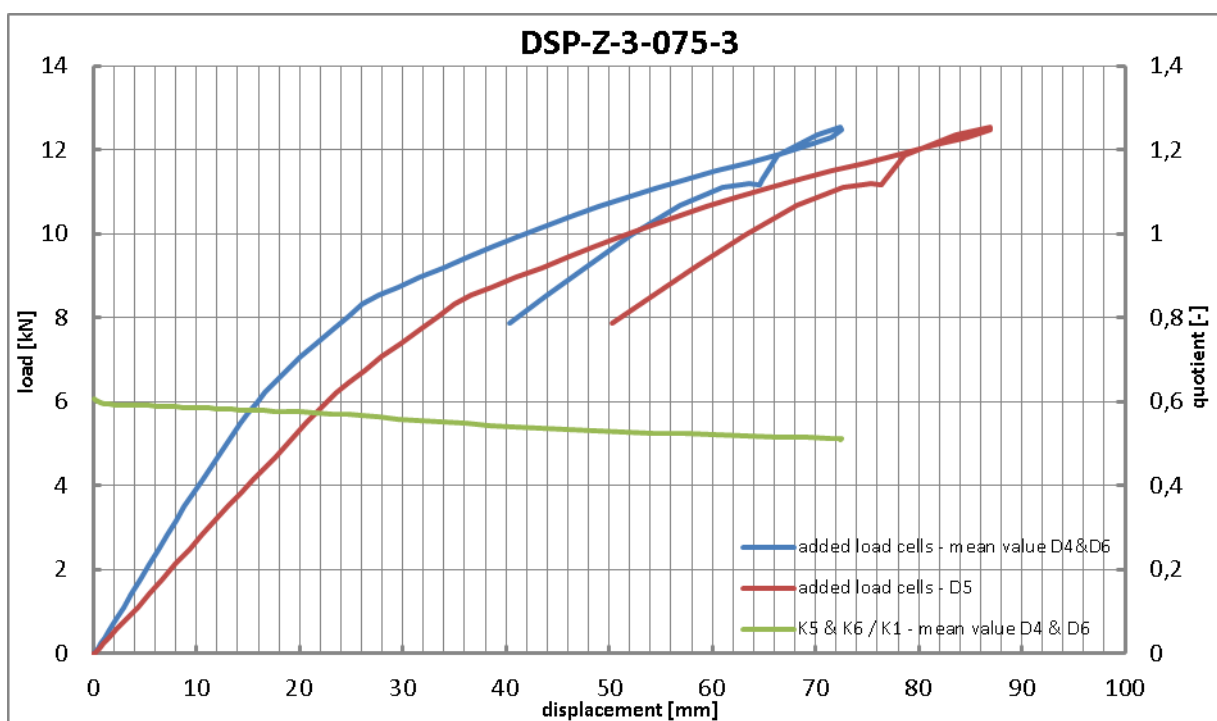
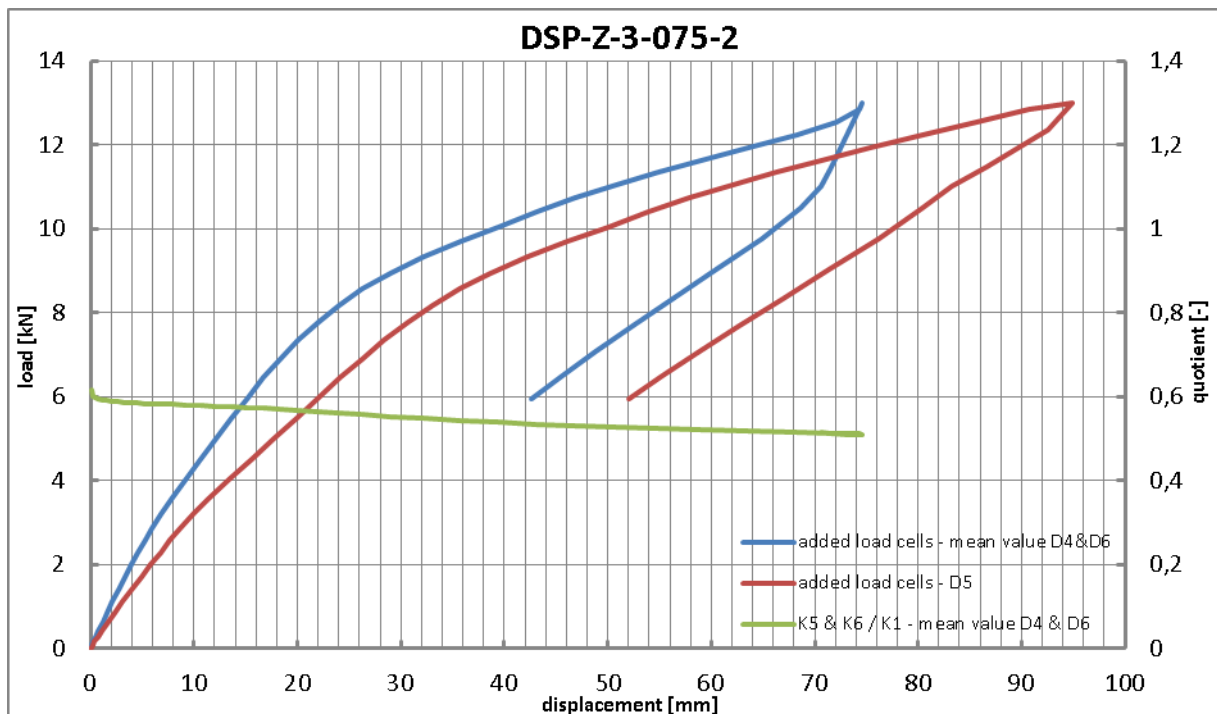


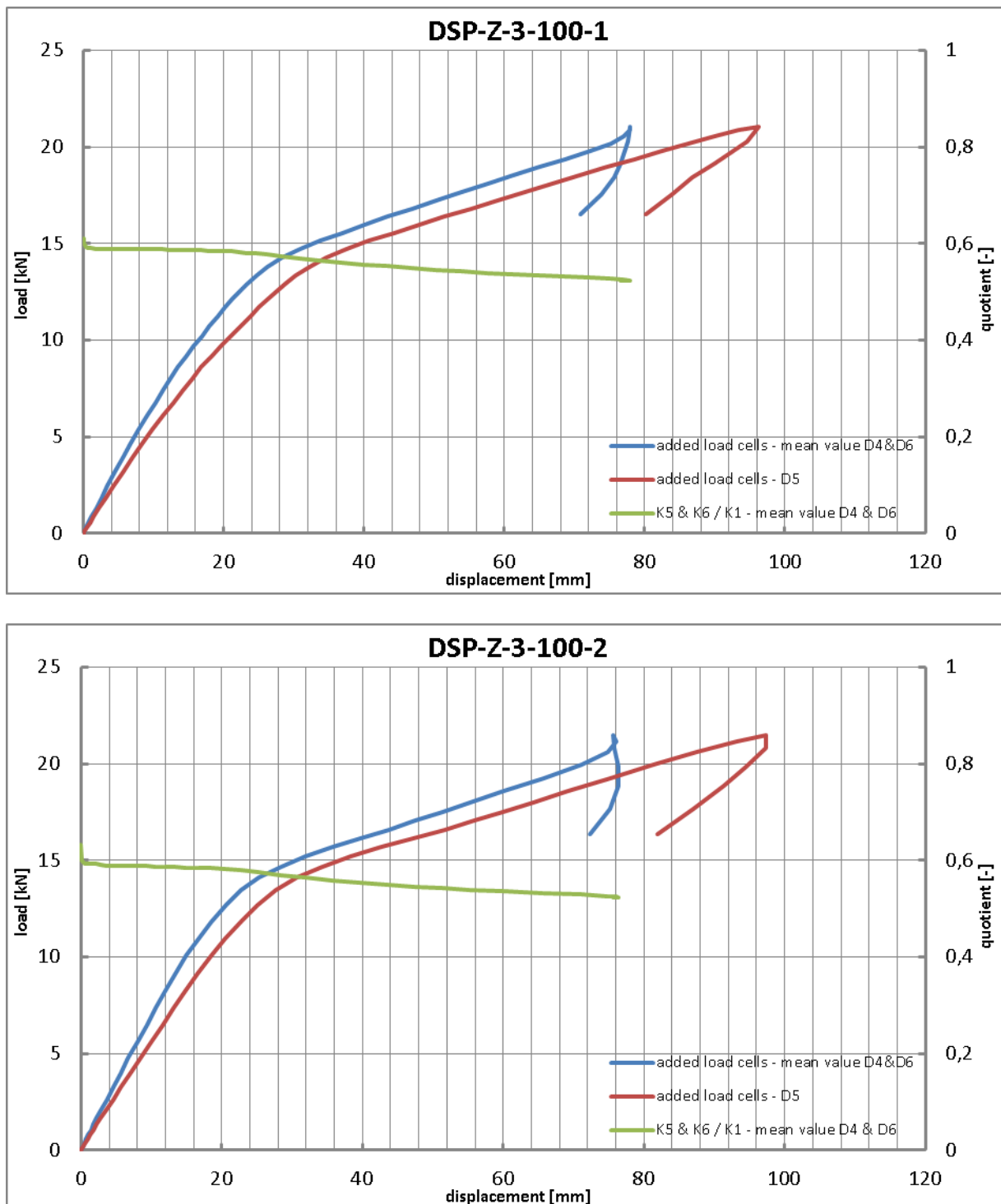


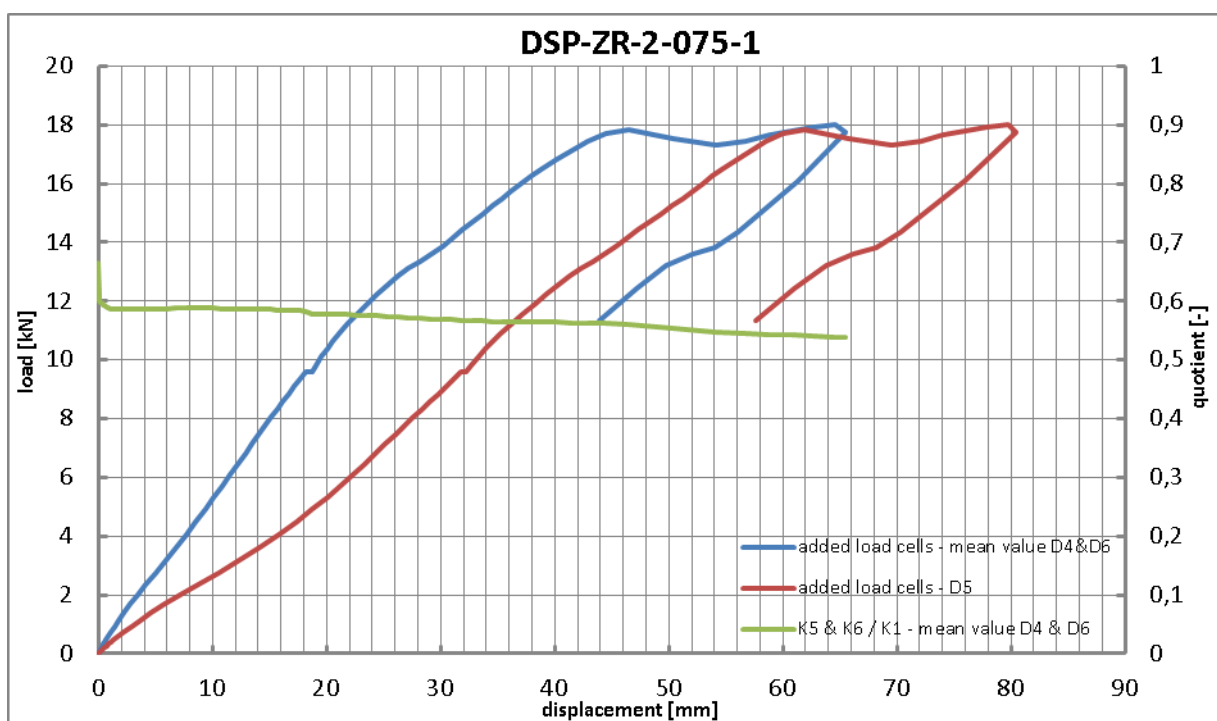
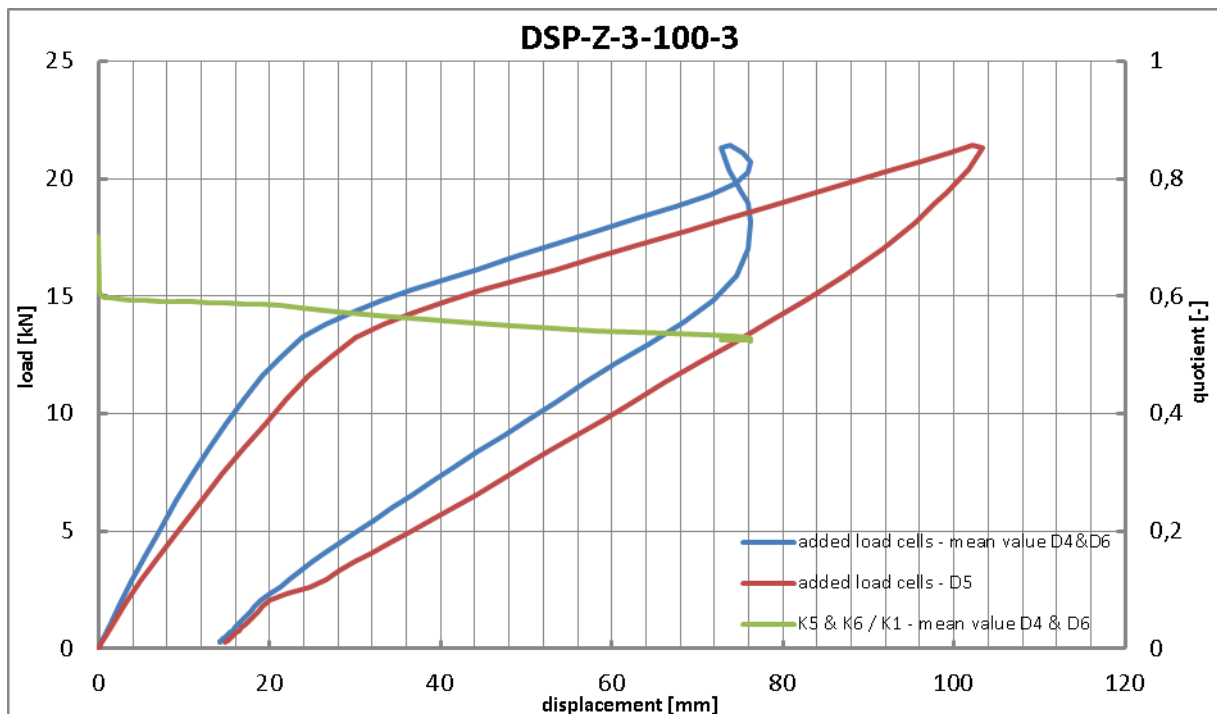


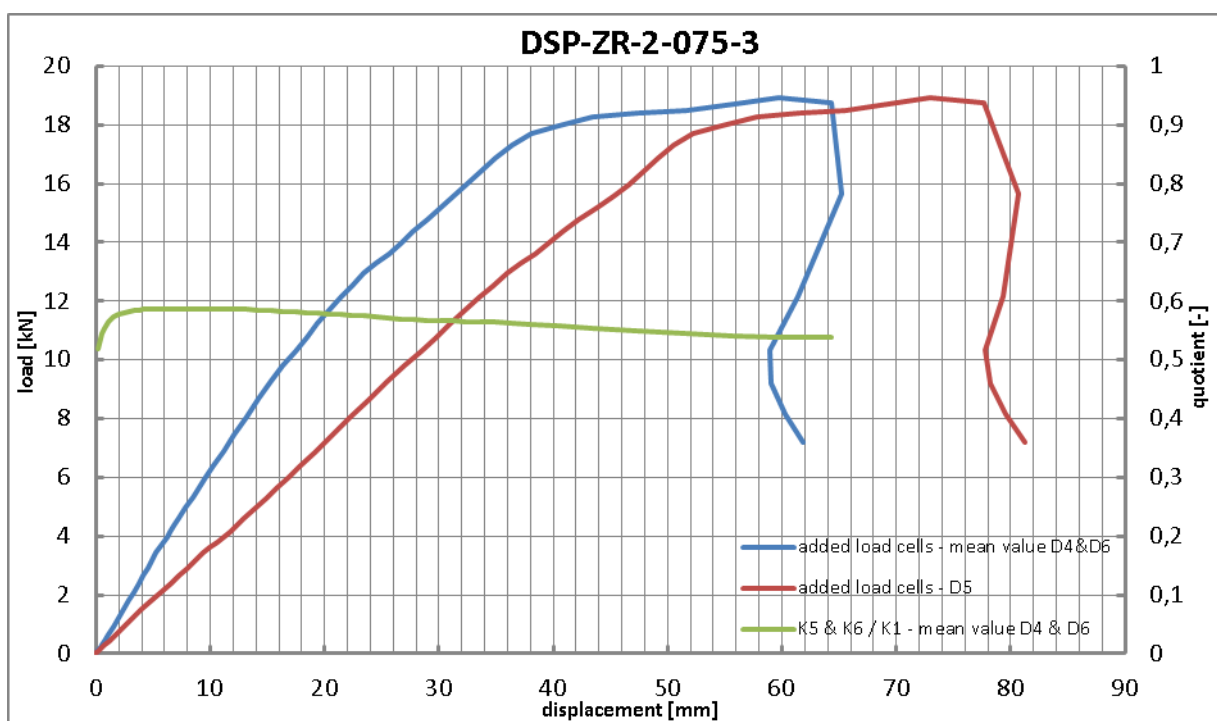
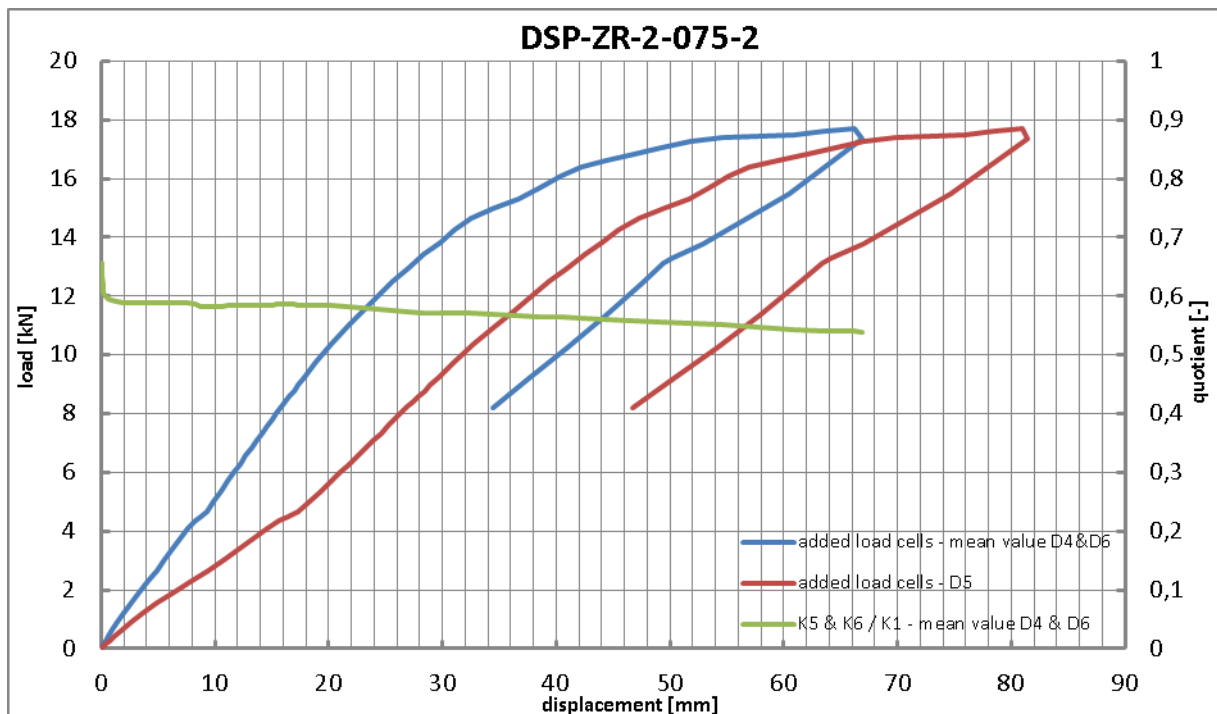


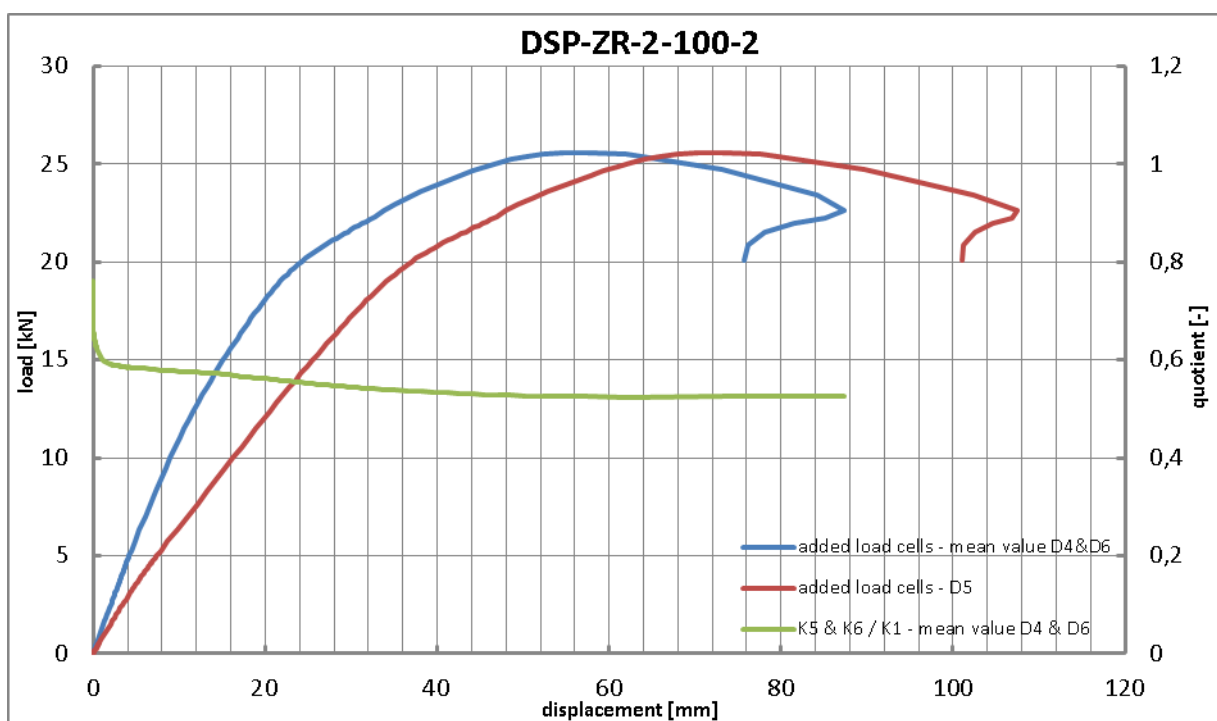
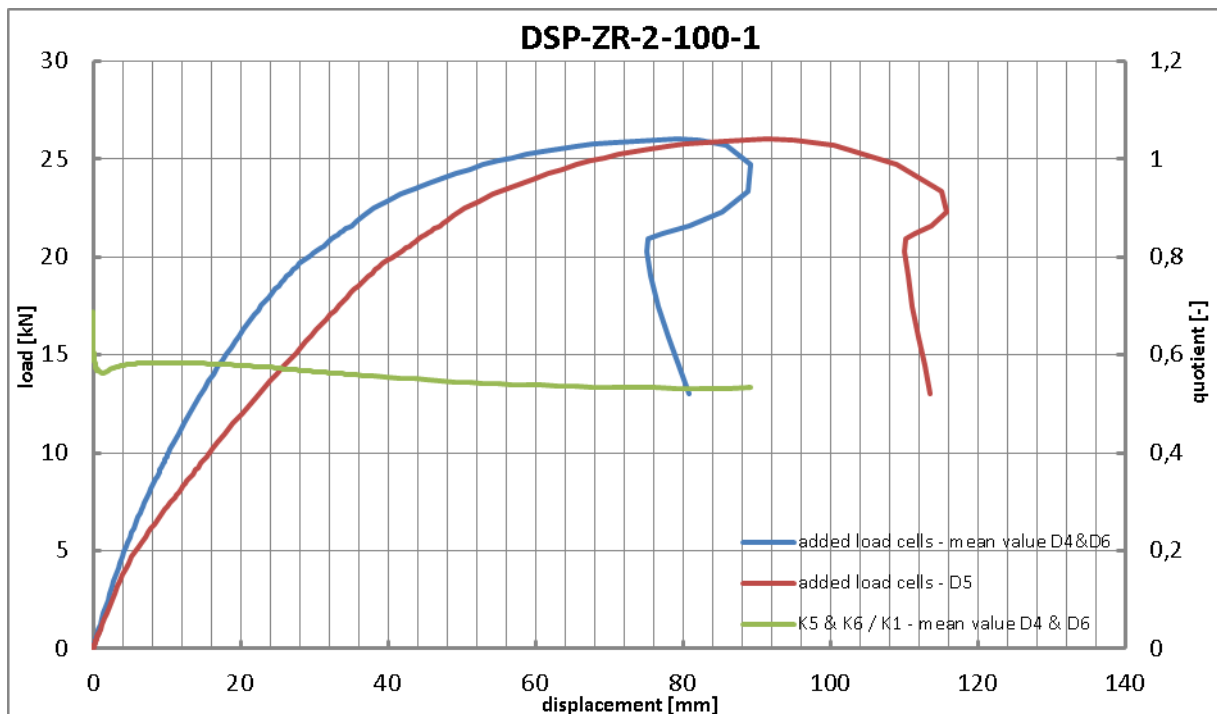


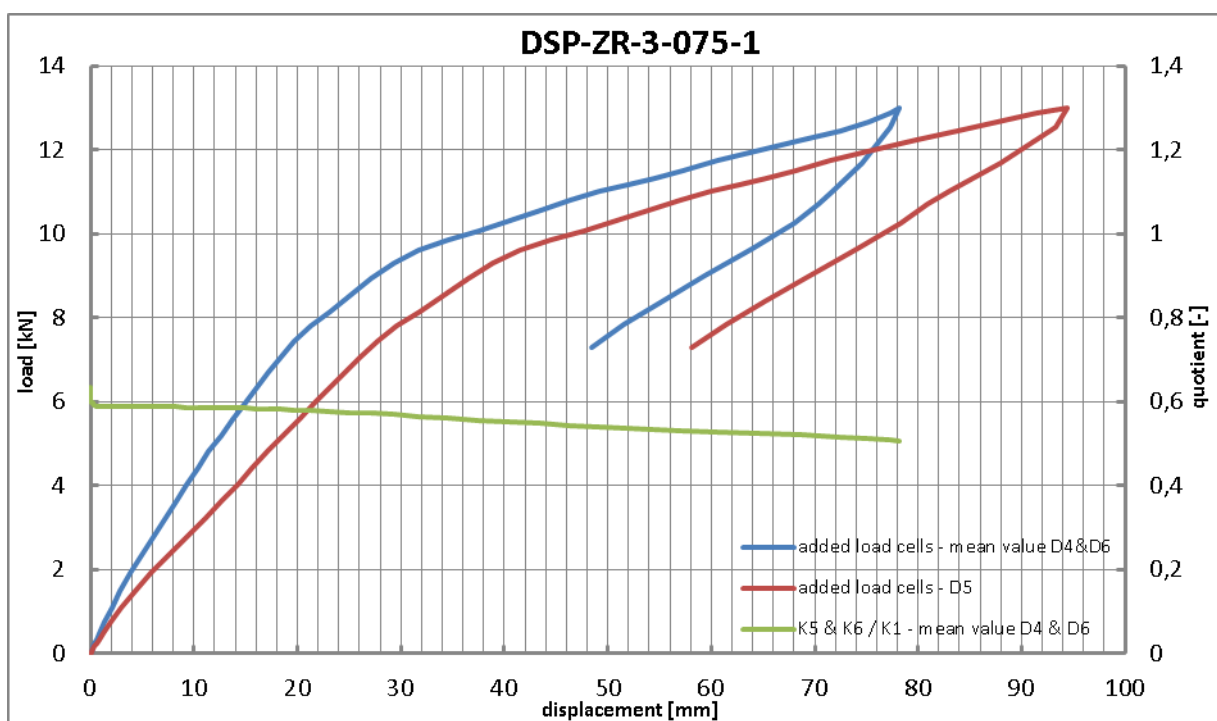
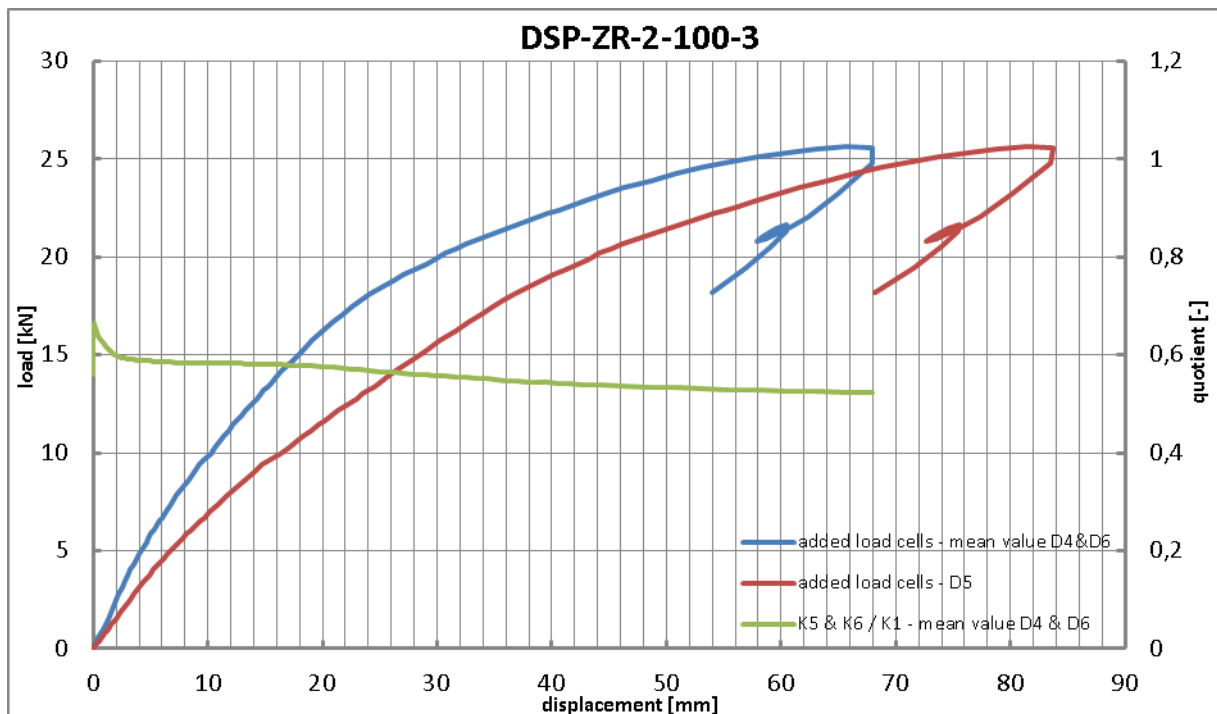


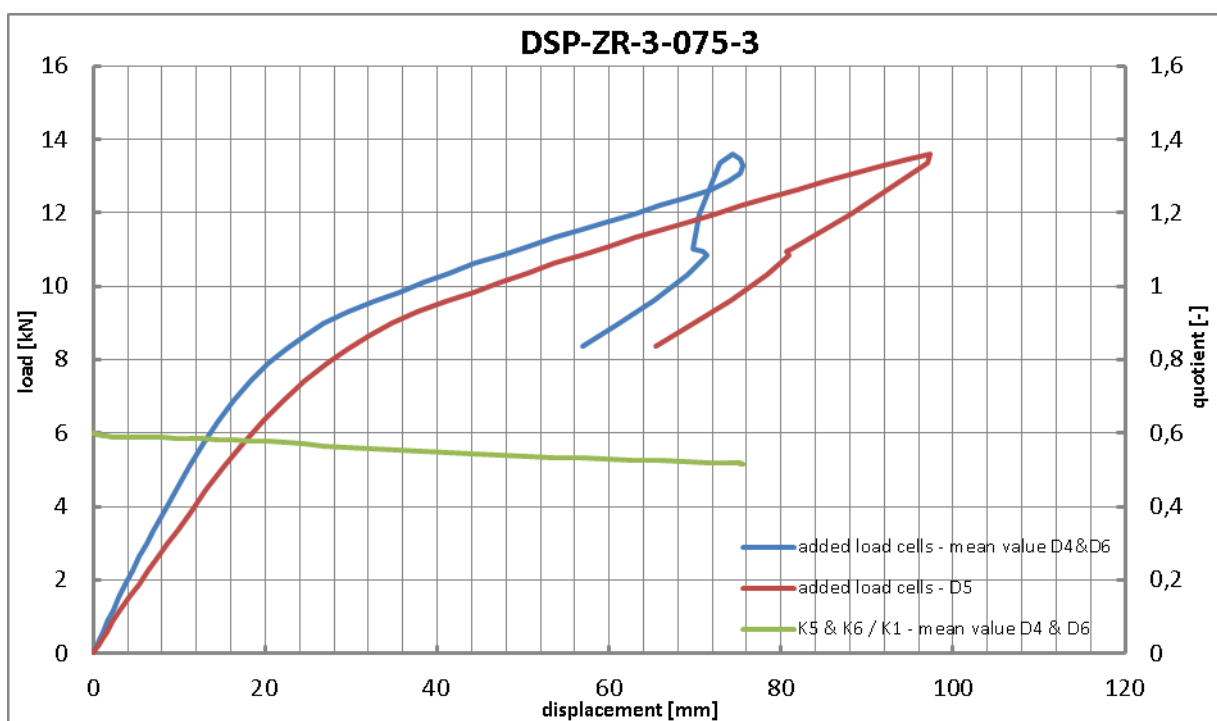
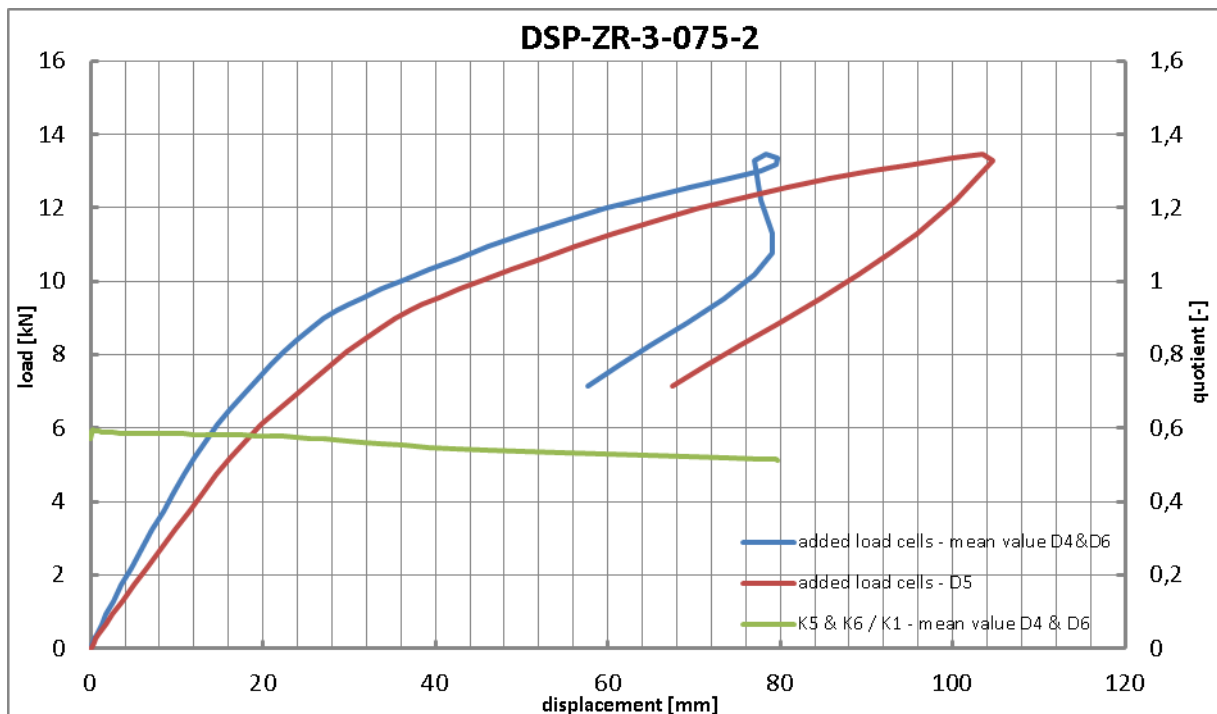


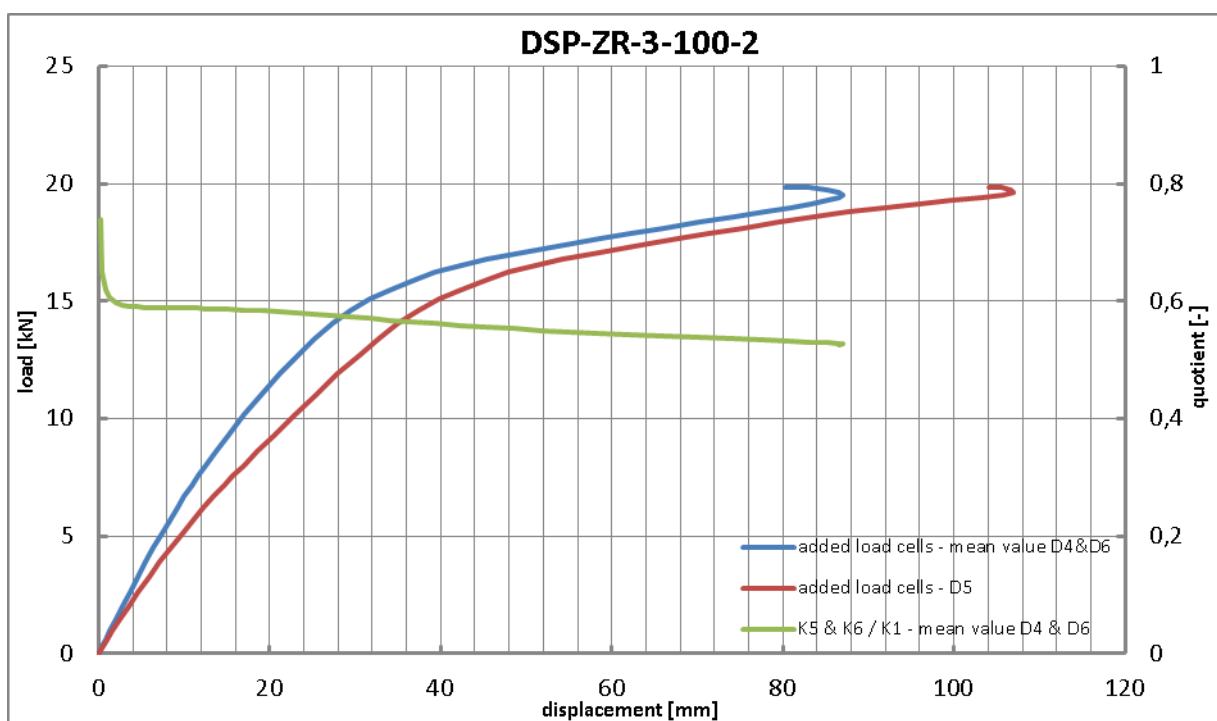
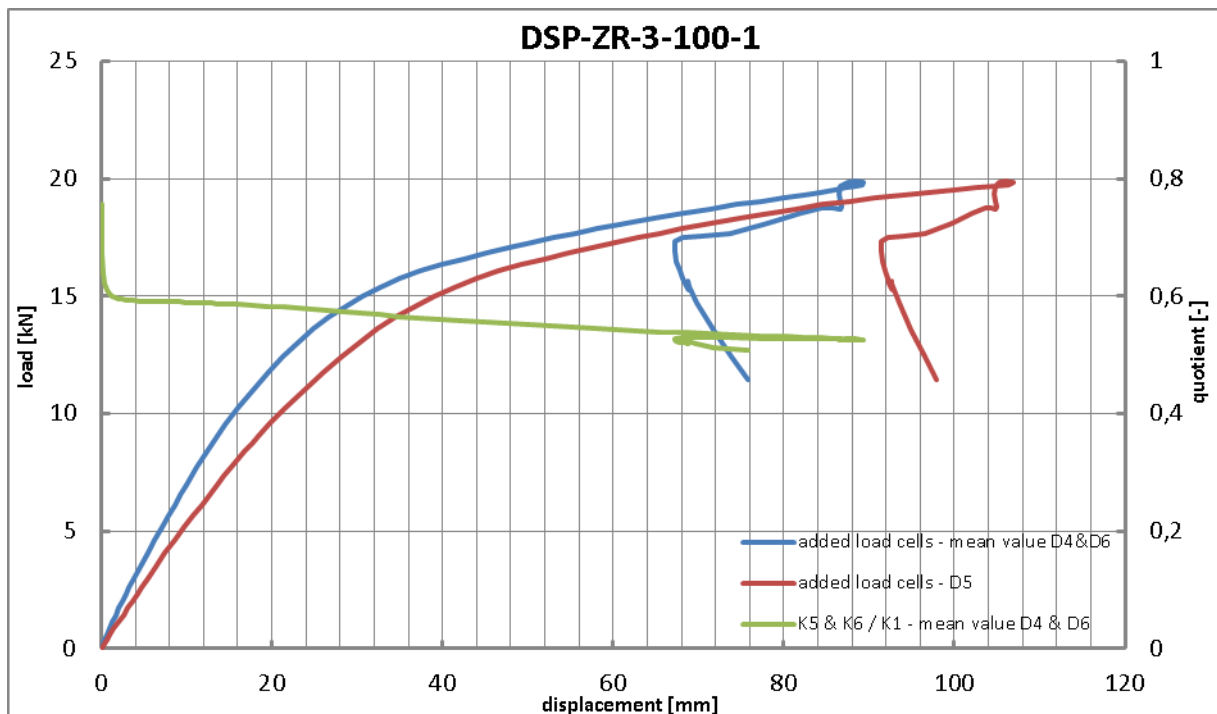


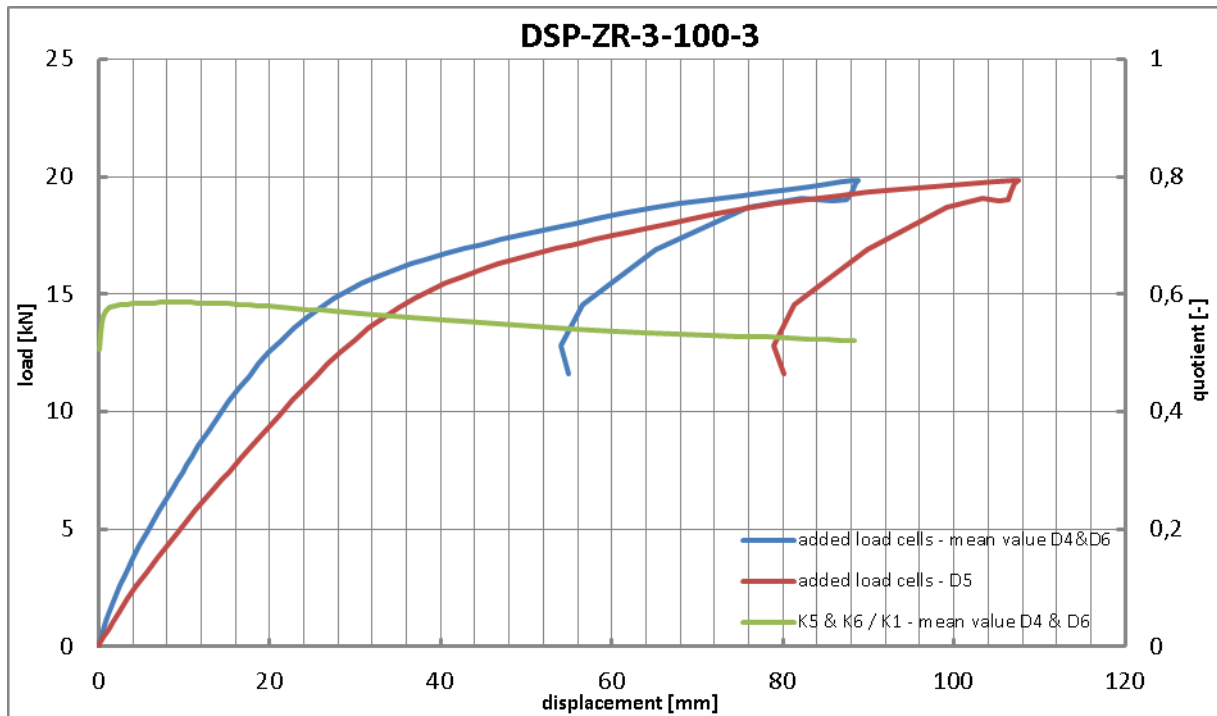












5 Annex E: Double span negative bending tests (suction tests)

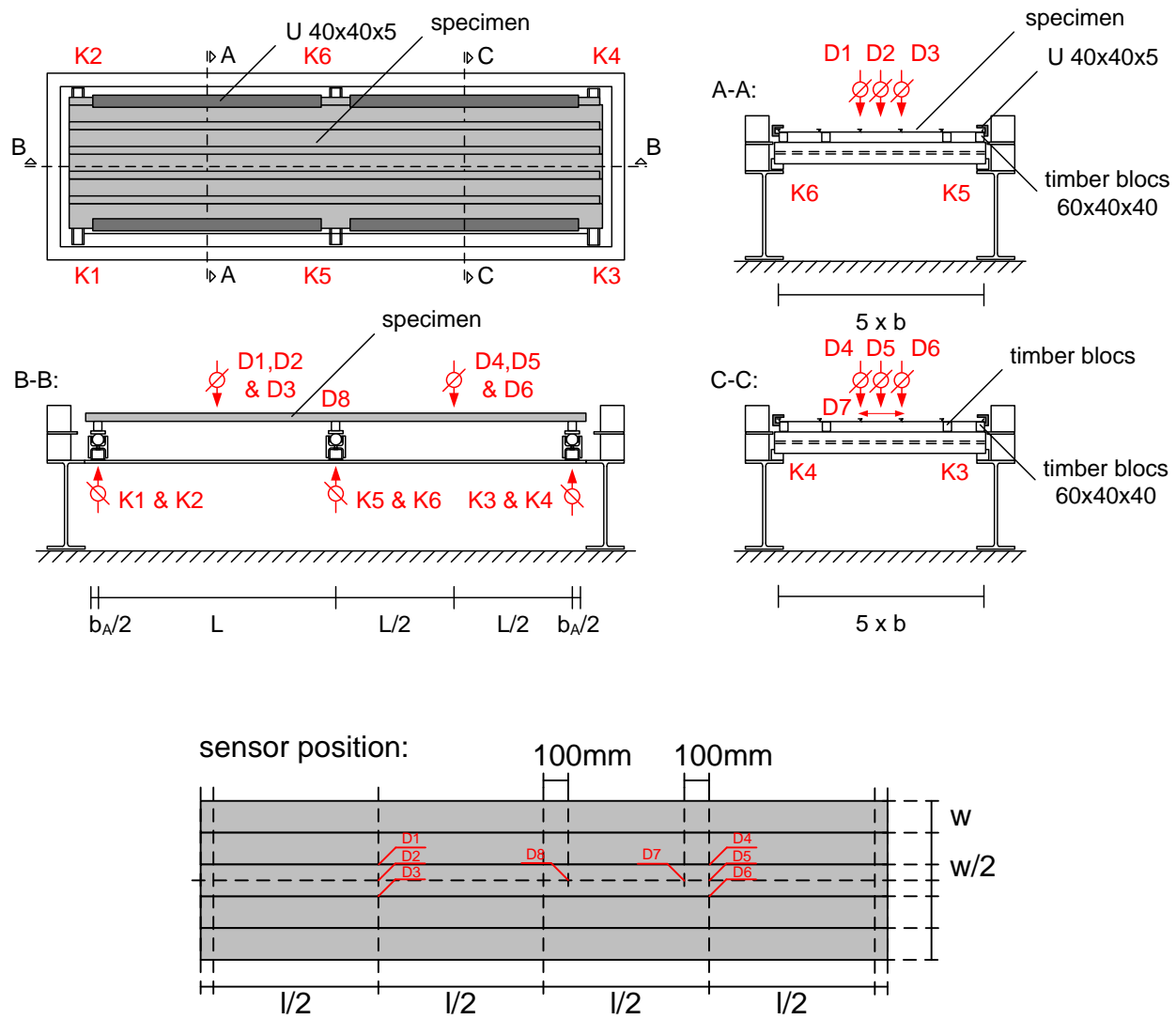


Fig. E.1: Schematic test setup



Fig. E.2: Test setup (without horizontal displacement sensors)

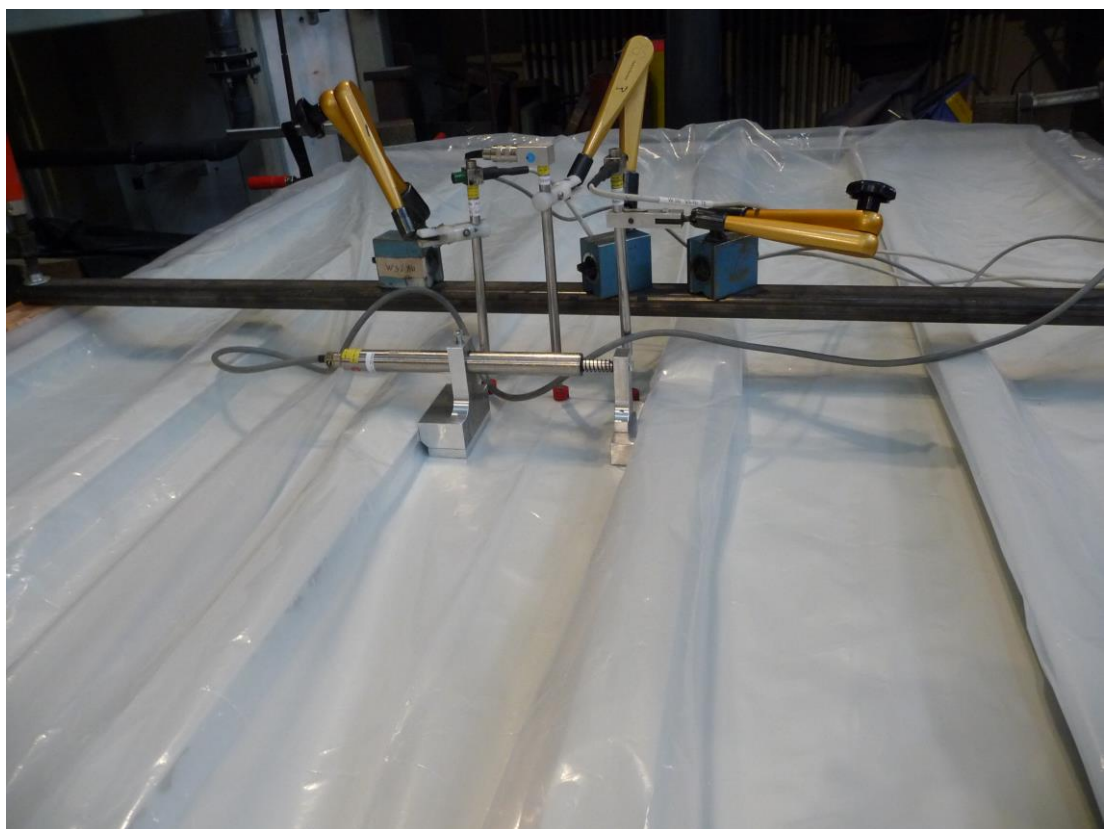


Fig. E.3: Test setup, horizontal displacement sensors

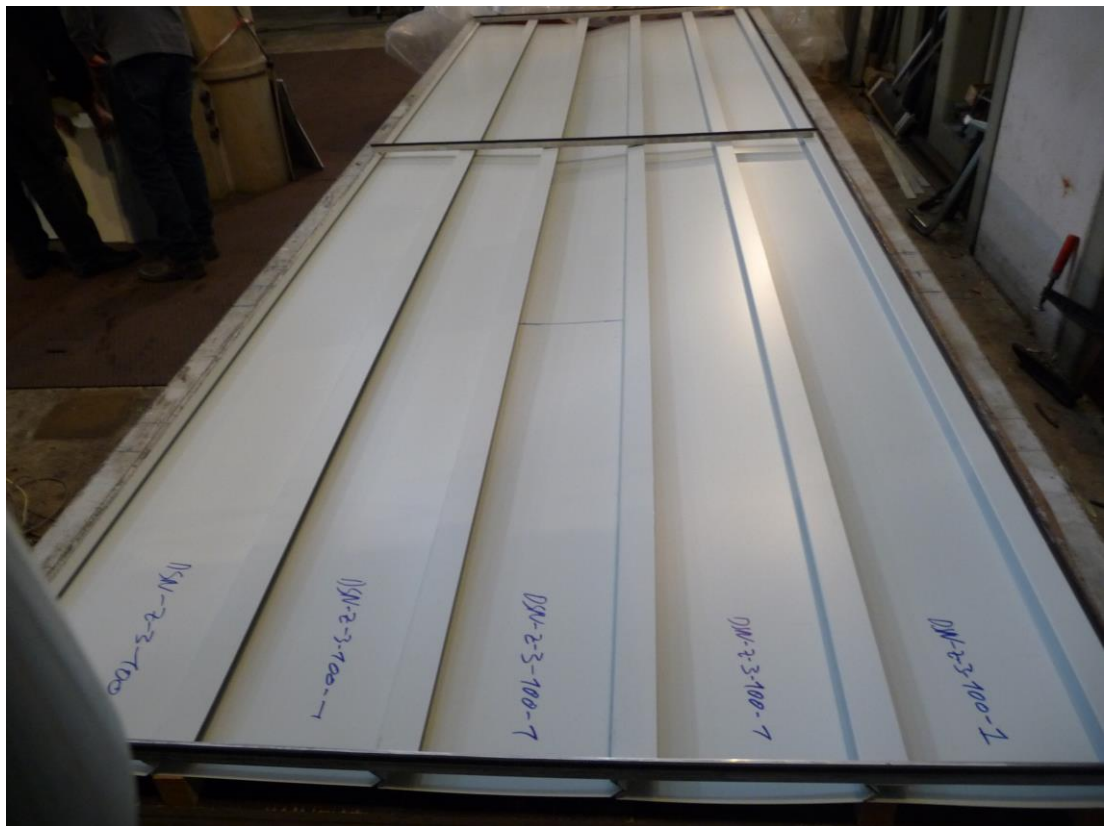


Fig. E.4: Failure by dislocation of the middle plank



Fig. E.5: Failure by local buckling of the compressed flanges

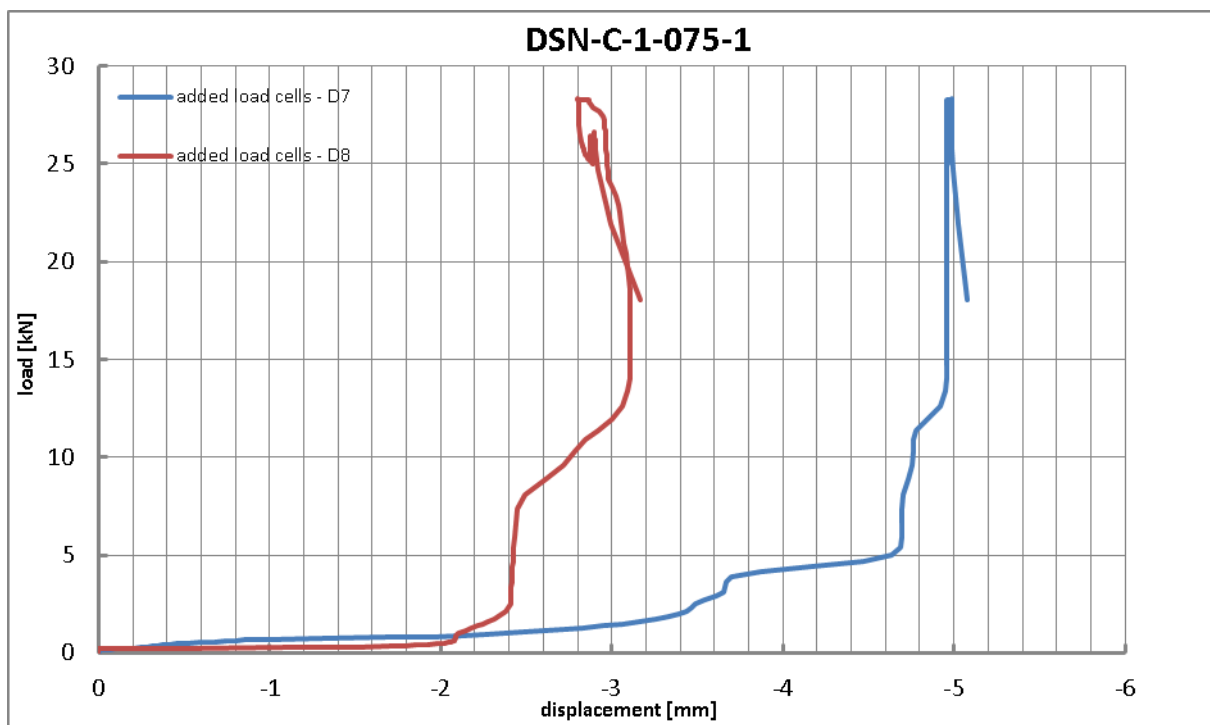
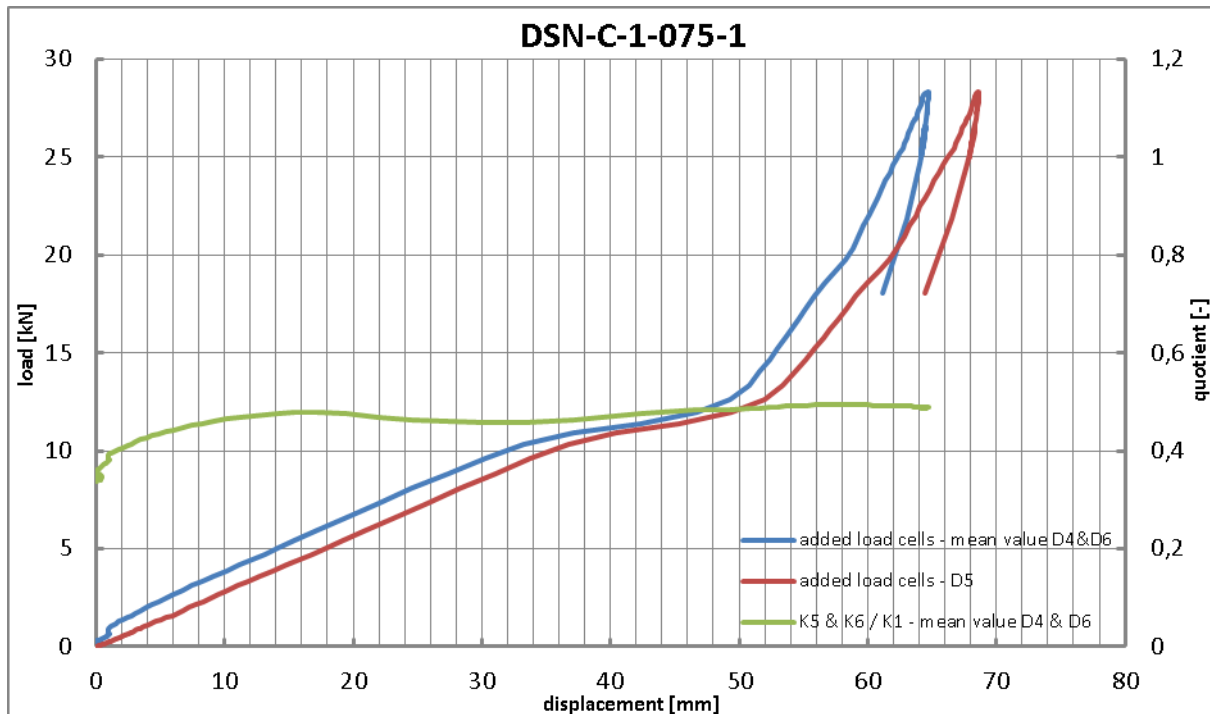


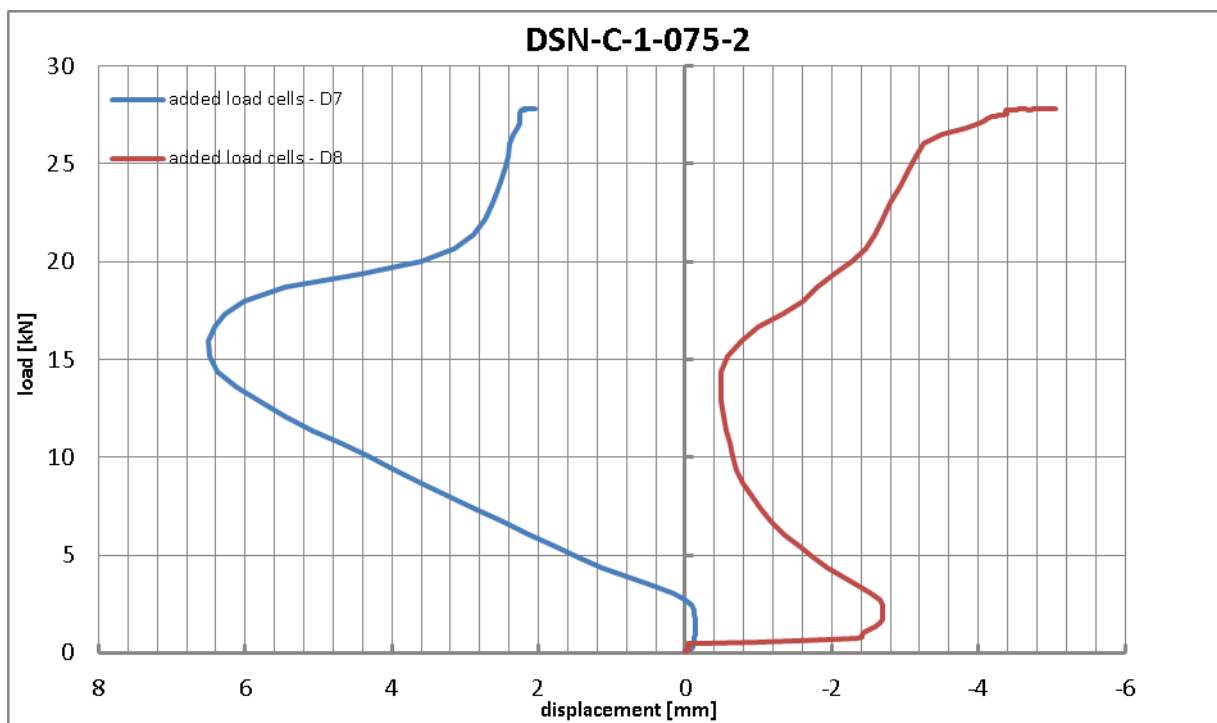
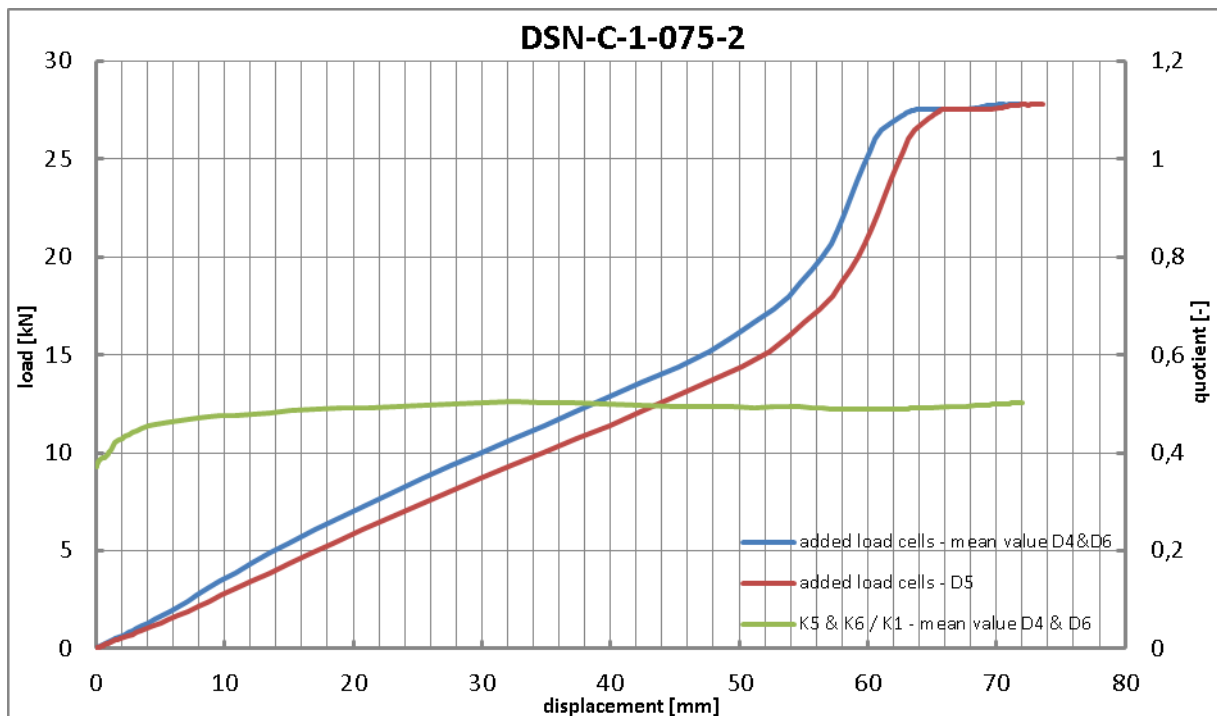
Fig. E.6: Failure by local buckling of the compressed flanges (DSN-Z-2-075-2)

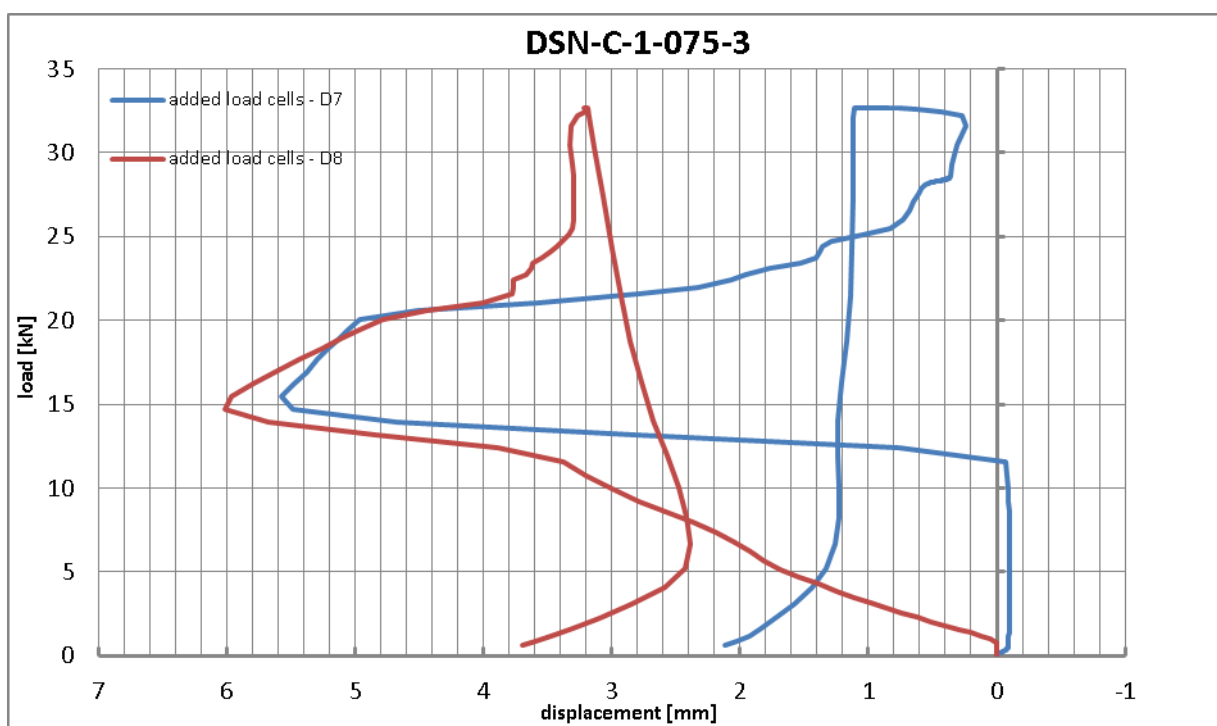
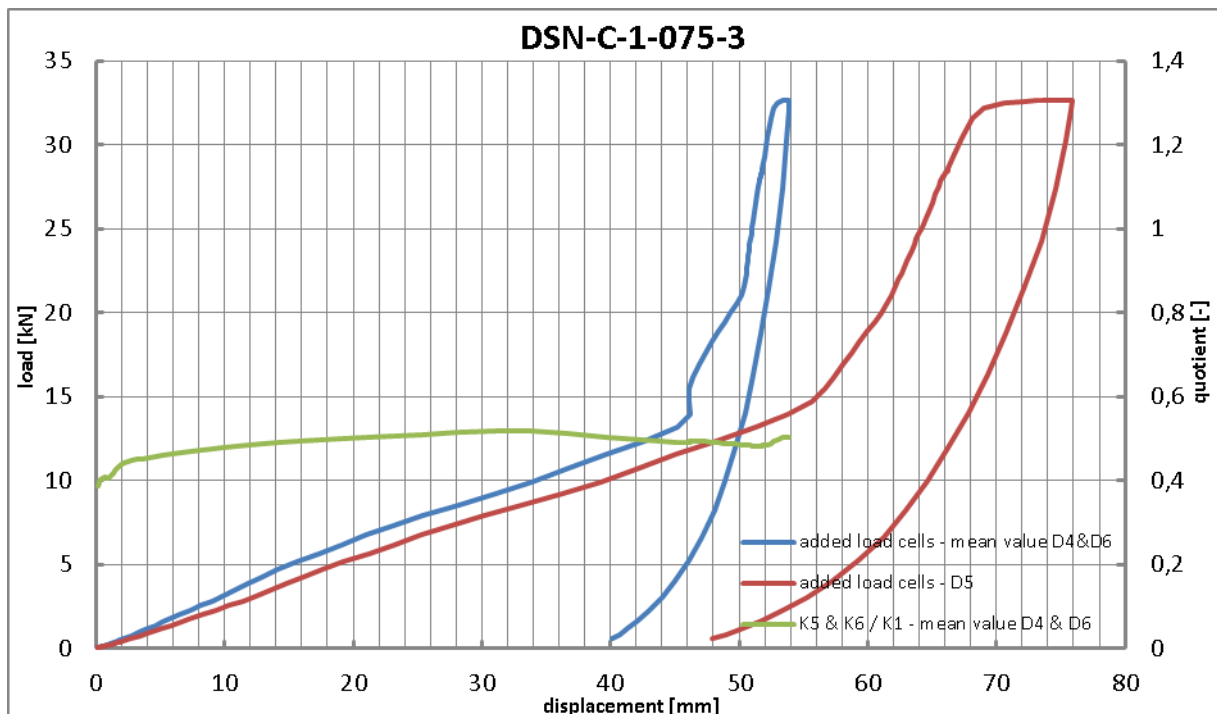


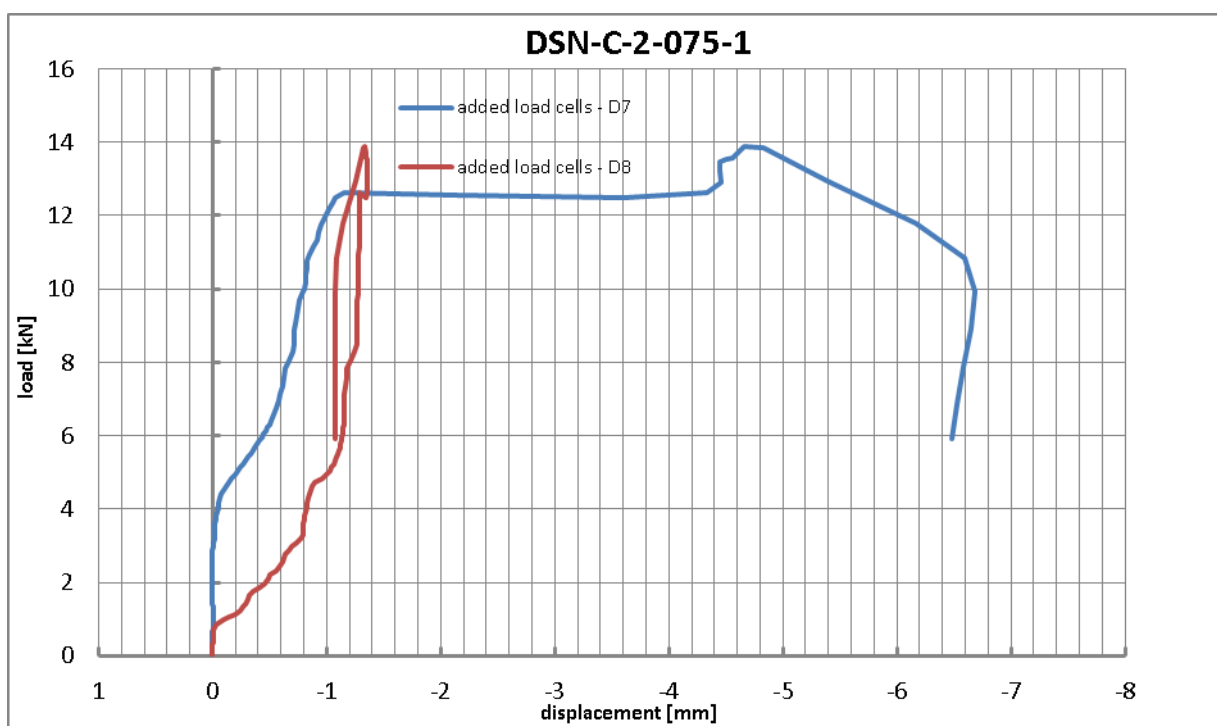
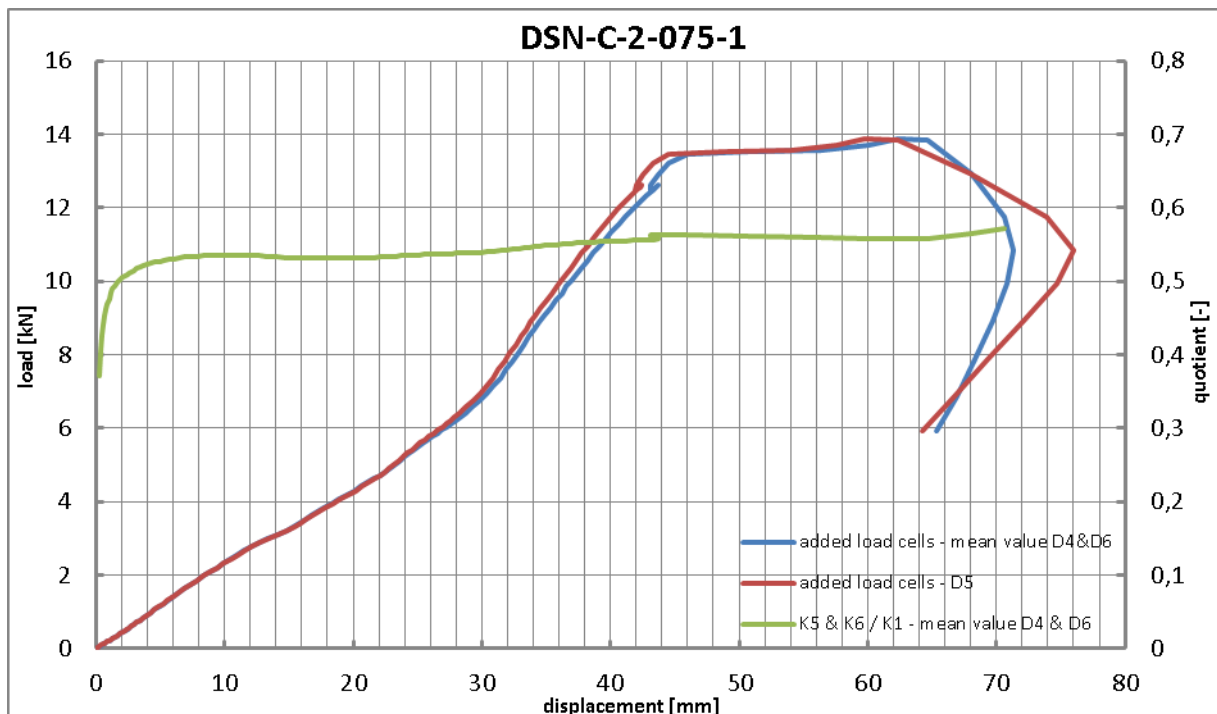
Fig. E.7: Failure by local buckling of the compressed flanges (DSN-C-1-075-2)

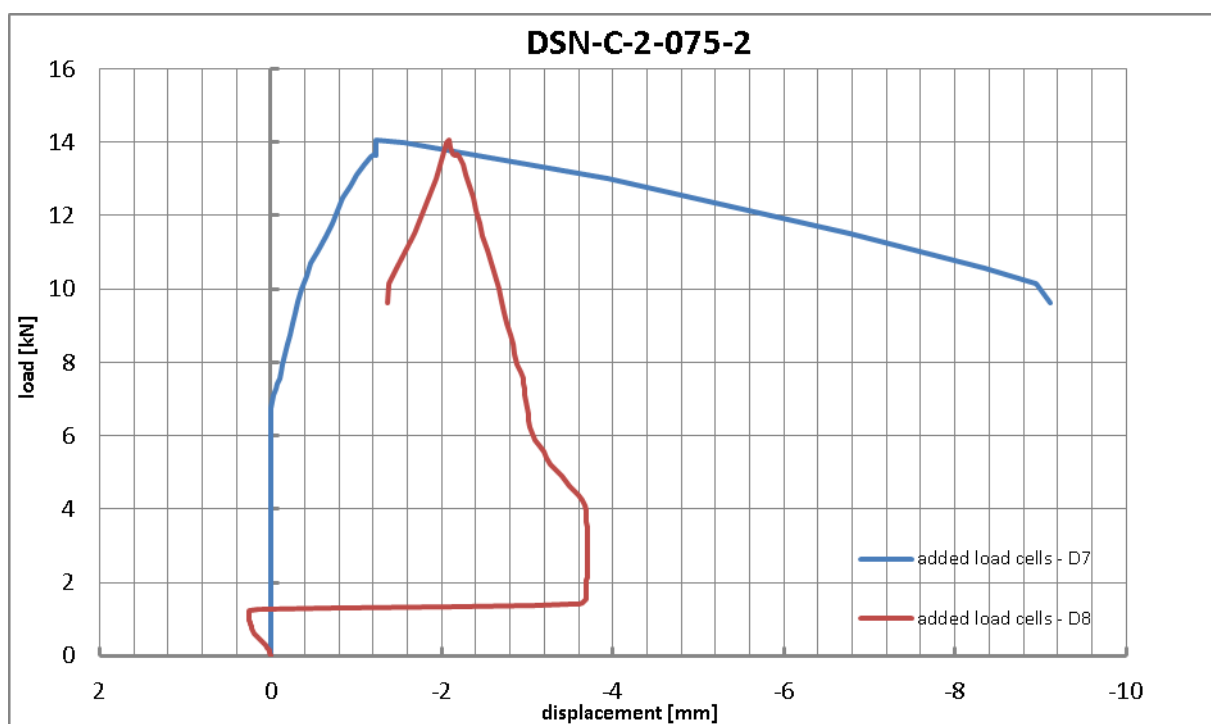
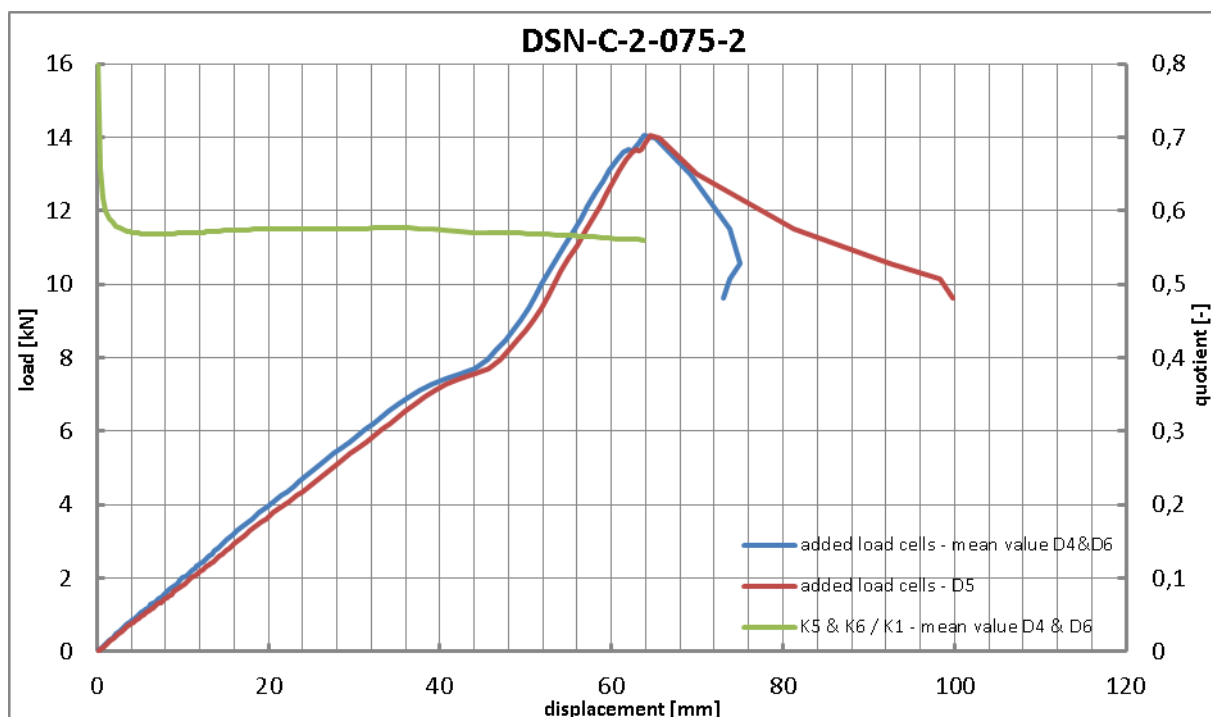
Load-deflection-curves:

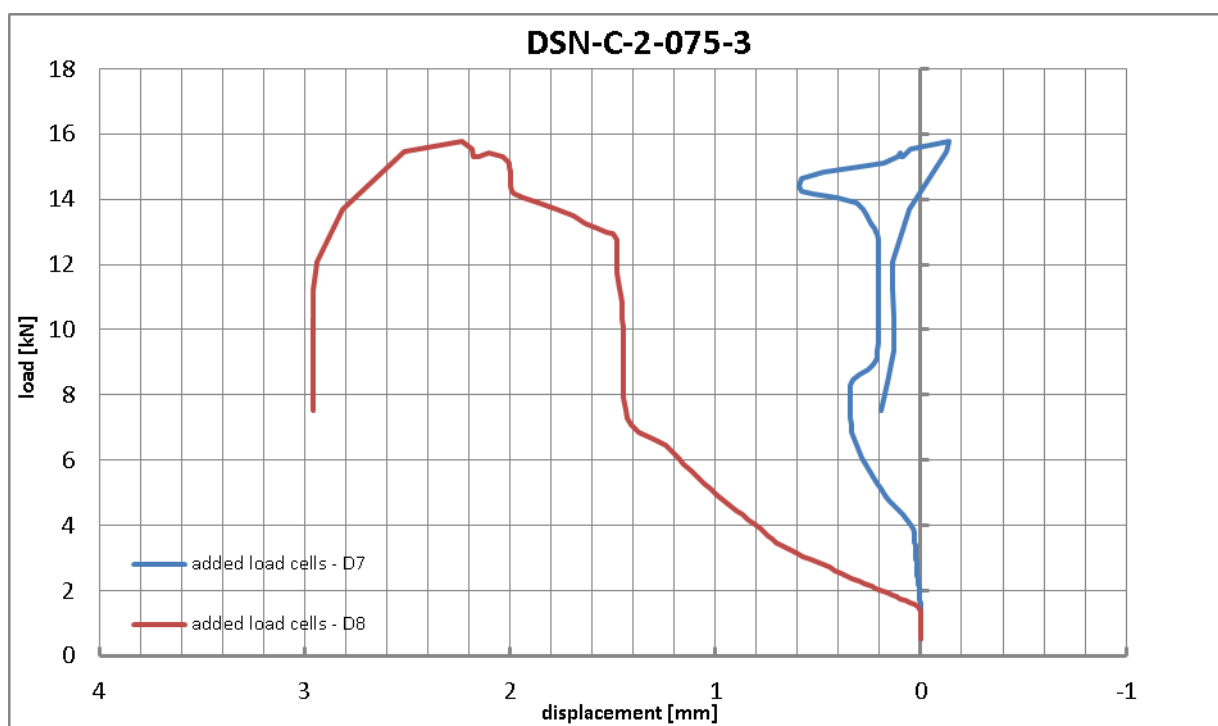
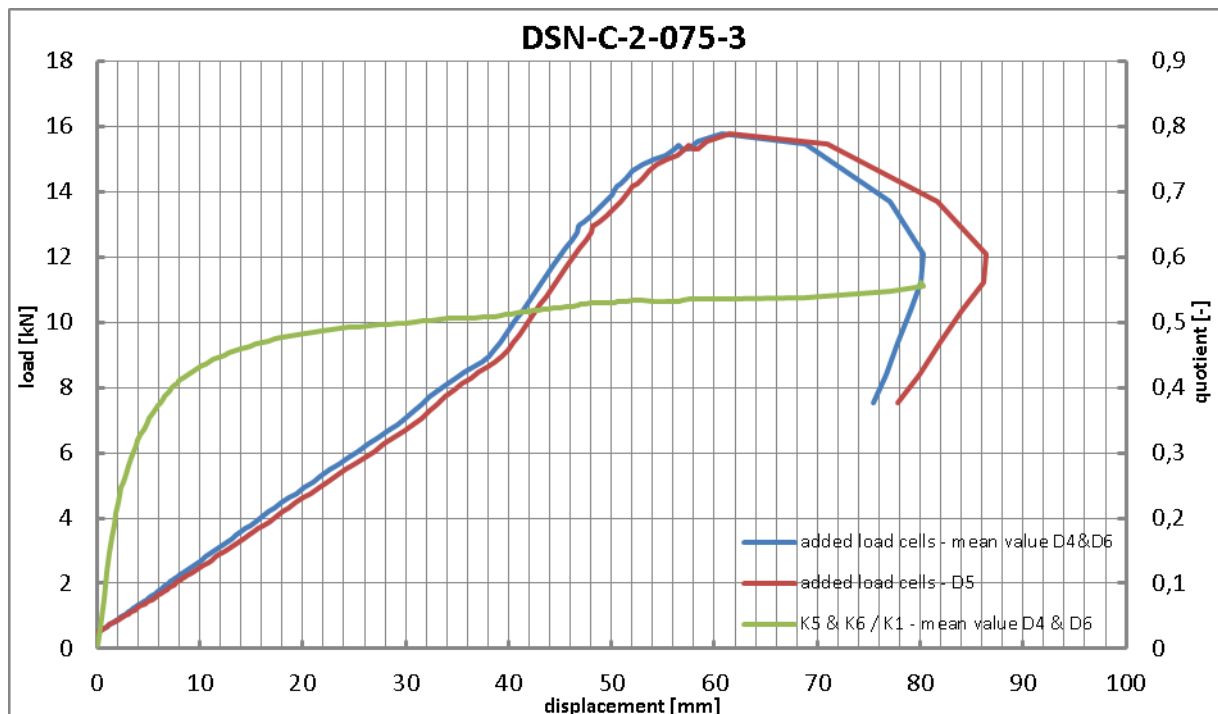


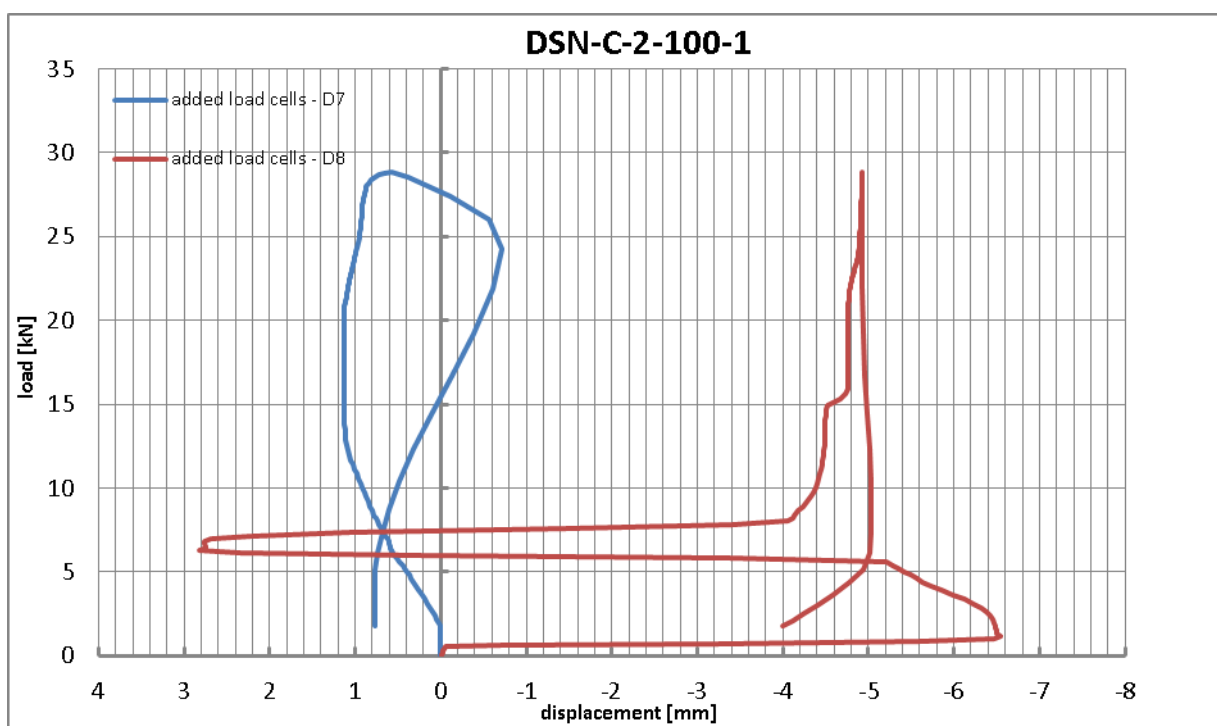
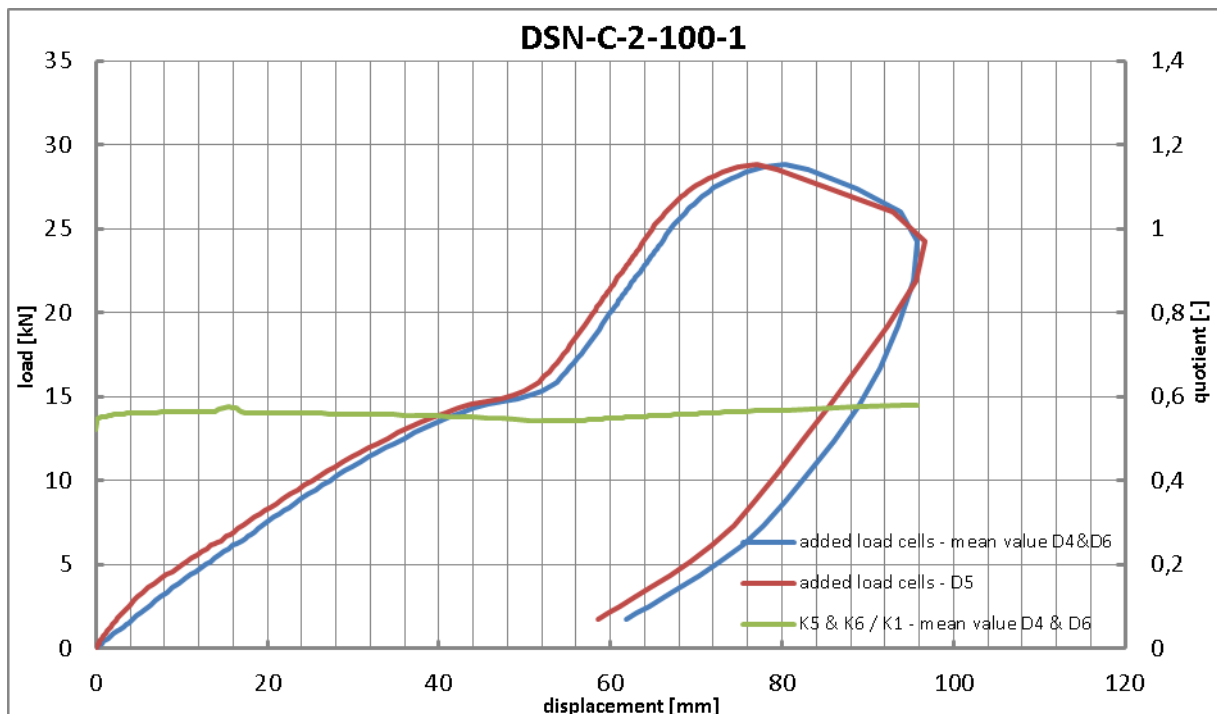


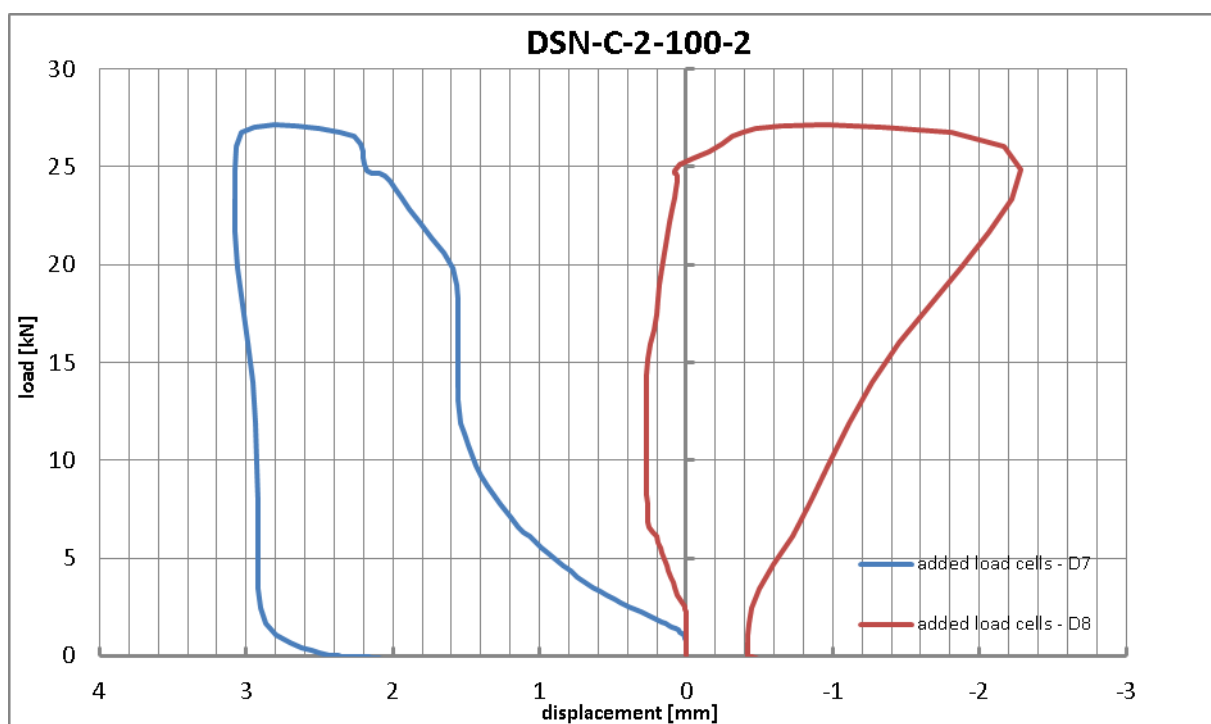
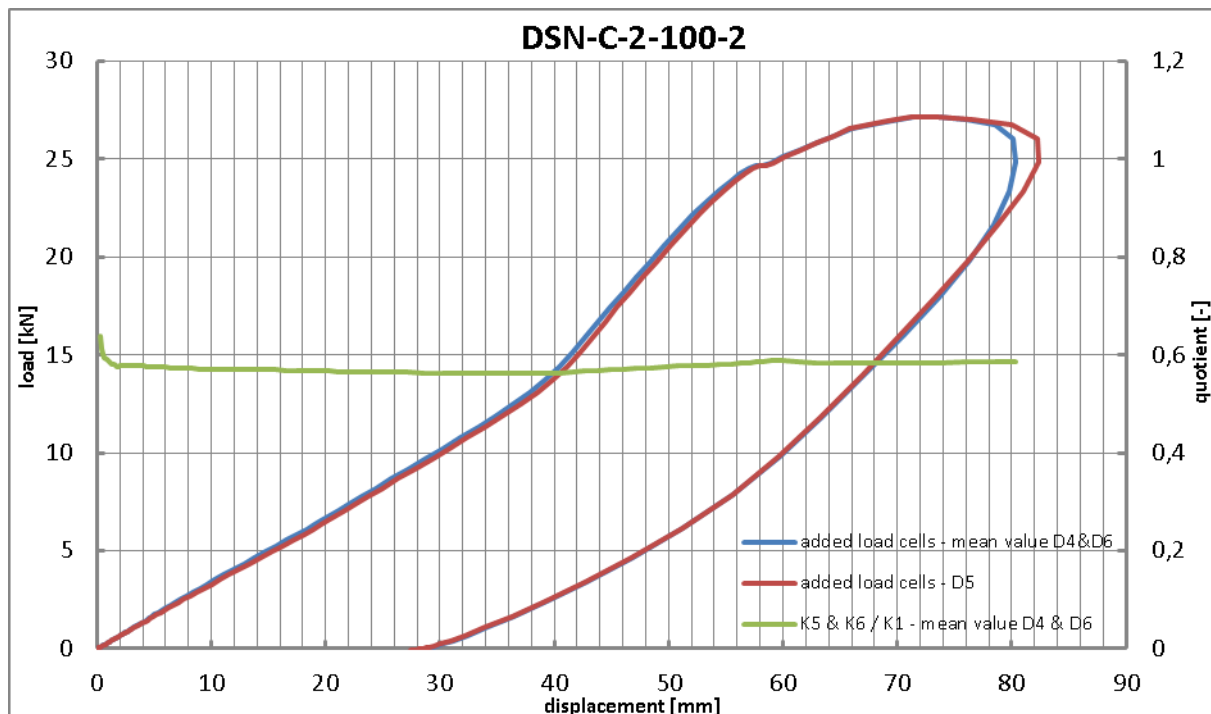


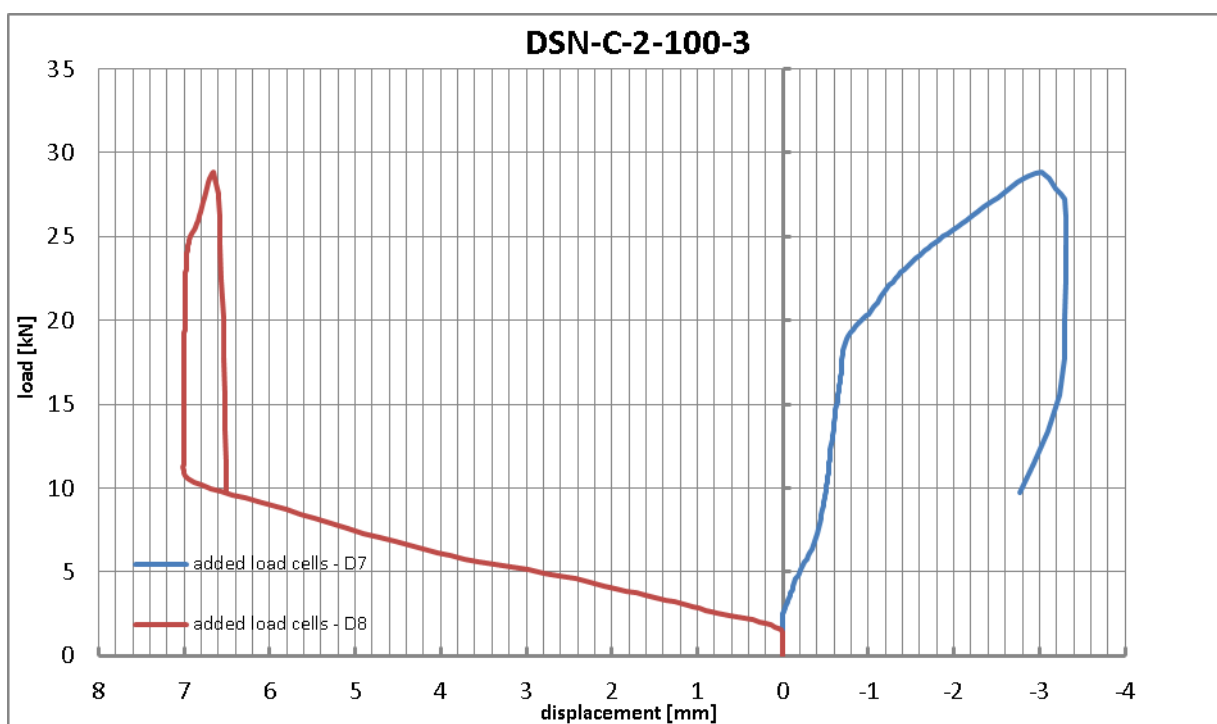
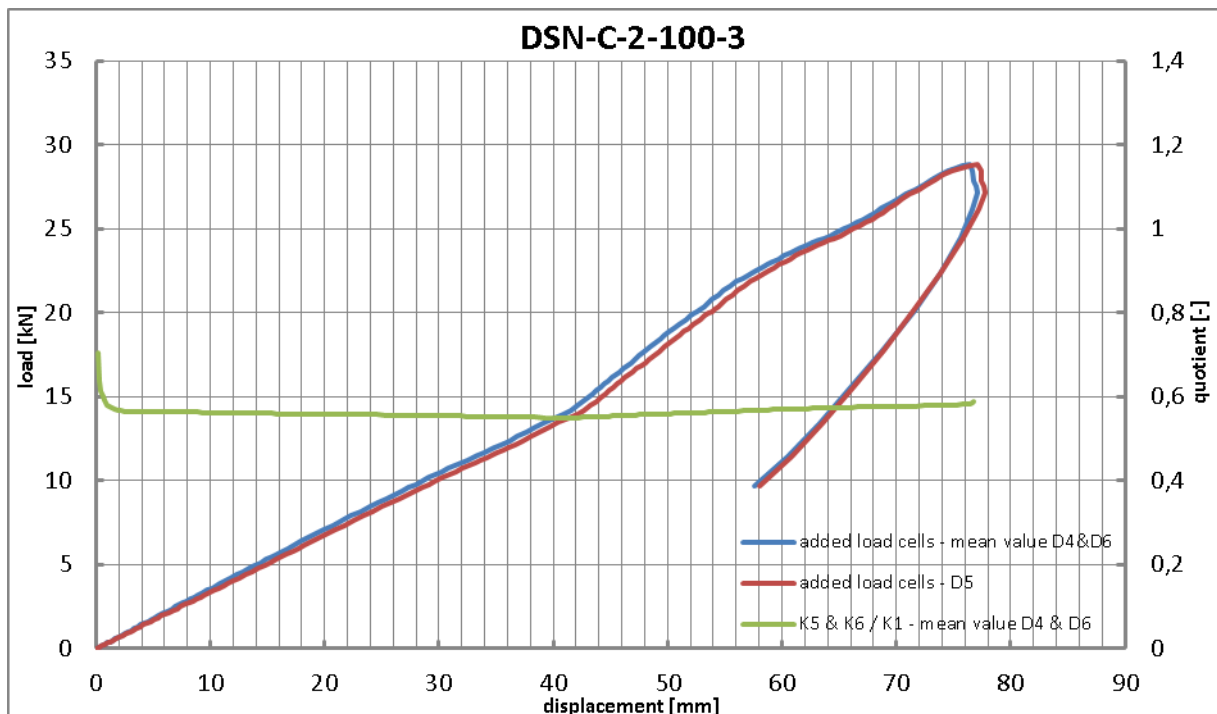


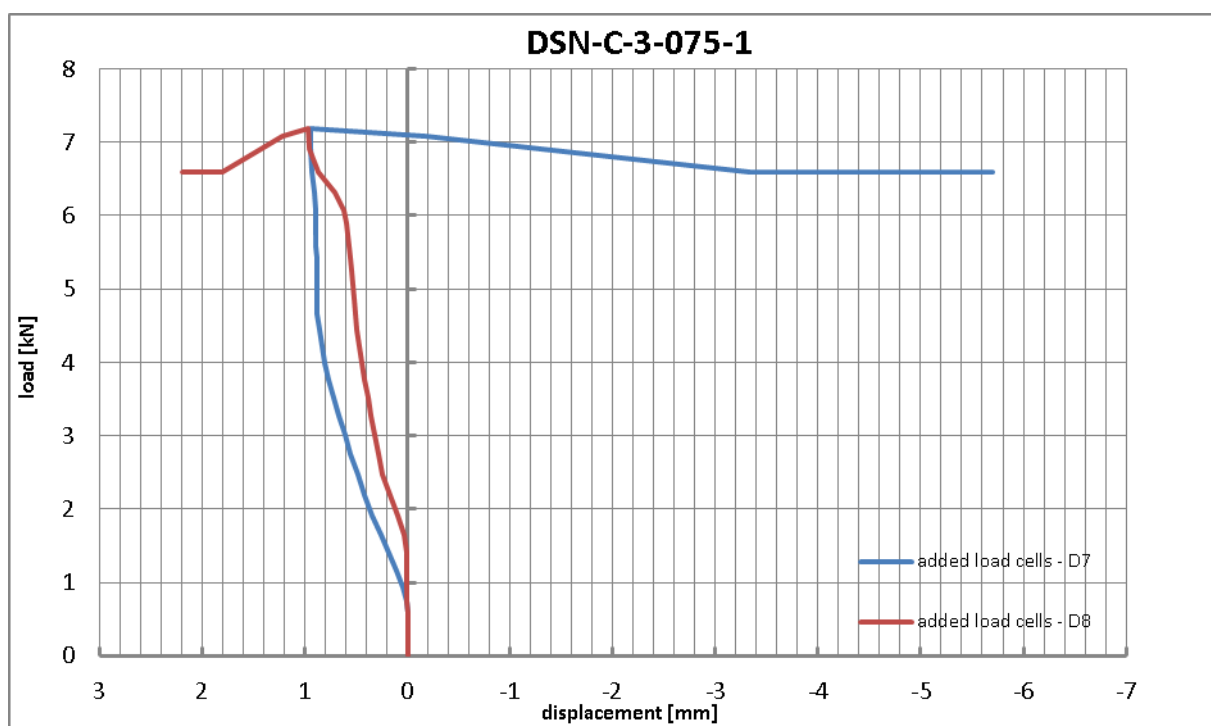
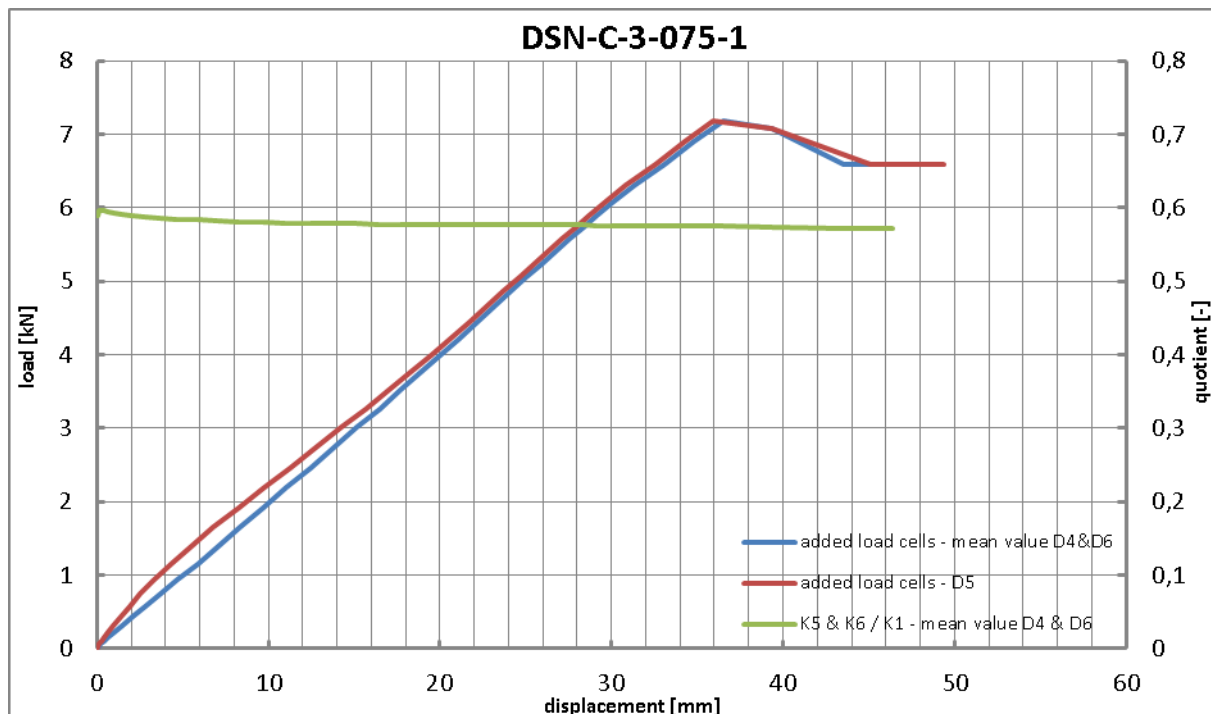


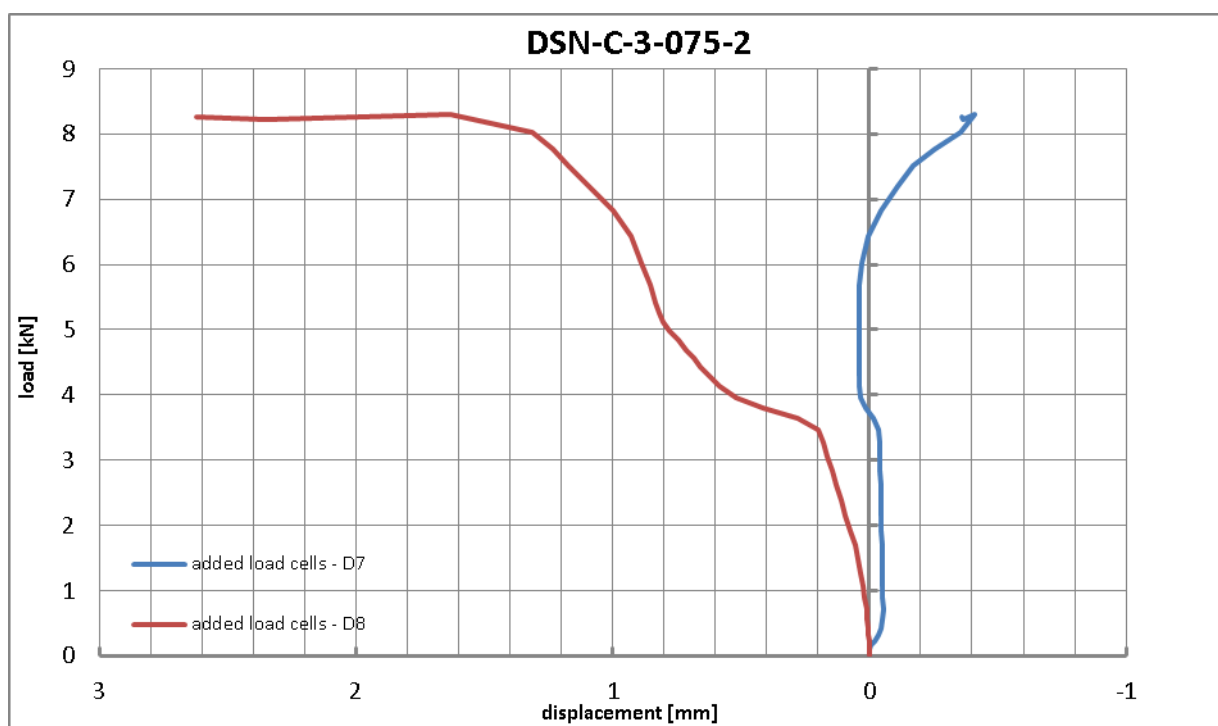
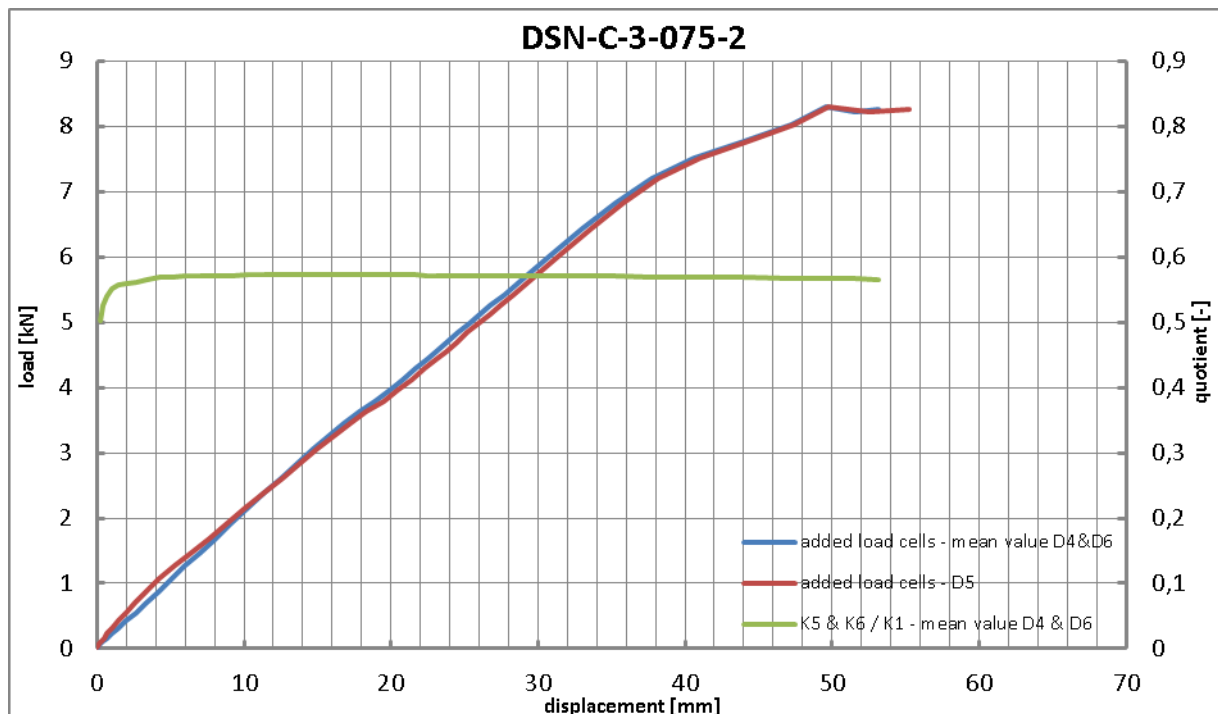


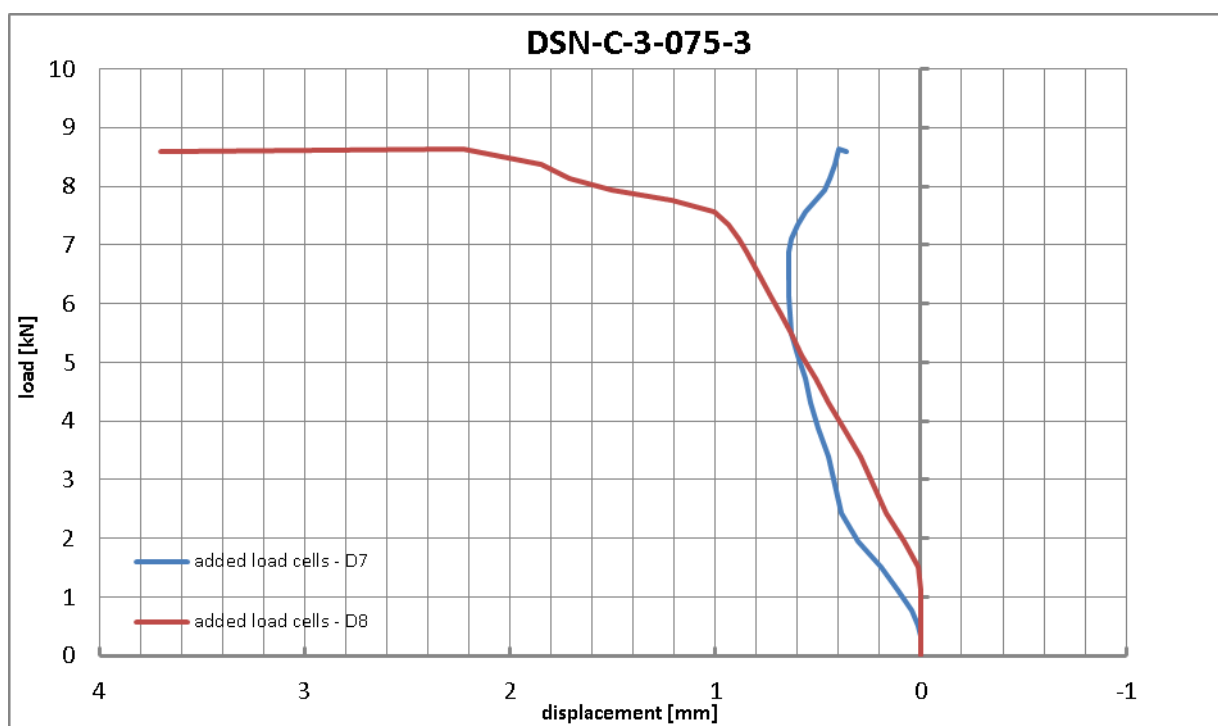
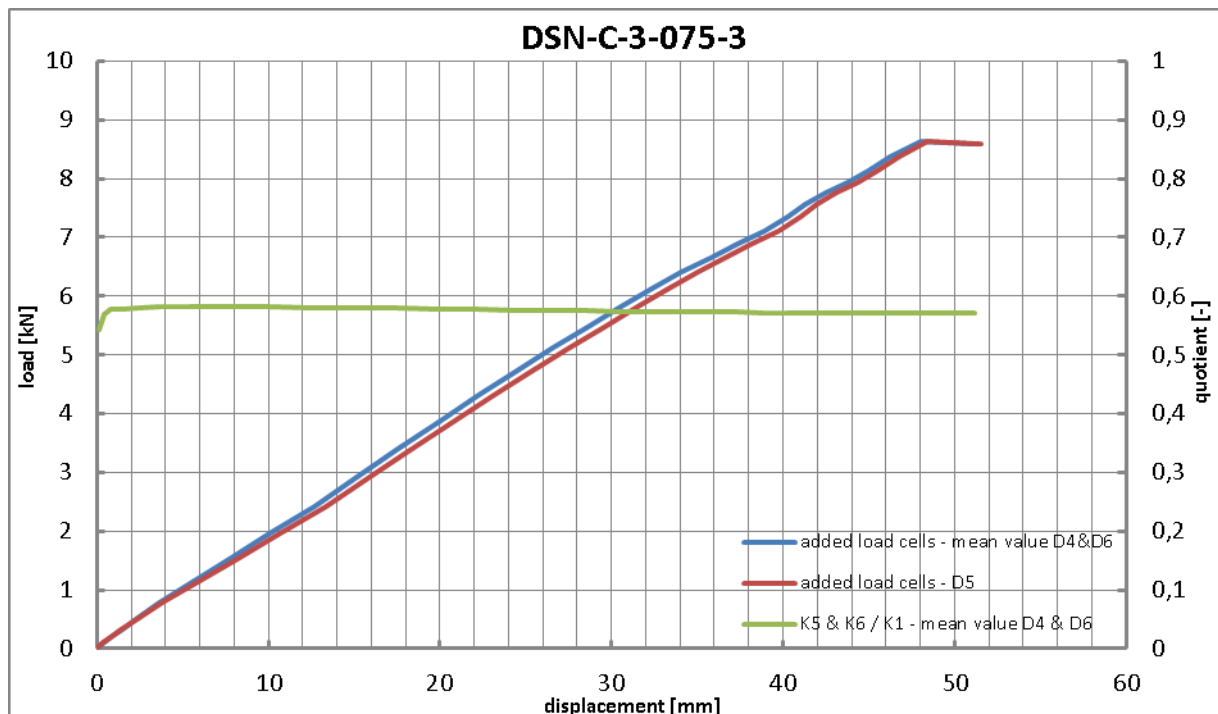


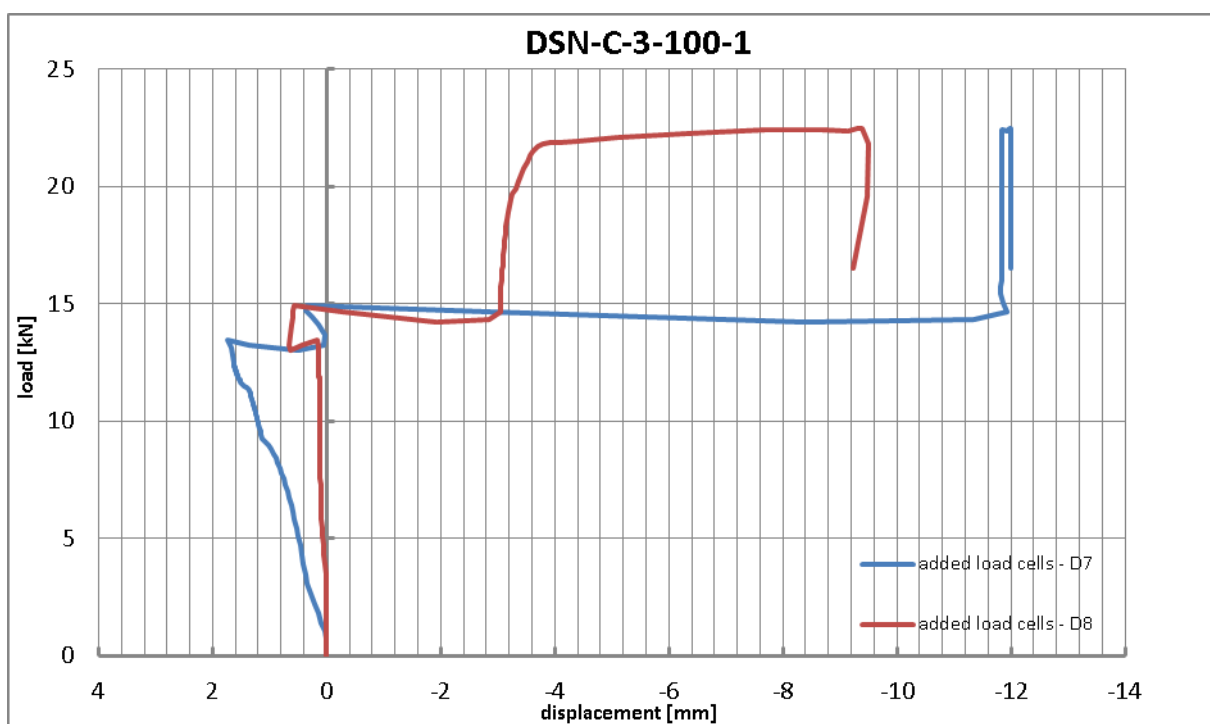
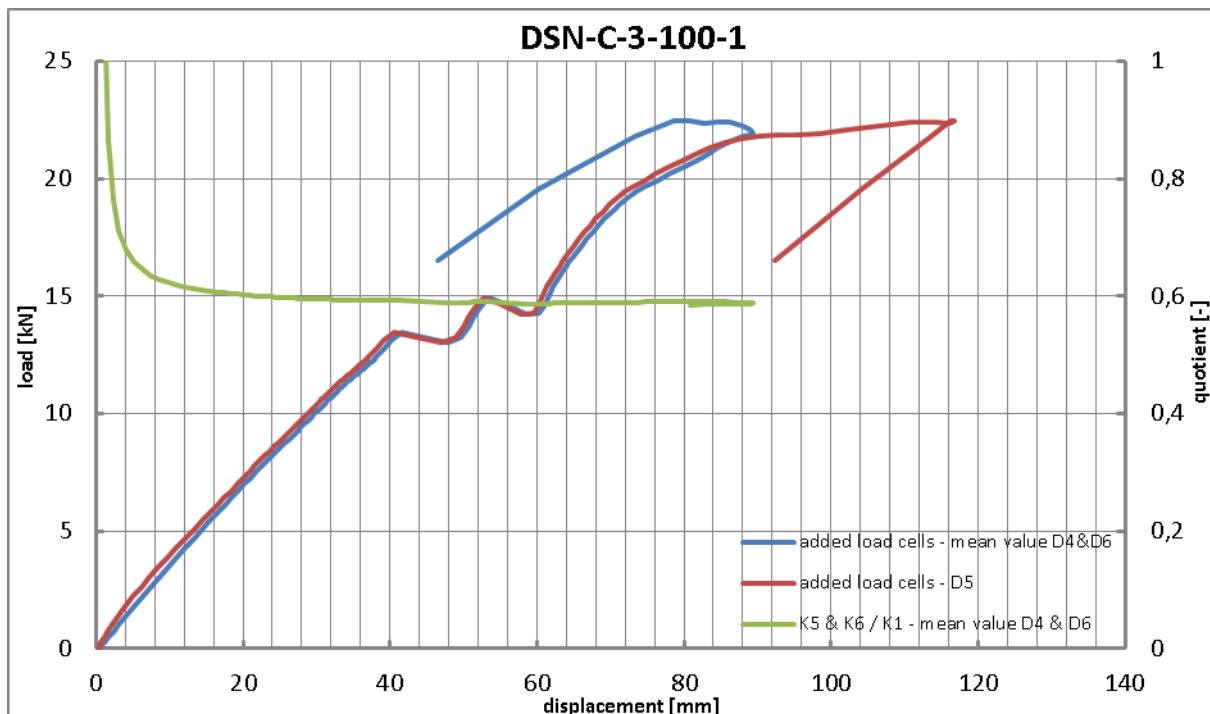


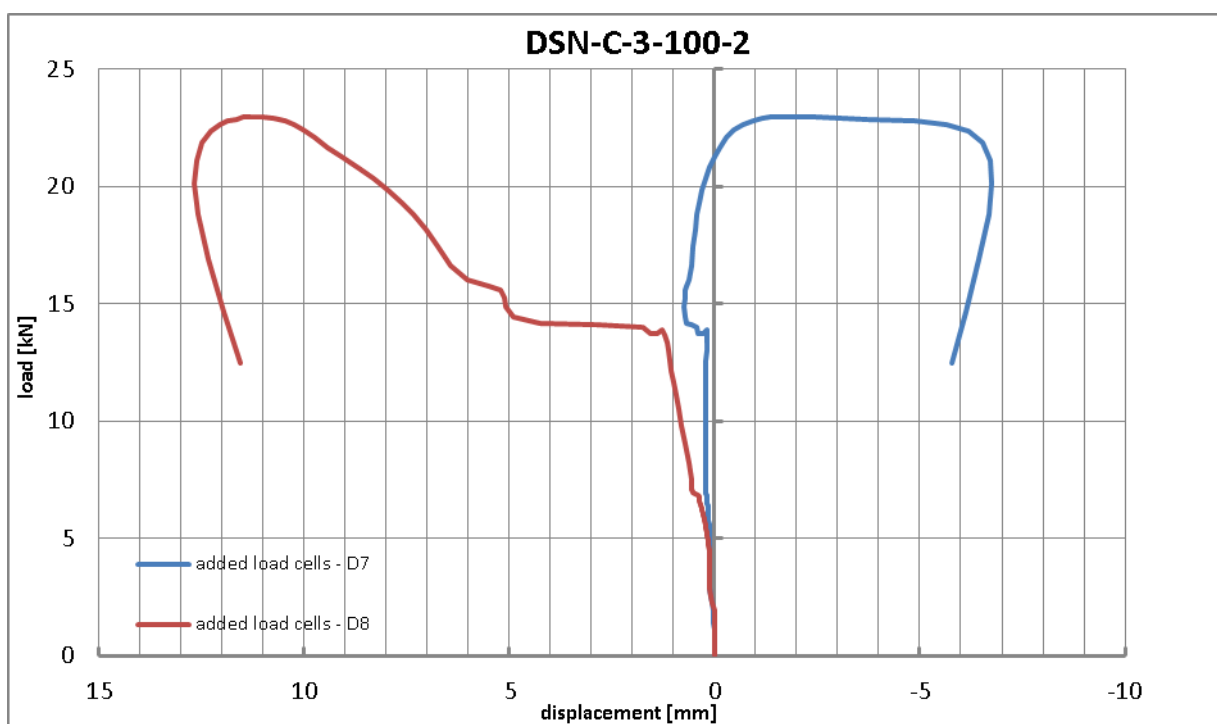
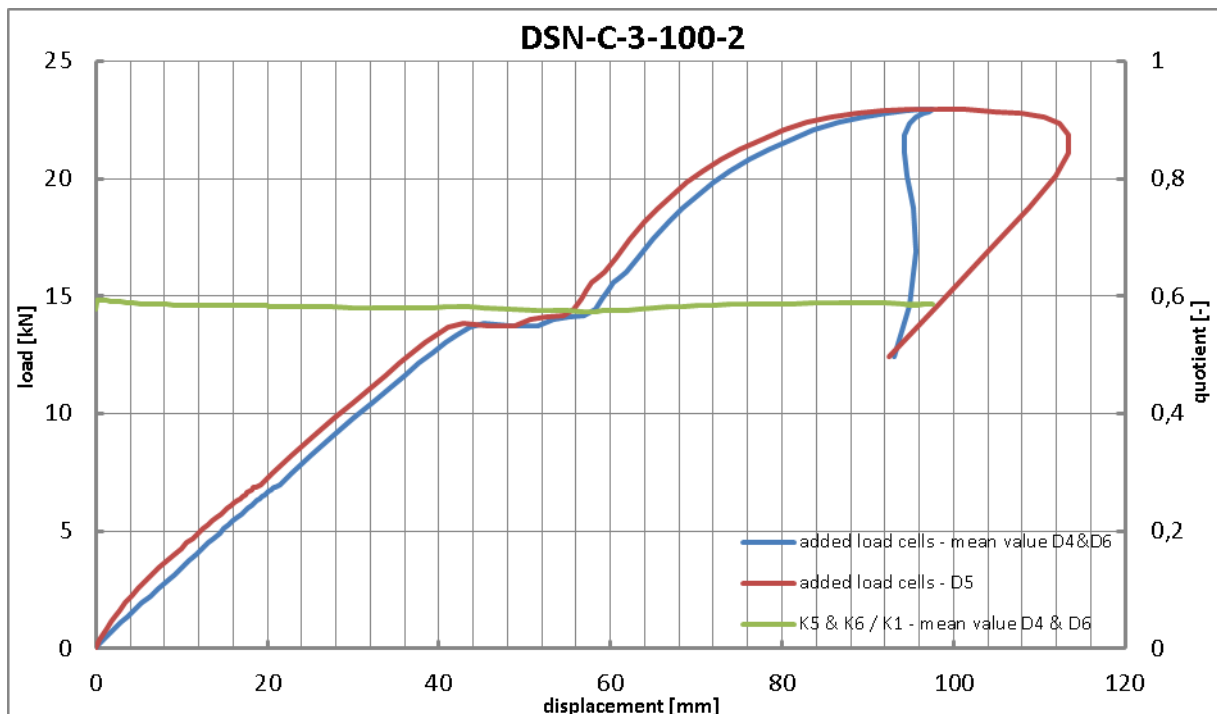


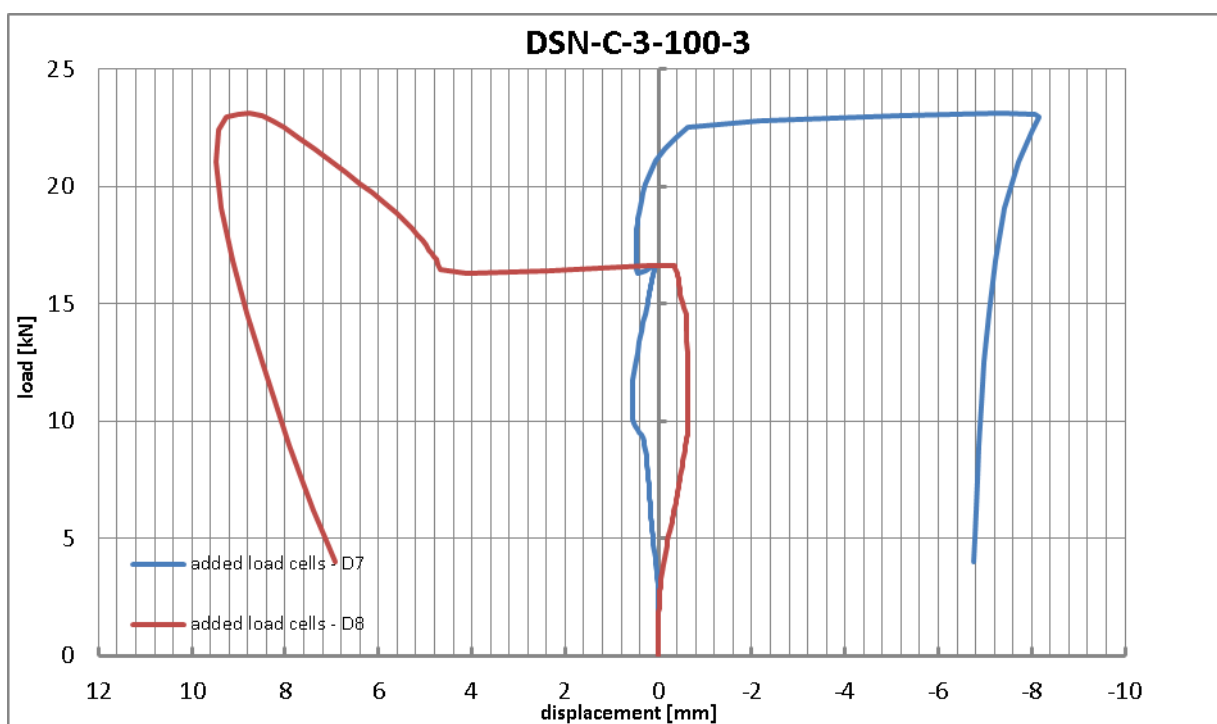
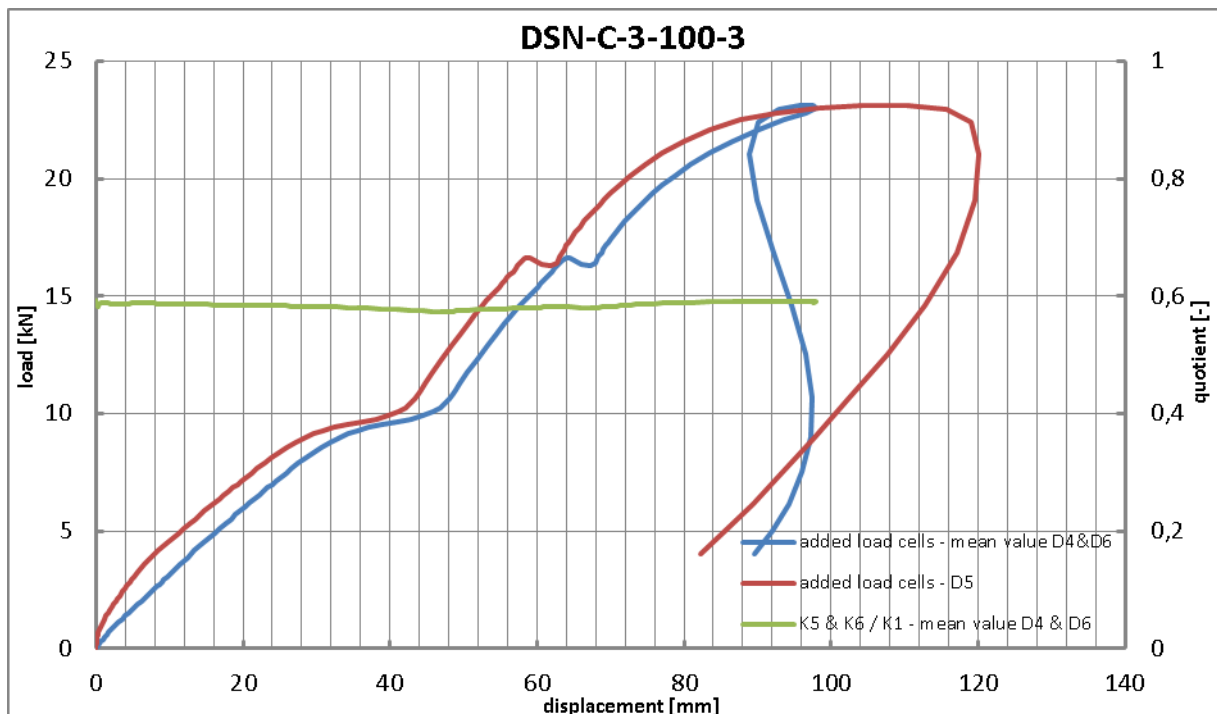


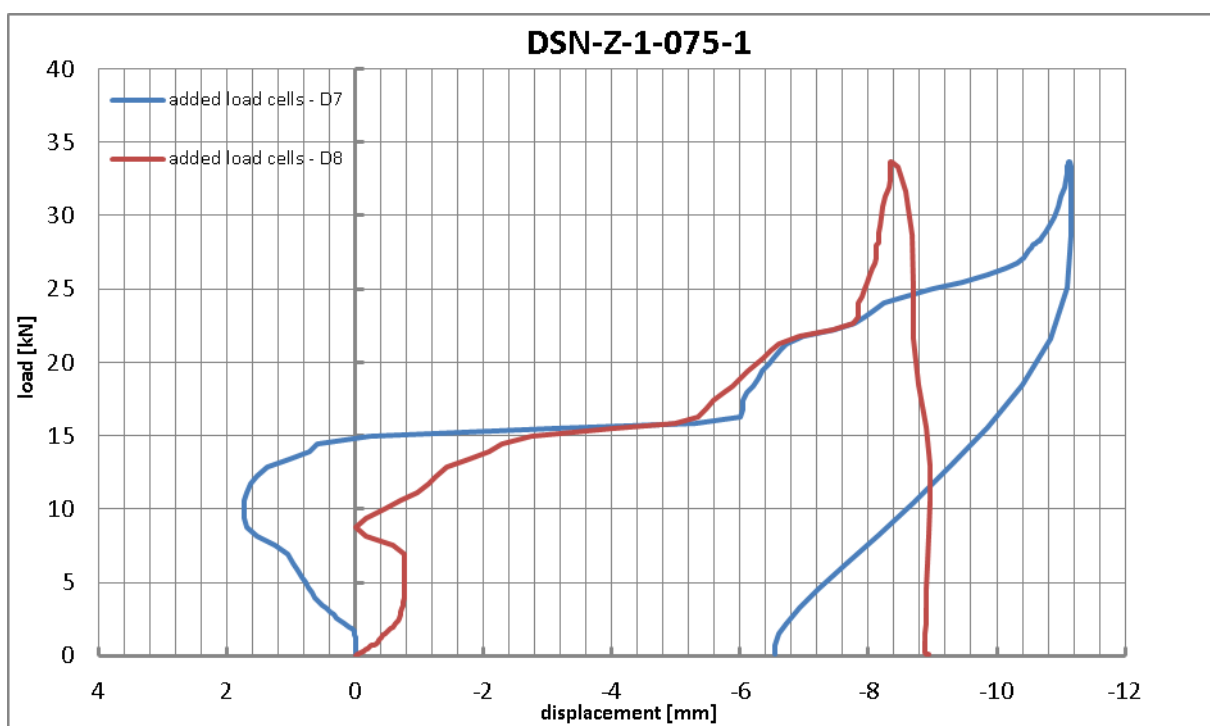
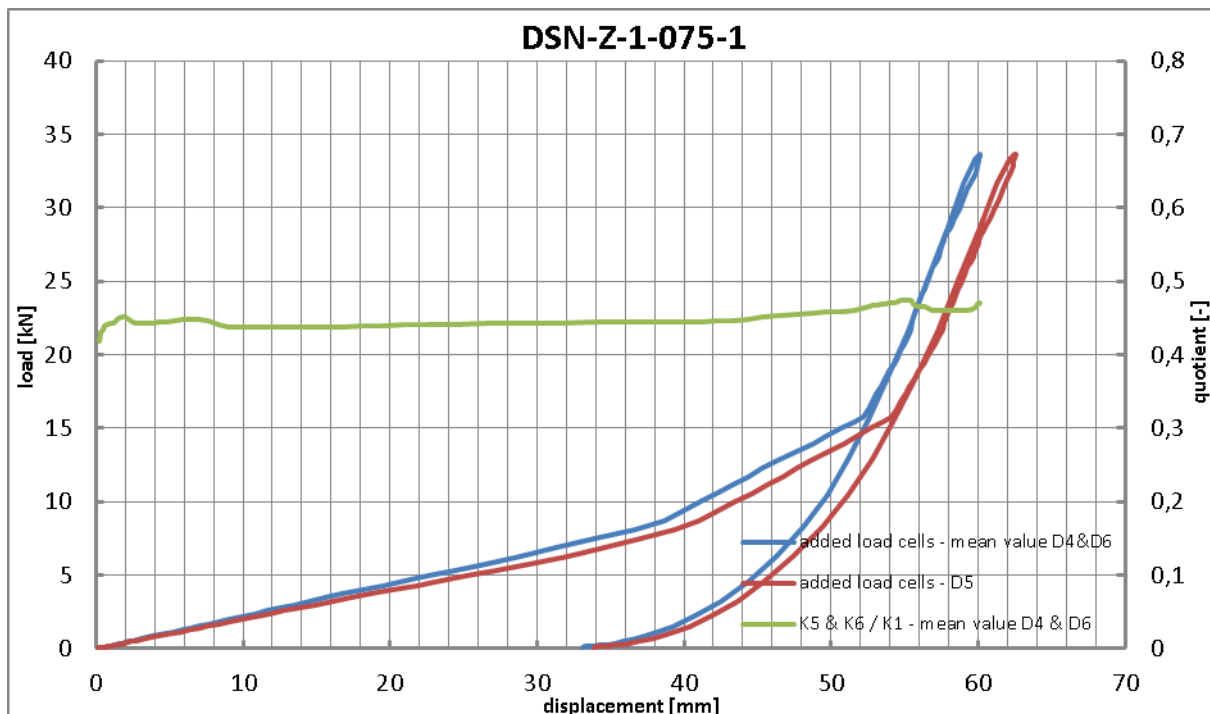


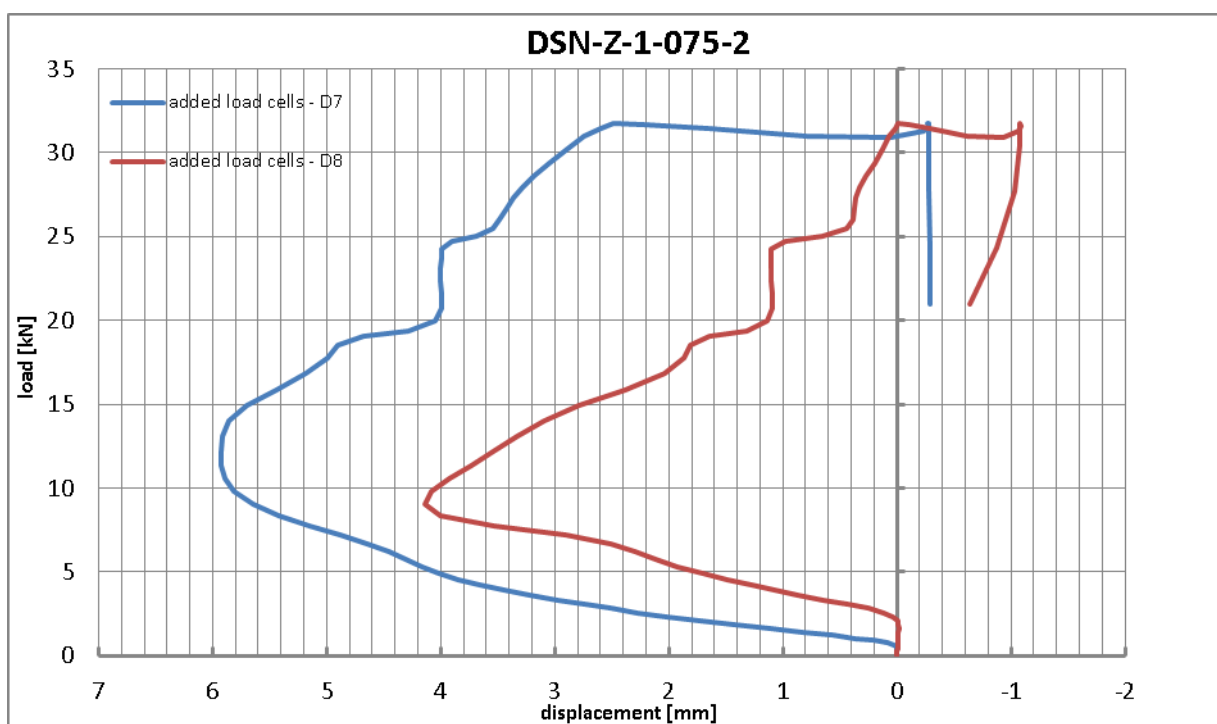
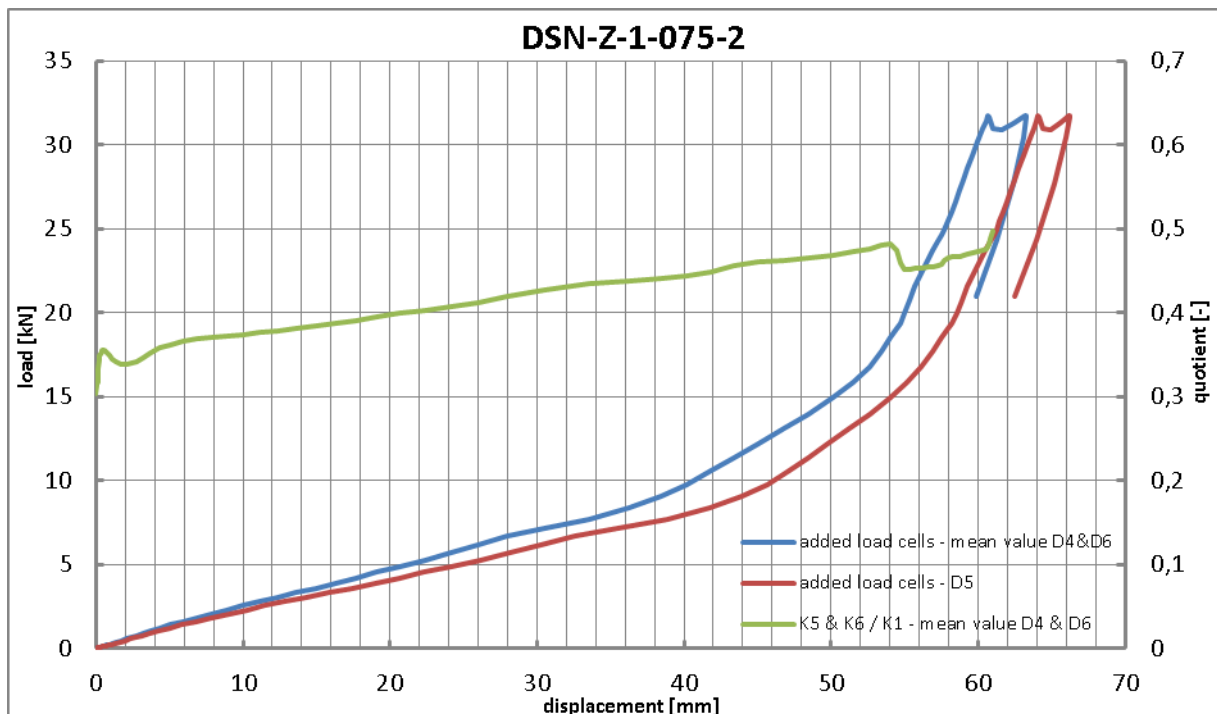


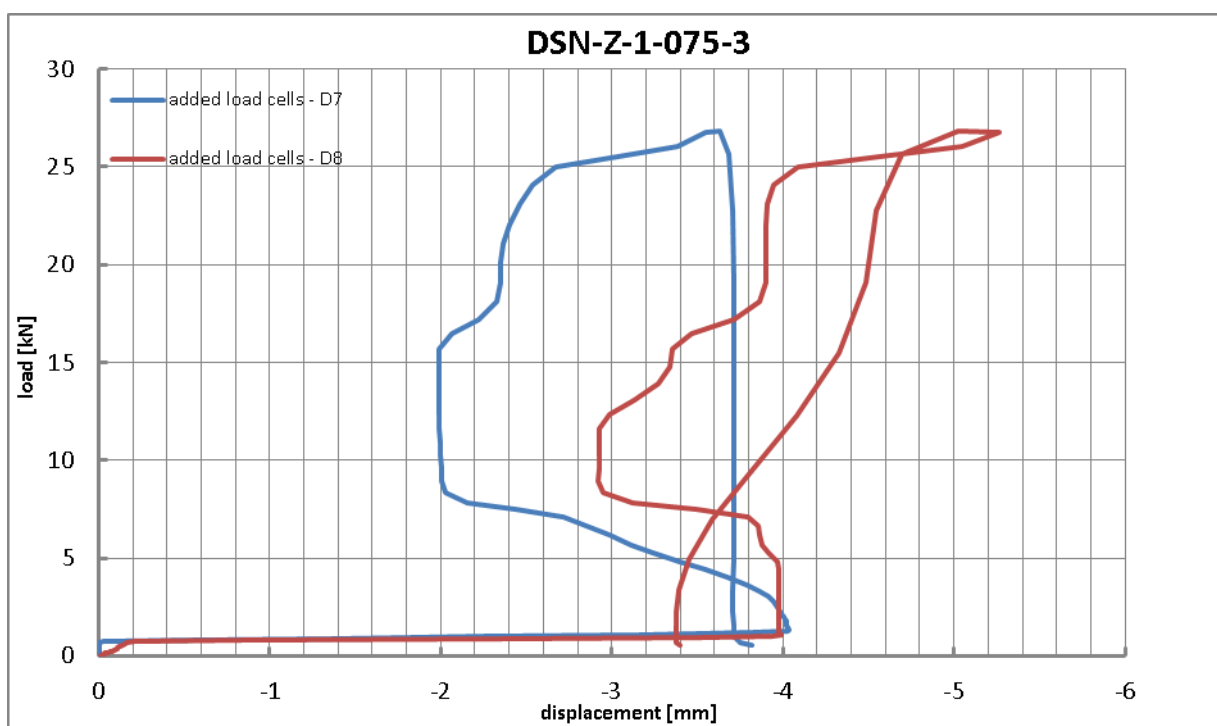
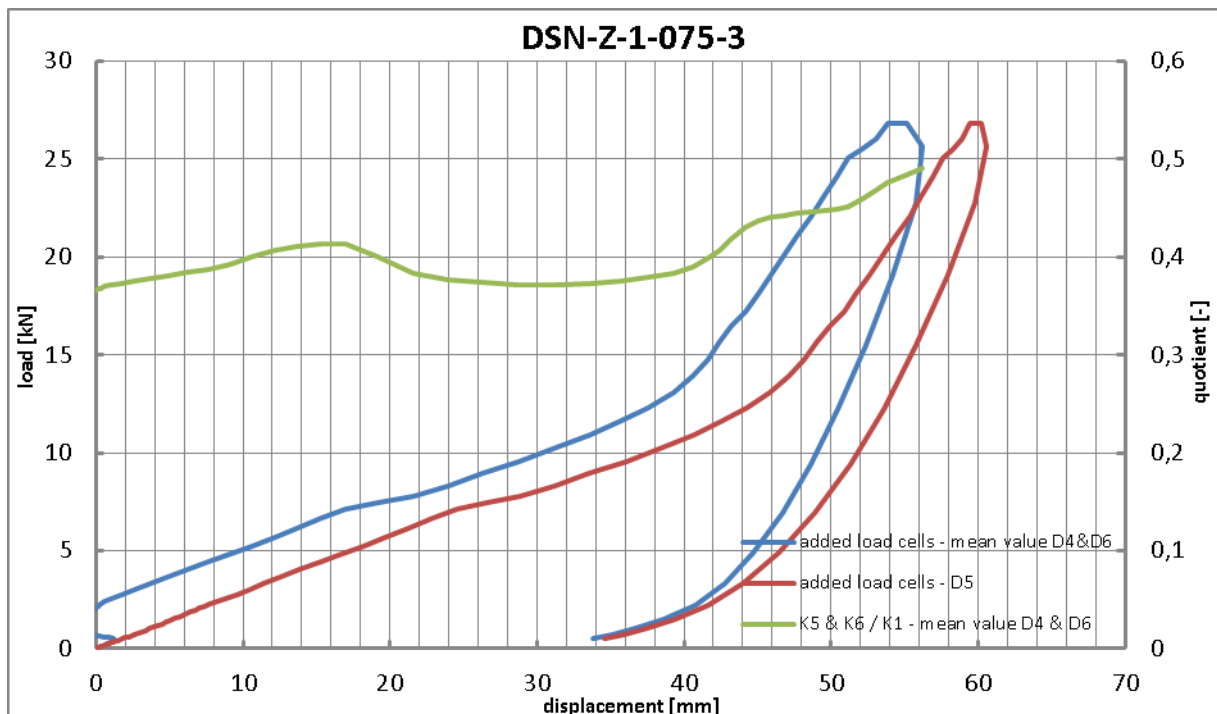


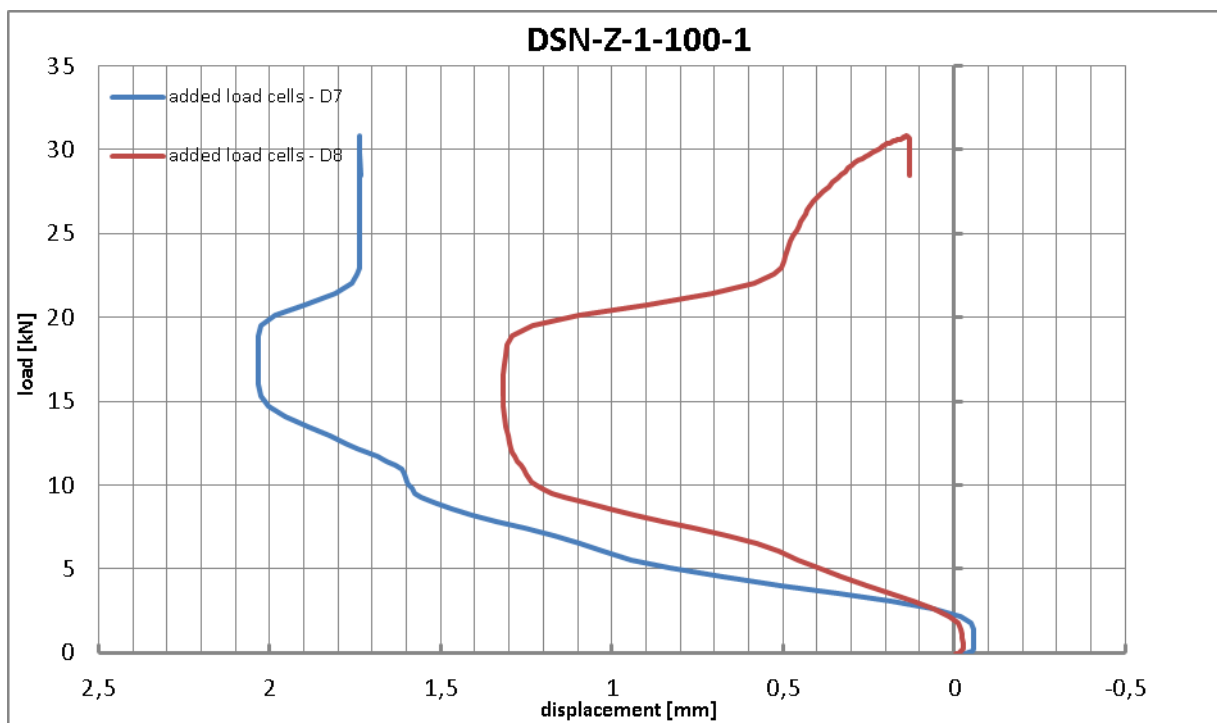
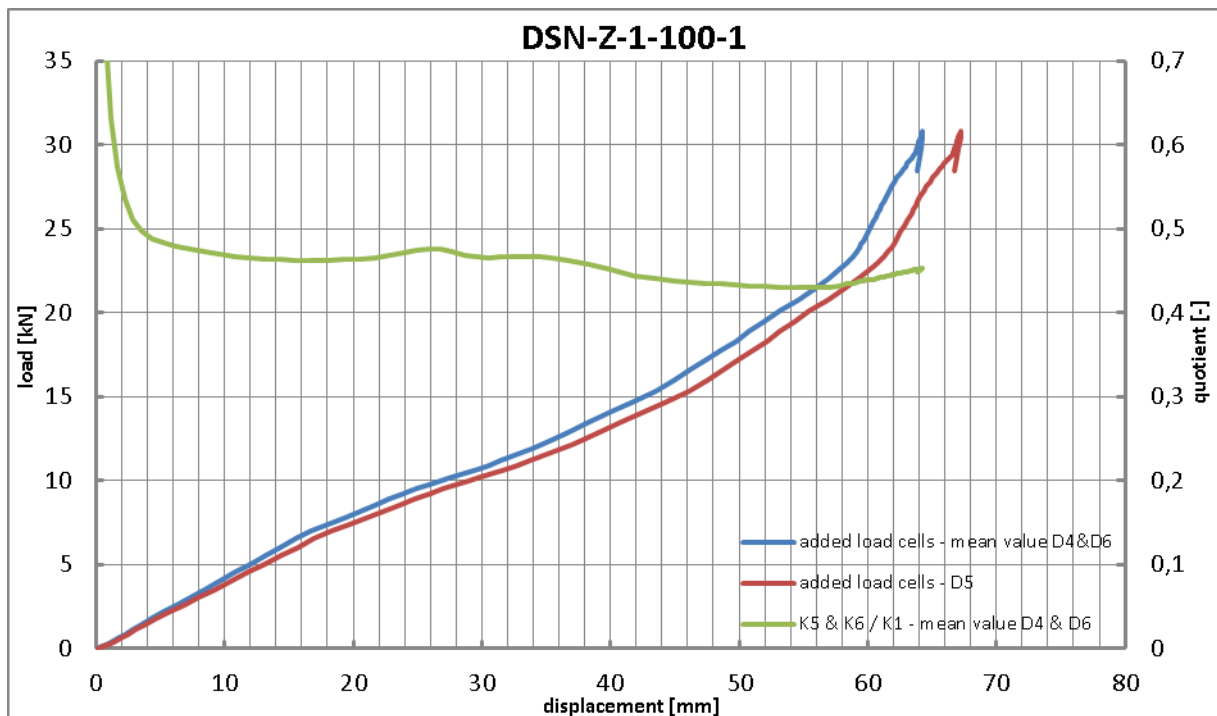


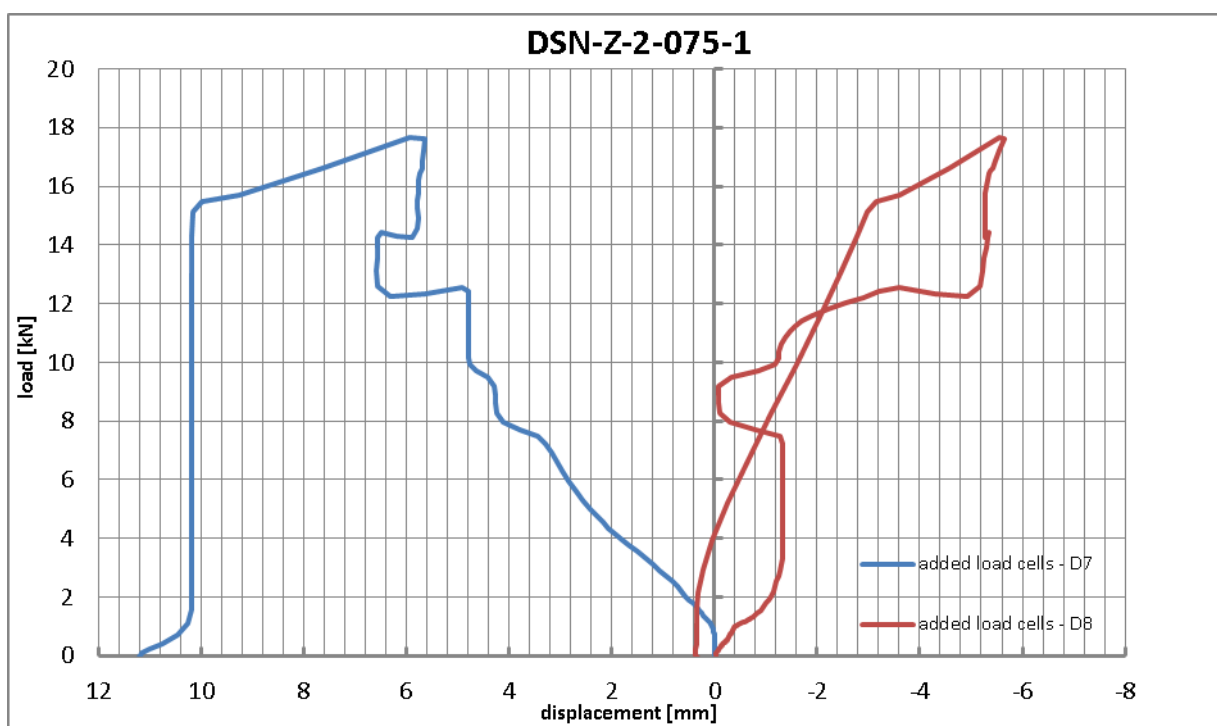
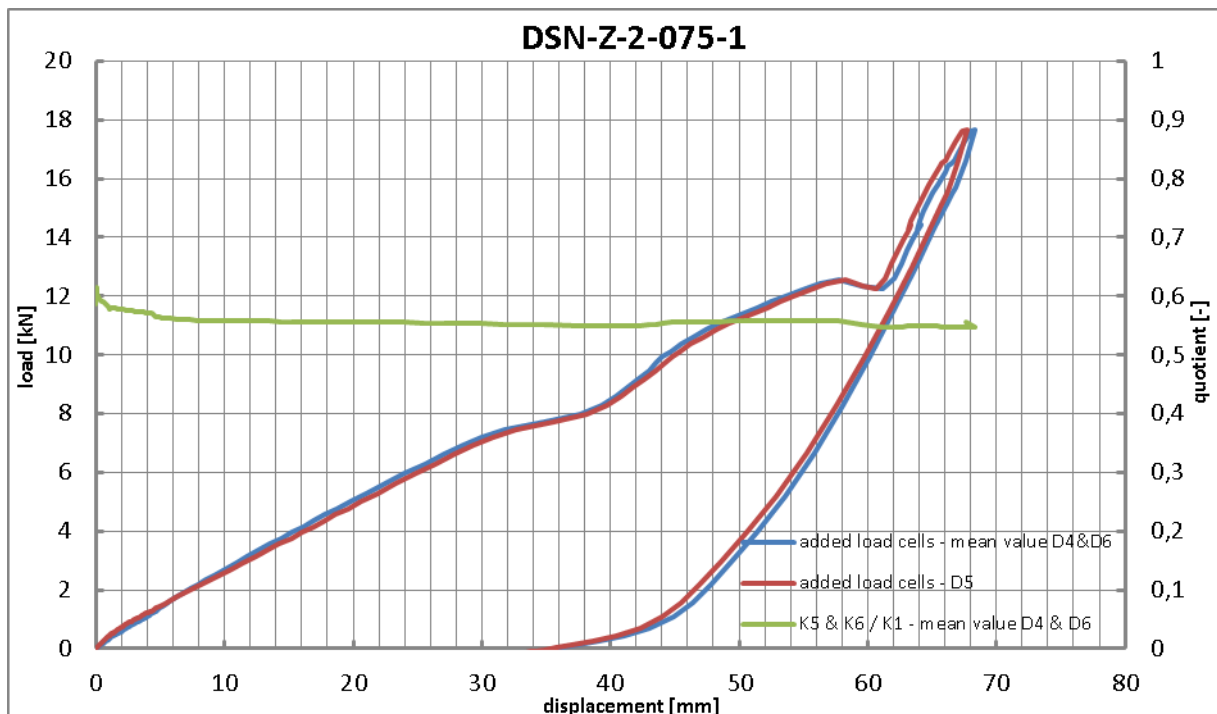


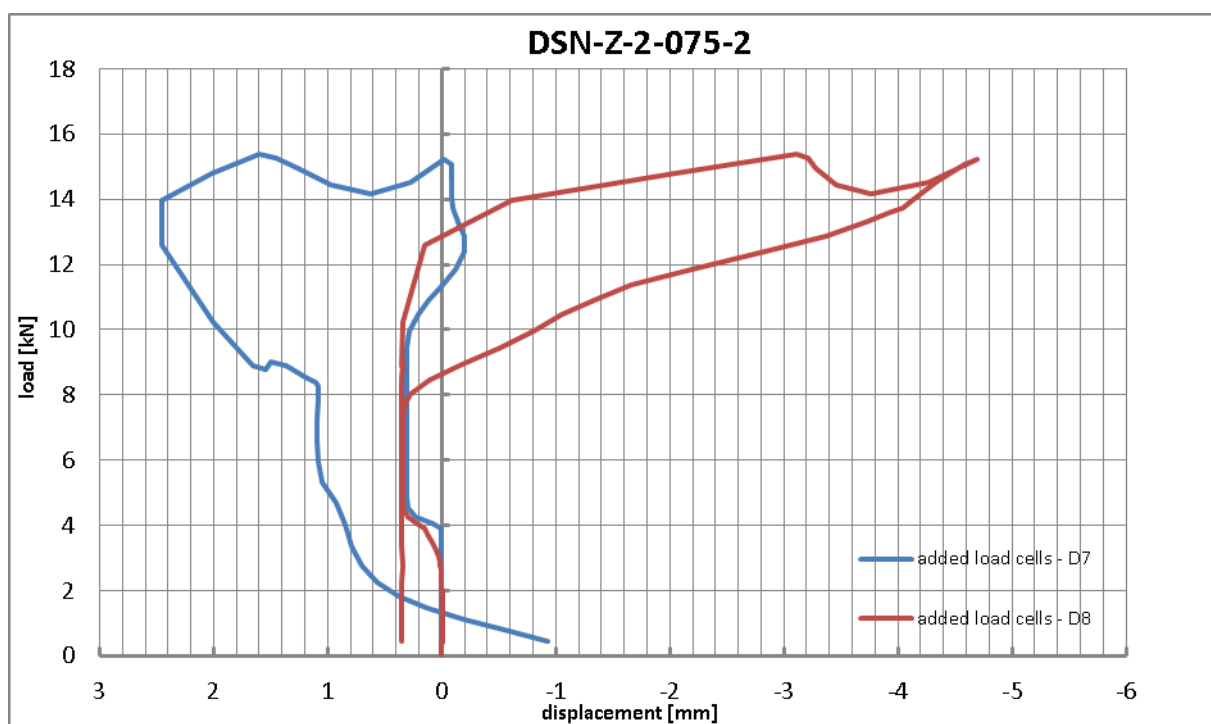
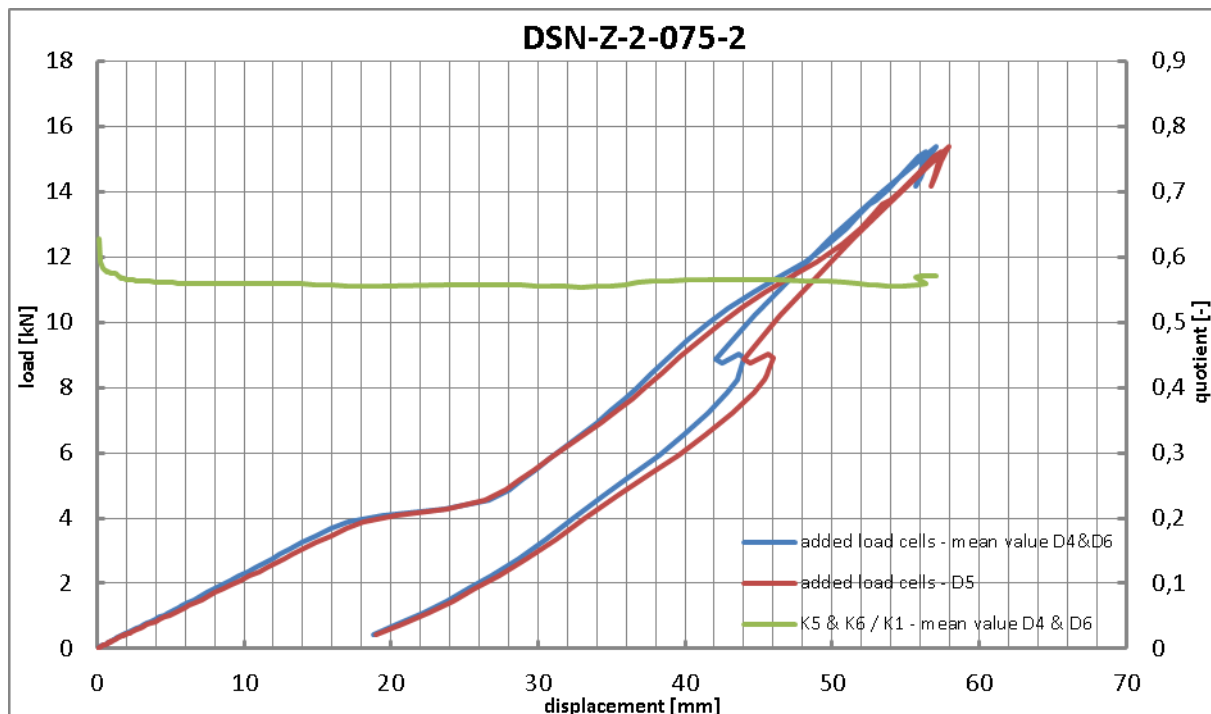


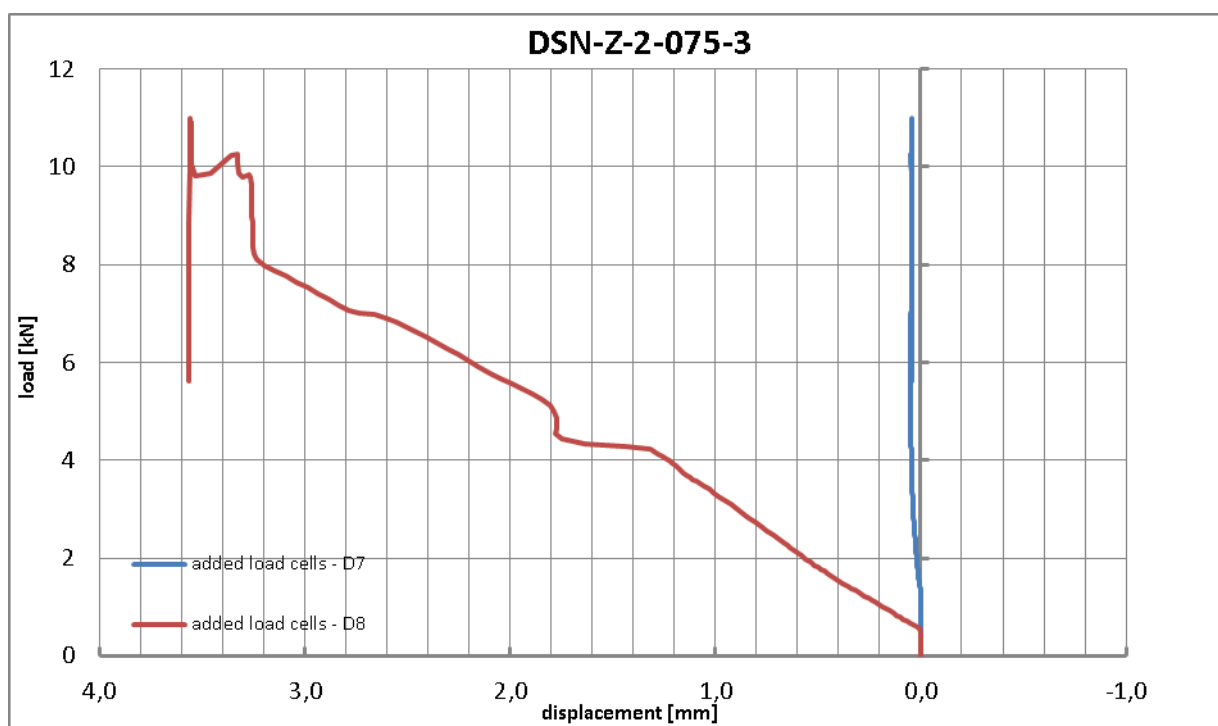
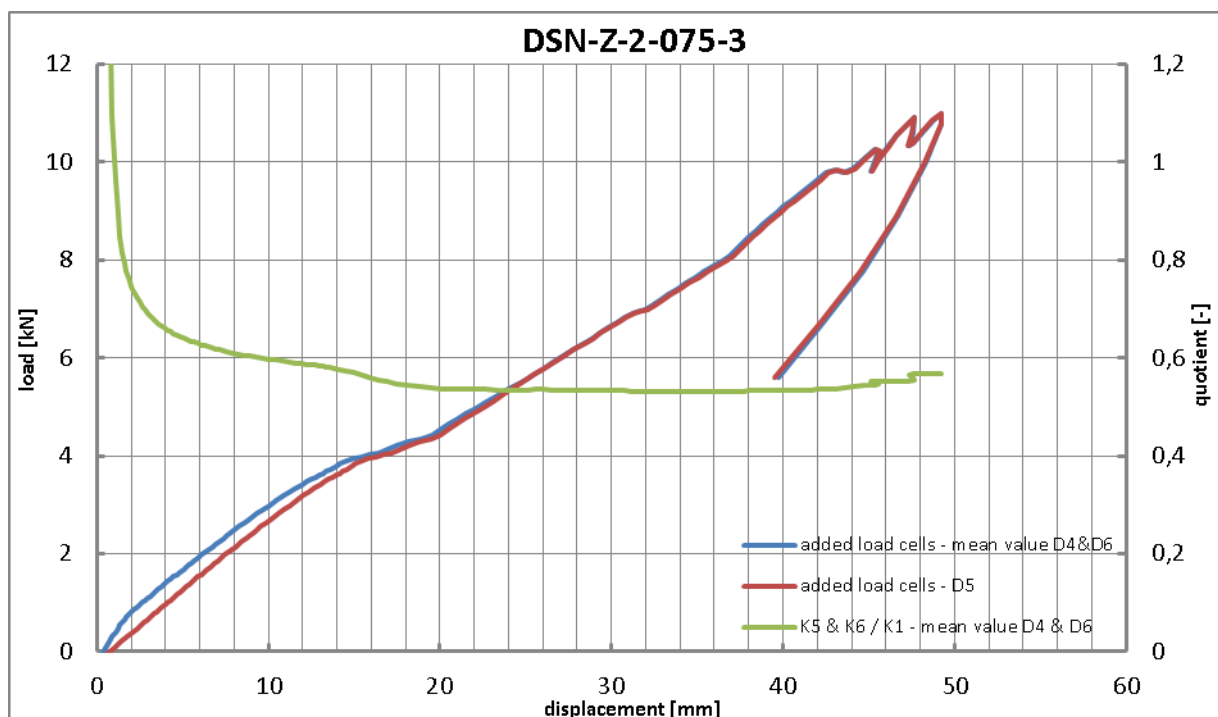


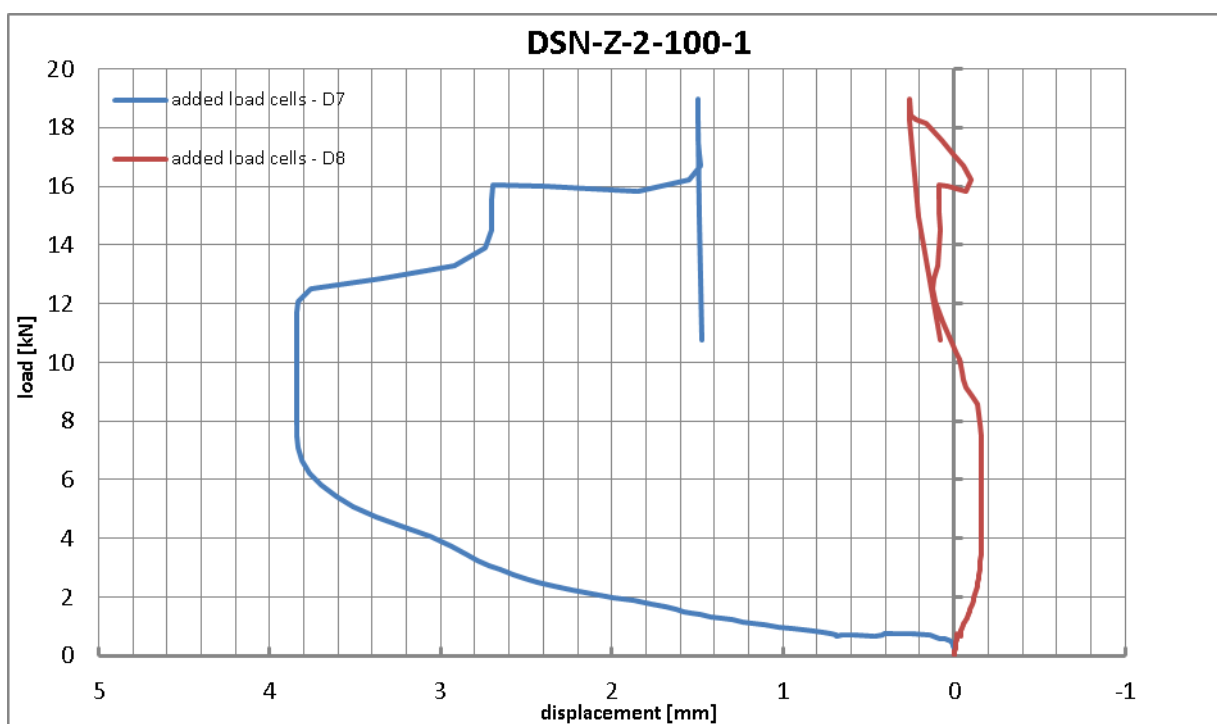
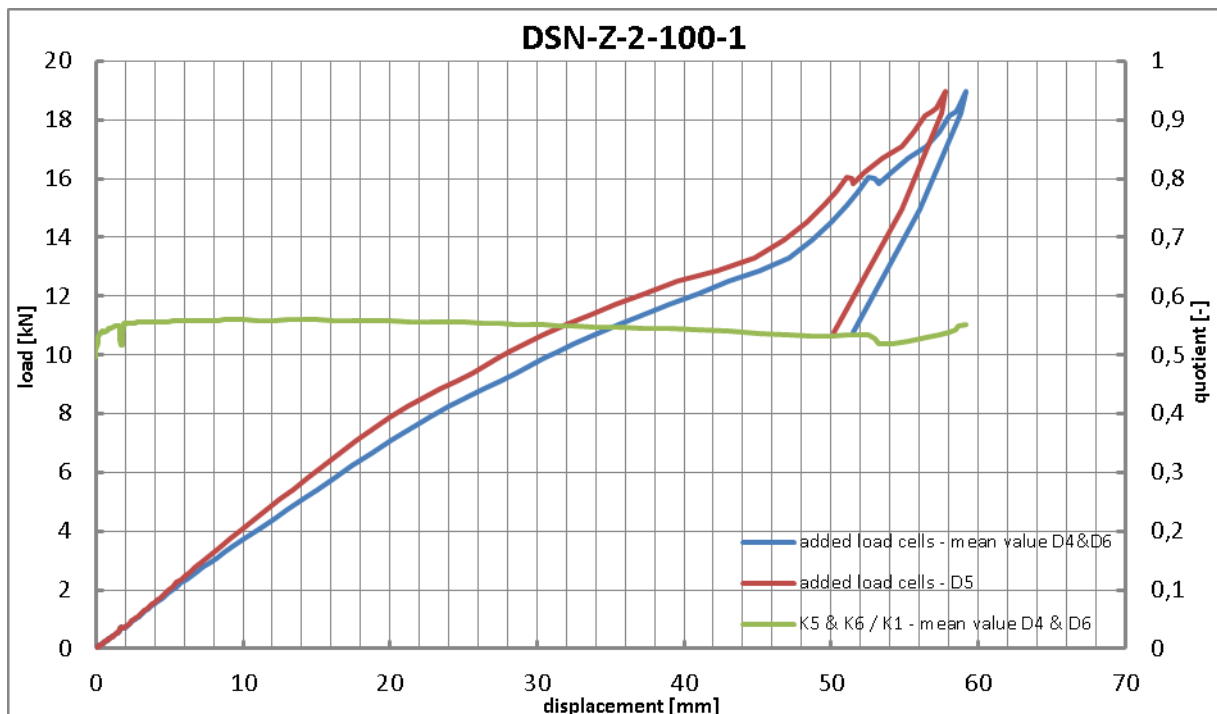


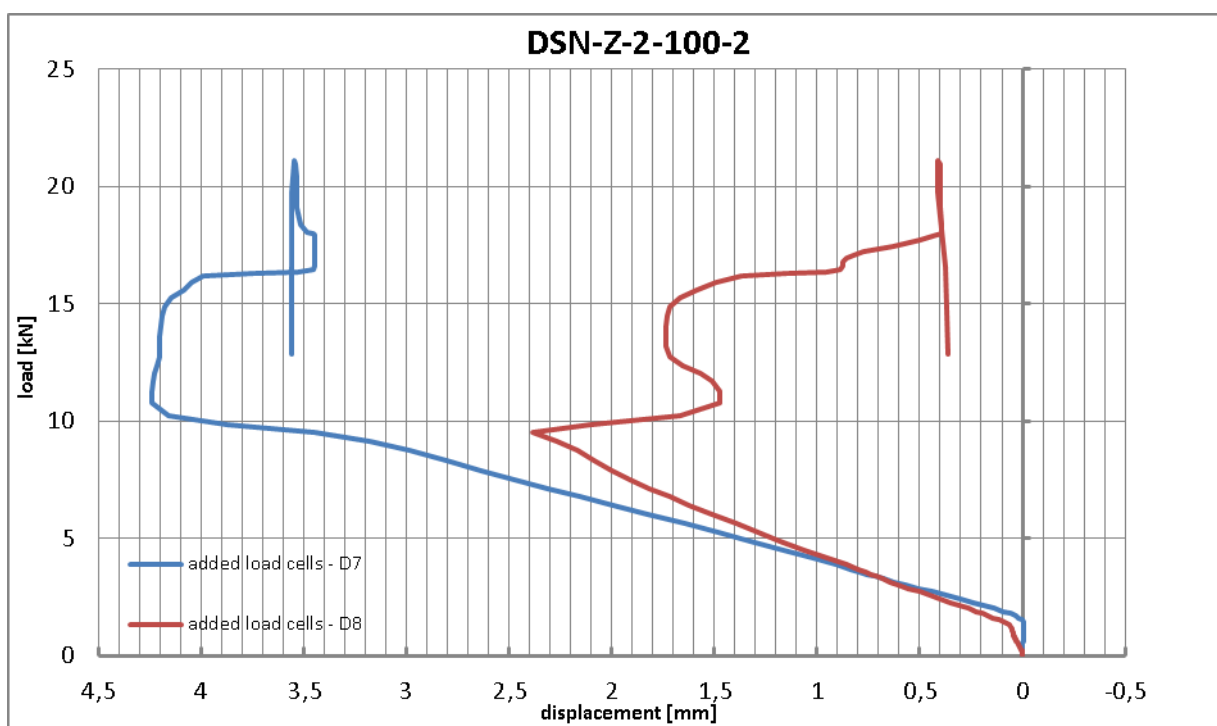
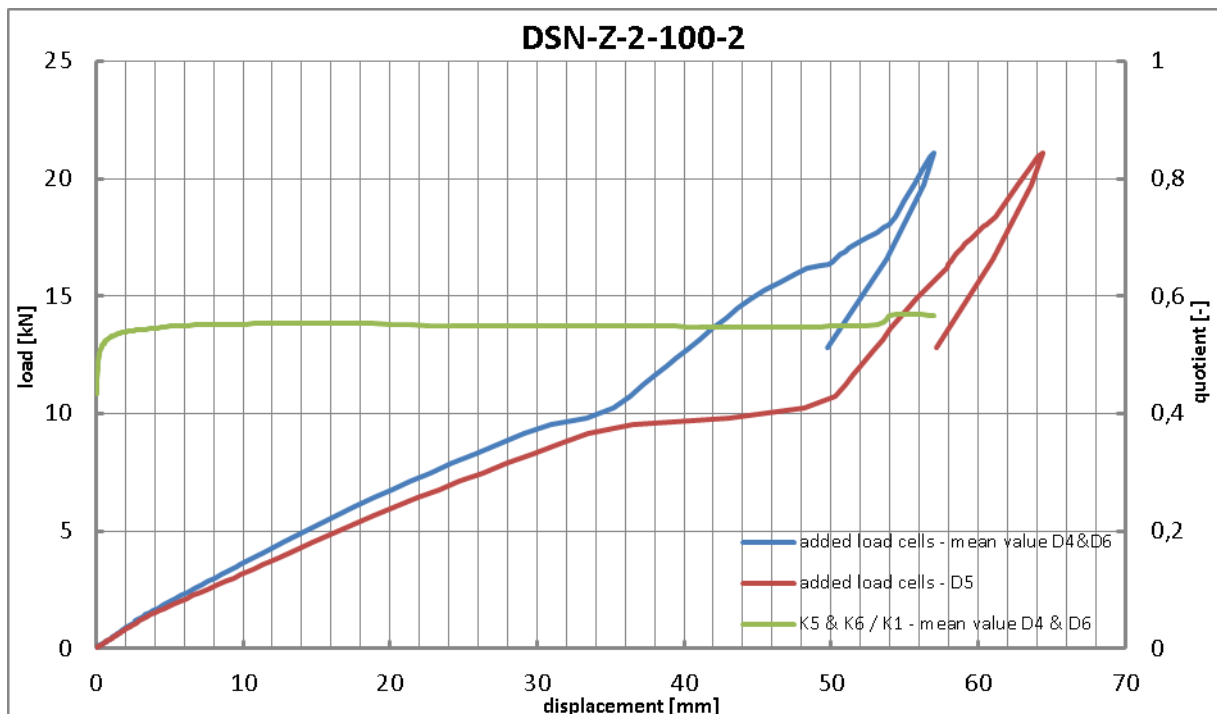


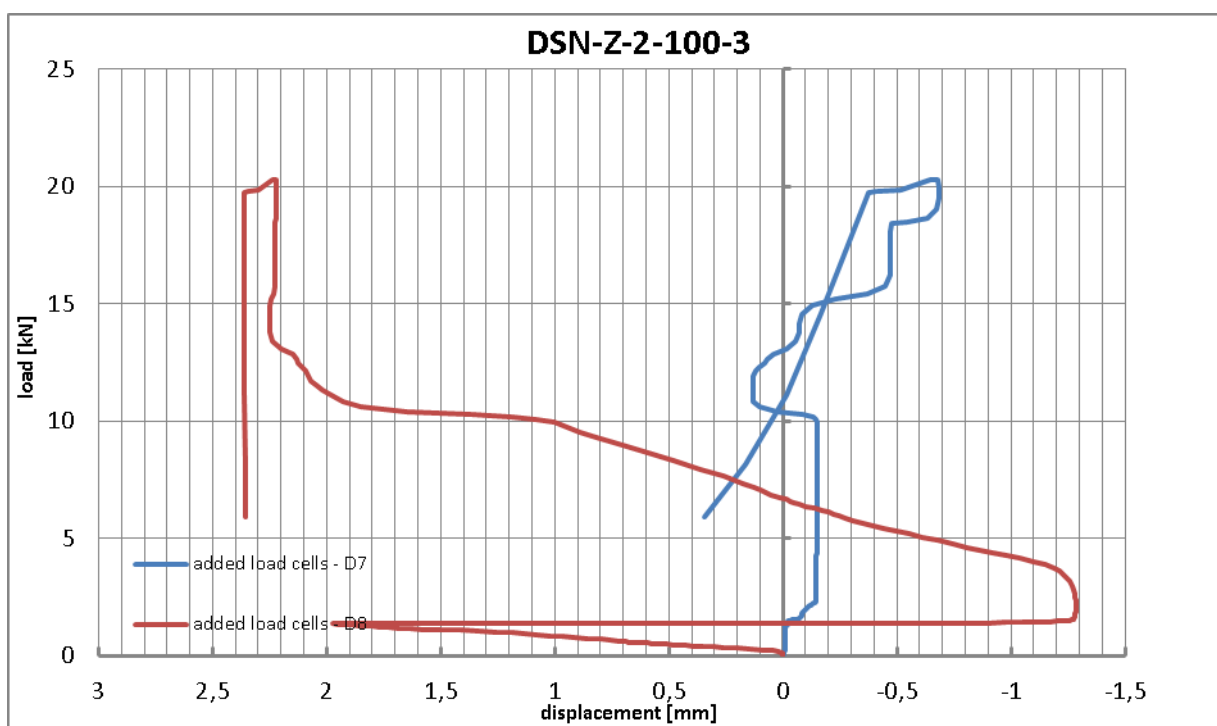
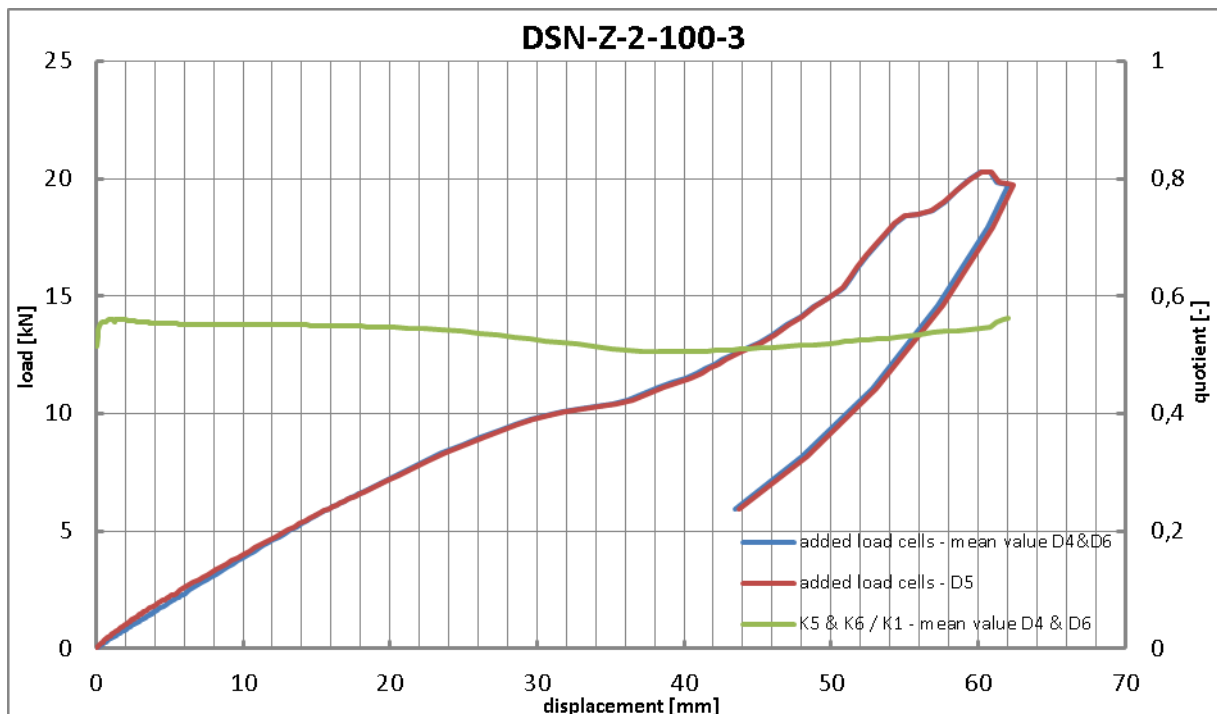


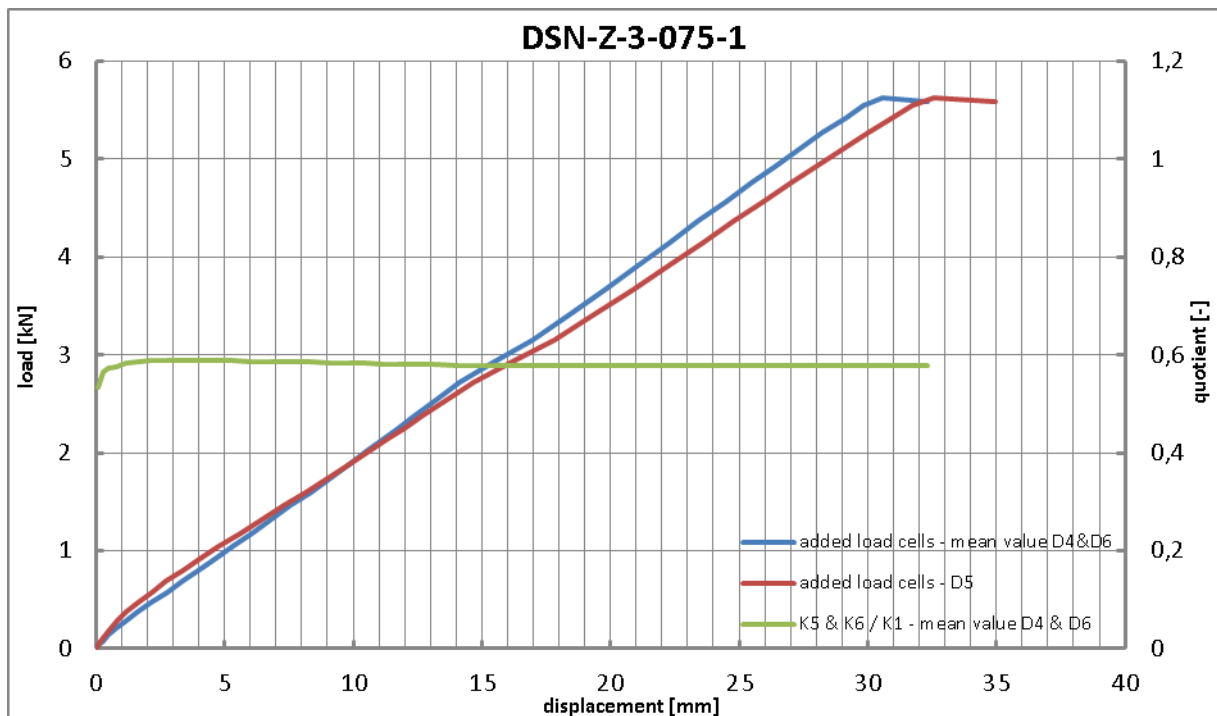


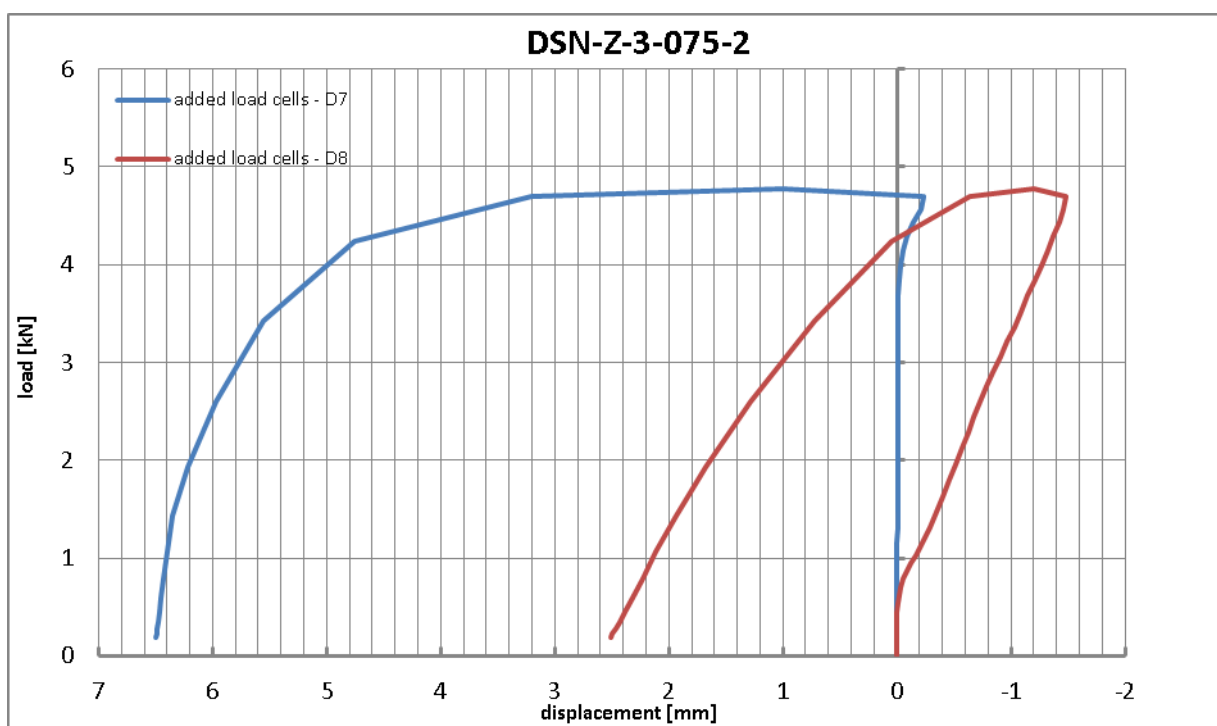
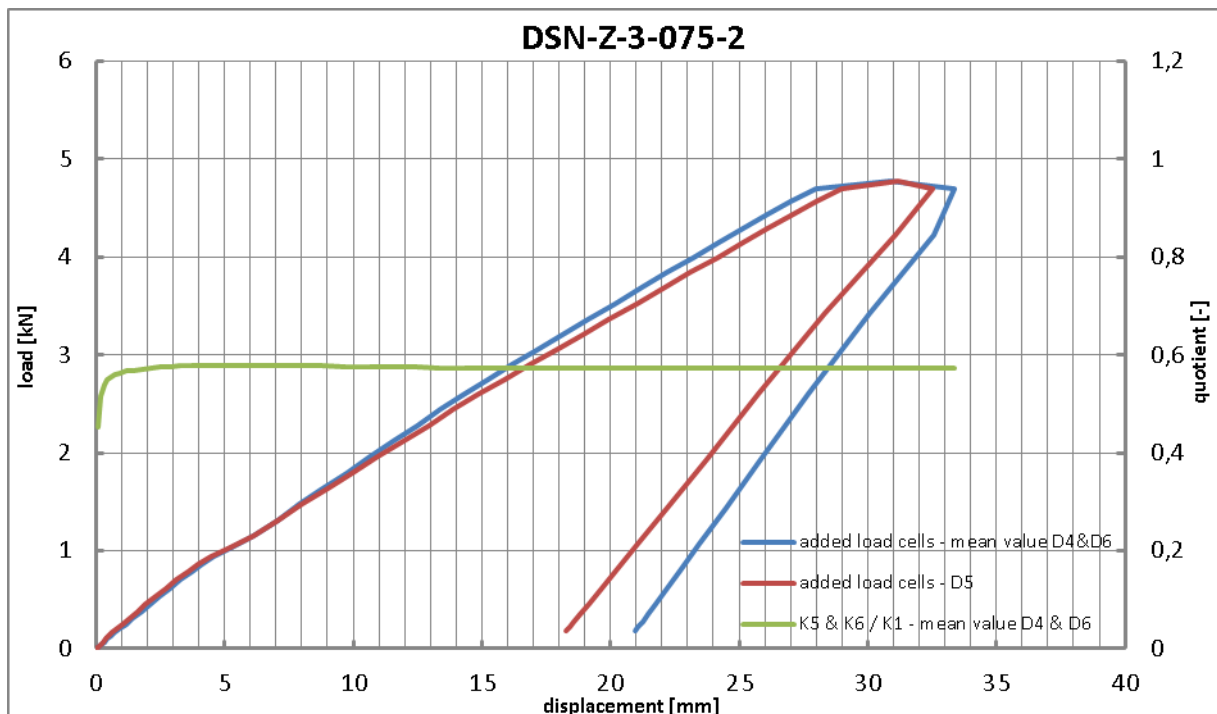


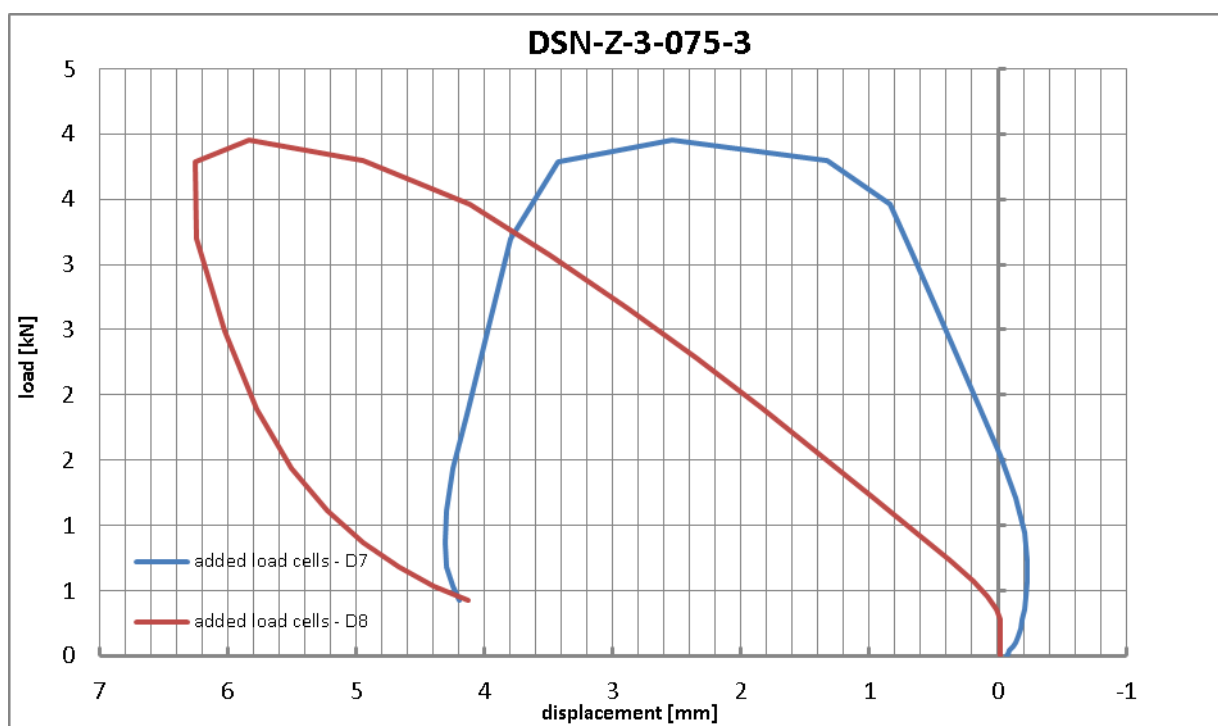
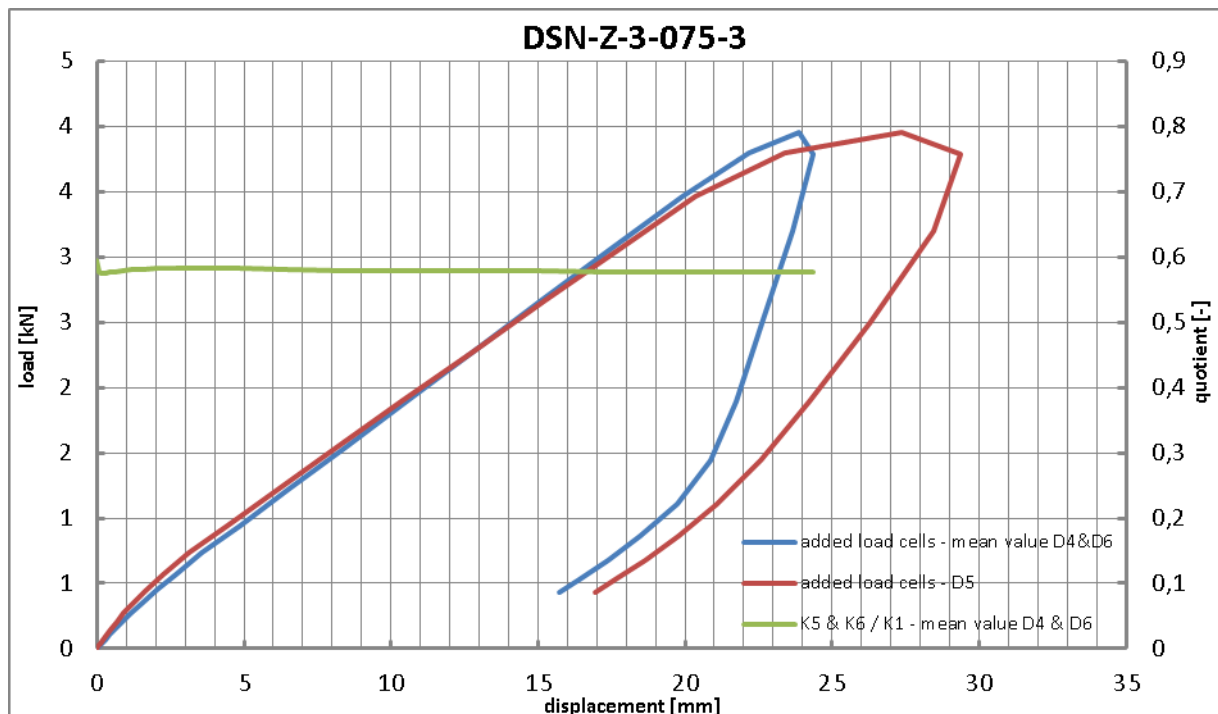


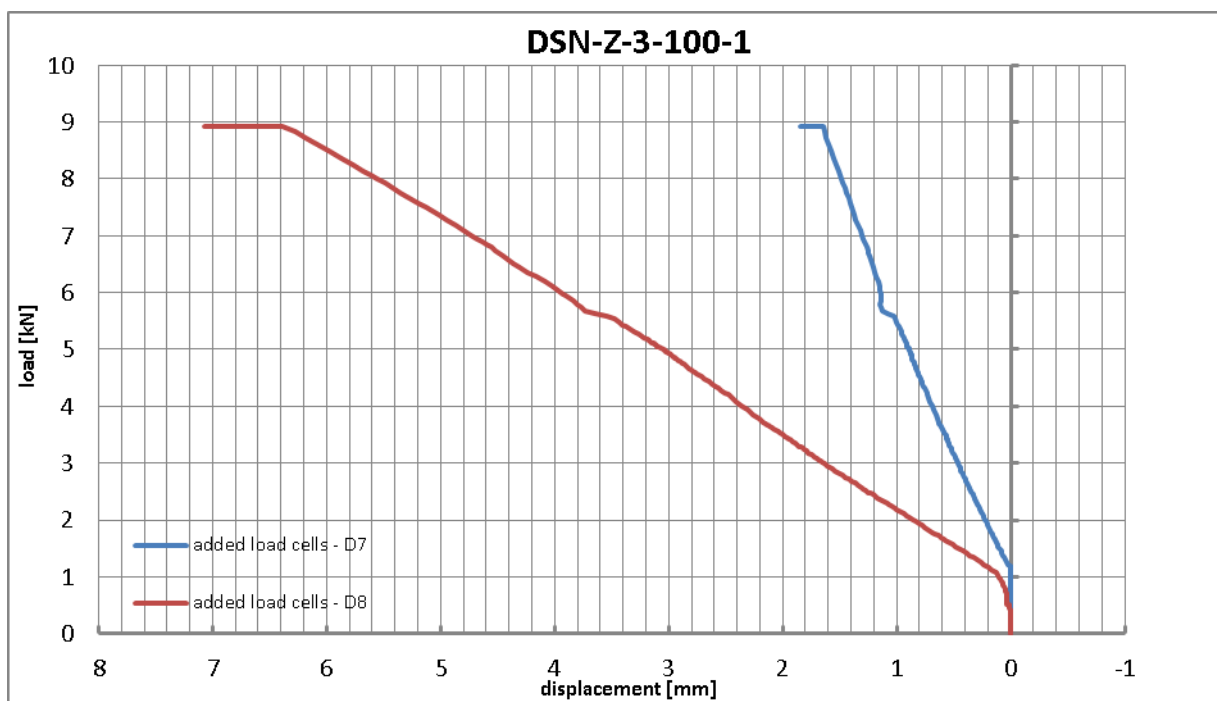
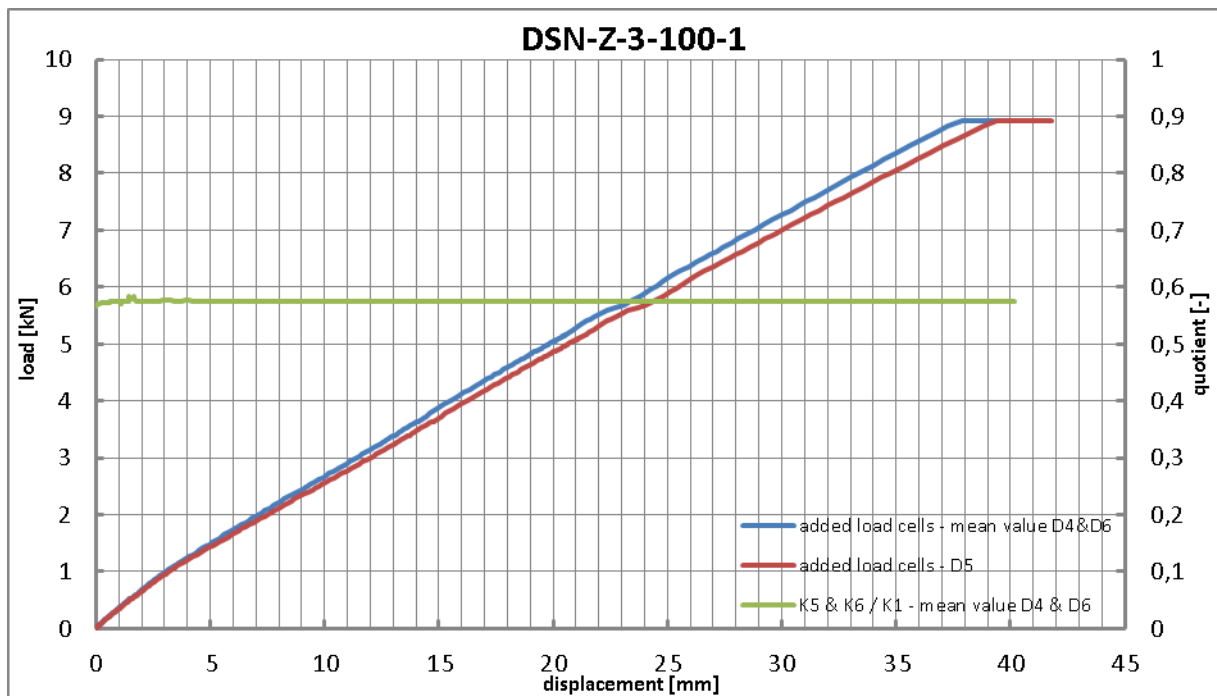


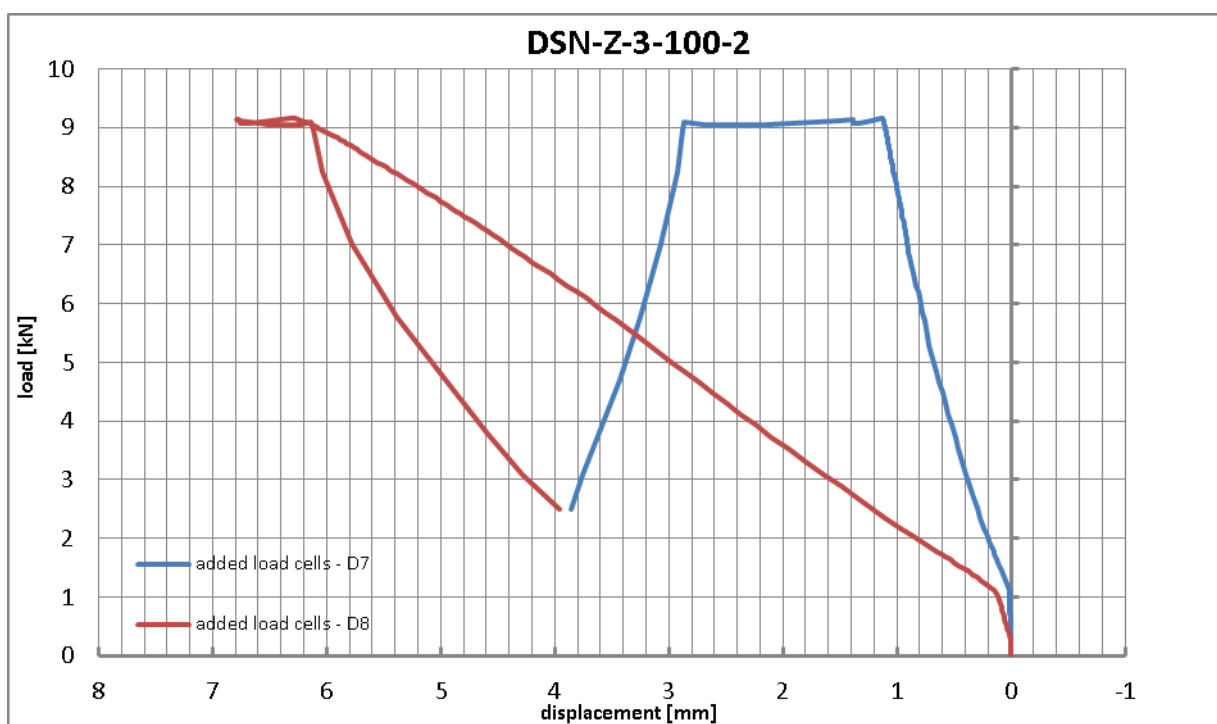
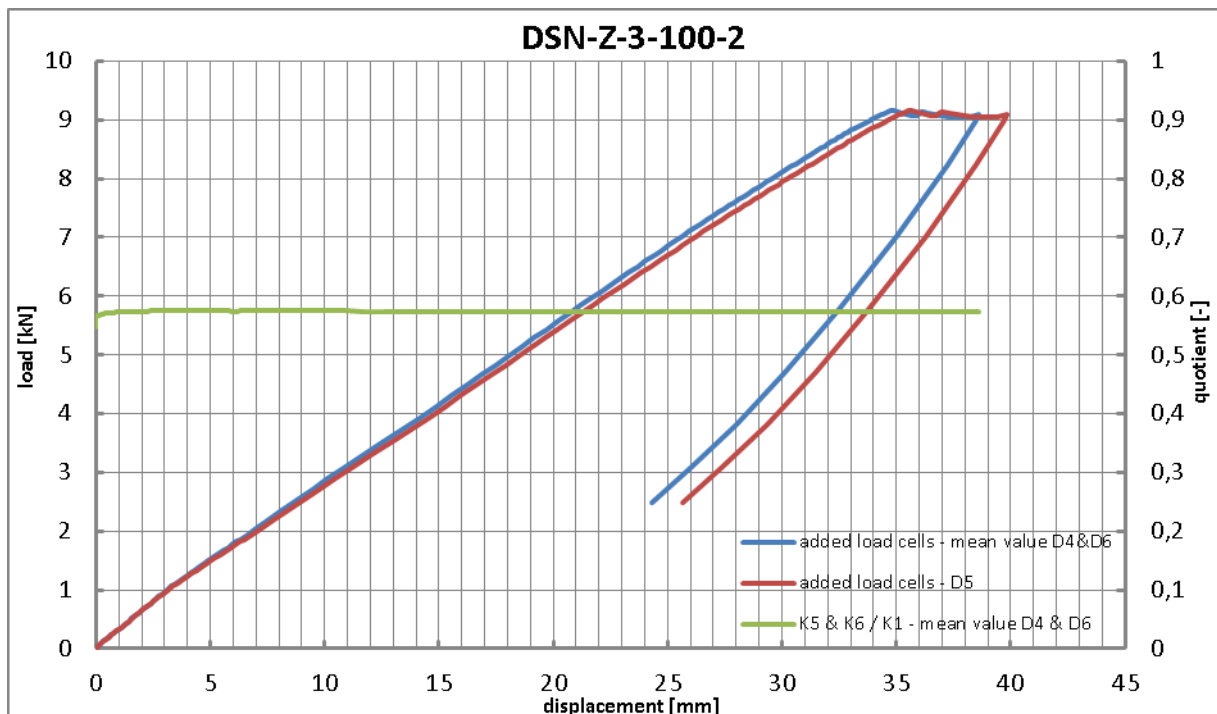


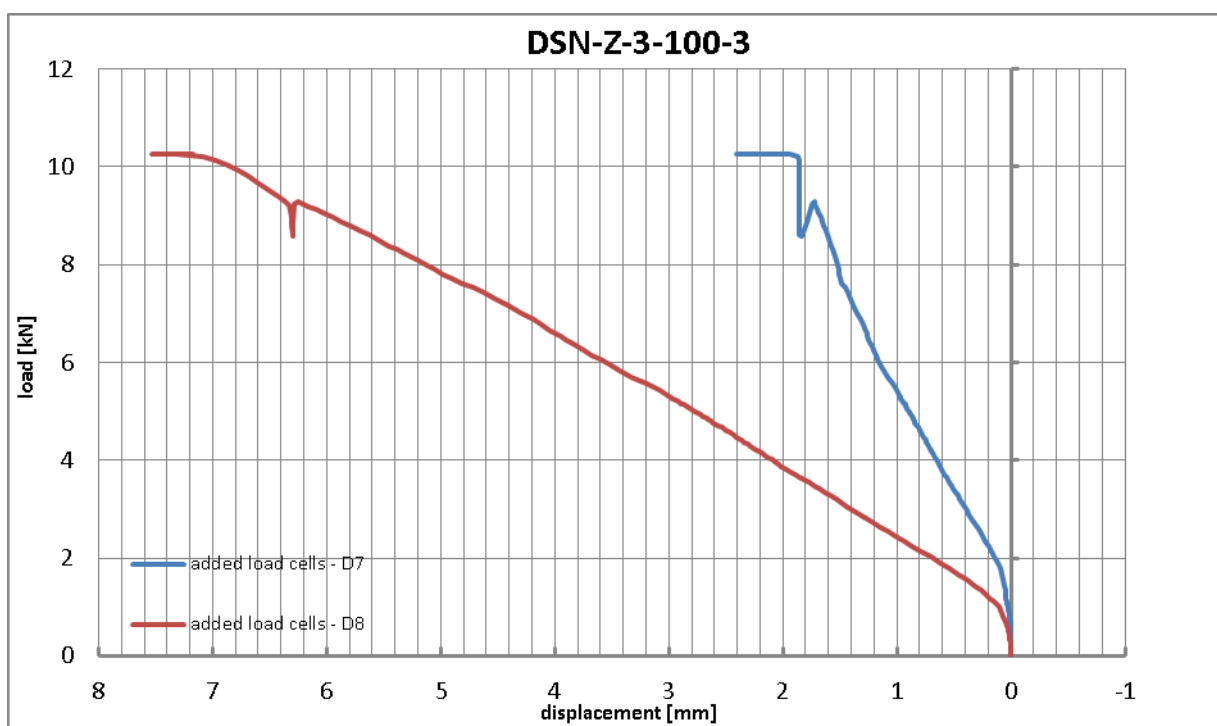
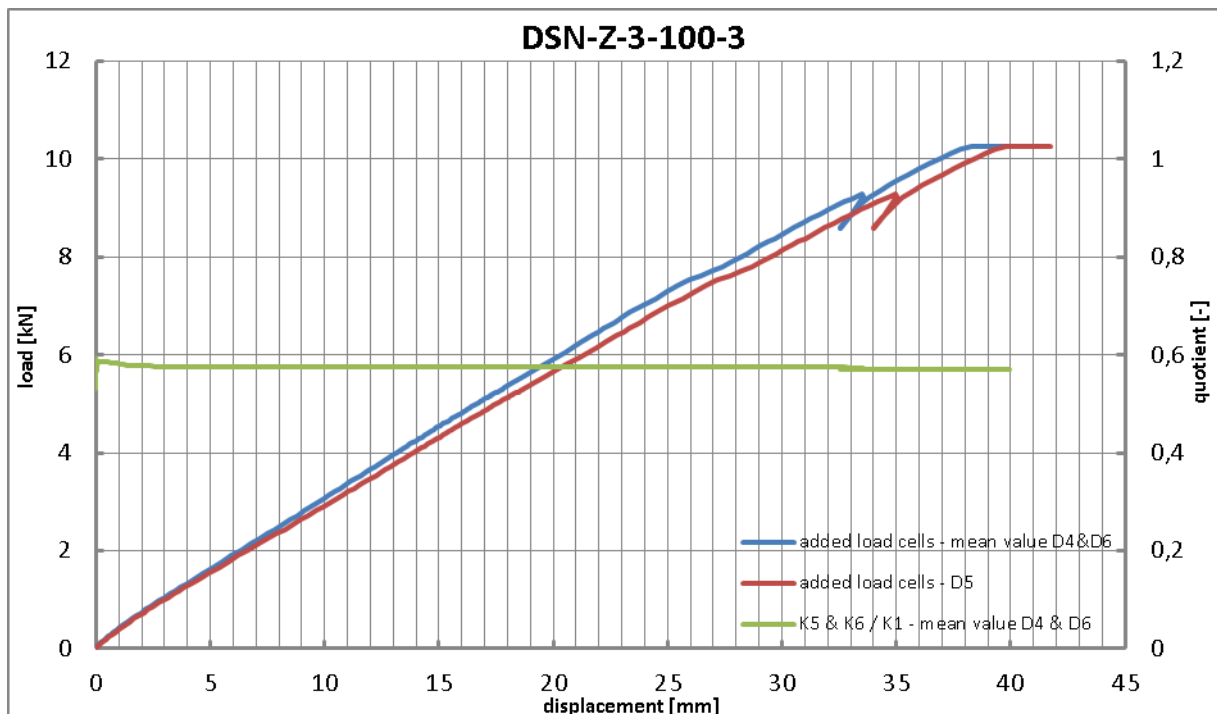


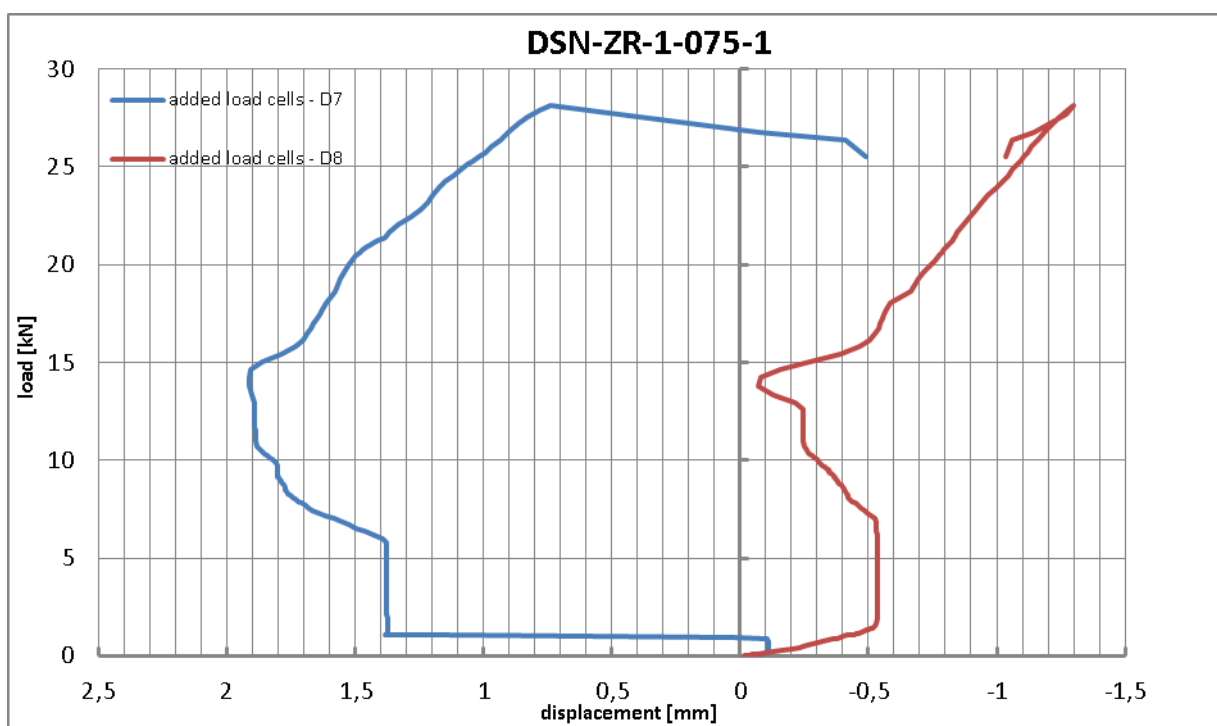
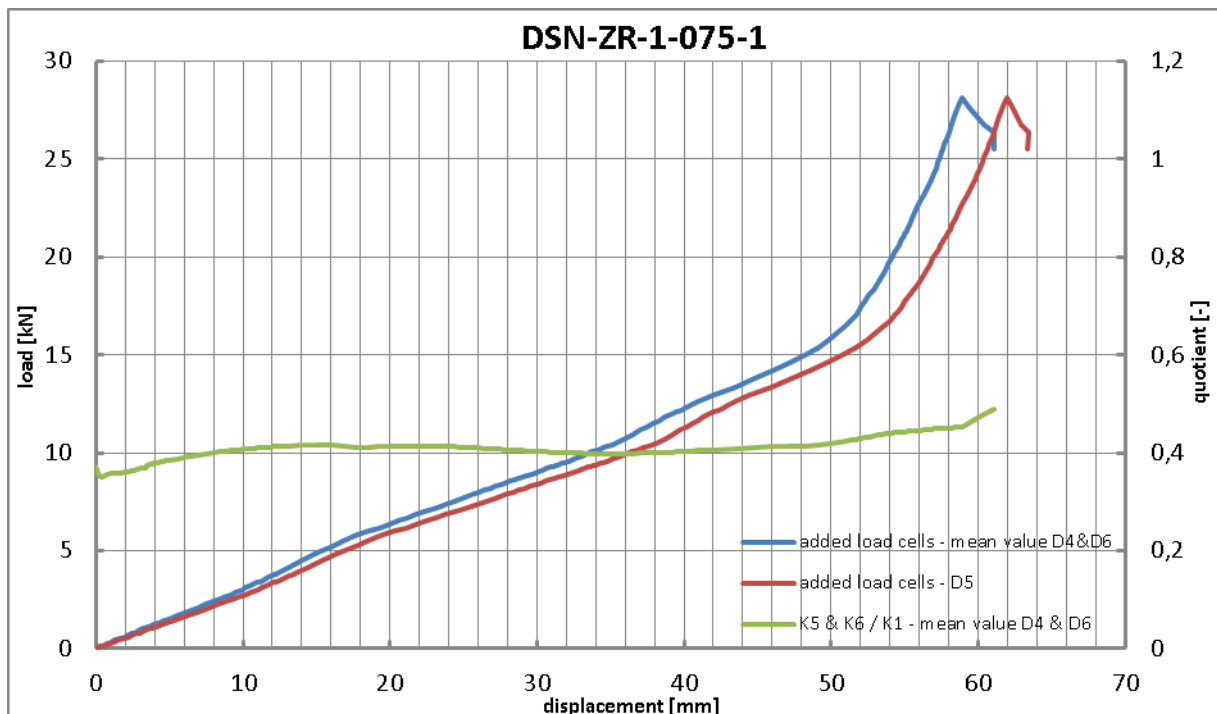


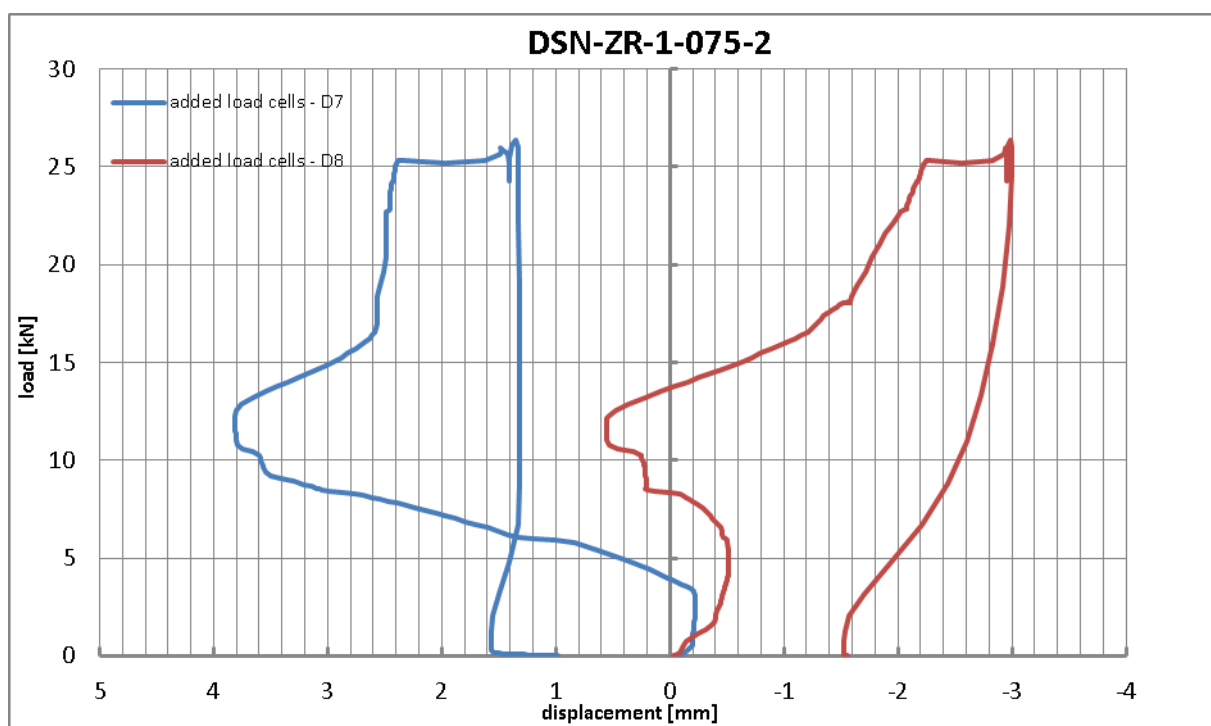
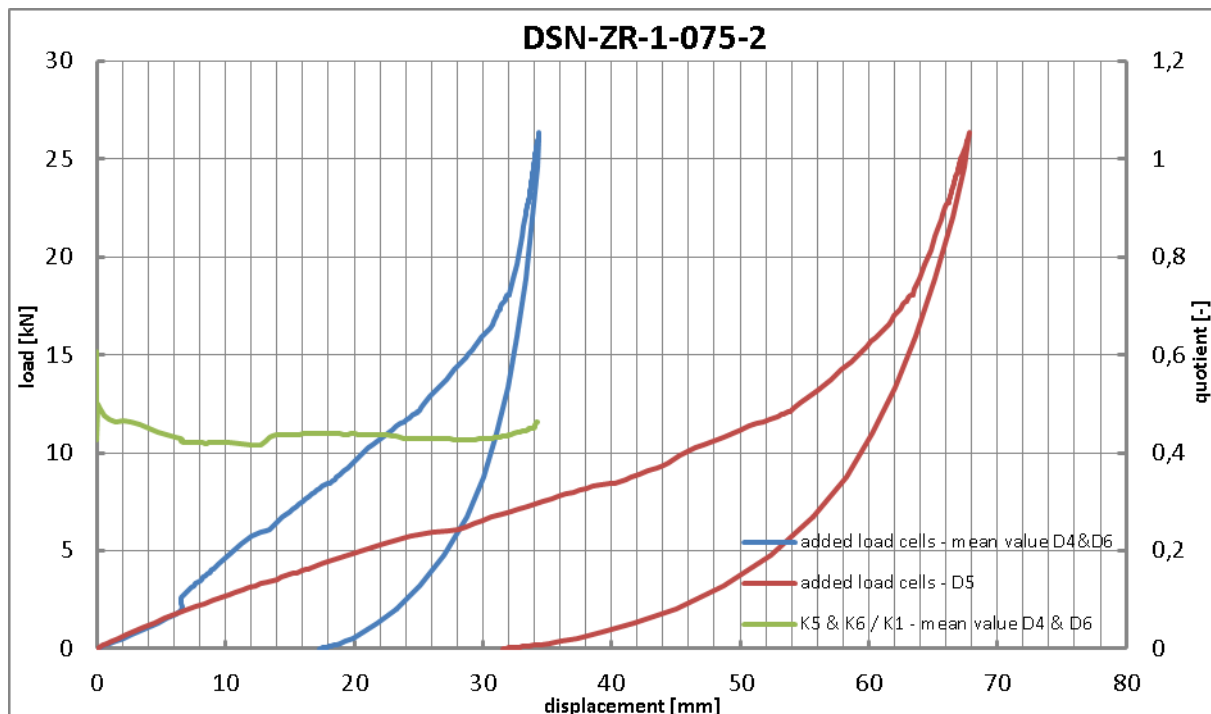


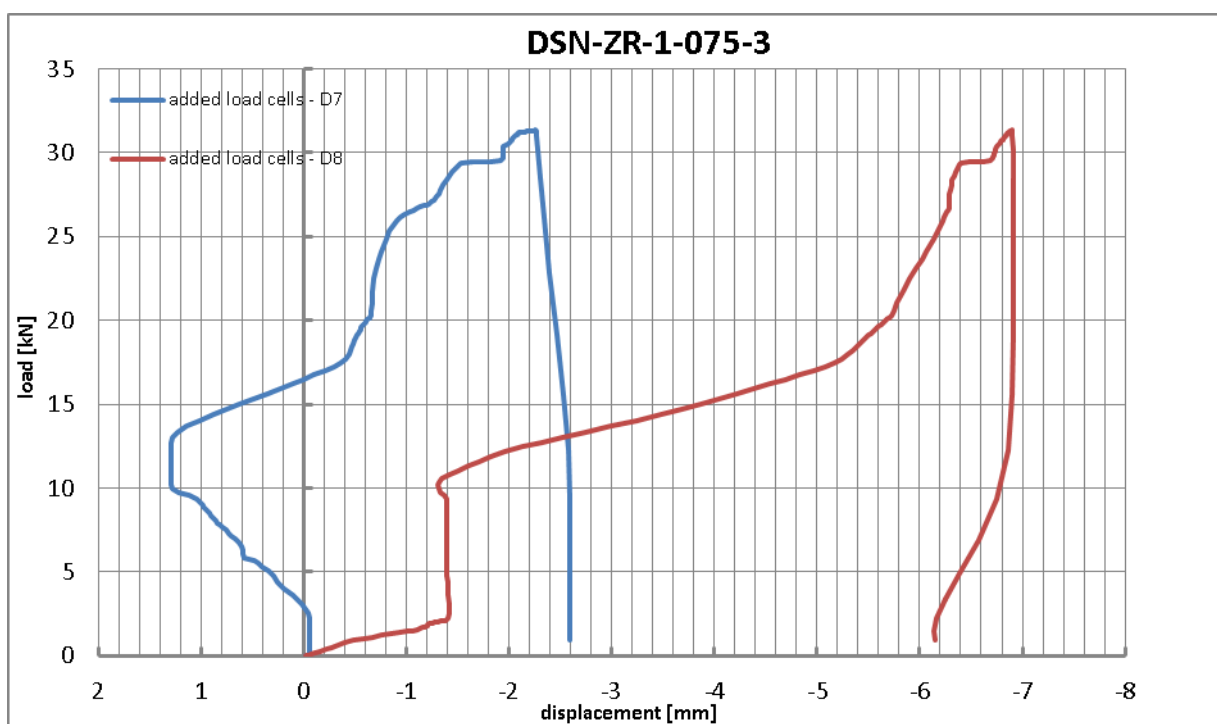
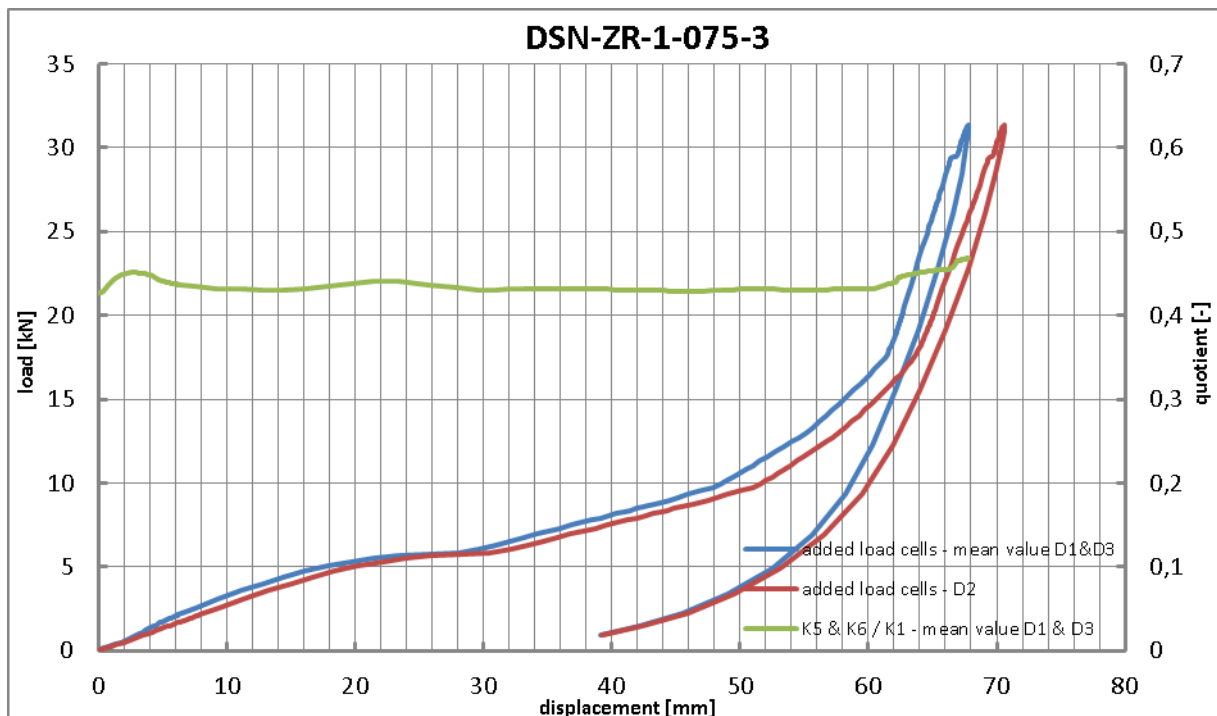


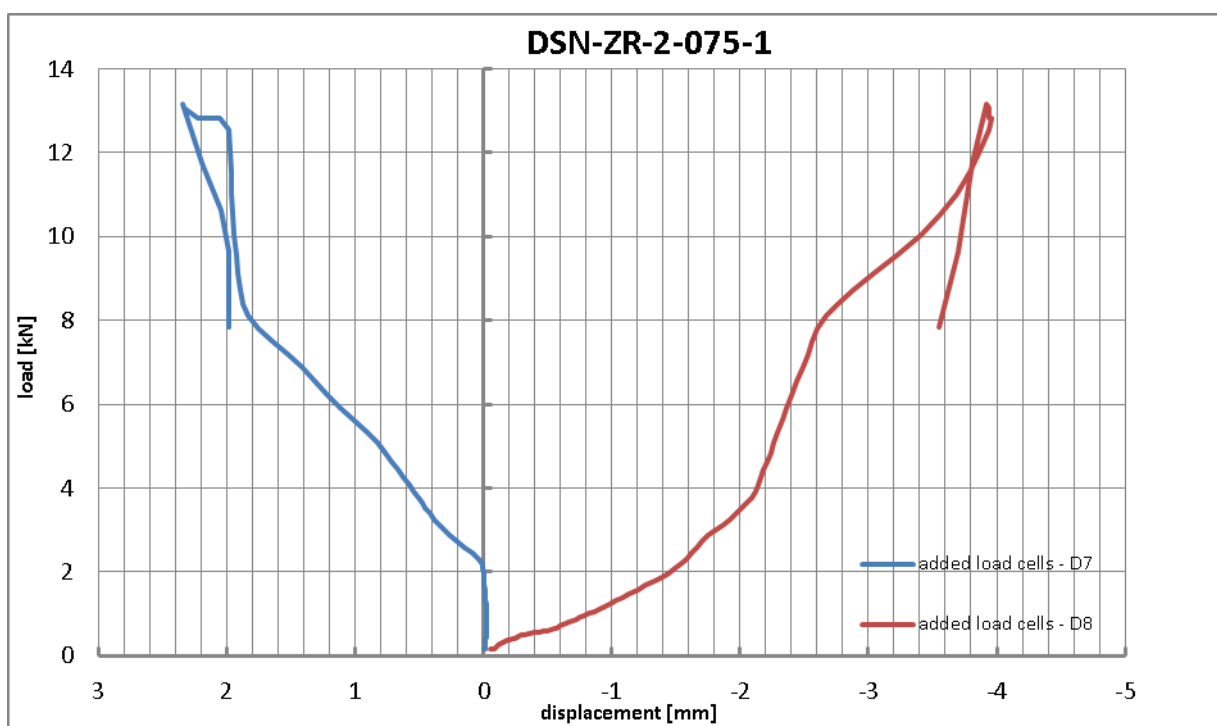
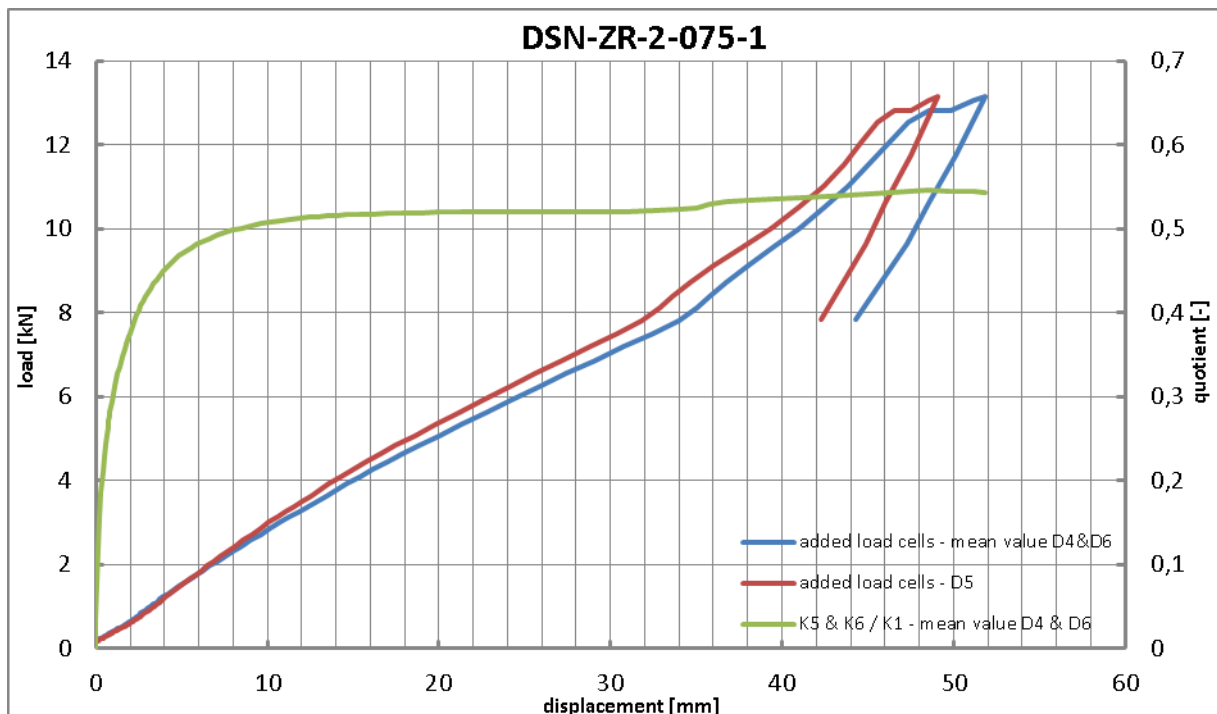


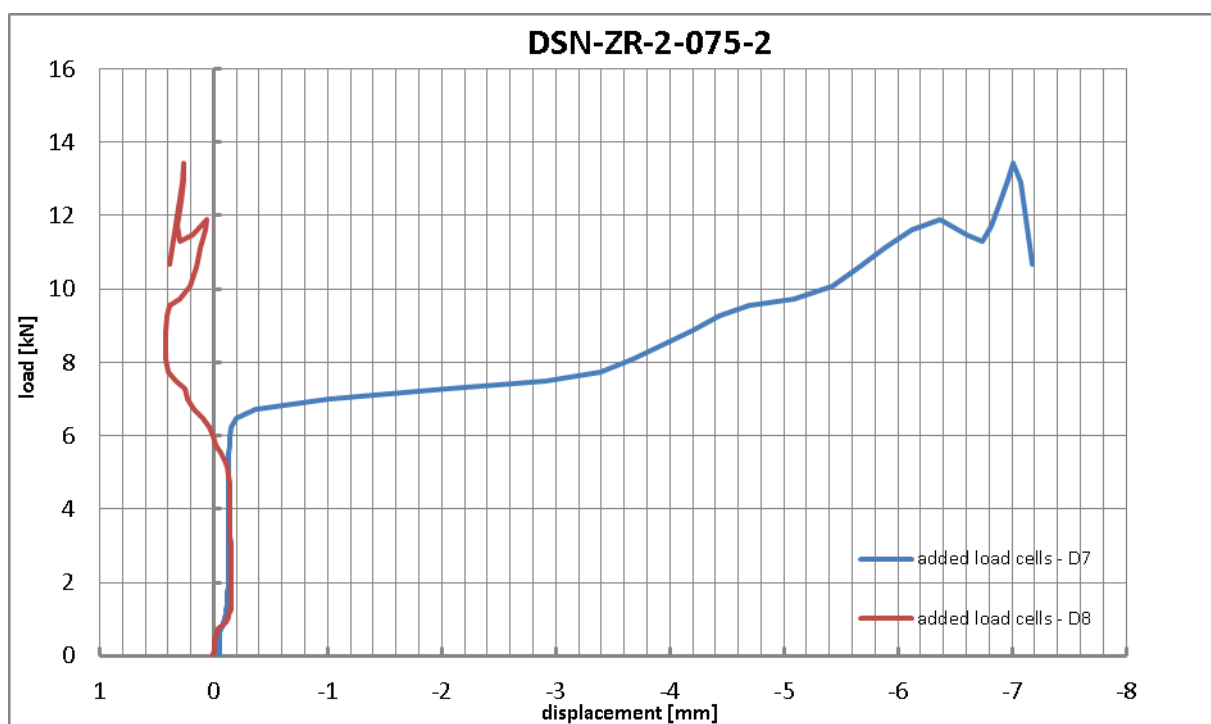
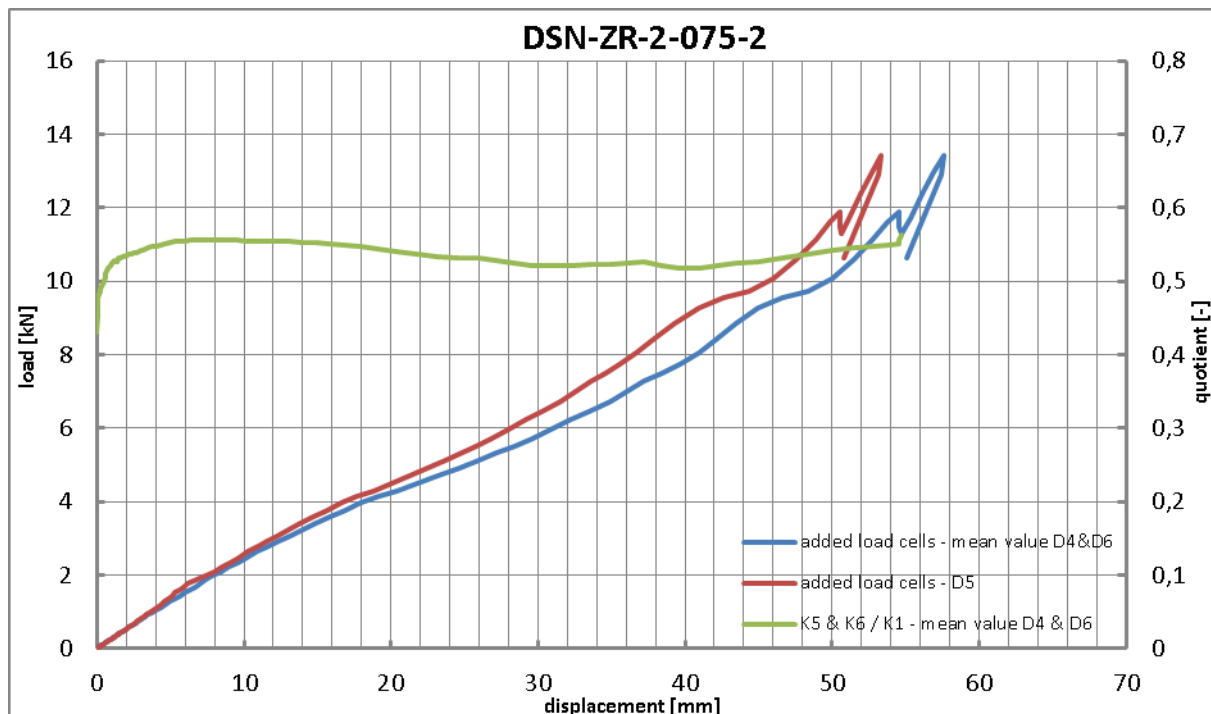


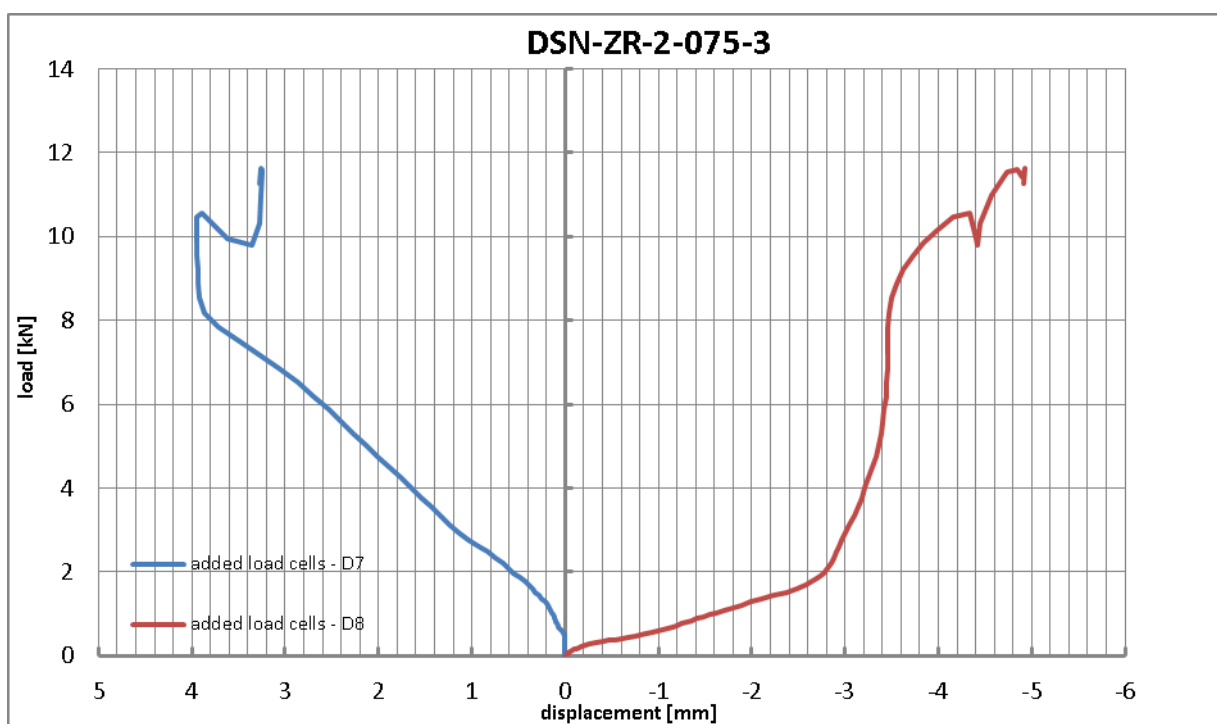
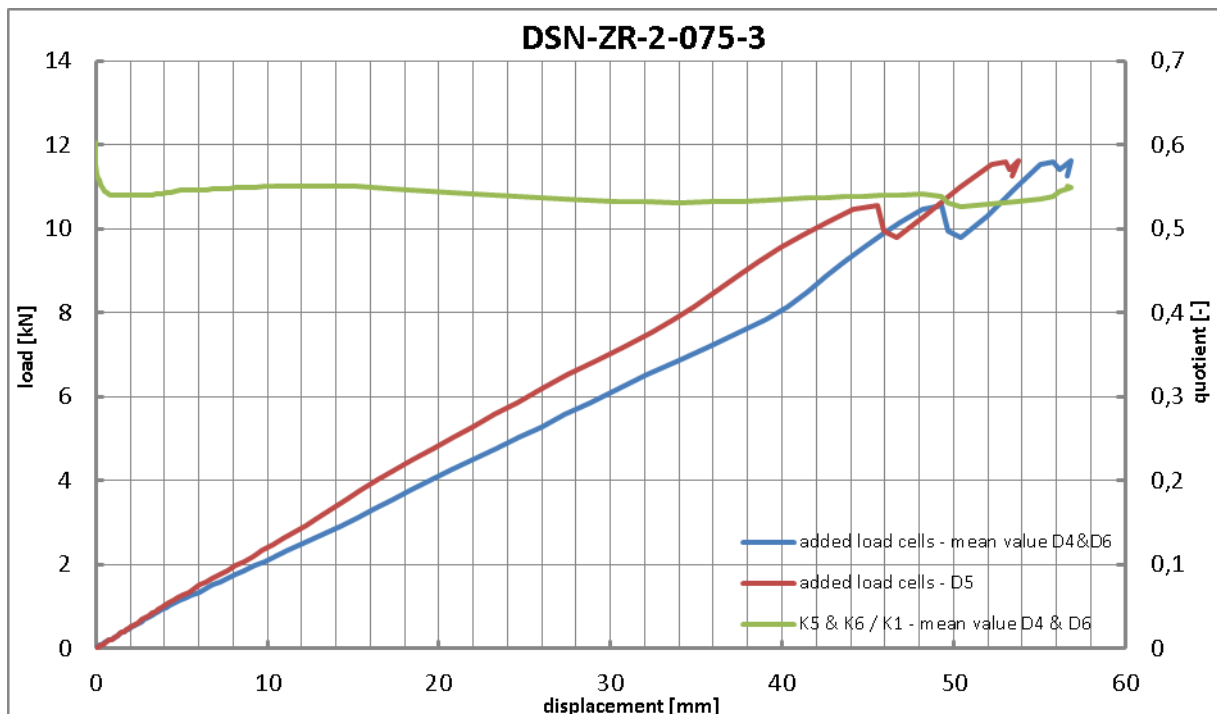


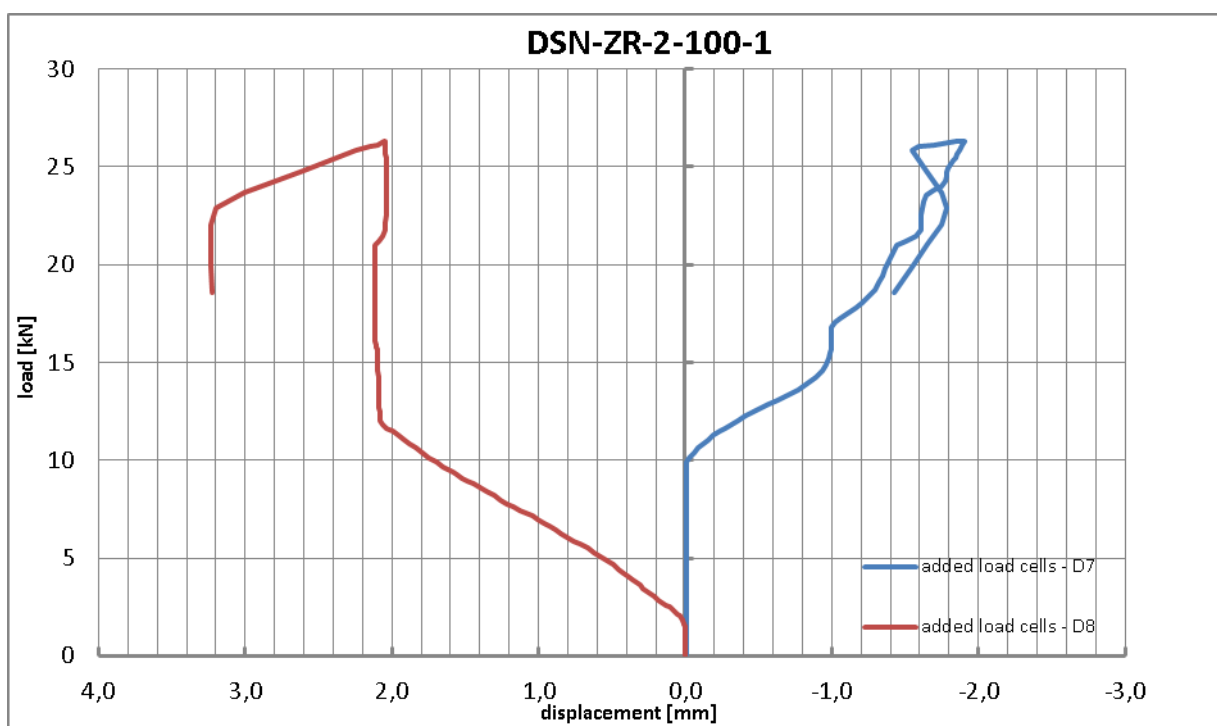
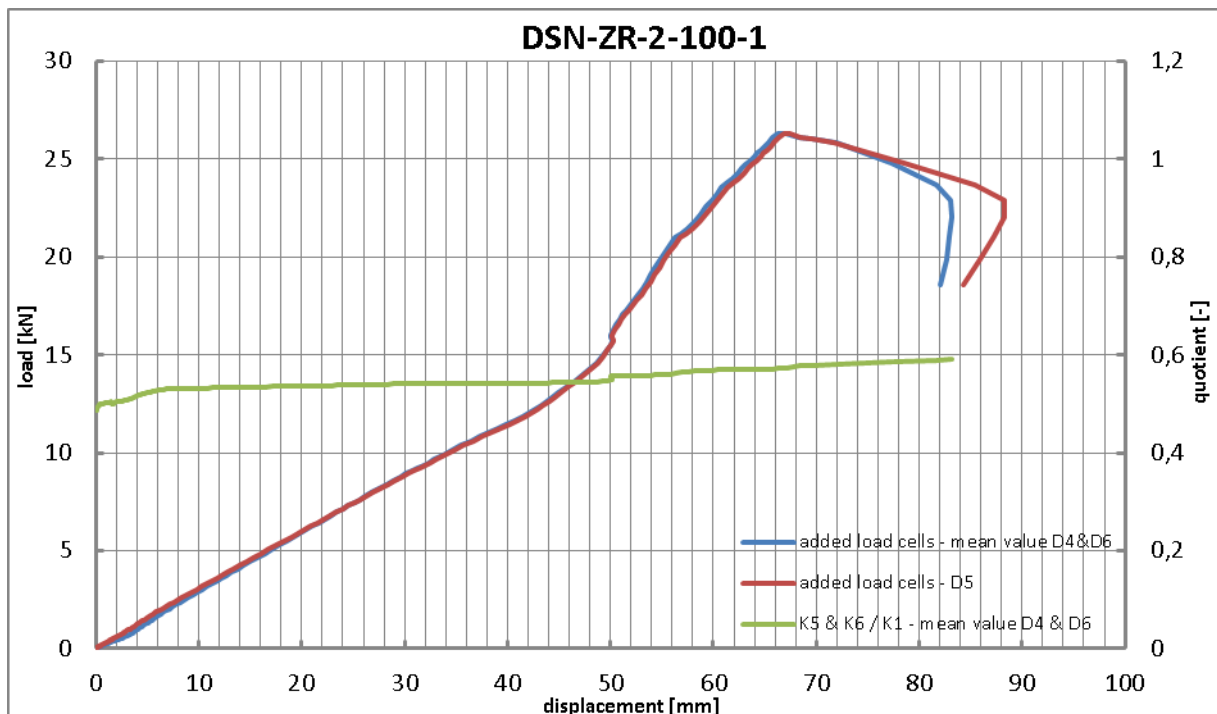


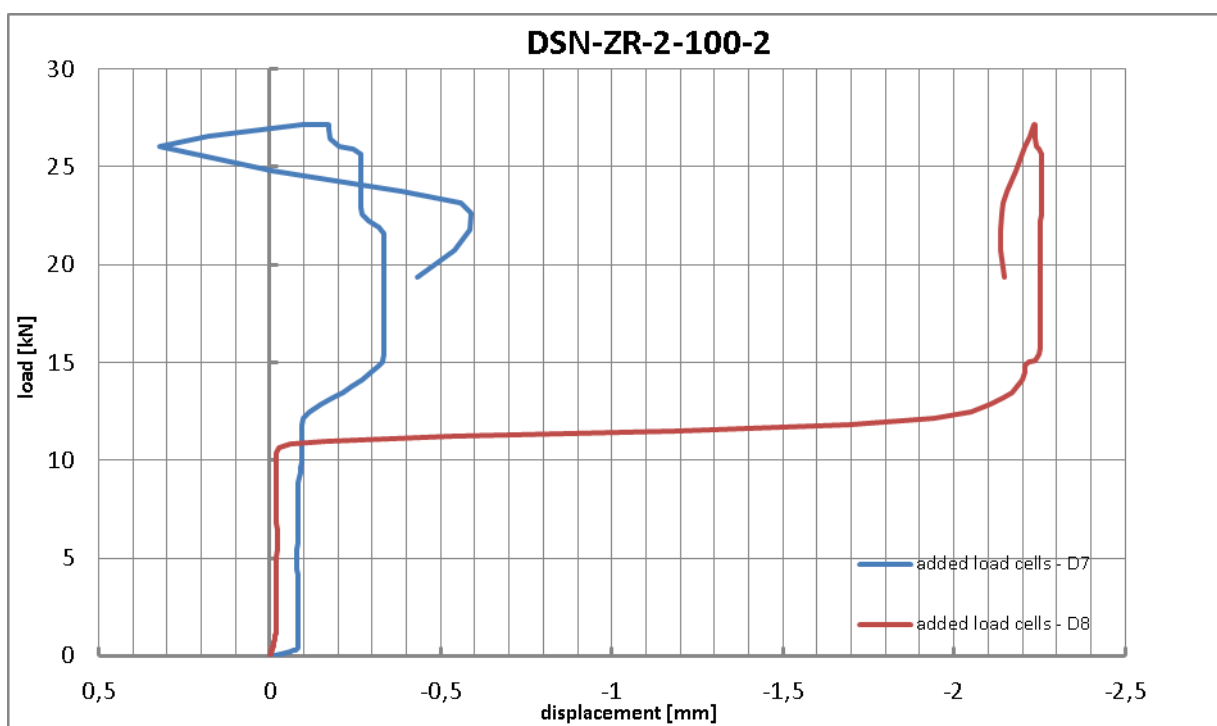
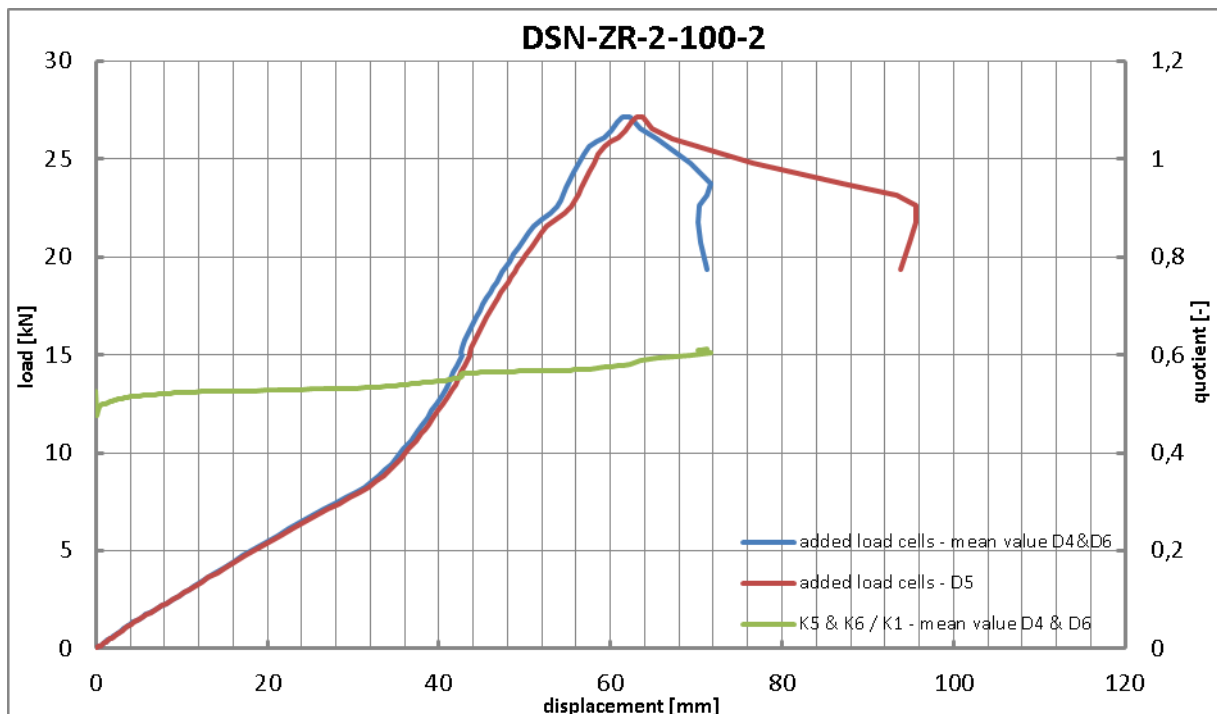


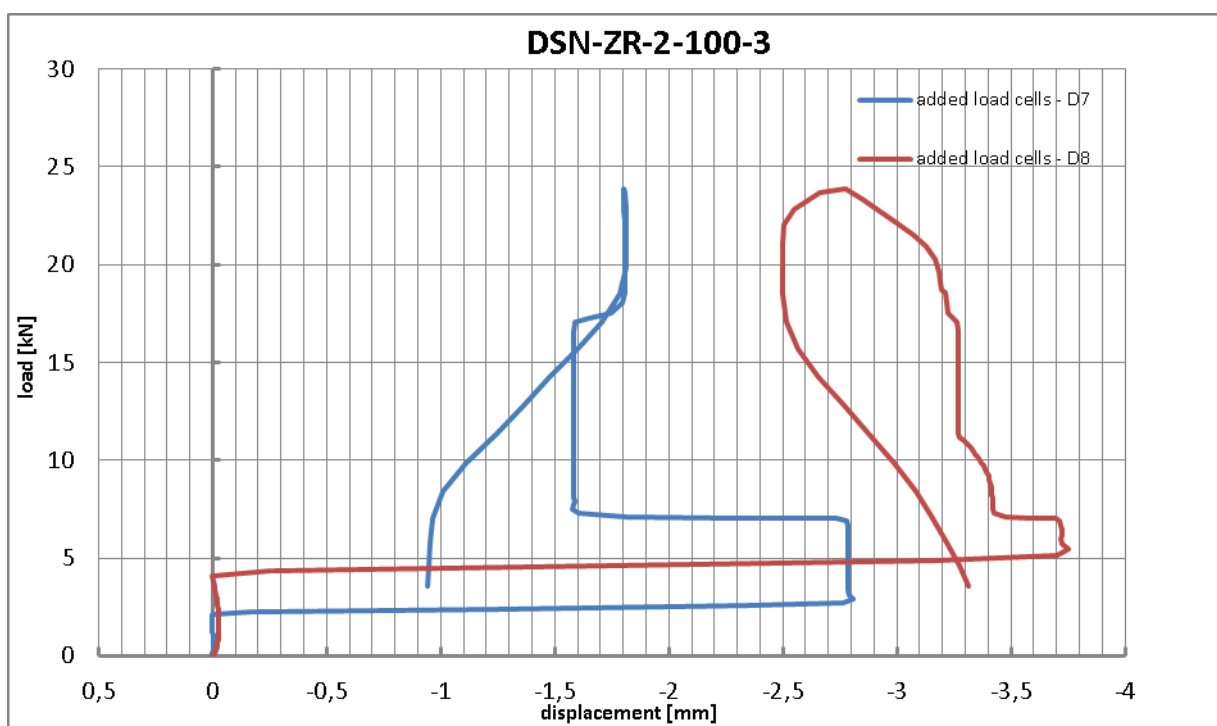
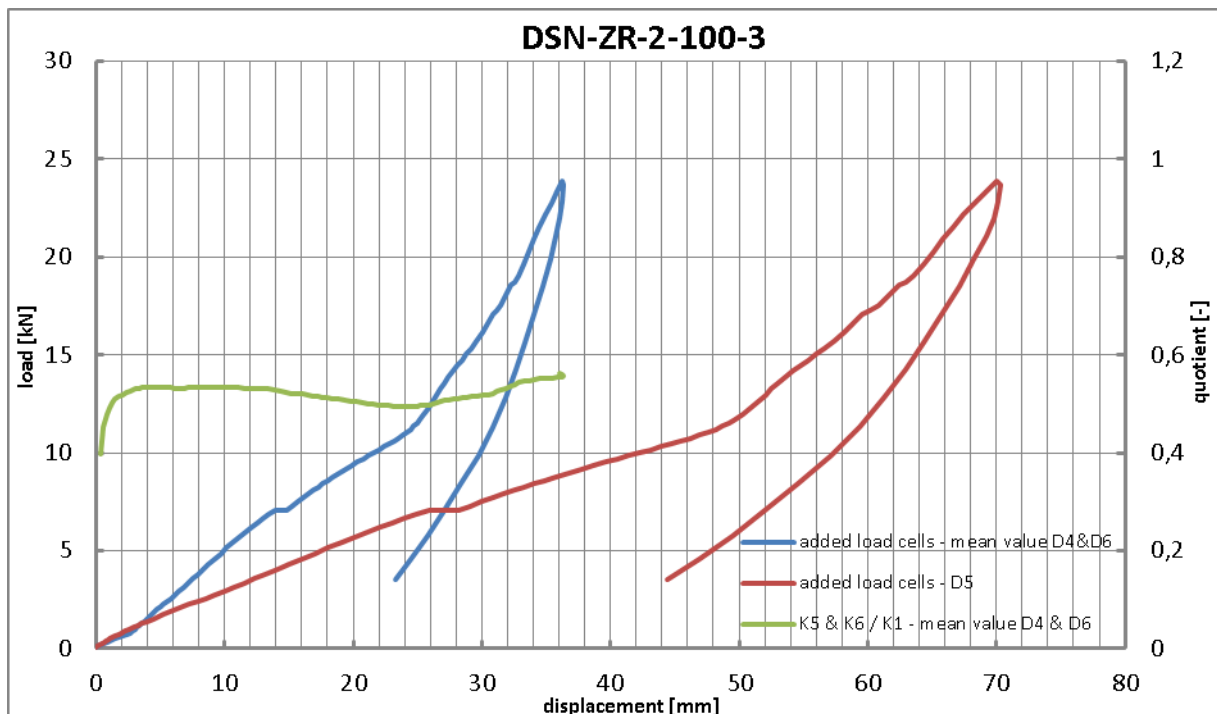


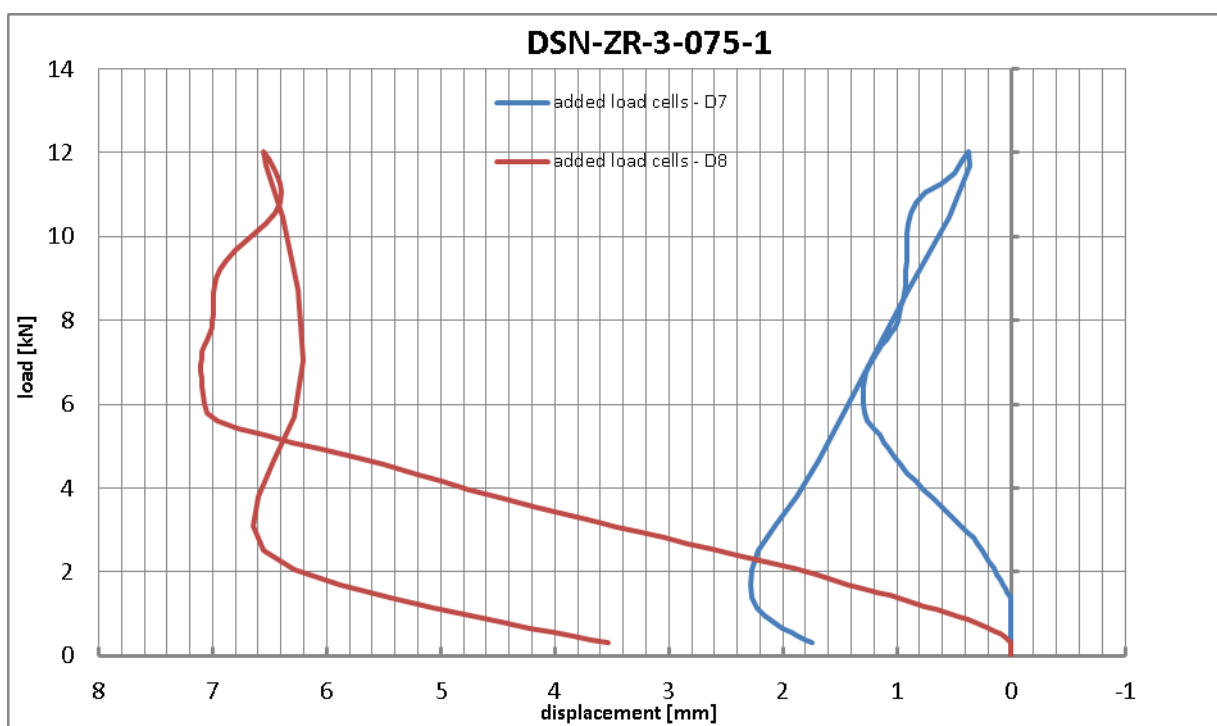
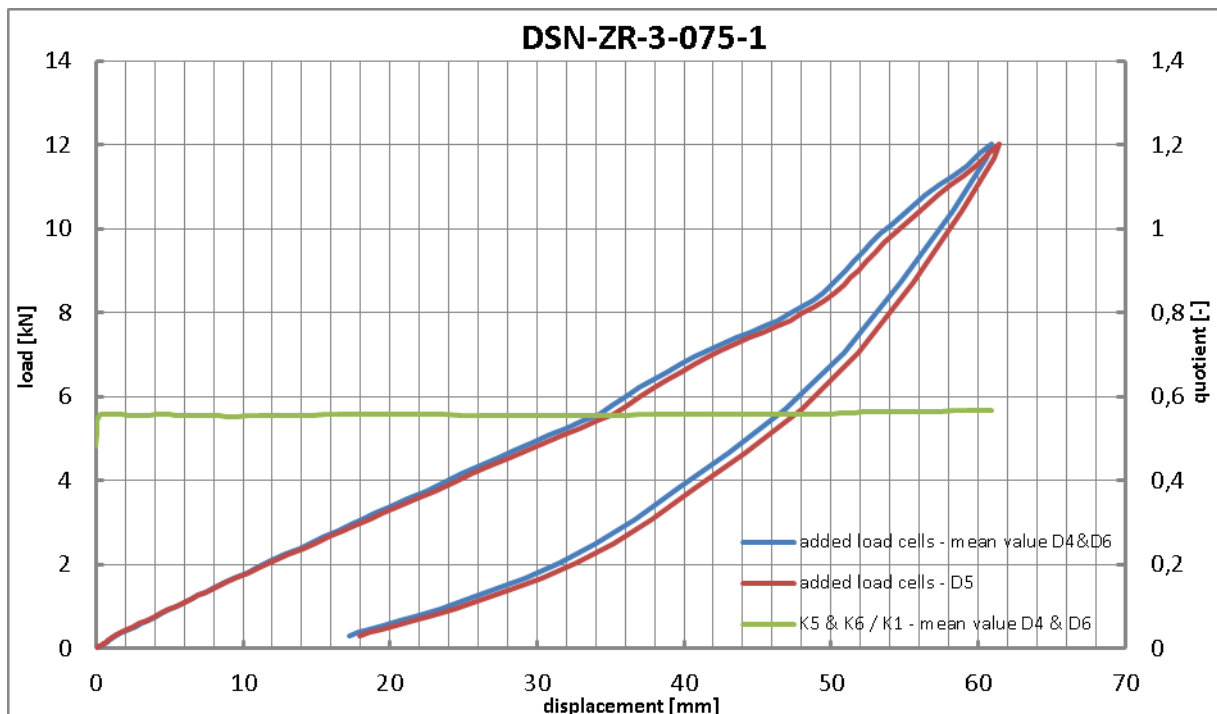


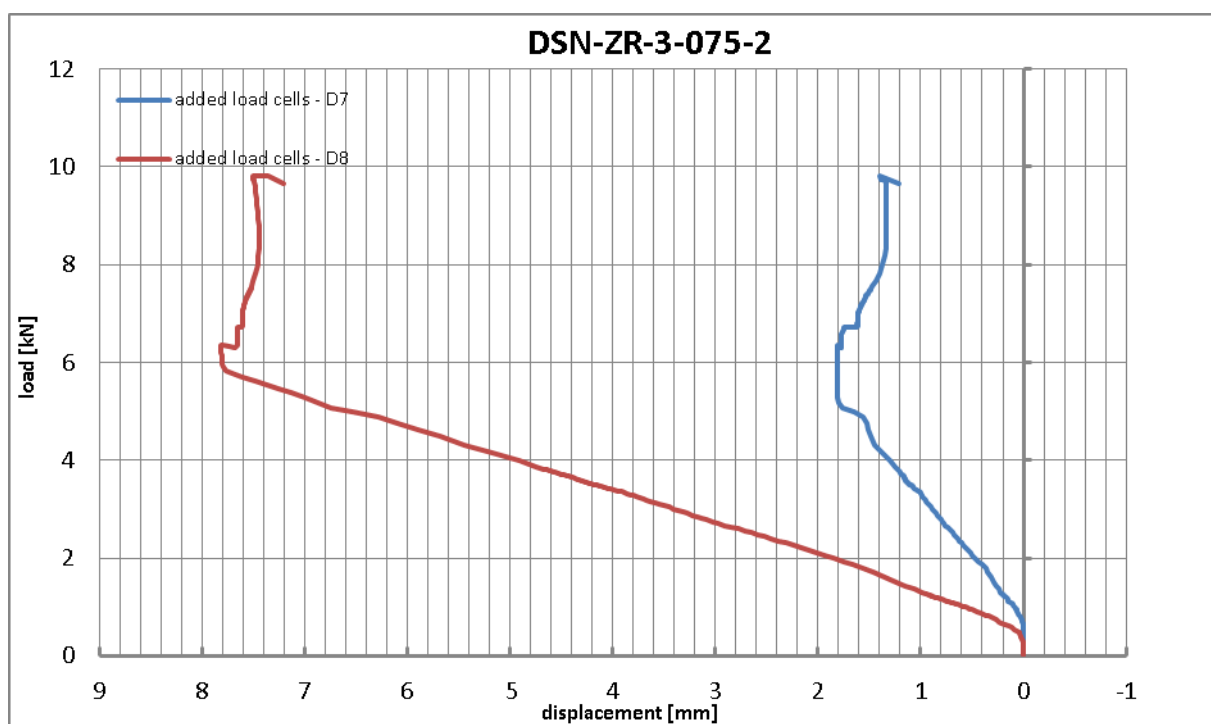
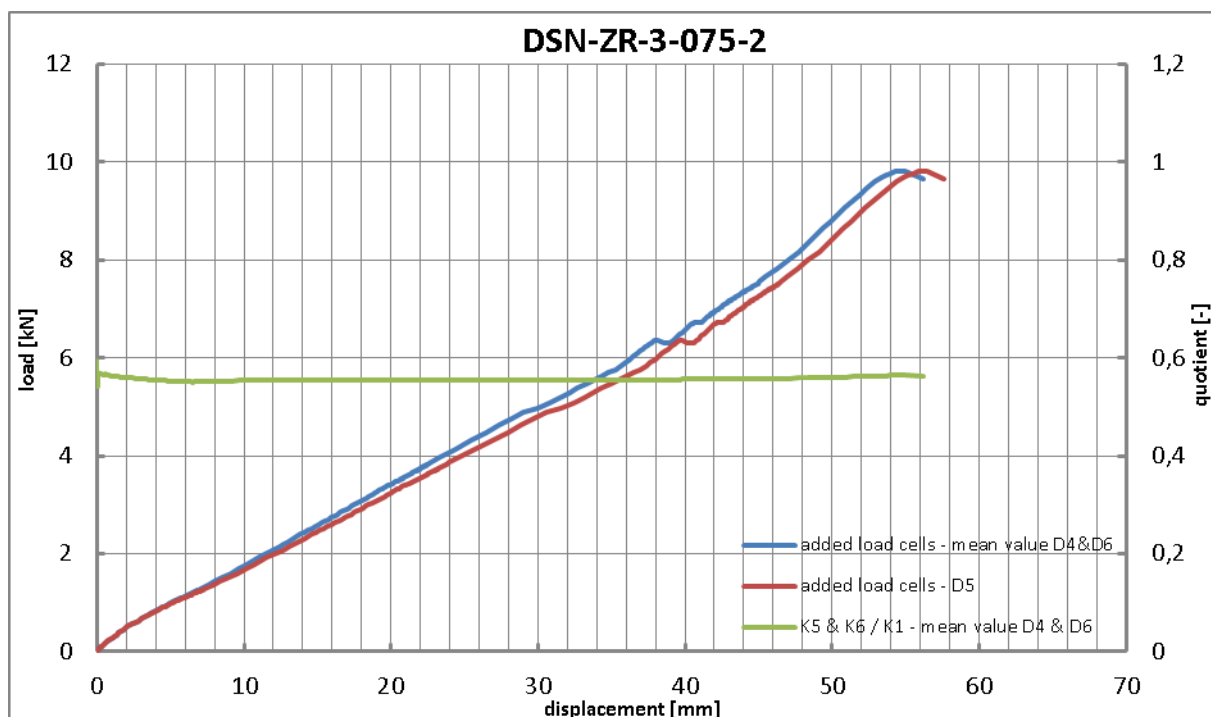


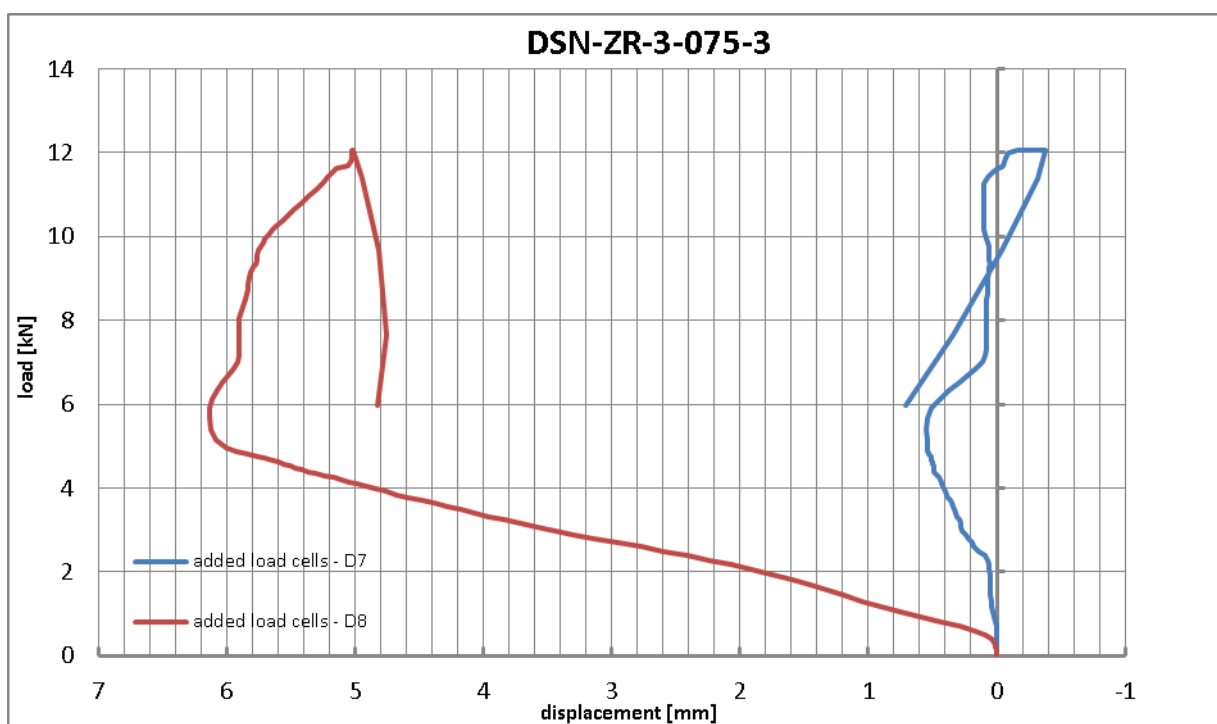
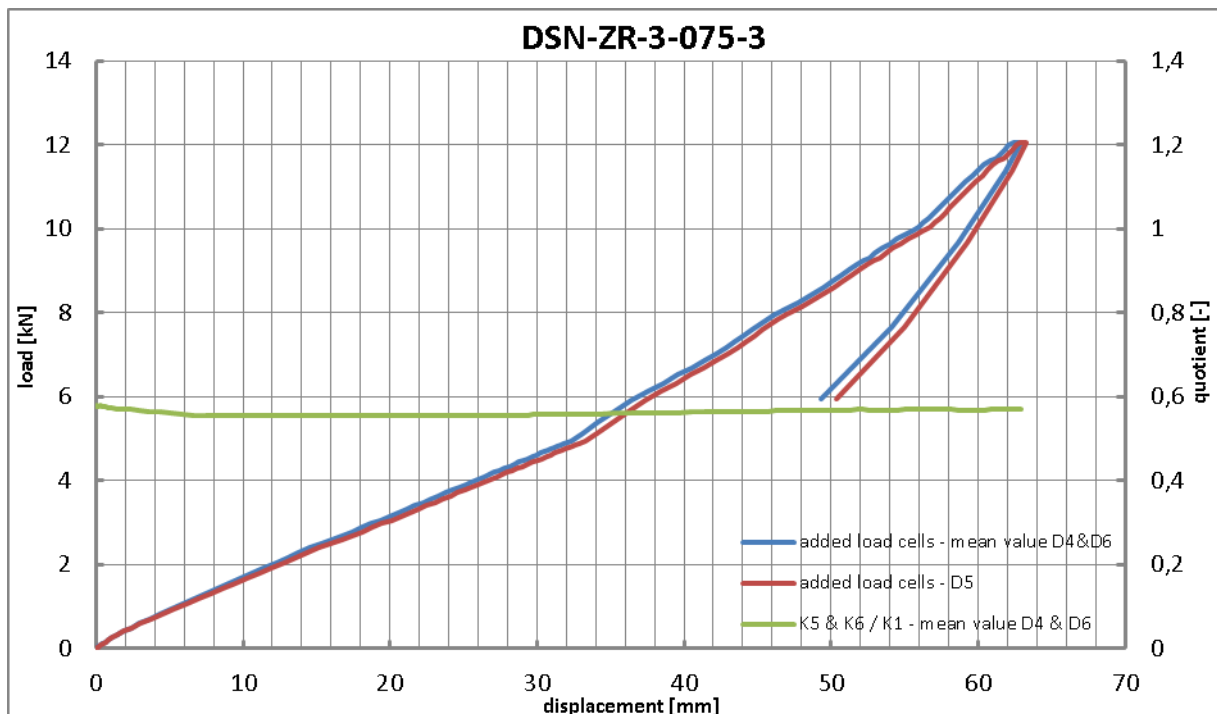


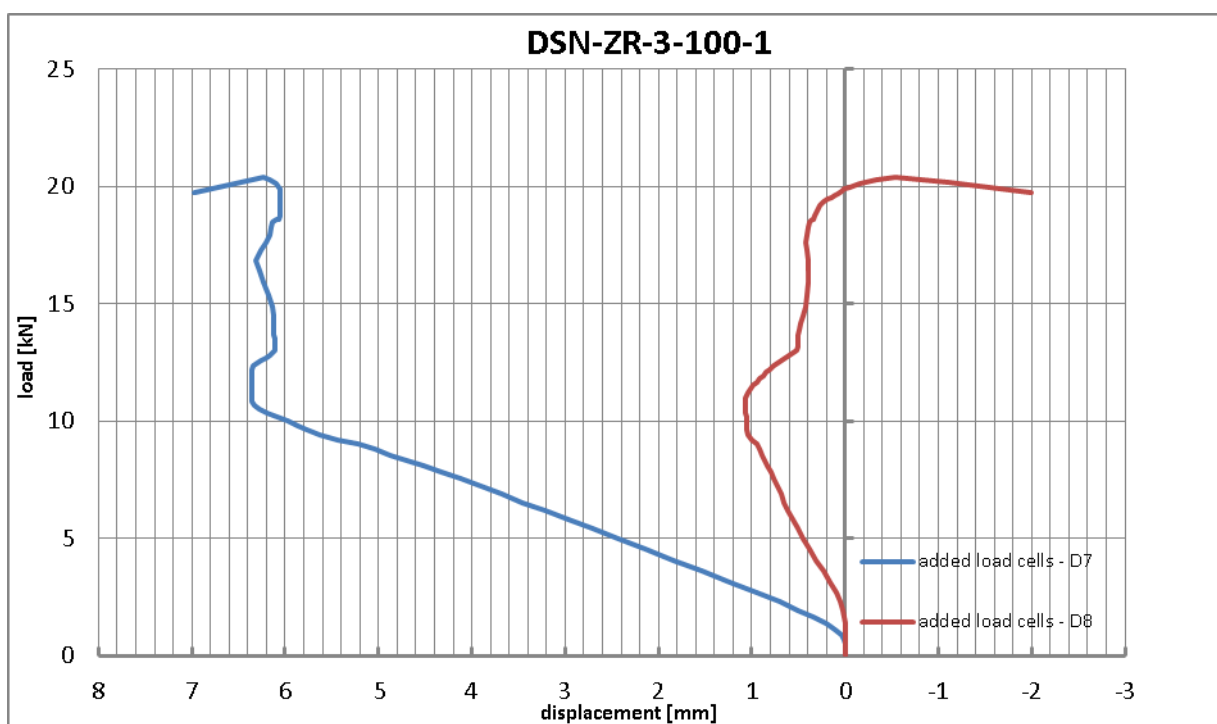
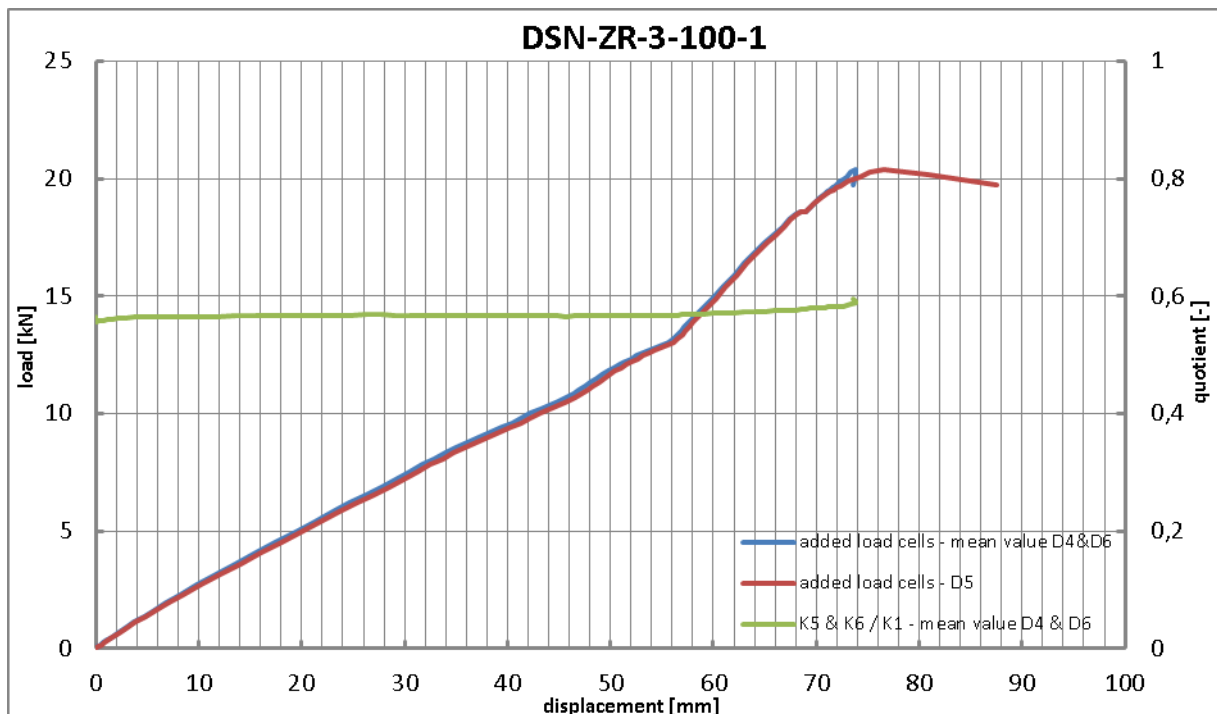


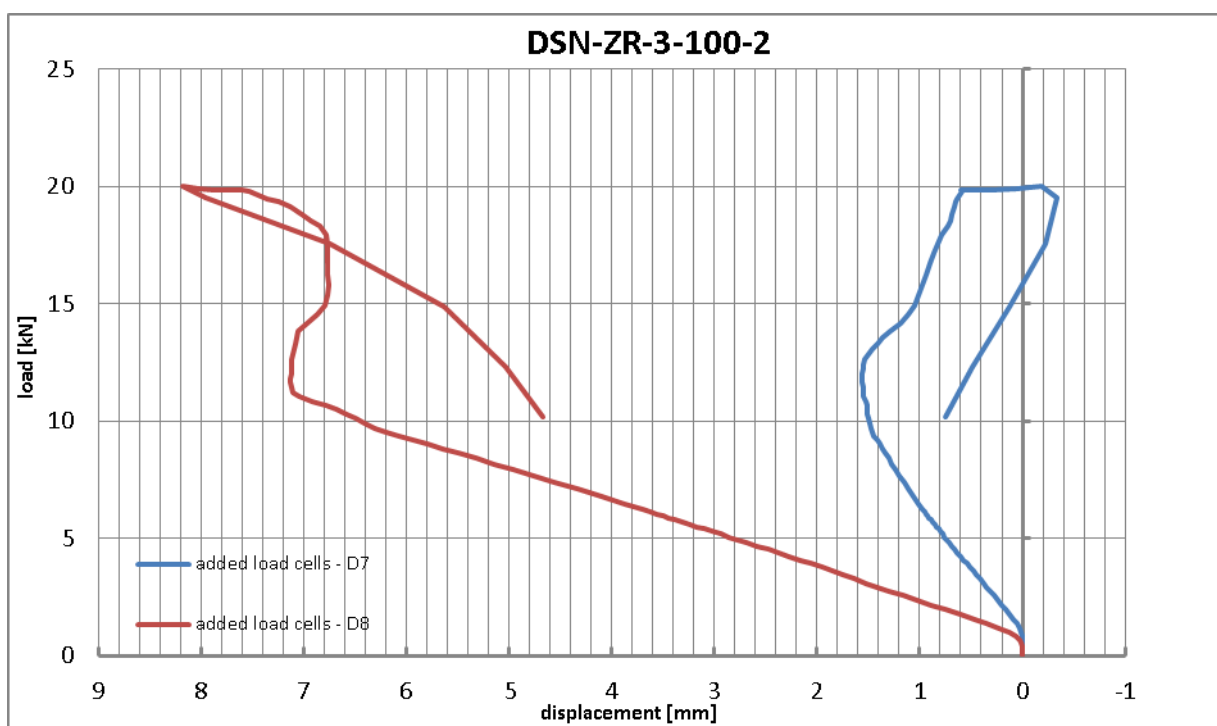
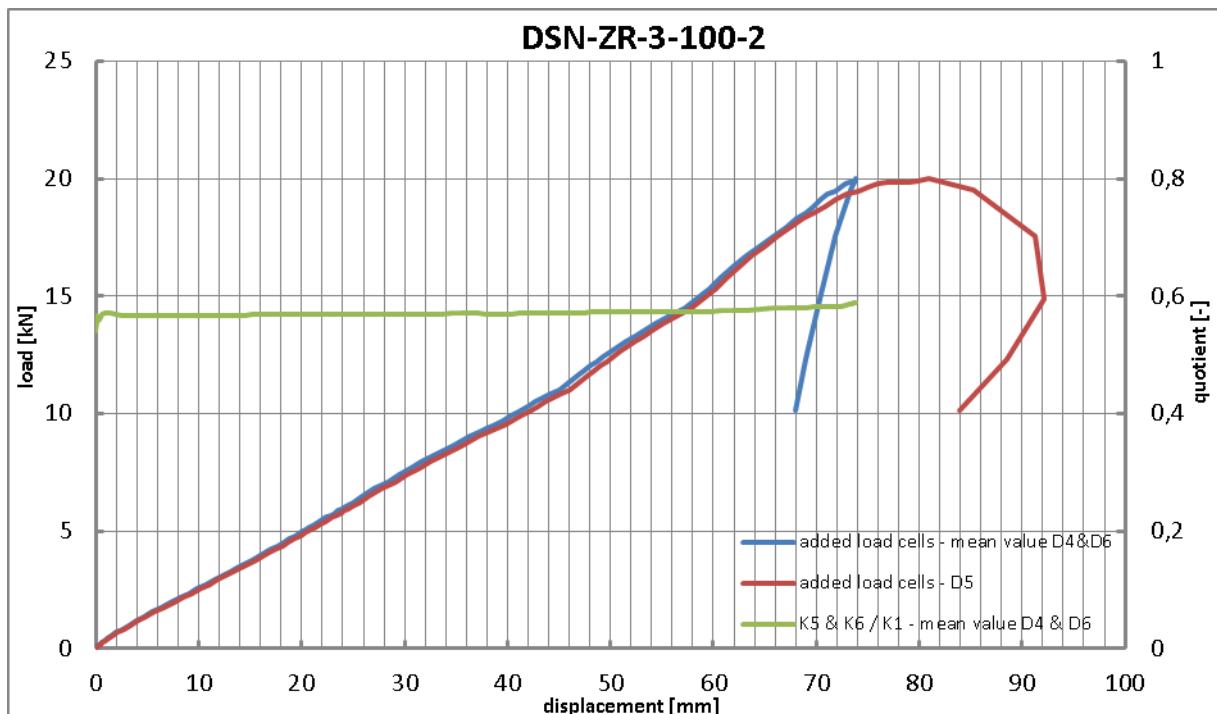


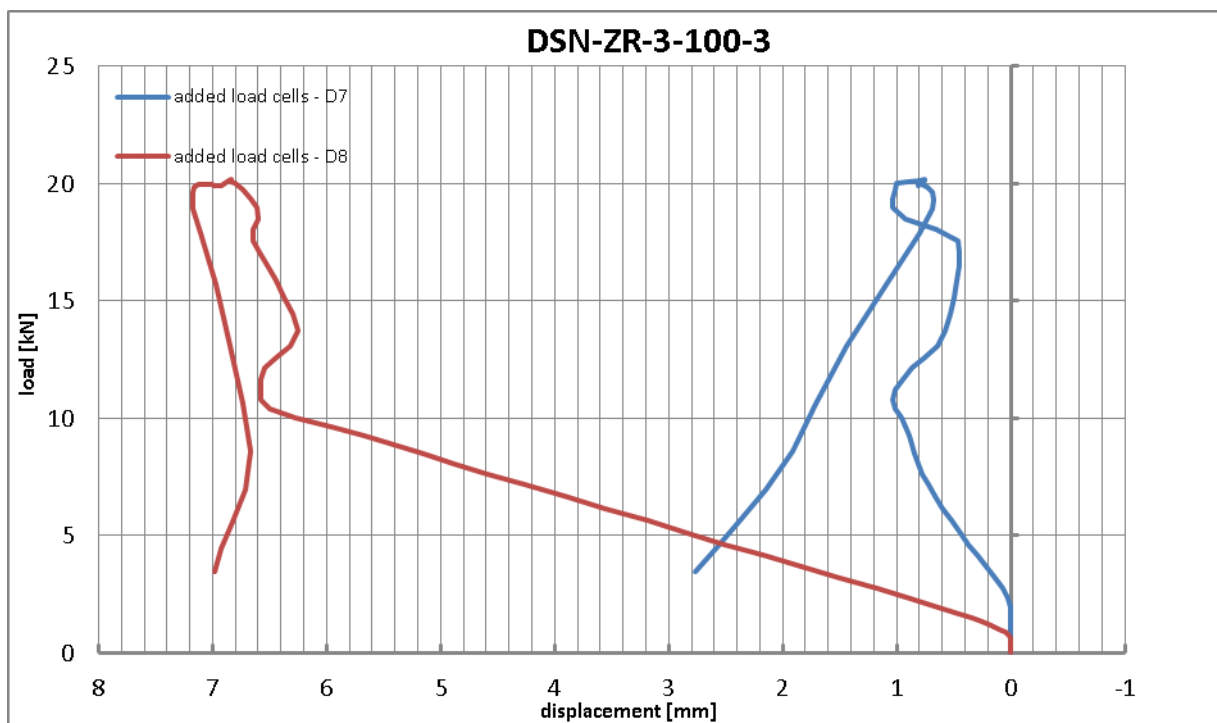
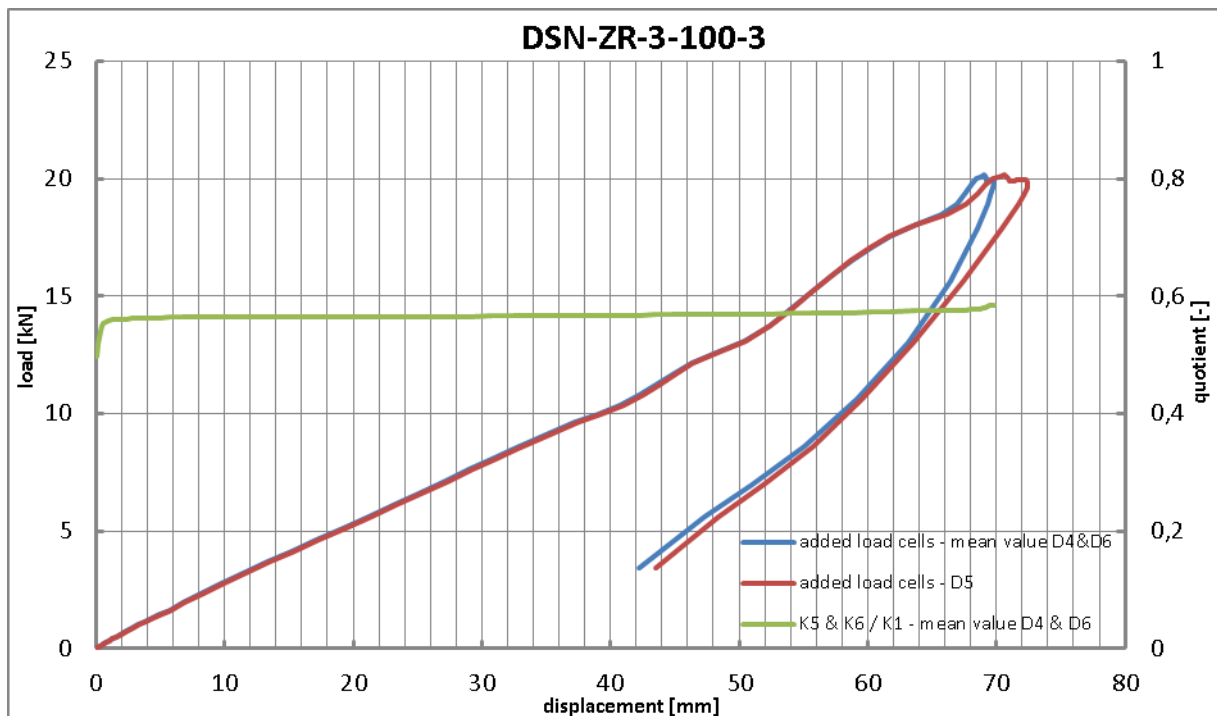












6 Annex F: End support tests (pressure)

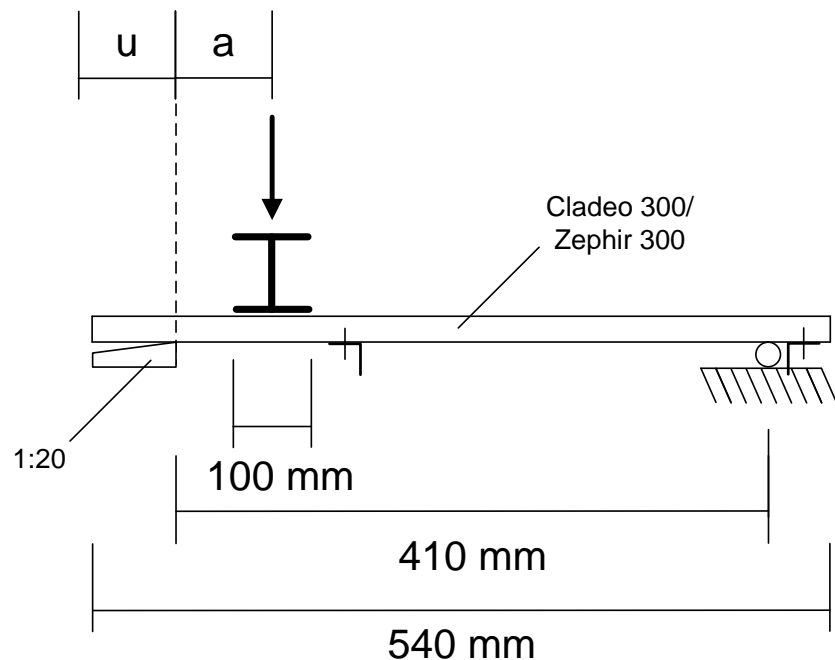


Fig. F.1: Schematic test setup



Fig. F.2: Test setup, side view



Fig. F.3: Test setup, front view



Fig. F.4: Web-crippling (Cladeo)



Fig. F.5: Local buckling under the load applying traverse (Cladeo)

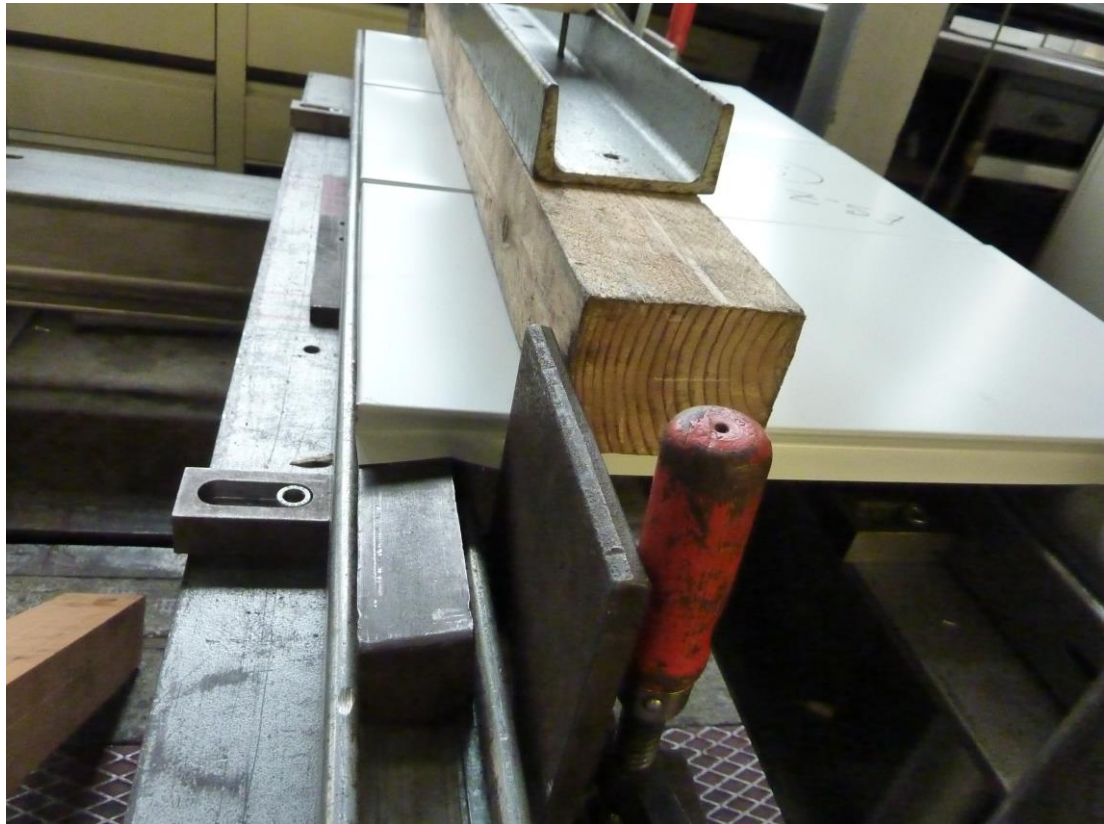
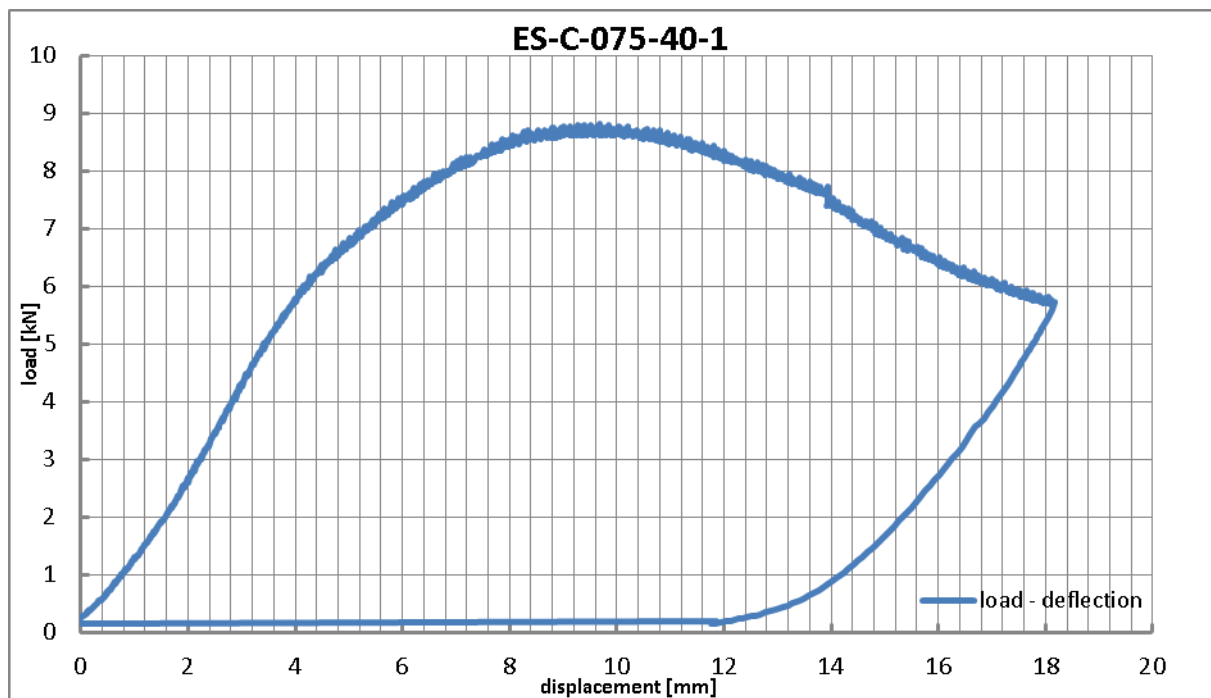


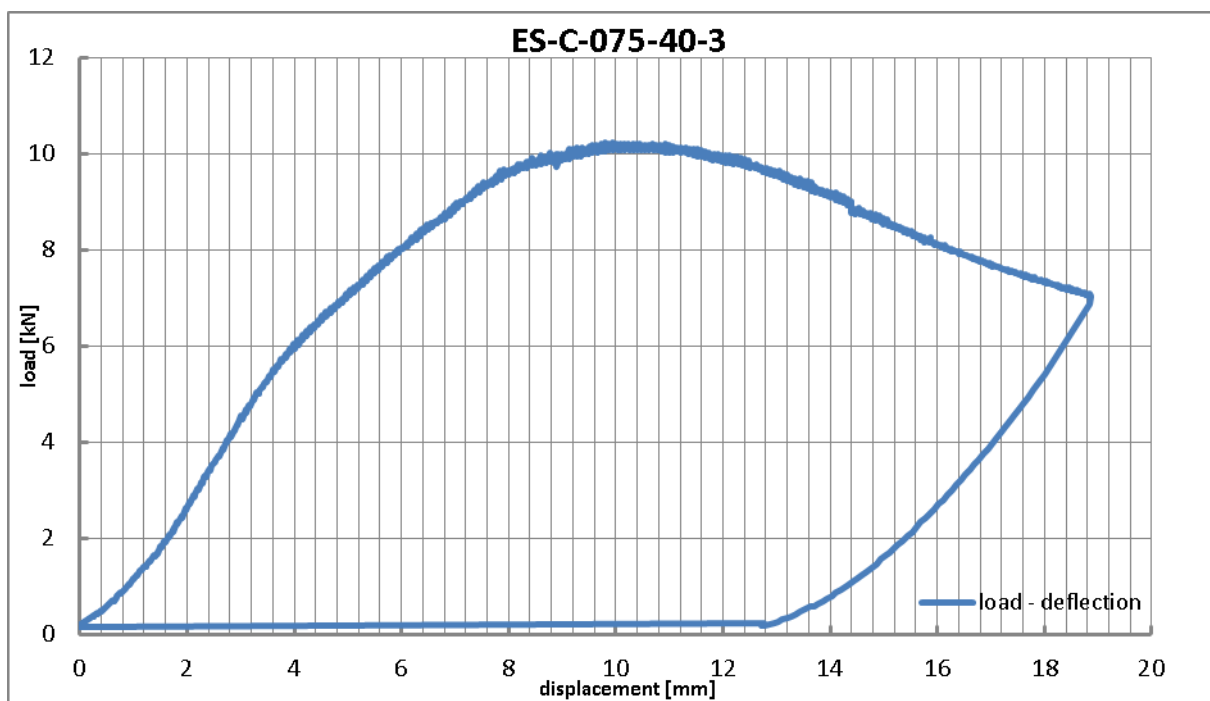
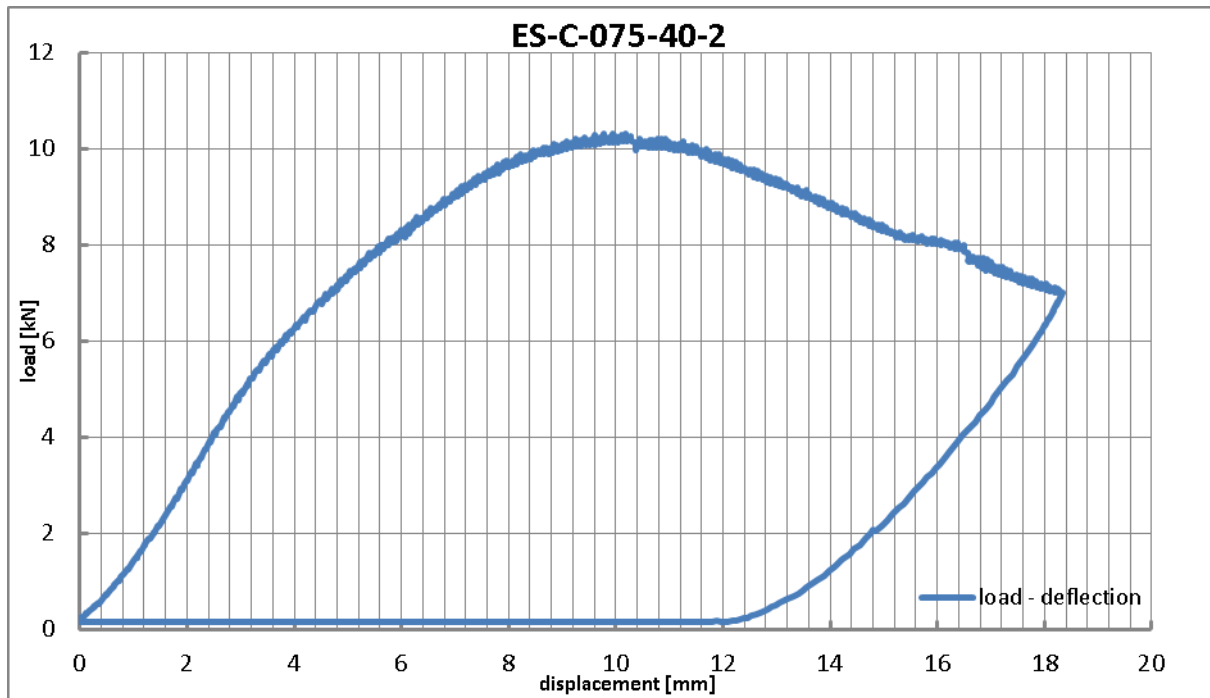
Fig. F.6: Web-crippling (Zephir)

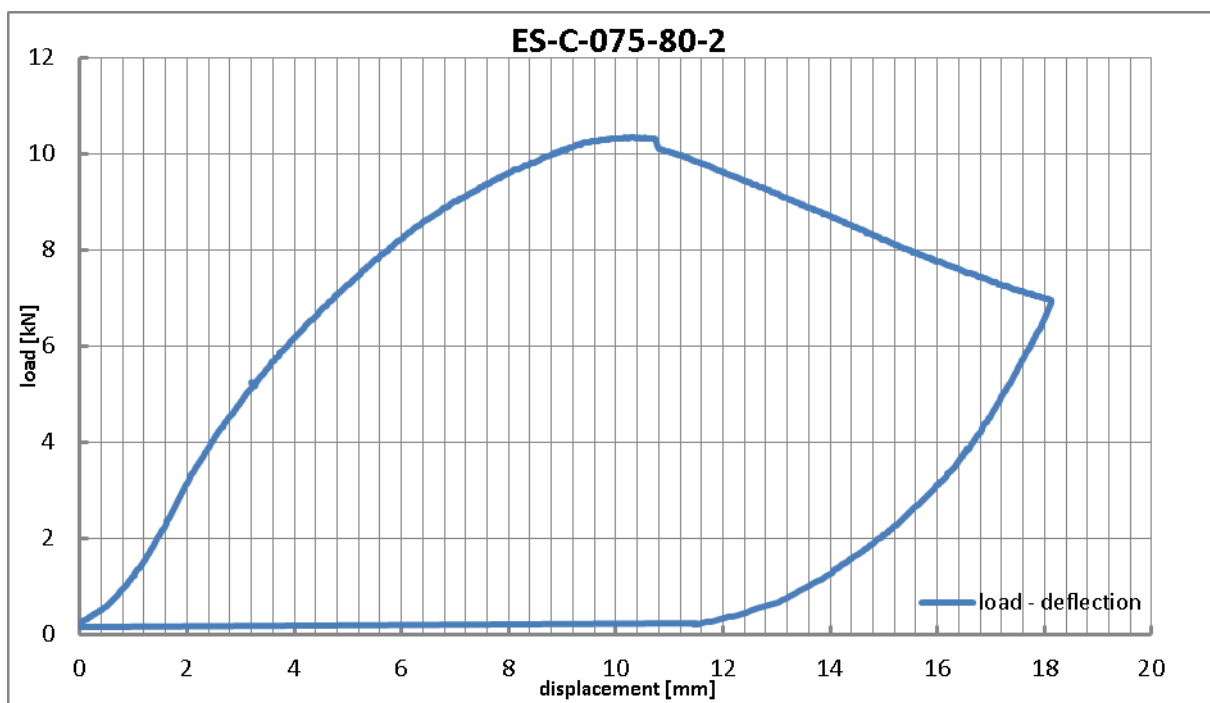
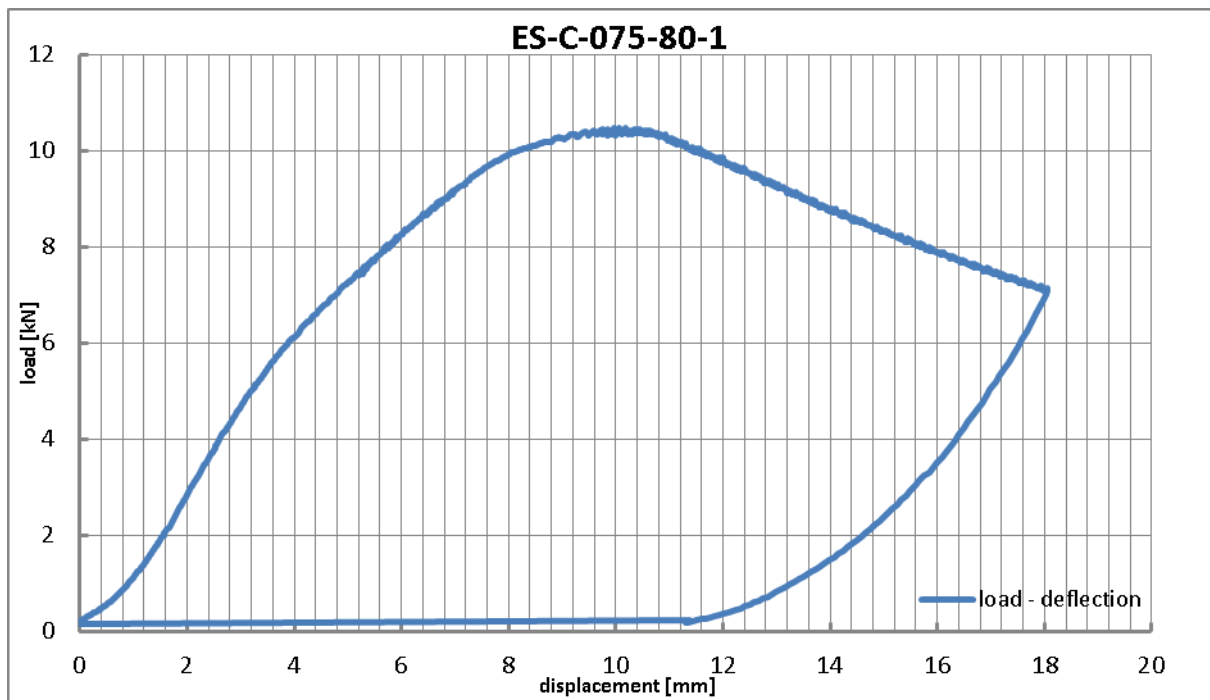


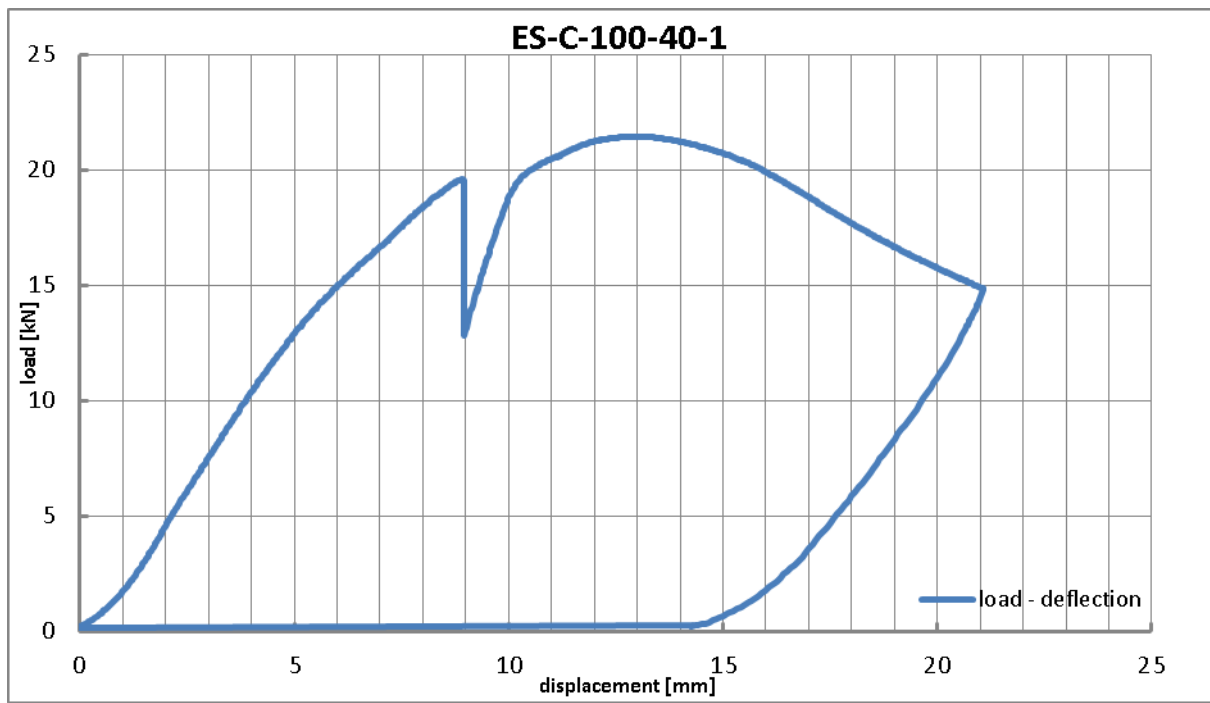
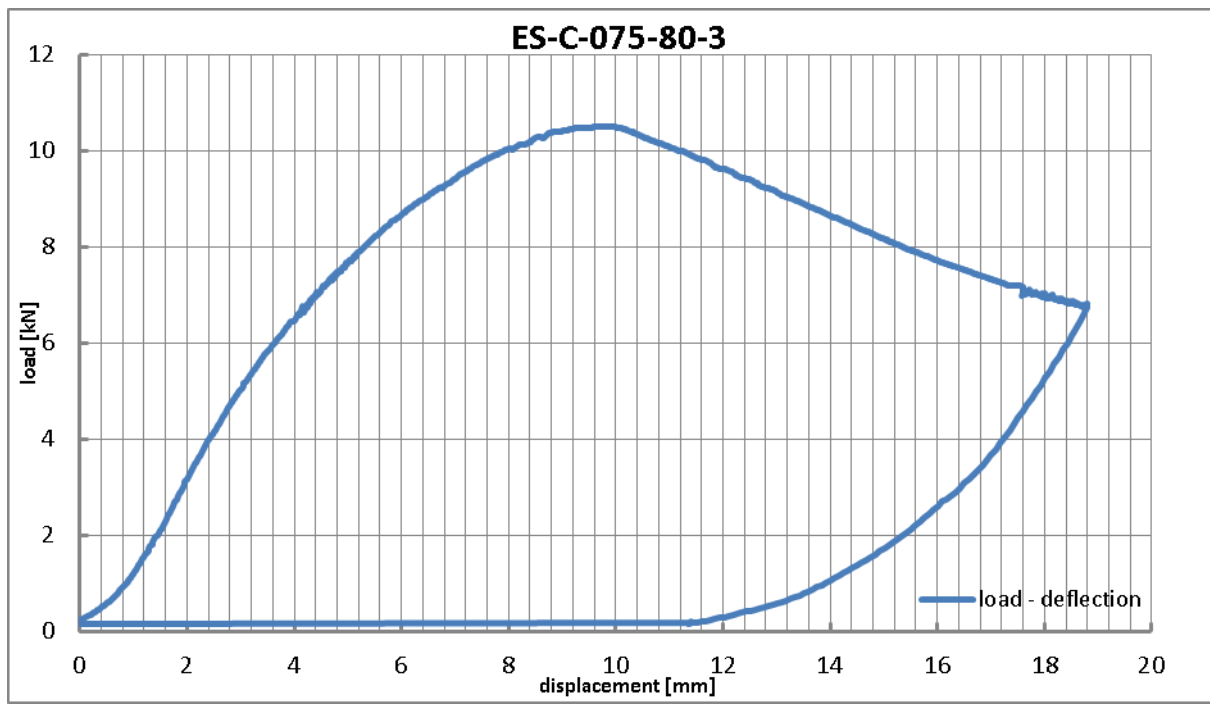
Fig. F.7: Local buckling under the load applying traverse (Zephir)

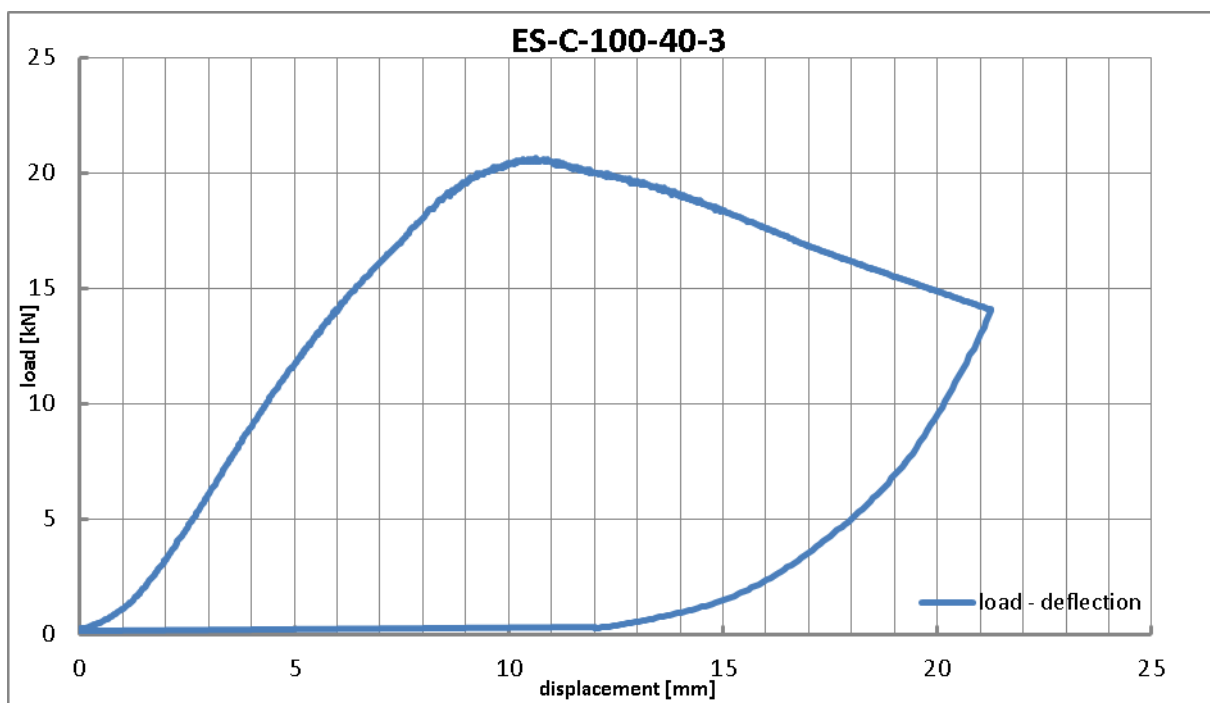
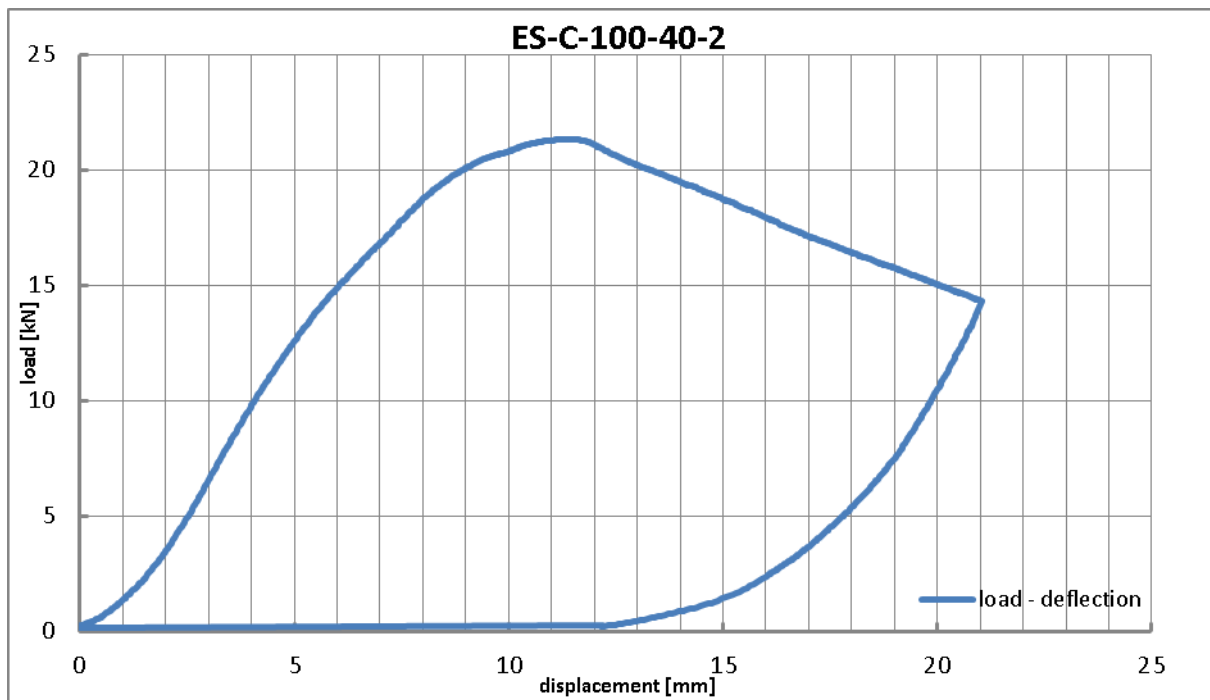
Load-deflection-curves:

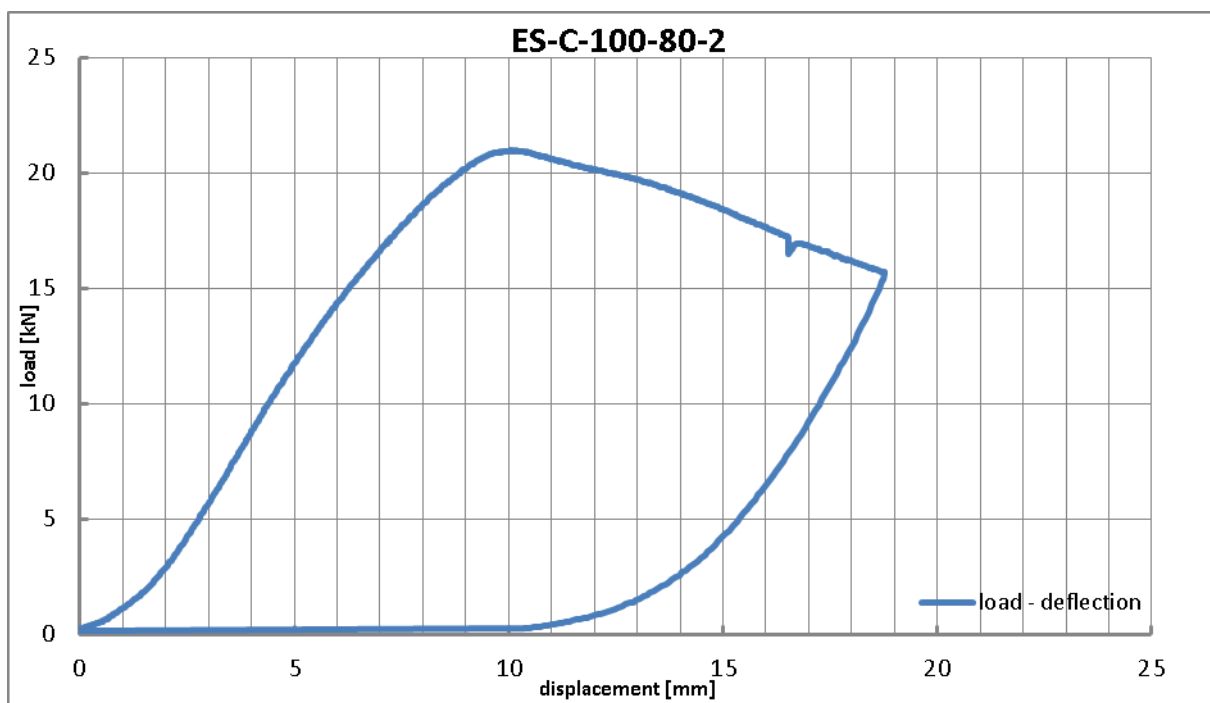
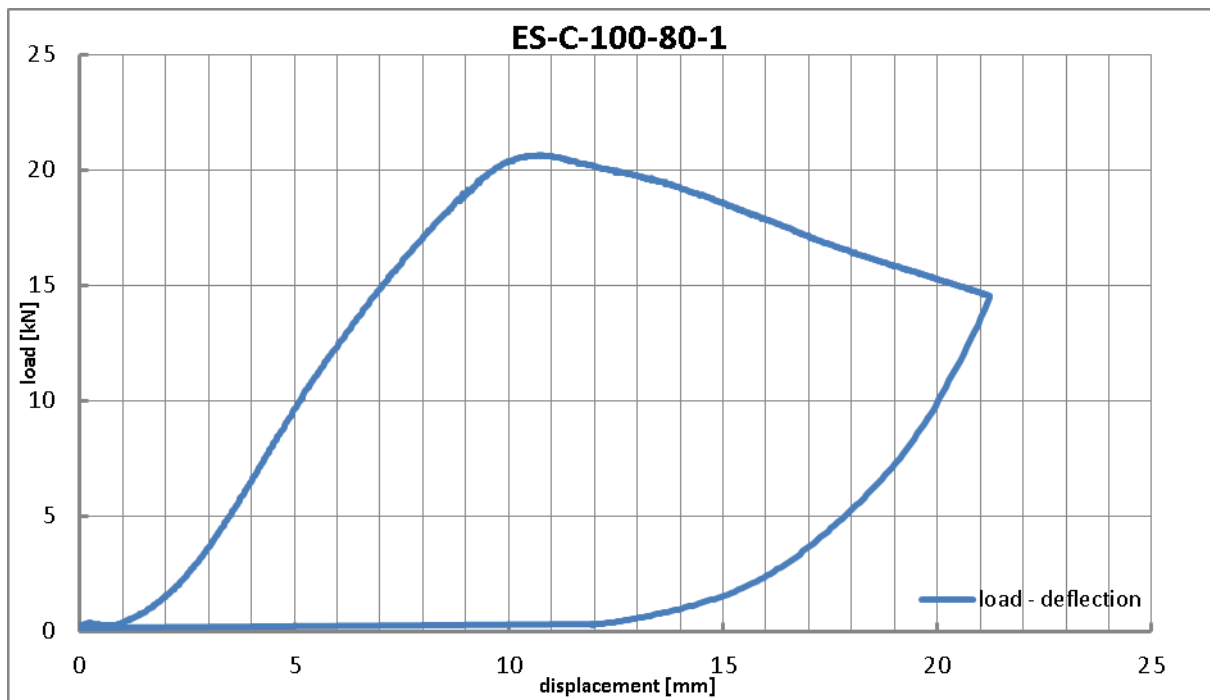


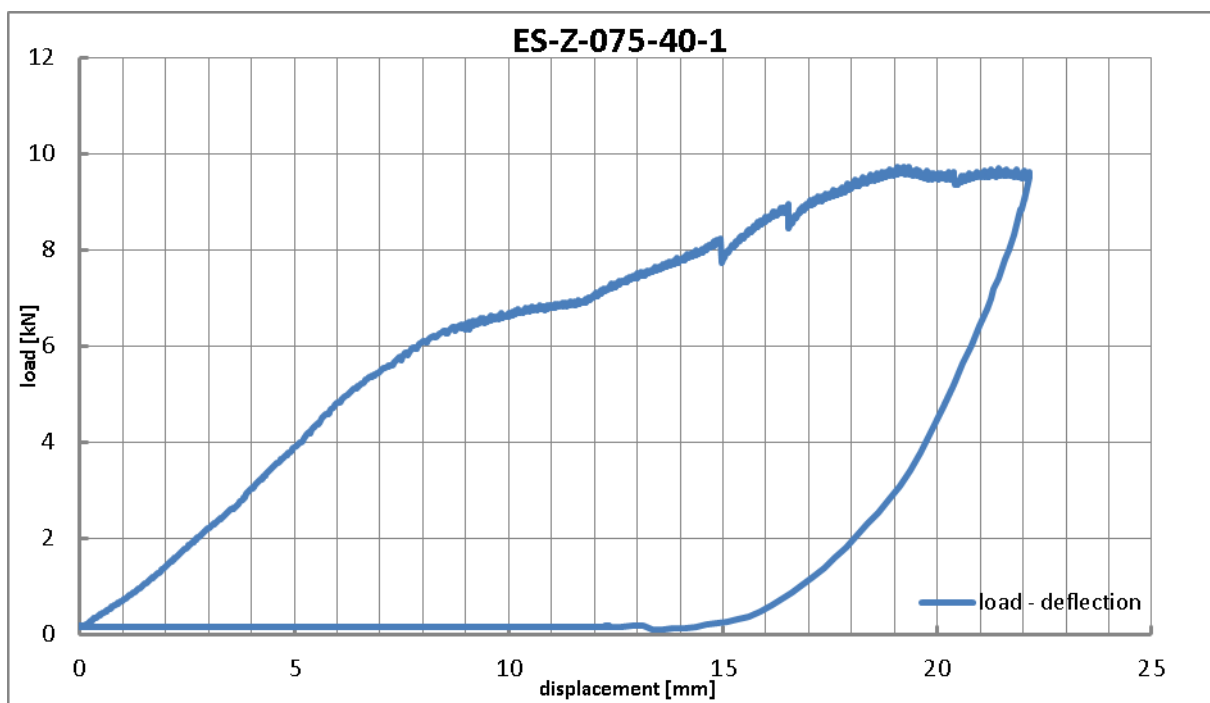
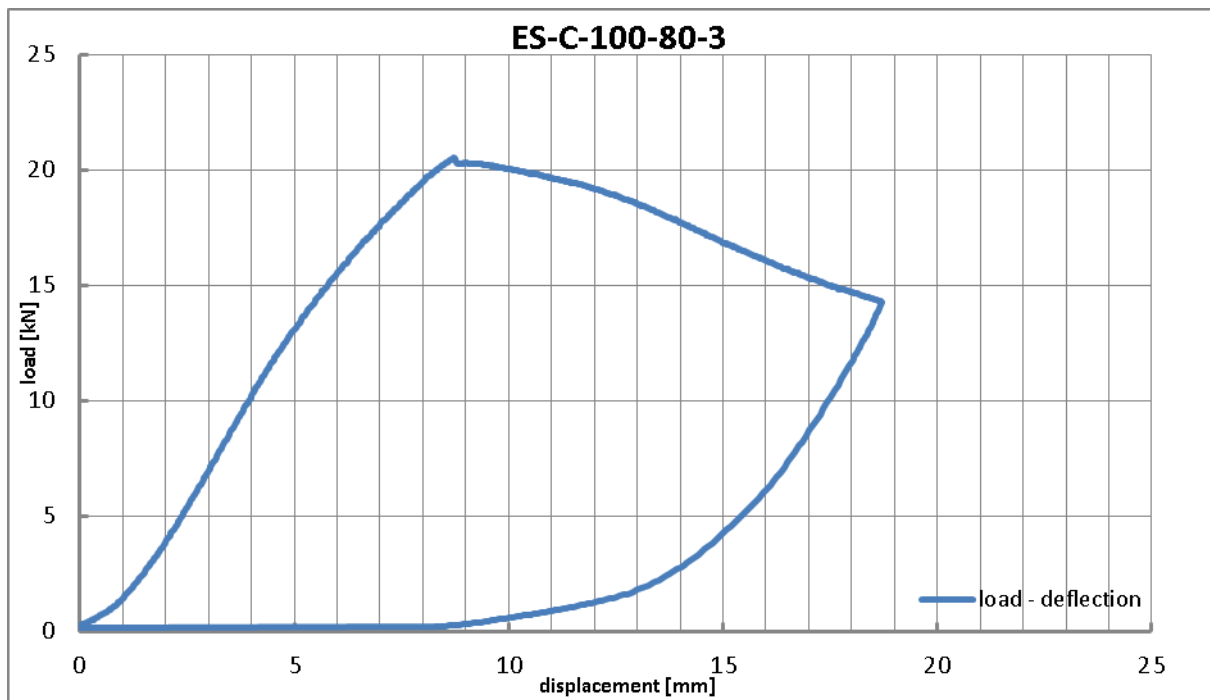


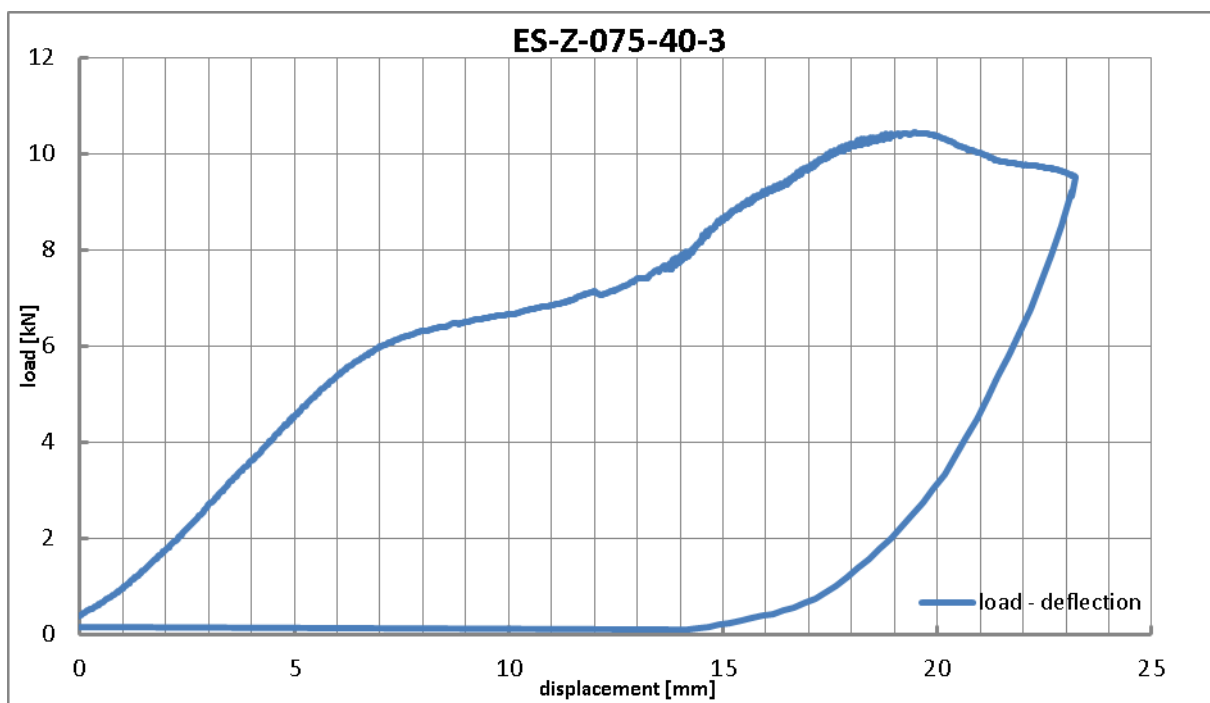
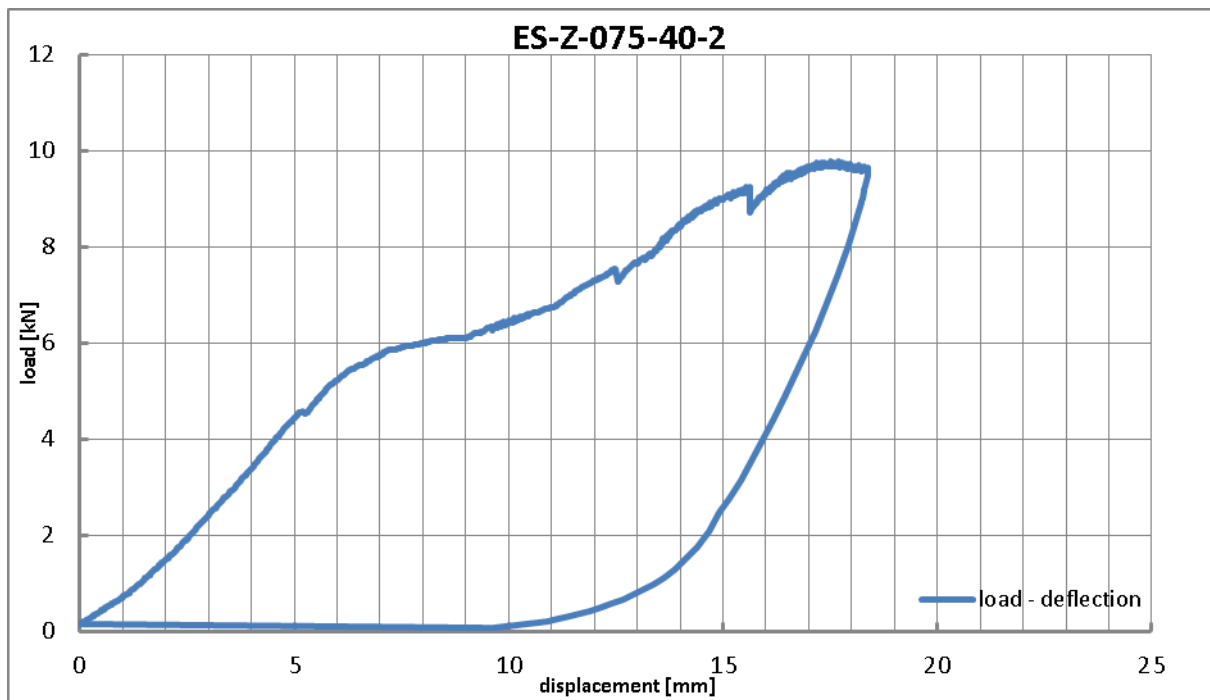


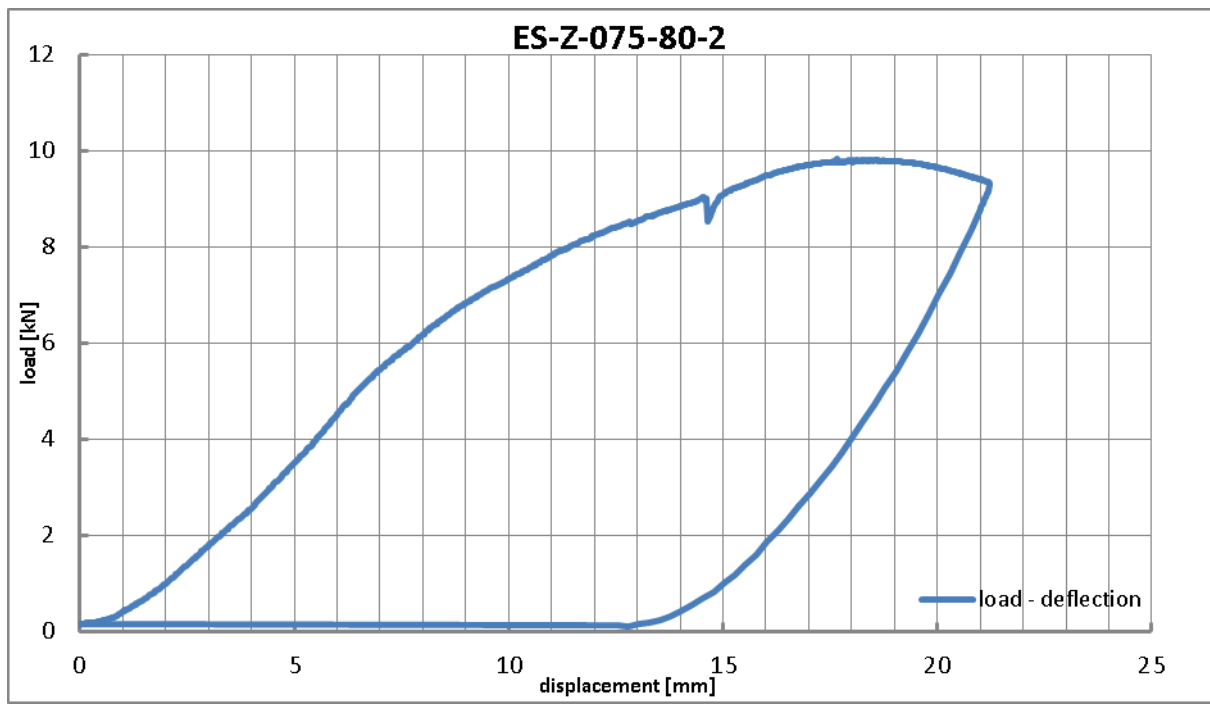
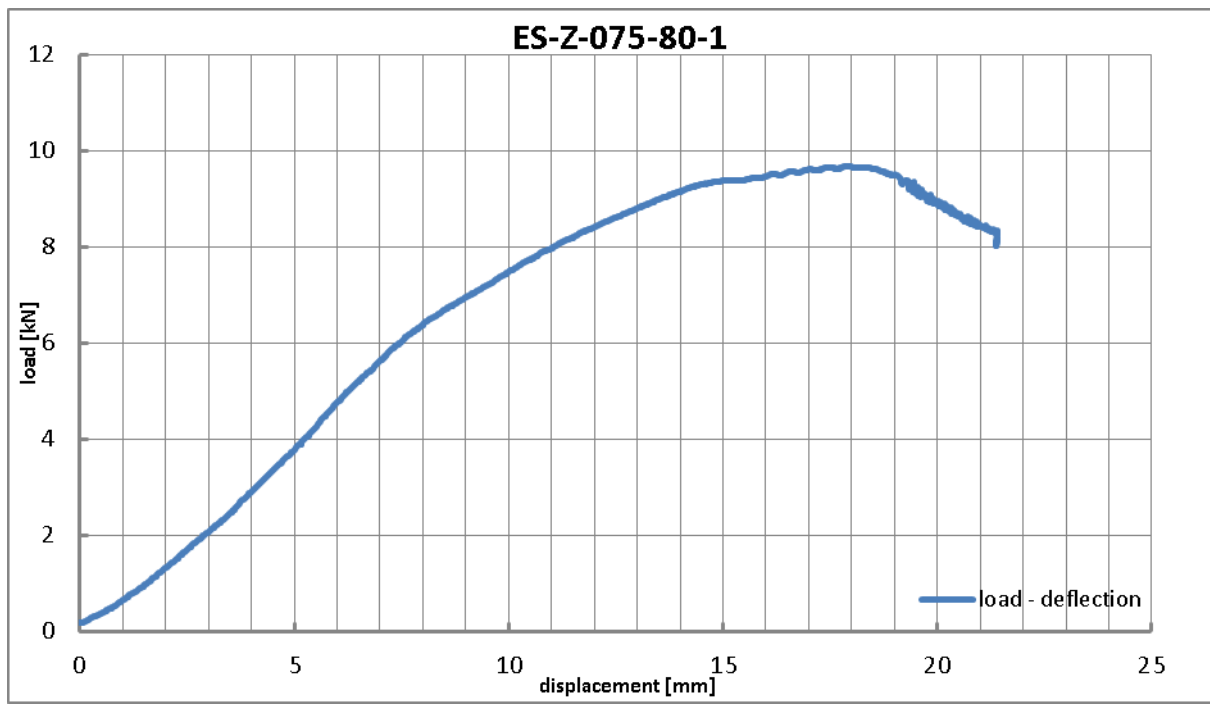


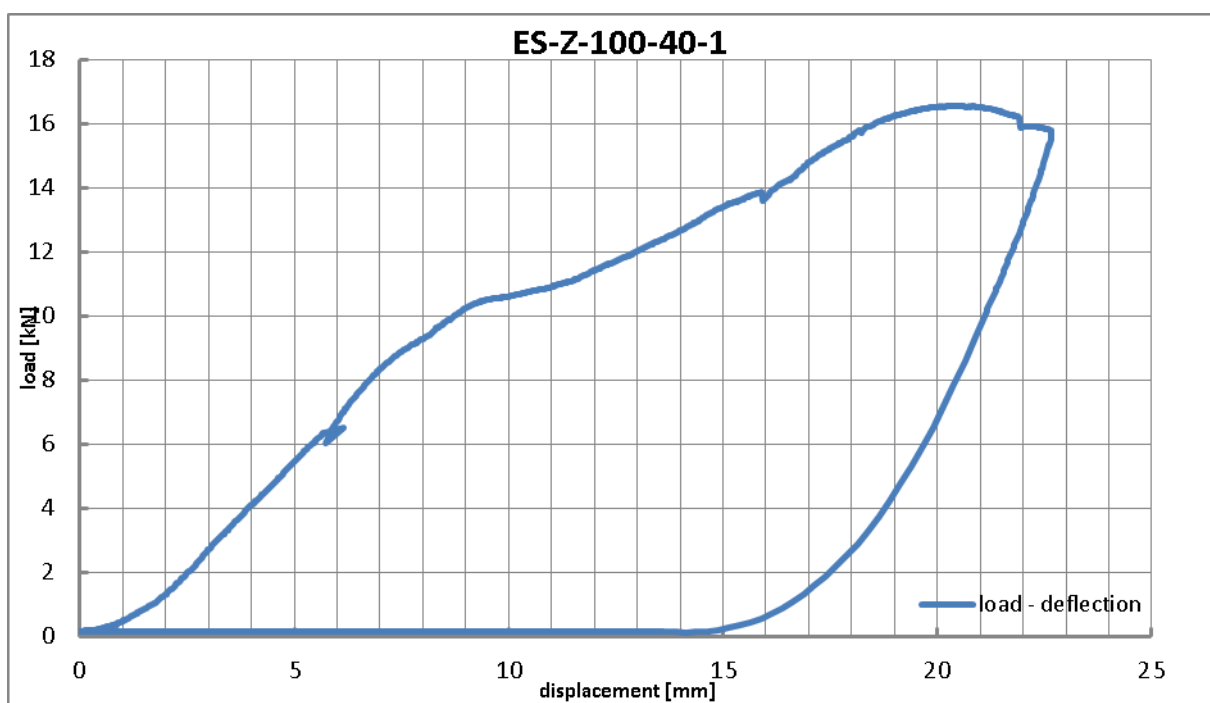
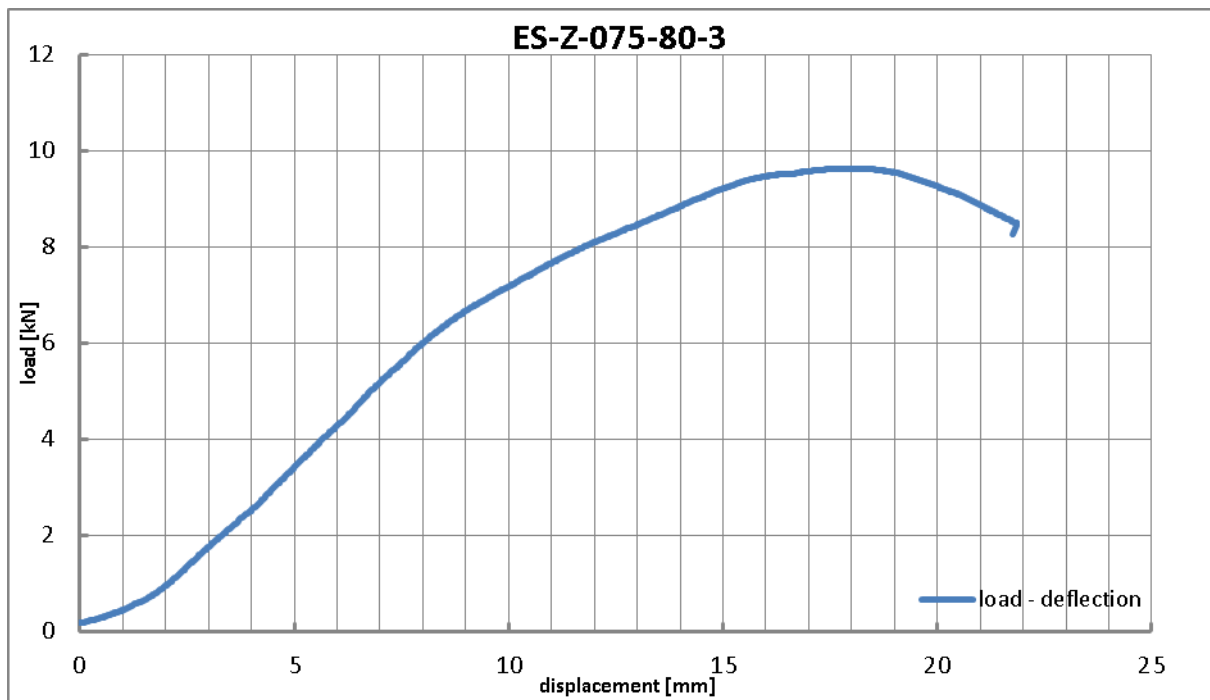


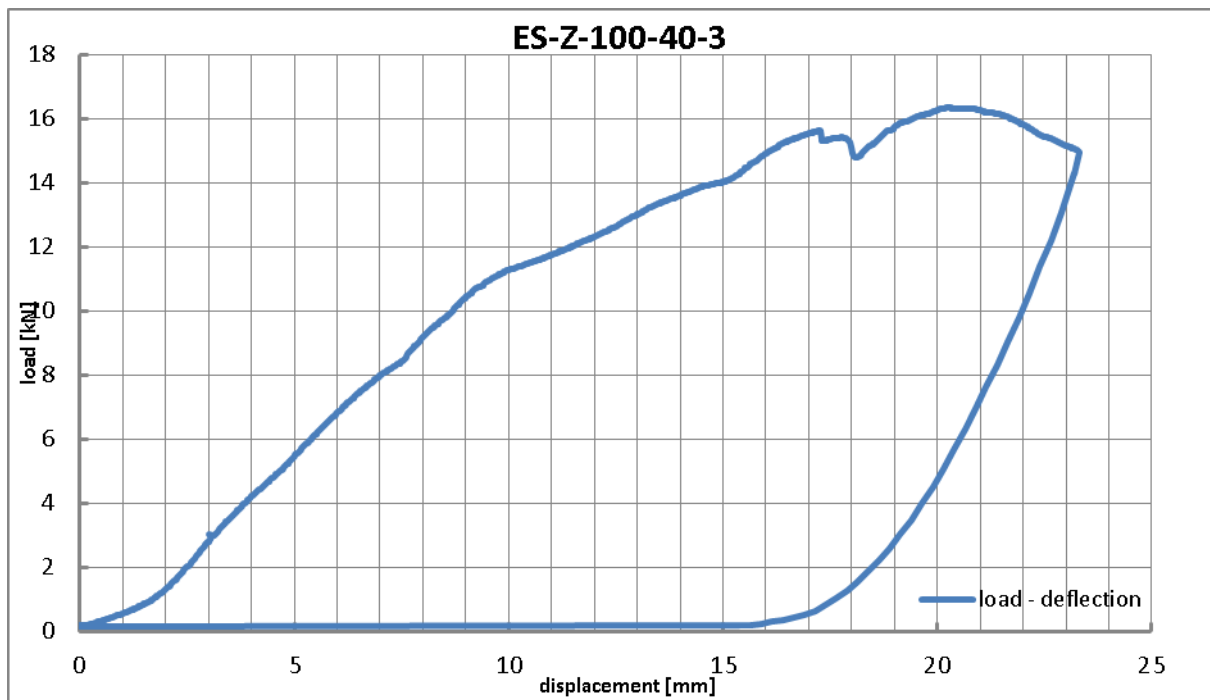
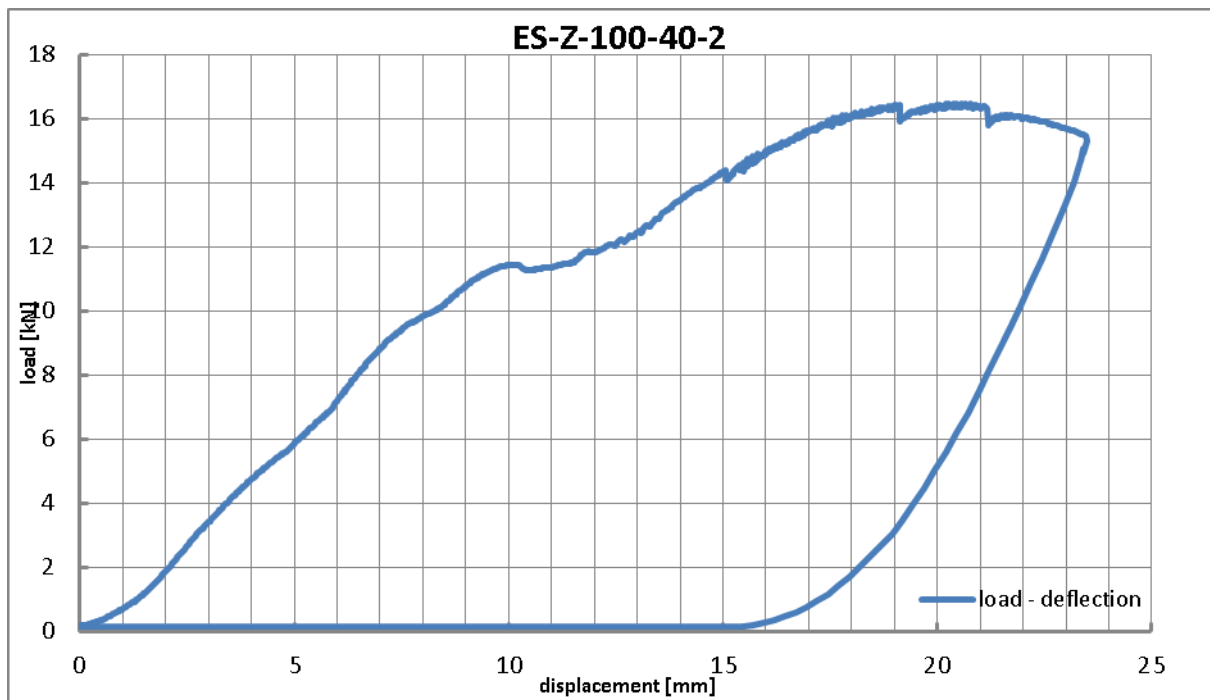


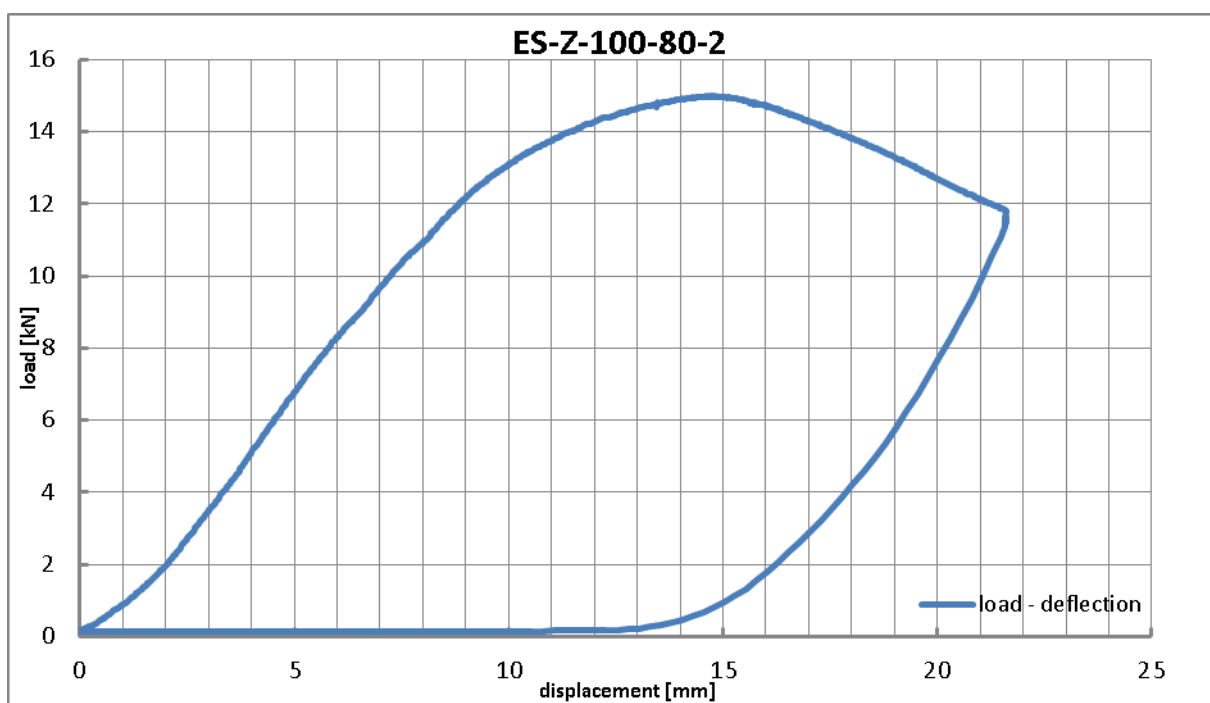
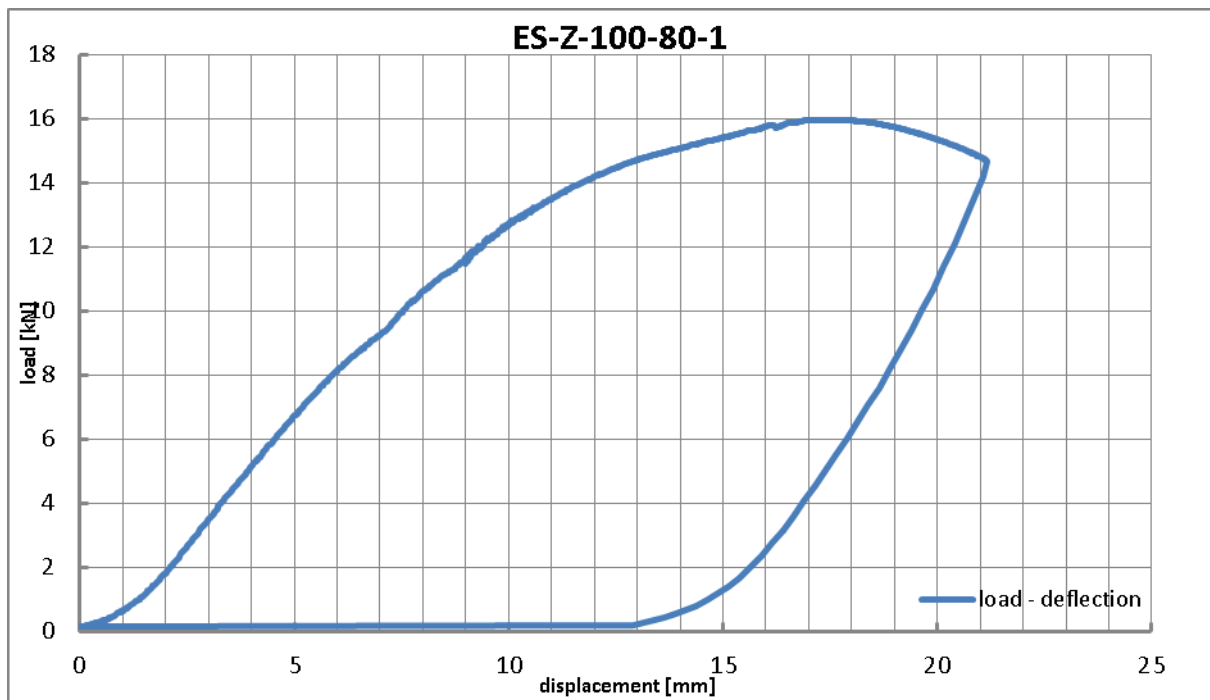


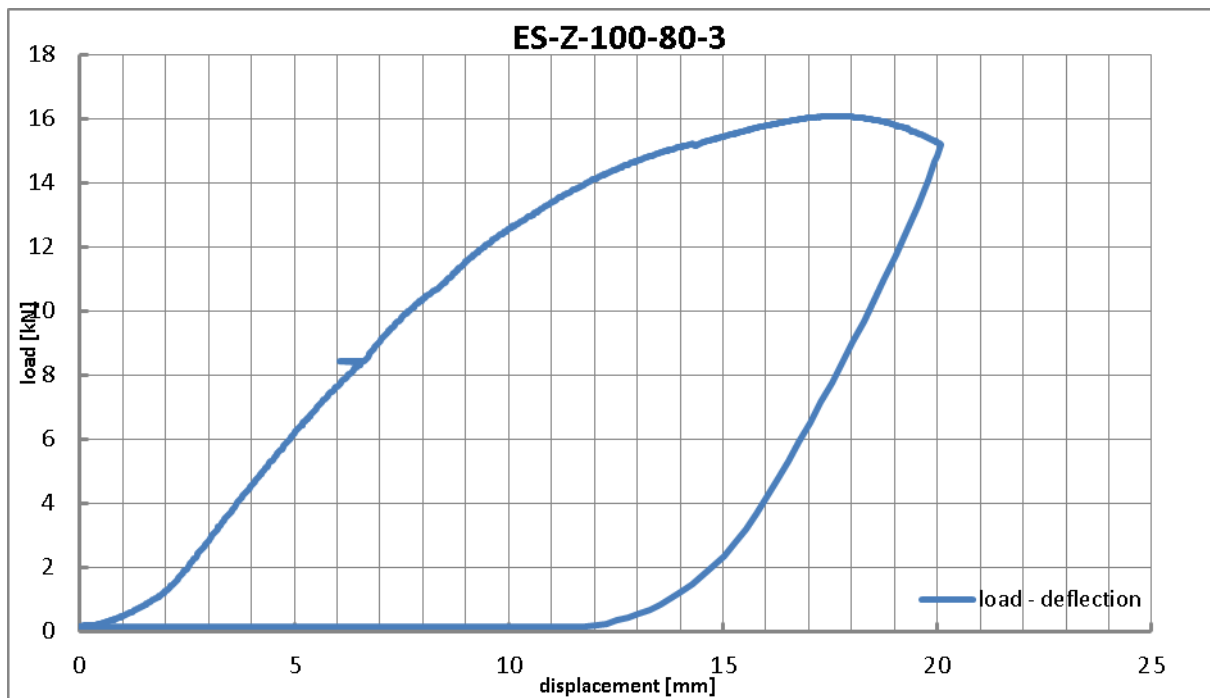




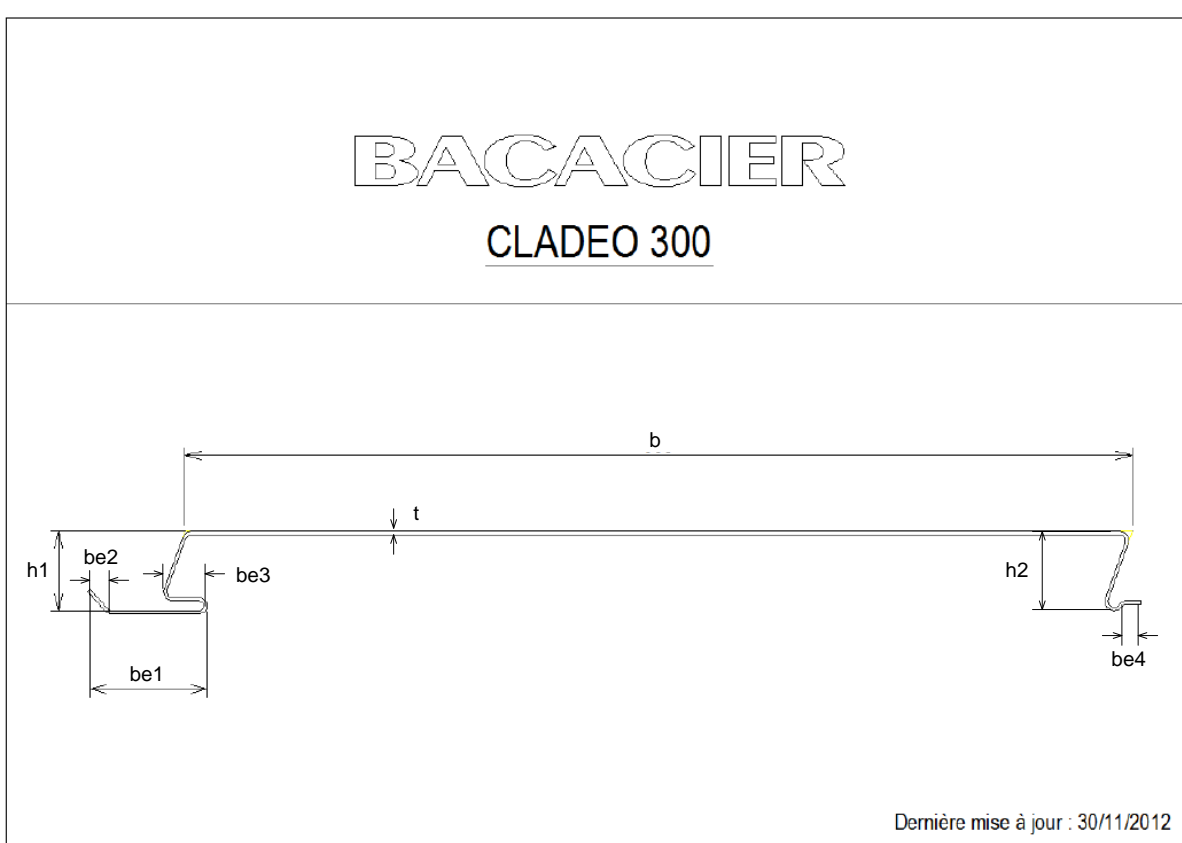








7 Annex G: Measurement of the profile geometry



profile	b [mm]	h1 [mm]	h2 [mm]	be1 [mm]	be2 [mm]	be3 [mm]	be4 [mm]	be5 [mm]	t [mm]
Cladeo $t_N = 0.75 \text{ mm}$	29.70	28.08	26.58	34.60	5.09	11.99	9.28	-	0.86
	29.80	28.47	26.25	34.73	4.95	12.10	8.08	-	0.85
	29.80	28.36	26.16	33.06	4.95	12.07	7.78	-	0.80
Cladeo $t_N = 1.00 \text{ mm}$	29.70	28.61	26.40	39.02	6.79	12.92	7.97	-	1.15
	29.80	28.22	26.49	38.99	6.82	12.82	7.62	-	1.20
	29.70	28.34	26.49	39.20	6.95	12.87	8.03	-	1.12
Zephir $t_N = 0.75 \text{ mm}$	29.50	35.44	30.39	24.73	21.66	58.71	21.30	18.46	0.84
	29.50	35.54	30.12	24.18	22.17	57.64	21.92	19.05	0.79
	29.50	35.62	30.48	24.55	22.40	59.76	21.17	18.87	0.79
Zephir $t_N = 1.00 \text{ mm}$	29.60	35.54	32.08	24.49	22.73	58.12	22.08	19.60	1.08
	29.60	35.50	31.81	25.79	22.46	58.36	21.91	20.17	1.22
	29.60	35.38	31.85	25.78	23.10	57.94	22.30	19.57	1.07
Zephir R $t_N = 0.75 \text{ mm}$	29.60	31.51	30.48	24.68	21.46	62.04	21.65	17.38	0.82
	29.60	34.13	30.33	23.90	22.20	61.84	22.69	17.12	0.83
	29.60	34.03	30.21	24.49	21.01	59.40	21.22	17.47	0.88
Zephir R $t_N = 1.00 \text{ mm}$	29.60	34.51	30.15	25.59	22.72	61.06	21.57	17.06	1.09
	29.50	34.79	30.01	24.51	22.64	60.60	22.78	16.26	1.09
	29.70	34.53	30.39	25.35	22.78	59.88	21.65	17.23	1.04

8 Annex H: Tensile tests

Test	Core thickness t_k [mm]	Yield strength $R_{p0.2}$ [N/mm ²]	Tensile strength R_m [N/mm ²]	Elongation at fracture $A_{L=80\text{mm}}$ [%]	Mean value	
					$R_{p0.2}$ [N/mm ²]	R_m [N/mm ²]
SSP-C-075-1	0.64	353	403	28.3	358	396
SSP-C-075-2	0.64	359	401	27.6		
SSP-C-075-3	0.64	362	385	27.6		
SSP-C-100-1	0.97	352	421	28.4	356	422
SSP-C-100-2	0.97	349	422	27.9		
SSP-C-100-3	0.97	366	424	27.5		
SSP-Z-075-1	0.71	392	468	23.5	392	466
SSP-Z-075-2	0.71	391	466	23.6		
SSP-Z-075-3	0.71	394	465	23.0		
SSP-Z-100-1	0.94	374	430	24.9	383	429
SSP-Z-100-2	0.94	390	430	25.5		
SSP-Z-100-3	0.94	385	427	24.7		
SSP-ZR-075-1	0.71	386	469	23.4	390	469
SSP-ZR-075-2	0.71	392	470	23.1		
SSP-ZR-075-3	0.71	393	467	23.7		
SSP-ZR-100-1	0.94	380	429	26.3	381	428
SSP-ZR-100-2	0.94	374	427	25.7		
SSP-ZR-100-3	0.94	388	427	25.9		
SSN-C-100-1	0.97	353	423	27.8	355	422
SSN-C-100-2	0.97	357	421	28.5		
SSN-C-100-3	0.97	354	423	28.4		
SSN-Z-075-1	0.72	389	469	24.3	389	467
SSN-Z-075-2	0.72	387	467	24.8		
SSN-Z-075-3	0.71	391	466	23.9		
SSN-Z-100-1	0.94	383	430	25.5	383	429
SSN-Z-100-2	0.94	383	430	25.6		
SSN-Z-100-3	0.94	384	428	25.3		
SSN-ZR-075-1	0.70	394	467	23.9	391	465
SSN-ZR-075-2	0.71	391	465	23.6		
SSN-ZR-075-3	0.71	389	464	23.9		
SSN-ZR-100-1	0.93	377	427	26.3	381	428
SSN-ZR-100-2	0.93	384	428	25.4		
SSN-ZR-100-3	0.93	383	428	26.6		

Test	Core thickness t_k [mm]	Yield strength $R_{p0.2}$ [N/mm ²]	Tensile strength R_m [N/mm ²]	Elongation at fracture $A_{L=80mm}$ [%]	Mean value	
					$R_{p0.2}$ [N/mm ²]	R_m [N/mm ²]
DSP-C-2-075-1	0.64	345	401	27.6	340	401
DSP-C-2-075-2	0.64	337	399	27.2		
DSP-C-2-075-3	0.63	337	404	28.7		
DSP-C-2-100-1	0.97	351	425	28.2	351	426
DSP-C-2-100-2	0.97	351	425	28.6		
DSP-C-2-100-3	0.97	350	427	28.6		
DSP-C-3-075-1	0.64	336	400	28.0	356	402
DSP-C-3-075-2	0.64	365	402	28.3		
DSP-C-3-075-3	0.64	367	403	28.7		
DSP-C-3-100-1	0.97	351	424	27.6	351	424
DSP-C-3-100-2	0.97	354	426	28.0		
DSP-C-3-100-3	0.97	347	422	27.6		
DSP-Z-2-075-1	0.71	402	467	24.5	399	466
DSP-Z-2-075-2	0.71	398	464	24.0		
DSP-Z-2-075-3	0.70	396	467	24.0		
DSP-Z-2-100-1	0.93	376	425	25.2	378	425
DSP-Z-2-100-2	0.93	378	425	26.4		
DSP-Z-2-100-3	0.94	379	426	26.4		
DSP-Z-3-075-1	0.71	400	465	22.9	397	465
DSP-Z-3-075-2	0.71	397	464	23.7		
DSP-Z-3-075-3	0.71	394	465	23.7		
DSP-Z-3-100-1	0.94	376	424	26.8	379	423
DSP-Z-3-100-2	0.94	382	424	26.5		
DSP-Z-3-100-3	0.93	380	422	27.0		
DSP-ZR-2-075-1	0.72	394	467	25.2	398	466
DSP-ZR-2-075-2	0.71	399	464	24.1		
DSP-ZR-2-075-3	0.71	401	466	24.6		
DSP-ZR-2-100-1	0.94	353	470	25.3	357	468
DSP-ZR-2-100-2	0.95	362	469	25.4		
DSP-ZR-2-100-3	0.94	356	465	26.0		
DSP-ZR-3-075-1	0.71	403	465	25.1	401	464
DSP-ZR-3-075-2	0.71	398	463	23.7		
DSP-ZR-3-075-3	0.71	402	465	24.6		

Test	Core thickness t_k [mm]	Yield strength $R_{p0.2}$ [N/mm ²]	Tensile strength R_m [N/mm ²]	Elongation at fracture $A_{L=80mm}$ [%]	Mean value	
					$R_{p0.2}$ [N/mm ²]	R_m [N/mm ²]
DSP-ZR-3-100-1	0.95	348	467	26.8	352	468
DSP-ZR-3-100-2	0.94	354	467	26.5		
DSP-ZR-3-100-3	0.94	355	469	27.0		
DSN-C-1-075-1	0.64	366	404	28.4	359	402
DSN-C-1-075-2	0.64	352	400	27.8		
DSN-C-1-075-3	0.65	358	401	28.4		
DSN-C-2-075-1	0.64	358	404	27.1	350	403
DSN-C-2-075-2	0.64	336	400	26.7		
DSN-C-2-075-3	0.63	355	405	26.6		
DSN-C-2-100-1	0.97	352	425	26.3	350	424
DSN-C-2-100-2	0.97	349	423	26.7		
DSN-C-2-100-3	0.97	350	425	26.7		
DSN-C-3-075-1	0.64	368	403	26.3	365	402
DSN-C-3-075-2	0.64	367	402	26.0		
DSN-C-3-075-3	0.64	360	402	27.1		
DSN-C-3-100-1	0.97	355	425	27.0	354	425
DSN-C-3-100-2	0.97	350	425	26.5		
DSN-C-3-100-3	0.97	356	425	26.3		
DSN-Z-1-075-1	0.71	390	468	24.1	391	468
DSN-Z-1-075-2	0.71	387	468	23.4		
DSN-Z-1-075-3	0.71	396	468	24.2		
DSN-Z-2-075-1	0.71	395	466	23.1	394	468
DSN-Z-2-075-2	0.72	393	467	23.2		
DSN-Z-2-075-3	0.71	394	470	23.0		
DSN-Z-2-100-1	0.93	384	427	25.7	380	428
DSN-Z-2-100-2	0.93	375	428	25.9		
DSN-Z-2-100-3	0.93	382	429	25.4		
DSN-Z-3-075-1	0.70	396	465	24.1	396	465
DSN-Z-3-075-2	0.71	396	467	24.2		
DSN-Z-3-075-3	0.71	395	464	24.6		
DSN-Z-3-100-1	0.94	375	426	26.2	376	425
DSN-Z-3-100-2	0.94	375	423	25.2		
DSN-Z-3-100-3	0.93	378	426	26.7		

Test	Core thickness t_k [mm]	Yield strength $R_{p0.2}$ [N/mm ²]	Tensile strength R_m [N/mm ²]	Elongation at fracture $A_{L=80mm}$ [%]	Mean value	
					$R_{p0.2}$ [N/mm ²]	R_m [N/mm ²]
DSN-ZR-1-075-1	0.71	405	468	23.9	398	468
DSN-ZR-1-075-2	0.71	395	467	23.9		
DSN-ZR-1-075-3	0.72	394	470	24.0		
DSN-ZR-2-075-1	0.71	400	464	24.6	397	466
DSN-ZR-2-075-2	0.71	397	465	24.2		
DSN-ZR-2-075-3	0.71	395	469	24.6		
DSN-ZR-2-100-1	0.95	358	467	25.5	361	418
DSN-ZR-2-100-2	0.95	362	467	25.3		
DSN-ZR-2-100-3	0.94	364	420	26.3		
DSN-ZR-3-075-1	0.71	396	466	23.8	394	467
DSN-ZR-3-075-2	0.72	397	466	23.4		
DSN-ZR-3-075-3	0.72	388	470	23.1		
DSN-ZR-3-100-1	0.94	354	468	25.2	358	467
DSN-ZR-3-100-2	0.95	361	466	25.3		
DSN-ZR-3-100-3	0.95	359	467	25.4		

Test	Core thickness t_k [mm]	Yield strength $R_{p0.2}$ [N/mm ²]	Tensile strength R_m [N/mm ²]	Elongation at fracture $A_{L=80mm}$ [%]	Mean value	
					$R_{p0.2}$ [N/mm ²]	R_m [N/mm ²]
ES-C-075-40-1	0.64	360	400	27.3	364	396
ES-C-075-40-2	0.64	363	393	27.2		
ES-C-075-40-3	0.64	368	394	28.8		
ES-C-075-80-1	0.64	359	399	27.3	363	395
ES-C-075-80-2	0.64	363	393	27.3		
ES-C-075-80-3	0.64	367	393	28.8		
ES-C-100-40-1	0.97	344	421	27.2	350	423
ES-C-100-40-2	0.97	353	424	27.4		
ES-C-100-40-3	0.97	353	423	27.7		
ES-C-100-80-1	0.97	345	422	27.1	350	423
ES-C-100-80-2	0.97	353	424	27.5		
ES-C-100-80-3	0.97	353	423	27.6		
ES-Z-075-40-1	0.71	387	470	23.9	389	468
ES-Z-075-40-2	0.71	387	467	23.9		
ES-Z-075-40-3	0.71	394	466	24.0		
ES-Z-075-80-1	0.71	388	467	23.6	390	468
ES-Z-075-80-2	0.71	392	469	23.5		
ES-Z-075-80-3	0.71	389	467	23.4		
ES-Z-100-40-1	0.94	371	430	25.7	378	429
ES-Z-100-40-2	0.94	385	427	25.2		
ES-Z-100-40-3	0.94	379	430	25.9		
ES-Z-100-80-1	0.94	370	429	25.7	378	429
ES-Z-100-80-2	0.93	385	427	25.1		
ES-Z-100-80-3	0.94	379	430	25.8		